Roles of Sirtuin 1 Activity and Tomato Carotenoids in the Development of Non-Alcoholic Fatty Liver Disease and Hepatocellular Carcinoma

A dissertation

submitted by

Junrui Cheng

In partial fulfillment of the requirements

for the degree of

Doctor of Philosophy

in

Biochemical and Molecular Nutrition

TUFTS UNIVERSITY

December 2017

Advisor:

Dr. Xiang-Dong Wang

Gerald J. and Dorothy R. Friedman School of Nutrition Science and Policy

Nutrition and Cancer Biology Laboratory

Jean Mayer – USDA Human Nutrition Research Center on Aging at Tufts University

ABSTRACT

The prevalence of non-alcoholic fatty liver disease (NAFLD) is positively associated with the obesity epidemic and the risks for hepatocellular carcinoma (HCC), which is the second most cause of cancer mortality worldwide. Sirtuin 1 (SIRT1) is a NAD+-dependent deacetylase that has emerged as a key metabolic sensor that links environmental signals to metabolic homeostasis, NAFLD, and to metabolic syndrome-associated HCC. Previous studies have shown that supplementation of tomato carotenoids, such as apo-10'-lycopenoic acid (ALA) which is an oxidized metabolite of apo-10'-lycopenal through lycopene cleavage by beta-carotene-9', 10'-oxygenase, can increase the expression and activity of SIRT1 and impede the development of NAFLD and HCC. However, whether tomato carotenoids protect against NAFLD and HCC dependent on SIRT1 signaling is enigmatic, and the causality between SIRT1 activity and the pathogenesis of NAFLD and HCC remains unknown. The primary objective of this thesis is to investigate the causal role of systemic SIRT1 activity in the development of NAFLD and HCC, and whether dietary tomato and tomato carotenoids, such as ALA, protect against NAFLD and HCC in a SIRT1-dependent manner.

In the 1st project, by utilizing SIRT1 homozygous mutation mice ablated of the catalytic activity of SIRT1 (MT) and their corresponding wild type (WT) littermates, we showed that SIRT1 loss-of-function aggravated high fat diet (HFD)-induced NAFLD progression, intriguingly, by promoting the mobility of free fatty acid (FFA) from mesenteric adipose tissue (MAT) to the liver. This study revealed a critical role of SIRT1 in preventing NAFLD, and addressed the underlying mechanism that people without 'belly fat' still develop fatty liver when SIRTt1 activity decreases due to certain factors such as aging, unhealthy diet, or stress. In the 2nd project, both WT and MT mice were treated with hepatic carcinogen diethylnitrosamine, followed by HFD feeding with or without tomato powder (TP, representative of whole tomato) for 34 weeks. Results revealed that TP supplementation significantly reduced liver steatosis in both WT and MT mice through different molecular mechanisms. The protective effect of TP in WT mice was mediated by increasing SIRT1 protein expression and activity, and decreasing hepatic fatty acid binding protein 1 expression and FFA uptake. While in MT mice, TP decreased hepatic fatty acid synthesis through inactivating hepatic acetyl-CoA carboxylase mediated by AMPK phosphorylation, independent of SIRT1. Additionally, TP lowered il-6 mRNA expression in MAT and IL-6 concentration in plasma, as compared with MT mice without TP. In WT mice, dietary TP decreased caspase-1 mediated IL-1β maturation. However, we did not detect significant hepatic inflammatory cell infiltration in both WT and MT mice. Neither the mutation of SIRT1 activity nor TP supplementation altered incidence or multiplicity of HCC in both WT and MT mice. This could be due to the lack of inflammation as a target of TP protection or limited efficacy of SIRT1 in ameliorating HCC development in this mouse model. Our final project

demonstrated that ALA supplementation at 10 mg/kg diet in WT and MT mice for 34 weeks achieved a comparable effect against NAFLD between WT and MT mice. Unexpectedly, MT mice developed less hepatic tumor multiplicity, as compared with WT mice fed the same dose of ALA. Interestingly, the ablation of SIRT1 activity resulted in increased expression of hepatic nuclear receptors (rxrα, lxrα, pparγ) and vitamin A transporter cd36, and hepatic retinol concentration, but decreased cyclin D1 protein levels, suggesting potential contribution of these nuclear receptors and retinol as well as cell cycle arrest to the reduction of hepatic tumor multiplicity. This study demonstrated that ALA protects against NAFLD and HCC independent of SIRT1 activity and the lack of SIRT1 activity reduced the progression of HCC in mice given HFD and ALA supplementation.

In summary, through this thesis work, we first demonstrated the causal role of absence of SIRT1 activity in the pathogenesis of NAFLD, which underscores the key role of SIRT1 in ameliorating NAFLD progression through involving multiple organs. Secondly by exploring an efficient dietary strategy against NAFLD, we demonstrated that dietary TP as a whole food approach acts as an effective disease prevention strategy against NAFLD independent of SIRT1 activity. Lastly, we demonstrated that lack of SIRT1 activity inhibited HCC development in mice given HFD and ALA supplementation, highlighting the complex regulation of SIRT1 in hepatic tumorigenesis with paradoxical functions as tumor suppressor or tumor promoter.

ACKNOWLEDGEMENTS

I would like to take the time to acknowledge several people who have been instrumental in the successful completion of this thesis work. First and foremost, I want to thank my advisor and mentor, Dr. Xiang-Dong Wang, whose continuous support and contagious positive attitude toward research encouraged me moving on throughout the entire PhD study. His abundant knowledge in nutrition, molecular biology and cell biology helps me to overcome the inevitable setbacks and unexpected changes I encountered throughout my research. Dr. Wang's dedication of time, funding, and thoughtful instructions were essential to make my Ph.D. experience productive and stimulating.

Thank you to my additional committee members, Dr. Dayong Wu, Dr. Lynne Ausman and Dr. Andrew Greenberg, who have also played a large supporting role in the completion of this thesis work. The ELISA studies would not have been possible without the help and instruction from Dr. Dayong at the Nutrition and Immunology Lab, where I gained my first 'hands-on' experience in bench study during my lab rotation as a master student. Dr. Ausman has been a constant source of support throughout my entire time at the Friedman School in matters of academics, school politics, and scientific insight. She truly has the student's best interest at heart, and is an invaluable part of this school. I want to thank Dr. Greenberg who also undertook as my thesis committee member despite his many other academic and professional commitments. He was always willing to discuss my latest

findings and provided insightful comments regarding the mechanistic details of my thesis work. His wisdom, knowledge and commitment to the highest standards inspired and motivated me. I am incredibly grateful for the support and guidance I received from all members of my committee.

Additionally, my fellow colleagues of the Nutrition and Cancer Biology Laboratory have all provided a welcoming and supportive environment in which to complete my thesis research over the past four years. My heartful thanks to Connie Hu, who taught me how to perform PCR, western blotting, HPLC, and other bench researches with great patience, even at her busy times. Dr. Chun Liu provided countless hours of his time processing liver samples for histological analysis and was always willing to spend the time to convey his knowledge and teach his skills. Rachel Chiaverelli, Jelena Mustra Rakic, Ji Ye Lim, fellow graduate students in our lab, have provided the perfect combination of friendship, stimulating suggestions, and helpful encouragement to help me navigate through this experience. I have truly enjoyed learning from and collaborating with everyone in this lab.

I would also like to acknowledge the Comparative Biology Unit here at the HNRCA. I would not have been able to complete the numerous animal studies that formed the basis of this thesis without the help and expertise of Dr. Donald Smith and his team.

Last but not the least, I want to thank my family for their love and long-time support throughout my thesis work. For my dearest parents who raised me with a love of science and an attitude of being serious and responsible. I give a heart-felt thank you to my loving parents, and my significant other, Timmy, who has stood by my side through this stressful time with unwavering support. I will be forever grateful for your love and dedication to my success and happiness.

TABLE OF CONTENTS

LIST OF ABBREVIATIONS

ACOX1 – acyl-CoA oxidase 1

ACOX3 – acyl-CoA oxidase 3

AMPK – AMP-activated protein kinase

ANOVA – analysis of variance

APO10LA – ALA

ATGL – adipose triglyceride lipase

CPT-1 – carnitine palmitoyltransferase-1

DEN – diethylnitrosamine

DGAT – diglyceride acyltransferase

EDTA – ethylenediaminetetraacetic acid

FFA – free fatty acid

H&E – hemotoxylin & eosin

HCC – hepatocellular carcinoma

HPLC – high performance liquid chromatography

HFD – high fat diet

HSL – hormone sensitive lipase

i.p. – intraperitoneal

IFNγ – interferon γ

IL-1β – interleukin 1β

IL-6 – interleukin 6

JNK – c-jun-N-terminal kinase

KO – knockout

LKB1 – liver kinase b1

LXR – liver X receptor

LKB1 – liver kinase B1

MAP – mitogen-activated protein

MAT – mesenteric adipose tissue

SIRT1 activity mutant – MT

MTTP – microsomal triglyceride transfer protein

NAD+ – nicotinamide adenine dinucleotide

NADH – reduced nicotinamide adenine dinucleotide

NAFLD – non-alcoholic fatty liver disease

NAM – Nicotinamide

NAMPT – Nicotinamide phosphoribosyltransferase

NASH – non-alcoholic steatohepatitis

NMNAT – Nicotinamide mononucleotide adenylyltransferase

PCR – polymerase chain reaction

PGC1α – peroxisome proliferator-activated receptor gamma coactivator 1-α

PLIN – perilipin

PPAR - peroxisome proliferator-activated receptor

PPRE – peroxisomal proliferator response element

RXR – retinoid X receptor

RAC – retinoic acid

RAR – retinoic acid receptor

SAS – Statistical Analysis System

SCD1 – Stearoyl-CoA desaturase

SEM – standard error of the means

SIRT1 – sirtuin 1

SREBP-1 – sterol regulatory element-binding protein 1

TNFα – tumor necrosis factor α

TP – tomato powder

WT – wild-type

CHAPTER I

INTRODUCTION

BACKGROUND

Obesity has become a leading epidemic concern worldwide, and the escalating incidence of nonalcoholic fatty liver disease (NAFLD) parallels the increasing obesity rates [1]. NAFLD is observed in 65%-85% of obese patients, with a higher prevalence in men compared to women [2]. NAFLD describes a range of related disorders that begin with hepatic steatosis, which can proceed to nonalcoholic steatohepatitis, non-alcoholic steatohepatitis (NASH), and fibrosis or cirrhosis as the final stage [3, 4].

Hepatocellular carcinoma (HCC) accounted for 85%-90% of primary liver cancers [5, 6], and is the second most common cause of cancer mortality worldwide [7]. According to the 18th Annual Report to the Nation on the Status of Cancer, the mortality of HCC is still increasing, despite of the decline in overall cancer death rates [8, 9]. NAFLD has been observed in 30%-40% of HCC patients in the US [5]. Indeed, with the involvement of inflammatory cytokines such as IL-1β, IL-6 and TNFα, simple steatosis can further progress to NASH, to severe fibrosis [10], which was observed in approximately 90% of HCC cases [11], highlighting the critical role of metabolism disorder on HCC development. Considering the lack of effective medical treatments for both NAFLD and HCC, preventing the incidence of NAFLD, or ameliorate NAFLD development at an early stage could be an important strategy.

It is well understood that consumption of tomato and tomato products is inversely associated with the incidence of a number of chronic diseases and ameliorates risk factors of metabolic diseases [12]. In addition, the consumption of tomato products can inhibit systemic inflammation by reducing pro-inflammatory cytokines [13], decrease hallmarks of liver steatosis, and accelerate hepatic lipid metabolism [14]. Tomatoes are good

sources of the colorless carotenoids phytoene, phytofluene, and other micronutrients such as vitamin C, E, and flavonoids, which are all considered as good anti-oxidant agents [15]. Previous studies have established beneficial effects of tomato and tomato products against inflammation [16, 17], oxidative stress [18, 19] and various cancers [20] including lung, stomach, colorectal, prostate cancer, etc. Two studies in our lab have revealed the anti-hepatic inflammation [21] and anti-hepatic lesion [15] effect of tomato extract, which contains only fat-soluble nutrients of tomatoes. Unlike tomato extract, tomato powder (TP) contains water-soluble nutrients, making dietary TP supplementation contain public health relevance.

. Lycopene, the pigment principally responsible for the characteristic deep-red color of ripe tomato and tomato products, is the most predominant carotenoid in human plasma. Lycopene has attracted attention due to its biological and physicochemical properties, especially related to its effects as a natural antioxidant, anti-inflammatory and anti-carcinogenic agent against certain types of cancers, including those of the liver [22] and lung [23]. We have previously demonstrated that in mammalian tissues, lycopene can be preferentially cleaved by beta-carotene 9',10'-oxygenase, resulting in apo-10'-lycopenal, which can be subsequently oxidized to apo-10'-lycopenoic acid (ALA) [24]. Intriguingly, both in vitro and in vivo studies found that ALA presented substantial anti-carcinogenesis characteristic in lung and liver through reducing cyclin D1 by promoting p21 expression [25, 26]. Further exploring the mechanism, Ip et al. found that ALA ameliorated HCC by dose-dependently up-regulating sirtuin 1 (SIRT1) protein, which is concordant with previous report that ALA increased SIRT1 mRNA and protein levels in

genetically-induced obese (ob/ob) mice [27]. However, whether ALA inhibits HCC dependent on SIRT1 signaling remains to be explored.

SIRT1 is an evolutionarily conserved NAD+-dependent histone and non-histone protein deacetylase [28, 29]. As a metabolic regulator, SIRT1 has been identified to control a series of physiological activities, including reducing fatty acid synthesis [30, 31], increasing β-oxidation [32, 33], and decreasing adipocyte generation [34]. These functions of SIRT1 are exerted through coupling with NAD+ hydrolysis, transferring the acetyl group of the substrate to cleaved NAD+ (ADP-ribose), and generating O-acetyl-ADP-ribose [29, 35, 36]. By virtue of these functions, SIRT1 has been widely studied as a molecular target to inhibit the pathogenesis of various diseases, including HFD-induced NAFLD [31, 37, 38]. Both animal and human studies suggest an inverse correlation between SIRT1 levels and NAFLD incidence [39, 40]. However, the causality of SIRT1 in the development of NALFD remains unknown.

SIGNIFICANCE

Considering the high mortality rate for those withHCC, avoidance of carcinogenesis initiation is the best protection against HCC. While the connection between SIRT1, NAFLD, and HCC development has been established, a deeper understanding of the causality of SIRT1 on the development of these diseases and the specific mechanisms are essential. Utilization of systemic SIRT1 ablation mouse model and use of carefully designed experimental animal protocols are excellent tools with which to provide additional knowledge regarding the signaling mechanisms involved in NAFLD and related hepatocarcinogenesis.

In addition, dietary intervention represents a promising disease control strategy for the prevention of NAFLD and HCC. Many experimental models focus on supplemental intervention with isolated compounds, enabling researchers to identify specific mechanisms of action by these compounds. However, this thesis also involves the efficacy of whole food intervention. Whole foods contain a diverse collection of nutrients and bioactive compounds that provide additive, complementary, and/or synergistic beneficial effects that are lacking from supplementation with a single compound. Therefore, supplementation with whole tomato may provide an effective nutritional approach to help reduce the severity of HFD-induced NAFLD and related carcinogenesis.

In summary, the significance of our study lies in: 1) revealing underlying targets for future hepatic steatosis and HCC treatment; and 2) providing a dietary-oriented, public health-meaningful means to reduce hepatic steatosis and HCC development. Considering the high prevalence of HCC and its notorious mortality rate, this thesis work provides critical insight into future treatment of HCC, and establishes guidance for dietary recommendations and clinical trials involving tomato intake for the prevention of NAFLD and HCC.

HYPOTHESIS

The primary objective of this thesis was to investigate the causality of SIRT1 activity on the development of NAFLD and HCC, and to determine whether the efficacy of tomato powder and ALA are dependent on SIRT1 signaling. We hypothesized that i) systemic SIRT1 ablation would accelerate the development of NAFLD and HCC, ii)

tomato powder supplements containing multiple tomato nutrients would provide protection against NAFLD and HCC independent of SIRT1, and iii) the efficacy of ALA is SIRT1 dependent. To test our hypotheses we developed four specific aims.

SPECIFIC AIMS

Specific Aim 1: To investigate the causality of sirtuin 1 in the development of non-alcoholic fatty liver disease.

To investigate Specific Aim 1, both sirtuin 1 (SIRT1) homozygous mice with the catalytic activity (MT) ablated and their corresponding wild type littermates (WT) were fed a high fat diet (HFD, 60% calories from fat) for 34 weeks. MT mice showed significantly higher levels of hepatic triglycerides which were accompanied with higher levels of SREBP-1 and SCD1and decreased phosphorylation of LKB1 and AMPK in the liver. Compared with WT mice, mRNA expression of lipogenic genes (*lxrα*, *srebp-1c*, s*cd1* and *fas*) in the mesenteric adipose tissue (MAT) increased significantly in MT mice. Fatty acid oxidation biomarkers (*acox1*, *acox3*, *cpt*, *ucp1*, *sirt3*) in both liver and MAT were comparable between groups. Interestingly, we observed that in MT mice, the mRNA level of hormone sensitive lipase (*hsl*), adipose triglyceride lipase (*atgl*) and perilipin-2 (*plin-2*), all involved in lipolysis, significantly increased in MAT, but not in epididymal adipose tissue. These changes positively correlated with circulating free fatty acid (FFA) concentrations and higher hepatic mRNA expression of *cd36* for FFA uptake. The present study has provided novel evidence to suggest that under HFD-induced metabolic surplus, the lack of SIRT1 catalytic activity promotes release of FFA from

MAT and escalate non-alcoholic fatty liver disease (NAFLD) by interfering with lipid homeostasis in both liver and MAT.

Specific Aim 2: To mechanistically examine the role of dietary tomato in preventing against NAFLD and HCC development.

To investigate Specific Aim 2, we utilized the same systemic SIRT1 ablated mice in Specific Aim 1 and their WT counterparts. Both WT and MT mice were injected with diethylnitrosamine (DEN), and fed a high fat diet (HFD) with or without tomato powder (TP) for 34 weeks.

As a result, we found that dietary TP significantly decreased liver steatosis and inflammation biomarkers in both MT and WT mice. In WT mice, TP decreased liver long chain fatty acid (FA) uptake by decreasing mRNA of fatty acid binding protein 1. Dietary TP also increased SIRT1 expression and IL-1β maturation associated with decreasing caspase 1. In MT group, TP decreased hepatic FA synthesis through inactivating hepatic acetyl-CoA carboxylase mediated by AMPK phosphorylation, and lowered il-6 expression in mesenteric adipose tissue (MAT), contributing to lowered IL-6 concentration in plasma and liver. Additionally, TP decreased mRNA levels of lipogenic genes (*acc*, *fas*, *scd1*, *dgat1*, *dgat2*) and pro-inflammatory biomarkers (*il-1β*, mcp1) in MAT. However, no significant effects of TP or SIRT1 activity were observed in HCC development.

Therefore, we conclude that dietary TP supplementation can ameliorate HFD-induced NAFLD and inflammatory responses independent of SIRT1 activity, but not affect carcinogen-induced HCC development.

Specific Aim 3: To investigate whether the efficacy of apo-10'-lycopenoic acid is SIRT1-dependent.

ALA naturally exists in tomato and tomato products. Furthermore, it is also a cleavage product from lycopene, a major carotenoid in dietary tomatoes. In the second project, we found that TP, as whole food, can prevent against NAFLD and HCC. This led us to propose that ALA, as a biological metabolite from tomatoes, might play a role in preventing the development of NAFLD and HCC. To complete Specific Aim 3, the same WT and MT mice described in Specific Aim 1 were used. Both mice were injected with DEN, and fed a HFD with apo-10'-lycopenoic acid (ALA) for 34 weeks.

Our results revealed that MT mice presented significantly higher acetylated-FoxO1/total-FoxO1 ratios than WT mice. Dietary ALA resulted in comparable liver steatosis and HCC incidence between WT and MT mice. HCC tumor multiplicity was moderately decreased in MT mice, compared to WT mice ($P = 0.08$). In MT mice, hepatic retinol and retinyl palmitate concentration significantly increased, which was associated with elevated hepatic *cd36* mRNA expression. Compared to WT mice, hepatic mRNA expressions of *rxrα*, *rarγ* and *pparγ*, as well as hepatic RXRα protein levels significantly increased in MT mice. In addition, hepatic cyclinD1 mRNA and protein levels significantly decreased in MT mice, which was associated with increased hepatic *p21*, *p27* and *p53* mRNA expressions. Hepatic levels of lipid metabolism-related genes and inflammatory biomarkers were comparable between WT and MT mice.

As conclusion, the efficacy of ALA protecting against liver steatosis and HCC was not SIRT1-dependent. Systemic SIRT1 activity ablation can moderately inhibit HCC development, potentially mediated by elevating hepatic retinol concentration.

SUMMARY

This thesis addresses the specific molecular mechanisms by which the lack of systemic SIRT1 activity accelerates HFD-induced NAFLD as well as prevention of carcinogen-initiated, HFD-promoted HCC by TP and ALA independent of SIRT1 activity. Specifically, we have demonstrated the crucial role that SIRT1 plays in the development of NAFLD by involving not only liver, but also adipose tissue, providing a deeper understanding concerning the participation of multi-organs in the pathogenesis of NAFLD and proposing the underlying mechanism of the NAFLD incidence in lean population. In a second study, we revealed that TP supplementation was capable of preventing NAFLD including a reduction in steatosis and liver inflammation, but did not present significant benefits in impeding HCC development. The lack of SIRT1 promoted the severity of hepatic triglyceride accumulation and increased hepatic inflammatory biomarkers, but did not alter HCC development. This study demonstrated that as a whole food, TP had potent efficacy protecting against NAFLD at the initial step, but the efficacy of whole food against carcinogenesis is limited. Consistent with the first study, SIRT1 mutation resulted in increased hepatic triglyceride deposit, but the role of SIRT1 in HCC development is still under debate since the 129/SvJ strain we utilized in this thesis presented impaired immune response. In our last study, in which we gave ALA, which presented substantial anti-HCC efficacy in the previous study from our lab, to both WT mice and mice lack of SIRT1 activity. The comparable HCC severity between WT and MT mice indicates that SIRT1 is not the only molecular target of ALA. Interestingly,

under the surplus of HFD and ALA, the lack of SIRT1 activity inhibited HCC, which was associated with increased hepatic retinol concentration. The inconsistent effect of SIRT1 on HCC development that we observed in the second and the third study might be due to the effect of ALA, but requires further investigation.

These studies revealed the unique biological activities exerted by SIRT1 that serve to inhibit HFD-induced NAFLD by affecting multiple organs. Our findings support whole food as an effective disease prevention strategy against NAFLD at the initial step. This thesis work also provided explanation in the necessity of utilizing C57BL6 backcrossed mice in the study of HCC development, as well as laid the groundwork for future studies examining the mechanisms by which tomato supplementation and tomato products prevent hepatic steatosis and inflammation.

LITERATURE CITED

[1] Aleksandrova, K., Stelmach-Mardas, M., Schlesinger, S., Obesity and Liver Cancer. Recent results in cancer research. Fortschritte der Krebsforschung. Progres dans les recherches sur le cancer 2016, 208, 177-198.

[2] Fabbrini, E., Sullivan, S., Klein, S., Obesity and nonalcoholic fatty liver disease: biochemical, metabolic, and clinical implications. Hepatology (Baltimore, Md.) 2010, 51, 679-689.

[3] Cohen, J. C., Horton, J. D., Hobbs, H. H., Human fatty liver disease: old questions and new insights. Science (New York, N.Y.) 2011, 332, 1519-1523.

[4] Baffy, G., Brunt, E. M., Caldwell, S. H., Hepatocellular carcinoma in non-alcoholic fatty liver disease: an emerging menace. Journal of hepatology 2012, 56, 1384-1391.

[5] El-Serag, H. B., Rudolph, K. L., Hepatocellular carcinoma: epidemiology and molecular carcinogenesis. Gastroenterology 2007, 132, 2557-2576.

[6] Parkin, D. M., Global cancer statistics in the year 2000. The Lancet. Oncology 2001, 2, 533-543.

[7] Ferlay, J., Soerjomataram, I., Dikshit, R., Eser, S., et al., Cancer incidence and mortality worldwide: sources, methods and major patterns in GLOBOCAN 2012. International journal of cancer 2015, 136, E359-386.

[8] Ryerson, A. B., Eheman, C. R., Altekruse, S. F., Ward, J. W., et al., Annual Report to the Nation on the Status of Cancer, 1975-2012, featuring the increasing incidence of liver cancer. Cancer 2016, 122, 1312-1337.

[9] Siegel, R. L., Miller, K. D., Jemal, A., Cancer Statistics, 2017. CA: a cancer journal for clinicians 2017, 67, 7-30.

[10] Dowman, J. K., Tomlinson, J. W., Newsome, P. N., Pathogenesis of non-alcoholic fatty liver disease. QJM: monthly journal of the Association of Physicians 2010, 103, 71-83.

[11] De Minicis, S., Marzioni, M., Saccomanno, S., Rychlicki, C., et al., Cellular and molecular mechanisms of hepatic fibrogenesis leading to liver cancer. Transl Gastrointest Cancer 2011, 1, 88-94.

[12] Story, E. N., Kopec, R. E., Schwartz, S. J., Harris, G. K., An update on the health effects of tomato lycopene. Annual review of food science and technology 2010, 1, 189-210.

[13] Ghavipour, M., Saedisomeolia, A., Djalali, M., Sotoudeh, G., et al., Tomato juice consumption reduces systemic inflammation in overweight and obese females. The British journal of nutrition 2013, 109, 2031-2035.

[14] Martin-Pozuelo, G., Navarro-Gonzalez, I., Gonzalez-Barrio, R., Santaella, M., et al., The effect of tomato juice supplementation on biomarkers and gene expression related to lipid metabolism in rats with induced hepatic steatosis. European journal of nutrition 2015, 54, 933-944.

[15] Melendez-Martinez, A. J., Nascimento, A. F., Wang, Y., Liu, C., et al., Effect of tomato extract supplementation against high-fat diet-induced hepatic lesions. Hepatobiliary Surg Nutr 2013, 2, 198-208.

[16] Garcia-Alonso, F. J., Jorge-Vidal, V., Ros, G., Periago, M. J., Effect of consumption of tomato juice enriched with n-3 polyunsaturated fatty acids on the lipid profile, antioxidant biomarker status, and cardiovascular disease risk in healthy women. Eur J Nutr 2012, 51, 415-424.

[17] Ghavipour, M., Sotoudeh, G., Ghorbani, M., Tomato juice consumption improves blood antioxidative biomarkers in overweight and obese females. Clin Nutr 2014.

[18] Basu, A., Imrhan, V., Tomatoes versus lycopene in oxidative stress and carcinogenesis: conclusions from clinical trials. Eur J Clin Nutr 2007, 61, 295-303.

[19] Jacob, K., Periago, M. J., Bohm, V., Berruezo, G. R., Influence of lycopene and vitamin C from tomato juice on biomarkers of oxidative stress and inflammation. Br J Nutr 2008, 99, 137-146.

[20] Giovannucci, E., Tomatoes, tomato-based products, lycopene, and cancer: review of the epidemiologic literature. J Natl Cancer Inst 1999, 91, 317-331.

[21] Wang, Y., Ausman, L. M., Greenberg, A. S., Russell, R. M., Wang, X. D., Dietary lycopene and tomato extract supplementations inhibit nonalcoholic steatohepatitis-promoted hepatocarcinogenesis in rats. Int J Cancer 2010, 126, 1788-1796.

[22] Ip, B. C., Wang, X. D., Non-alcoholic steatohepatitis and hepatocellular carcinoma: implications for lycopene intervention. Nutrients 2013, 6, 124-162.

[23] Palozza, P., Simone, R. E., Catalano, A., Mele, M. C., Tomato lycopene and lung cancer prevention: from experimental to human studies. Cancers 2011, 3, 2333-2357.

[24] Hu, K. Q., Liu, C., Ernst, H., Krinsky, N. I., et al., The biochemical characterization of ferret carotene-9',10'-monooxygenase catalyzing cleavage of carotenoids in vitro and in vivo. The Journal of biological chemistry 2006, 281, 19327-19338.

[25] Ip, B. C., Hu, K. Q., Liu, C., Smith, D. E., et al., Lycopene metabolite, apo-10'-lycopenoic acid, inhibits diethylnitrosamine-initiated, high fat diet-promoted hepatic inflammation and tumorigenesis in mice. Cancer prevention research (Philadelphia, Pa.) 2013, 6, 1304-1316.

[26] Lian, F., Smith, D. E., Ernst, H., Russell, R. M., Wang, X. D., Apo-10'-lycopenoic acid inhibits lung cancer cell growth in vitro, and suppresses lung tumorigenesis in the A/J mouse model in vivo. Carcinogenesis 2007, 28, 1567-1574.

[27] Chung, J., Koo, K., Lian, F., Hu, K. Q., et al., Apo-10'-lycopenoic acid, a lycopene metabolite, increases sirtuin 1 mRNA and protein levels and decreases hepatic fat accumulation in ob/ob mice. The Journal of nutrition 2012, 142, 405-410.

[28] Smith, J. S., Brachmann, C. B., Celic, I., Kenna, M. A., et al., A phylogenetically conserved NAD+-dependent protein deacetylase activity in the Sir2 protein family. Proceedings of the National Academy of Sciences of the United States of America 2000, 97, 6658-6663.

[29] Imai, S., Armstrong, C. M., Kaeberlein, M., Guarente, L., Transcriptional silencing and longevity protein Sir2 is an NAD-dependent histone deacetylase. Nature 2000, 403, 795-800.

[30] Lan, F., Cacicedo, J. M., Ruderman, N., Ido, Y., SIRT1 modulation of the acetylation status, cytosolic localization, and activity of LKB1. Possible role in AMP-activated protein kinase activation. The Journal of biological chemistry 2008, 283, 27628-27635.

[31] Hou, X., Xu, S., Maitland-Toolan, K. A., Sato, K., et al., SIRT1 regulates hepatocyte lipid metabolism through activating AMP-activated protein kinase. The Journal of biological chemistry 2008, 283, 20015-20026.

[32] Gerhart-Hines, Z., Rodgers, J. T., Bare, O., Lerin, C., et al., Metabolic control of muscle mitochondrial function and fatty acid oxidation through SIRT1/PGC-1alpha. The EMBO journal 2007, 26, 1913-1923.

[33] Purushotham, A., Schug, T. T., Xu, Q., Surapureddi, S., et al., Hepatocyte-specific deletion of SIRT1 alters fatty acid metabolism and results in hepatic steatosis and inflammation. Cell Metab 2009, 9, 327-338.

[34] Bai, L., Pang, W. J., Yang, Y. J., Yang, G. S., Modulation of Sirt1 by resveratrol and nicotinamide alters proliferation and differentiation of pig preadipocytes. Molecular and cellular biochemistry 2008, 307, 129-140.

[35] Canto, C., Houtkooper, R. H., Pirinen, E., Youn, D. Y., et al., The NAD(+) precursor nicotinamide riboside enhances oxidative metabolism and protects against high-fat diet-induced obesity. Cell metabolism 2012, 15, 838-847.

[36] Landry, J., Sutton, A., Tafrov, S. T., Heller, R. C., et al., The silencing protein SIR2 and its homologs are NAD-dependent protein deacetylases. Proceedings of the National Academy of Sciences of the United States of America 2000, 97, 5807-5811.

[37] Cheng, J., Liu, C., Hu, K., Greenberg, A., et al., Ablation of systemic SIRT1 activity promotes nonalcoholic fatty liver disease by affecting liver-mesenteric adipose tissue fatty acid mobilization. Biochimica et biophysica acta 2017.

[38] Purushotham, A., Xu, Q., Li, X., Systemic SIRT1 insufficiency results in disruption of energy homeostasis and steroid hormone metabolism upon high-fat-diet feeding. FASEB journal: official publication of the Federation of American Societies for Experimental Biology 2012, 26, 656-667.

[39] Deng, X. Q., Chen, L. L., Li, N. X., The expression of SIRT1 in nonalcoholic fatty liver disease induced by high-fat diet in rats. Liver international: official journal of the International Association for the Study of the Liver 2007, 27, 708-715.

[40] Mariani, S., Fiore, D., Basciani, S., Persichetti, A., et al., Plasma levels of SIRT1 associate with non-alcoholic fatty liver disease in obese patients. Endocrine 2015, 49, 711-716.

CHAPTER II

LITERATURE REVIEW

HEPATOCELLULAR CARCINOMA (HCC)

HCC accounts for 85-90% of primary liver cancers [1, 2]. It is the fifth most common cancer among men, and the second most common cause of cancer mortality worldwide [3]. According to the 18th Annual Report to the Nation on the Status of Cancer, the incidence of HCC is still increasing, and HCC mortality is increasing at the highest rate, despite the decline in overall cancer death rates [4, 5]. HCC is an aggressive malignancy, with a 5-year relative survival rate of 16.6%, and an even lower survival rate in those diagnosed at a regional or distant stage (10.7% and 3.1%) [5, 6]. The risk of HCC development is influenced by a variety of environmental cues, including viral hepatitis infections, excessive alcohol consumption, smoking, and a rising epidemic concern, non-alcoholic fatty liver disease (NAFLD) [7].

NON-ALCOHOLIC FATTY LIVER DISEASE (NAFLD)

NAFLD) is defined by ≥ 5% of hepatic lipid accumulation, in the absence of significant alcohol consumption (140 g/week for women and 210 g/week for men for periods longer than two years), hereditary disease, or use of medications that induce steatosis such as amiodarone or tamoxifen [8, 9]. NAFLD describes a broad spectrum of liver disease that ranges from liver steatosis to non-alcoholic steatohepatitis (NASH), and ultimately, to fibrosis and cirrhosis [10-13]. NAFLD is the most common liver disease in developed countries, with a prevalence of 23%-30% in the general population [14] and 80%-90% in obese adults [15]; the incidence of NAFLD is still escalating at an alarming rate paralleled with the increasing obesity rates [16]. NASH is a more advanced stage of NAFLD, which can be distinguished by the presence of inflammation and hepatocyte ballooning [11]. Robust evidence from several cohort studies have suggested that NASH

is a great risk for the incidence of liver fibrosis and cirrhosis [17-22], which is the excessive extracellular matrix deposition in liver, causing the replacement of normal hepatocytes with type I collagen-rich scar tissue and leading to the occurrence of hepatic dysfunction [23, 24]. Approximately 90% of HCC cases develop based on a natural history of severe fibrosis [24], with the involvement of oxidative stress [25-28], growth factors such as transforming growth factor-b1 (TGF-β1) and connective tissue growth factor (CTGF) [28, 29], inflammation-related biomarkers such as NF-κB and c-Jun NH2-terminal kinase (JNK) [25, 28, 30-32], and Toll-Like Receptors (TLRs) [23, 25, 28].

NAFLD and HCC

NAFLD has been observed in 30% - 40% of HCC patients in the US [1], highlighting the critical role of metabolism disorder on hepatocellular carcinoma (HCC) development. HCC is an aggressive liver malignancy with poor prognosis, and nowadays, we still lack efficient treatment of HCC [33]. Since HCC is a heterogenous disease with other modifiable risk factors also contributing to its cancer burden [5], researchers have made great efforts to discover novel targets to not only block the progress of HCC, but also reduce the predisposing factors of HCC, such as obesity, hepatic inflammation, and NAFLD. One meta-analysis observed that caloric restriction contained anticancer efficacy by reviewing 44 studies [34], in which three studies reported the protective role of caloric restriction against liver cancer [35-37]. Therefore, potentially effective molecular targets that mimic caloric restriction against HCC warrant further investigation.

SIRTUIN 1 (SIRT1)

SIRT1 Function

The sirtuins are a family of evolutionarily conserved NAD+-dependent histone and non-histone protein deacetylases [38]. Of these, the most intensively studied is silent information regulator T1 (SIRT1). SIRT1 can deacetylate a vast spectrum of protein substrates and therefore regulate gene transcription and protein signaling. This renders SIRT1 a wide range of biological and pathophysiological functions including promoting fat metabolism [39-42], enhancing insulin sensitivity [39, 43], inhibiting oxidative stress [44-46], and reducing chronic inflammation [47-49]. SIRT1 functions through coupling with NAD+ hydrolysis, and transferring the acetyl group of the substrate to cleaved NAD (ADP-ribose), generating O-acetyl-ADP-ribose [50-52].

SIRT1 Regulatory Activity

It is well known that NAD^+ as a rate-limiting substrate for SIRT1 and is critical to the regulation of SIRT1 activity [50]. Nicotinamide phosphoribosyltransferase (NAMPT) is a rate-limiting NAD^+ biosynthetic enzyme that produces nicotinamide mononucleotide (NMN) from nicotinamide (NAM) and 5′-phosphoribosyl-1-pyrophosphate (PRPP). With the involvement of a second enzyme, nicotinamide/nicotinic acid mononucleotide adenylyltransferase (NMNAT), NMN is then converted into NAD+, which is consumed by SIRT1 [53]. Studies have reported that depleting NAD+ results in decreased SIRT1 activity [54, 55], and increasing DNA damage is associated with decreased levels of NAMPT level and NAD+ , followed by a reduced SIRT1 activity while causing no change in SIRT1 protein level [54]. This leads us to hypothesize that elevated DNA

damage and oxidative stress are closely related only to SIRT1's activity, rather than its protein level.

SIRT1 AND NAFLD

It has been shown that FoxOs can regulate hepatic Nampt transcription level, and overexpression of NAMPT reduces total triglyceride levels in liver [56]. These results are aligned with a clinical study in which reduced hepatic NAMPT was observed in NAFLD patients [57]. Both animal and human studies suggest an inverse correlation between circulating SIRT1 levels and NAFLD incidence [58, 59]. Several SIRT1 transgenic mouse models have been established to explore the molecular mechanism of SIRT1 signaling against hepatic steatosis development [39, 41, 60-63]. For example, global overexpression of SIRT1 using a knock-in Sirt1 genomic construct was shown to enhance energy expenditure and decrease high fat diet-induced hepatic steatosis [60]; the hepatocyte-specific deletion of SIRT1 caused hepatic steatosis [41, 62, 63], hepatic inflammation and endoplasmic reticulum stress [41], and the phenotype of heterozygous SIRT1 knockout mice fed a high-fat diet presented severe hepatic steatosis [64]. However, these mouse models either showed the effect of partial SIRT1 function, or focused on liver-specific SIRT1 function, owing to the limitation that whole body SIRT1 gene knockout in mice would cause metabolic defects [65], developmental abnormality, and postnatal lethality [66, 67]. These shortcomings have become the challenge to expanded investigation for the causal effect of systemic SIRT1 activity on NALFD development, which thus highlights the need to develop a novel engineered animal model that can mimic whole-body SIRT1 knockout, but presents less fatal defects.

SIRT1 AND CANCER

Controversy regarding cancer and sirtuins exists, mainly because sirtuins could act as either a tumor suppressor or tumor promoter depending on the cellular context or its targets in specific signaling pathways or specific cancers. SIRT1 was reported to be overexpressed in many types of cancer, including pancreas cancer [68], prostate cancer [69], and bladder cancer [70]. In these cancers, overexpression of SIRT1 impedes apoptosis, while silencing of SIRT1 by RNA interference sensitizes cancer cells to certain chemotherapeutic agents [68]. On the other hand, SIRT1 expression was reported to be reduced in colon cancer [71, 72], glioblastoma [73], and breast cancer [74] through different mechanisms. Overexpression of SIRT1 in $APC^{Min/+}$ mouse inhibits colon cancer formation by SIRT1-dependent deacetylation and inactivation of β-catenin [72]. SIRT1 was also reported to be a downstream target of Brca1 as SIRT1 overexpression inhibits the growth of Brca1 mutant cancer cells [75]. In addition, it has been reported impaired DNA damage response, genome instability, and tumorigenesis in multiple tissues in SIRT1 heterozygous knockout mice [76].

SIRT1 AND HCC

SIRT1 Expression in HCC Tissue

Whether SIRT1 inhibits or promotes HCC incidence is controversial. Compared to normal liver cell lines, a higher level of SIRT1 expression was observed in HCC cell lines including Hep3B [77-79], HepG2 [77-83], HuH7 [77, 78, 82, 83], HLE [79], HLF [79, 81], SKHep1 [77-79], HKCI-4 [77], HKCI-1 [77], SNU-449 [77], SNU-423 [77], PLC5 [77, 78], SMMC-7721 [78, 82], MHCC97H [78] and liver cancer stem cells [84]. By examining clinical HCC specimens, 20 studies reported an increase of SIRT1 protein

expression in HCC tumorous tissue compared to non-tumorous tissue [77-82, 84-97], and SIRT1 was predominantly localized in the nucleus [77, 78, 81, 91, 92, 97]. However, the mRNA levels between HCC tissue and paired normal liver tissue were comparable [77, 85, 86, 94], indicating that SIRT1 affects HCC in a post-transcriptional manner. The expression of SIRT1 was positively correlated with tumor grade [77, 78, 98], but the association between SIRT1 and overall survival remains controversial. Four studies showed that high SIRT1 expression predicted a lower overall survival rate [84, 86, 92, 97] while three studies did not observe significant association between SIRT1 expression and HCC prognosis [77, 86, 96]. The inconsistent results might be due to variant expression of AMPK-α2, p-MEK, c-Myc and miR-34α expression, which have been reported to influence HCC prognosis [87, 90, 97, 98]. One showed that on the contrary to nuclear SIRT1, cytoplasmic SIRT1 predicted favorable prognosis [92], suggesting that SIRT1 might exert a different function on hepatic carcinogenesis depending on subcellular location. Although SIRT1 aberrant expression in HCC tissue was widely reported in previous studies, these results are observational, leaving the causal relationship between SIRT1 and hepatic carcinogenesis enigmatic.

SIRT1 and Cell Proliferation

Dual effects of SIRT1 on cell proliferation have been documented in previous publications. It has been reported that SIRT1 can transcriptionally and post-translationally inhibit key cell cycles and apoptosis regulatory proteins such as p53 [77, 96, 99], BCL6 [100], Ku-70 [101] and Smad7 [102]. In contrast, SIRT1 also contains a suppressive activity in tumor cell growth by interacting and deacetylating E2F1, which indirectly decreases pRb hyper-phosphorylation and induces cyclinD/cdk4 activity [71].

Additionally, SIRT1 has been shown to directly deacetylate NF-κB, which is well-known for its anti-apoptotic function [102]. Despite the discrepancies existed for the role of SIRT1 in cell growth, consistent causal effects have been reported with regard to SIRT1 promoting HCC cell proliferation [77-79, 81-89, 91, 93-96, 98, 103, 104] via blocking PARP-1, caspase-3 and c-Myc [77, 79, 83, 85, 91, 94, 97]. Considering the disparate effects of SIRT1 on cell proliferation in different cell context, the following paragraphs will focus on the pathways involved in SIRT1 regulating cell growth, specifically in human liver cancer cells.

SIRT1 and p53 Signaling

As one of the most important tumor suppressors, p53 was the first non-histone target identified for SIRT1 [105], and was widely discussed when investigating the role of SIRT1 in carcinogenesis. By deacetylating p53 C-terminal lysines, SIRT1 transcriptionally down-regulates p53 [106]; while by removing the acetyl group from k382 of p53, SIRT1 post-translationally decreases p53 protein stability, promoter binding affinity, and protein-protein association [99]. Since activated p53 has been reported to induce DNA repair, programmed cell death (apoptosis), autophagy, and cell migration, SIRT1 was identified to promote HCC by inhibiting p53 acetylation and transactivation in studies utilizing various liver cancer cell lines [77, 96, 97]. However, despite the preponderance of evidence from cell studies showing that inhibition of SIRT1 leads to increasing p53 levels, the association between SIRT1 and p53 in human HCC specimens was controversial. Zhang et al. found SIRT1 was correlated with p53 mutation [96], while such association was not observed in a study by Choi et al [81]. Mutant p53 tissue expressed higher p53 level [81], but two studies concluded opposite association between

p53 and SIRT1 levels in HCC tissue [80, 92]. The pathways involved in SIRT1 and cancer cell apoptosis revealed to be disparate in p53 wild-type and p53 mutant cells. In SK-Hep1 and HepG2 (p53 wild-type) cells, SIRT1 knockdown resulted in G1 arrest by enhancing p53 acetylation and p21 induction [77, 96], well known as required transcription factors for CDK2 inactivation [107]. On the other hand, silencing SIRT1 in Hep3B, PLC5 (p53 mutant) cells enhanced PARP cleavage, leading to cell apoptosis [77], indicating that the role of SIRT1 in cell apoptosis induction might be p53 independent. Interestingly, lower risk of disease recurrence and longer relapse-free survival were shown in p53 mutant HCC patients [96]. The knockdown of SIRT1 in PLC5 and Hep3B resulted in decreased AMPK phosphorylation and increased p70s6K1, and consistently, animals injected with SIRT1 knockdown PLC5 cells ended up with larger tumors. However, opposite effects of knocking down SIRT1 were observed in HepG2 cells [96]. Since p53 mutation was frequently occurred in HCC patients [106], future studies are needed to investigate the differential regulation of cell cycle arrest and apoptosis by SIRT1 in p53 wild-type and p53 mutant patients.

SIRT1 and the Yes-Associated Protein (YAP) Signaling

The Yes-associated protein (YAP) is the mammalian ortholog of Drosophila Yorkie (Yki), a downstream effector of the Hippo signaling pathway responsible for cell growth control [108, 109]. Both YAP and its homolog TAZ act as transcriptional co-activators of TEAD [110] and regulate an array of target genes including connective tissue growth factor (CTGF), which is responsible for cell proliferation, migration and epithelial-mesenchymal transition [108, 111, 112]. Utilizing comparative oncogenomics and expression analyses, YAP was pinpointed as the most likely driver genes in liver

cancer [109]. Cells harboring YAP mutation presented less proliferative activity [109], while transgenic YAP overexpression in liver caused tissue enlargement and hepatic tumorigenesis [113]. As a target gene of YAP/TEAD, CTGF has been also found over-expressed in HCCs [112].

Both in vivo and in vitro studies showed that transcription level of YAP was downregulated with SIRT1 knockdown and up-regulated with SIRT1 knock-in [93]. SIRT1 overexpression enhanced binding of YAP to MKK3 promoter, which depended on YAP recruiting RNA polymerase II to MKK3 promoter region [93]. This contributed to the activation of MKK3/p38 pathways, which upregulated FLNA and induced cell proliferation [93, 114]. As one of the isoforms of YAP family, YAP2 contains more transactivation activity than YAP1 [115]. Immunostaining HCC hepatic tissue revealed higher expression of YAP2 compared to normal self-paired tissue, and the expression of SIRT1 was positively associated with YAP2 expression [92]. SIRT1 can post-translationally deacetylate YAP2 and increase the interaction of YAP2 with TEAD4, subsequently decreasing YAP2-mediated CTGF and p21 transcription [91]. Therefore, SIRT1 not only regulates YAP2 expression, but also YAP2 transcriptional activity. Interestingly, mutating lysine to arginine on YAP2 on 4KR in C-terminus presented similar acetylation as wild-type YAP2, but SIRT1 overexpression did not increase the transcriptional activity of 4KR YAP2 [91], providing evidence that other HDACs might be involved in deacetylating YAP2. Consistent with this note, knockdown of YAP2 decreased colony formation with or without SIRT1 presence, accompanied with increased PARP-1 cleavage [91], indicating that YAP2 might act as a specific target for HCC treatment independent on SIRT1.

SIRT1 and β-catenin

Abnormal regulation of the transcription factor β-catenin is one of the most frequently reported events in the development of HCC [86, 116, 117]. As a key intracellular effector in the canonical Wnt signaling pathway, the level of β-catenin is low in hepatocytes under normal states via being degraded by a destruction complex comprised of APC, Axin, and GSK-3 [117-119]. However, when the canonical Wnt/ β-catenin pathway is activated, the destruction complex will be degraded, leading to accumulation of β-catenin in cytoplasm [118, 119]. Surplus of β-catenin leads to its translocation to the cell nucleus, where it binds to the transcription factors Tcf/Lef and acts as a coactivator to stimulate the transcription of many genes involved in cell proliferation, such as c-Myc, c-Jun and Cyclin D1 [117].

SIRT1 removes the acetylation of β-catenin at K345 [99], which promotes its accumulation at nucleus in mesenchymal stem cells [120], but limited evidence has been reported in terms of the effect of SIRT1 on β-catenin activation in HCC cells, and SIRT1 expression was more frequently seen in HCC without β-catenin mutation. Our results of negative association of SIRT1 expression and β-catenin mutation support these observations, indicating SIRT1 is more likely to drive tumor progression in the tumors not dependent on the Wnt/β-catenin pathway. Capurro et al. [36] have shown that GPC3 promotes the growth of HCC by stimulating canonical Wnt signaling in vivo and in vitro. Our study also found that Sirt1 up-regulation could increase the expression of GPC3. In the present study, we showed that Sirt1 up-regulation increased accumulation and nuclear translocation of the transcription factor β-catenin. SIRT1 is a direct target of miR-133b. This is consistent with one study in which mice receiving injection of SIRT1-

overexpression cells had comparable tumor development as wild-type mice [120]. These results indicated that the regulatory effects of SIRT1 on β-catenin may not affect HCC development.

SIRT1 in HCC Cell Senescence

Cellular senescence in p53 wild-type cells was associated with enhanced p53 acetylation on K382 and induction of p21, which were known for their role in senescence induction. SIRT1 plays a role in telomeric maintenance via regulating the expression of telomerase and members of the shelterin complex Mitogen-activated protein kinase (MAPK) cascades that are key signaling pathways responsible for the regulation of normal cell proliferation, survival and differentiation [121]. (MAP) kinase/extracellular signal-regulated kinase (ERK) kinase (MEK) is a dual threonine and tyrosine recognition kinase that phosphorylates and activates MAPK. Dysregulation of MAPK/ERK has been implicated in various cancers [122]. MKK3 preferentially activates p38a [123]. MEK1 is up-regulated in the genesis of a number of tumors, and is regarded as an oncogene which accelerates cancer formation, progression, and therapy resistance [124, 125]. MEK1-YAP interaction is critical for HCC proliferation and tumorigenesis [126]. The p38/MAPK signaling pathway controls both cell survival and cell apoptosis in the initiation and development of various cancers [127]. To date, four p38 MAPKs that might have overlapping functions have been identified: MAPK14 (p38α), MAPK11 (p38β), MAPK12 (p38γ), and MAPK13 (p38δ). While p38α is abundantly expressed in most tissues, the others seem to be expressed in a more tissue-specific manner. However, like SIRT1, activation of p38 can either suppress or stimulate tumorigenesis. On the one hand, it can stimulate premature senescence and p53-dependent growth arrest [128, 129]; on the

other hand, inactivation of p38 was reported to induce mitochondria-mediated apoptosis in HCC cells [130, 131]. Further studies on the role of SIRT1 in HCC cell senescence are warranted.

TOMATO CONSUMPTION

Tomatoes are good sources of the colorless carotenoids phytoene, phytofluene, and other micronutrients such as vitamin C, E and flavonoids, which are all considered as good anti-oxidant agents [132]. Tomato consumption has been demonstrated to be beneficial in populations of young and old alike. Specifically, one prospective cohort study has reported that the risk of cancer mortality significantly decreased by 50% in the highest tomato intake group, as compared to that in the lowest tomato intake group [133]. A more recent study showed that among Sudanese children, those who consumed 2~3 tomatoes developed 48%~83% less total mortality rates, compared to those who did not consume tomatoes at all. In addition, tomato intake significantly reduced the incidence of diarrheal and respiratory infections, as well as the risks of diarrhea- and fever-related deaths [134].

Tomato Consumption and HCC

Previous studies established additional evidence showing that the consumption of tomato and tomato products can protect against inflammation [135, 136], oxidative stress [137, 138] and various cancers including lung, stomach, colorectal, and prostate cancer [139]. Our two previous studies have revealed that tomato extract, which contains only fat-soluble nutrients of tomatoes, has beneficial effect in terms of anti-hepatic inflammation [140] and anti-hepatic lesion [132]. Unlike tomato extract, the constituting nutrients in fresh tomatoes are largely retained in the tomato powder, thus best mimic the

natural consumption of tomatoes, which renders our study to have public-health relevance. Considering the well-rounded beneficial nutrients contained in tomatoes and the protective effects against hepatic diseases of tomato extract, we expect tomato supplementation in our study to carry out a role in reducing DEN-initiated, HFD-promoted hepatic steatosis and HCC development.

APO-10'-LYCOPENOIC ACID (ALA)

Apo-10'-lycopenoic acid (ALA) is a compound found in tomato products. It is also a metabolite from lycopene (a red carotenoid pigment in tomatoes) being cleaved by enzyme 9',10'-monooxygenase (BCO2) [141, 142]. Accumulating evidence has suggested that ALA exhibits important biologic properties including anti-inflammation [143-145], reducing adipogenesis [146, 147] and inhibiting lung tumor development [148]. In addition, ALA has protective effects against HCC development. In a previous study we have shown that after diethylnitrosamine (DEN) injection and high fat diet (HFD) intervention, mice with ALA supplementation developed HCC with less multiplicity and volume, despite with the same tumor incidence [145]. However, the underlying mechanism of how ALA protects against hepatic steatosis and HCC development remains unclear.

ALA, Cell Migration and Angiogenesis

Peroxisome proliferator-activated receptor γ (PPARγ) is involved in regulation of angiogenesis, tumor progression and metastasis. We recently reported that ALA treatment in liver and lung cancer cells (HuH7 and A549) resulted in inhibited cell migration and cell invasion by utilizing transwell and wound healing models. Importantly, ALA can dose-dependently increase the mRNA and protein levels of

PPARγ, as well as the transactivity of PPARγ, a possible underlying mechanism by which ALA protects against tumor progression. The manuscript is attached as **Appendix I**.

ALA, HCC and SIRT1

Previous studies reported that resveratrol could promote SIRT1 activity, which was associated with ameliorated cancer progression [149]. Increased consumption of polyphenol-enriched fruits and vegetables is also associated with increased neuro-protective, anti-inflammatory, and anti-cancer function by targeting the SIRT1 gene [149]. These studies showed a promising opportunity of suppressing cancer development by utilizing dietary intervention means. Interestingly, two studies in our lab consistently revealed an improvement of SIRT1 deacetylation activity by feeding mice with APO10LA, coupling with the reduction of hepatic fat accumulation and hepatotumorigenesis [145, 146]. However, these two studies only identified a positive association between APO10LA supplementation and SIRT1 activity, but not causal-relationship, while whether SIRT1 is the direct target of APO10LA remains unknown.

LITERATURE CITED

[1] El-Serag, H. B., Rudolph, K. L., Hepatocellular carcinoma: epidemiology and molecular carcinogenesis. *Gastroenterology* 2007, *132*, 2557-2576.

[2] Parkin, D. M., Global cancer statistics in the year 2000. *The Lancet. Oncology* 2001, *2*, 533-543.

[3] Ferlay, J., Soerjomataram, I., Dikshit, R., Eser, S., *et al.*, Cancer incidence and mortality worldwide: sources, methods and major patterns in GLOBOCAN 2012. *International journal of cancer* 2015, *136*, E359-386.

[4] Siegel, R. L., Miller, K. D., Jemal, A., Cancer Statistics, 2017. *CA: a cancer journal for clinicians* 2017, *67*, 7-30.

[5] Ryerson, A. B., Eheman, C. R., Altekruse, S. F., Ward, J. W., *et al.*, Annual Report to the Nation on the Status of Cancer, 1975-2012, featuring the increasing incidence of liver cancer. *Cancer* 2016, *122*, 1312-1337.

[6] Howlader, N., Noone, A., Krapcho, M., Miller, D., *et al.*, Bethesda, MD 2017.

[7] Makarova-Rusher, O. V., Altekruse, S. F., McNeel, T. S., Ulahannan, S., *et al.*, Population attributable fractions of risk factors for hepatocellular carcinoma in the United States. *Cancer* 2016, *122*, 1757-1765.

[8] Younossi, Z. M., Koenig, A. B., Abdelatif, D., Fazel, Y., *et al.*, Global epidemiology of nonalcoholic fatty liver disease-Meta-analytic assessment of prevalence, incidence, and outcomes. *Hepatology (Baltimore, Md.)* 2016, *64*, 73-84.

[9] Chalasani, N., Younossi, Z., Lavine, J. E., Diehl, A. M., *et al.*, The diagnosis and management of non-alcoholic fatty liver disease: practice guideline by the American Gastroenterological Association, American Association for the Study of Liver Diseases, and American College of Gastroenterology. *Gastroenterology* 2012, *142*, 1592-1609.

[10] Silverman, J. F., Pories, W. J., Caro, J. F., Liver pathology in diabetes mellitus and morbid obesity. Clinical, pathological, and biochemical considerations. *Pathology annual* 1989, *24 Pt 1*, 275-302.

[11] Powell, E. E., Cooksley, W. G., Hanson, R., Searle, J., *et al.*, The natural history of nonalcoholic steatohepatitis: a follow-up study of forty-two patients for up to 21 years. *Hepatology (Baltimore, Md.)* 1990, *11*, 74-80.

[12] Matteoni, C. A., Younossi, Z. M., Gramlich, T., Boparai, N., *et al.*, Nonalcoholic fatty liver disease: a spectrum of clinical and pathological severity. *Gastroenterology* 1999, *116*, 1413-1419.

[13] Marchesini, G., Bugianesi, E., Forlani, G., Cerrelli, F., *et al.*, Nonalcoholic fatty liver, steatohepatitis, and the metabolic syndrome. *Hepatology (Baltimore, Md.)* 2003, *37*, 917-923.

[14] Clark, J. M., Brancati, F. L., Diehl, A. M., Nonalcoholic fatty liver disease. *Gastroenterology* 2002, *122*, 1649-1657.

[15] Bellentani, S., Scaglioni, F., Marino, M., Bedogni, G., Epidemiology of non-alcoholic fatty liver disease. *Digestive diseases (Basel, Switzerland)* 2010, *28*, 155-161.

[16] Loomba, R., Sanyal, A. J., The global NAFLD epidemic. *Nature reviews. Gastroenterology & hepatology* 2013, *10*, 686-690.

[17] Chan, W. K., Ida, N. H., Cheah, P. L., Goh, K. L., Progression of liver disease in non-alcoholic fatty liver disease: a prospective clinicopathological follow-up study. *Journal of digestive diseases* 2014, *15*, 545-552.

[18] McPherson, S., Hardy, T., Henderson, E., Burt, A. D., *et al.*, Evidence of NAFLD progression from steatosis to fibrosing-steatohepatitis using paired biopsies: implications for prognosis and clinical management. *Journal of hepatology* 2015, *62*, 1148-1155.

[19] Angulo, P., Keach, J. C., Batts, K. P., Lindor, K. D., Independent predictors of liver fibrosis in patients with nonalcoholic steatohepatitis. *Hepatology (Baltimore, Md.)* 1999, *30*, 1356-1362.

[20] Hossain, N., Afendy, A., Stepanova, M., Nader, F., *et al.*, Independent predictors of fibrosis in patients with nonalcoholic fatty liver disease. *Clinical gastroenterology and hepatology : the official clinical practice journal of the American Gastroenterological Association* 2009, *7*, 1224-1229, 1229.e1221-1222.

[21] Bacon, B. R., Farahvash, M. J., Janney, C. G., Neuschwander-Tetri, B. A., Nonalcoholic steatohepatitis: an expanded clinical entity. *Gastroenterology* 1994, *107*, 1103-1109.

[22] Evans, C. D., Oien, K. A., MacSween, R. N., Mills, P. R., Non-alcoholic steatohepatitis: a common cause of progressive chronic liver injury? *Journal of clinical pathology* 2002, *55*, 689-692.

[23] Novo, E., Cannito, S., Paternostro, C., Bocca, C., *et al.*, Cellular and molecular mechanisms in liver fibrogenesis. *Archives of biochemistry and biophysics* 2014, *548*, 20-37.

[24] De Minicis, S., Marzioni, M., Saccomanno, S., Rychlicki, C., *et al.*, Cellular and molecular mechanisms of hepatic fibrogenesis leading to liver cancer. *Transl Gastrointest Cancer* 2011, *1*, 88-94.

[25] Brenner, D. A., Seki, E., Taura, K., Kisseleva, T., *et al.*, Non-alcoholic steatohepatitis-induced fibrosis: Toll-like receptors, reactive oxygen species and Jun N-terminal kinase. *Hepatology research : the official journal of the Japan Society of Hepatology* 2011, *41*, 683-686.

[26] Tanaka, S., Mogushi, K., Yasen, M., Ban, D., *et al.*, Oxidative stress pathways in noncancerous human liver tissue to predict hepatocellular carcinoma recurrence: a prospective, multicenter study. *Hepatology (Baltimore, Md.)* 2011, *54*, 1273-1281.

[27] De Minicis, S., Seki, E., Paik, Y. H., Osterreicher, C. H., *et al.*, Role and cellular source of nicotinamide adenine dinucleotide phosphate oxidase in hepatic fibrosis. *Hepatology (Baltimore, Md.)* 2010, *52*, 1420-1430.

[28] Brenner, D. A., Molecular pathogenesis of liver fibrosis. *Transactions of the American Clinical and Climatological Association* 2009, *120*, 361-368.

[29] Meurer, S. K., Esser, M., Tihaa, L., Weiskirchen, R., BMP-7/TGF-beta1 signalling in myoblasts: components involved in signalling and BMP-7-dependent blockage of TGF-beta-mediated CTGF expression. *European journal of cell biology* 2012, *91*, 450-463.

[30] Kodama, Y., Kisseleva, T., Iwaisako, K., Miura, K., *et al.*, c-Jun N-terminal kinase-1 from hematopoietic cells mediates progression from hepatic steatosis to steatohepatitis and fibrosis in mice. *Gastroenterology* 2009, *137*, 1467-1477.e1465.

[31] Calvisi, D. F., Pascale, R. M., Feo, F., Dissection of signal transduction pathways as a tool for the development of targeted therapies of hepatocellular carcinoma. *Reviews on recent clinical trials* 2007, *2*, 217-236.

[32] Thevananther, S., Sun, H., Li, D., Arjunan, V., *et al.*, Extracellular ATP activates c-jun N-terminal kinase signaling and cell cycle progression in hepatocytes. *Hepatology (Baltimore, Md.)* 2004, *39*, 393-402.

[33] Zhou, Y., Li, Y., Zhou, T., Zheng, J., *et al.*, Dietary Natural Products for Prevention and Treatment of Liver Cancer. *Nutrients* 2016, *8*, 156.

[34] Lv, M., Zhu, X., Wang, H., Wang, F., Guan, W., Roles of caloric restriction, ketogenic diet and intermittent fasting during initiation, progression and metastasis of cancer in animal models: a systematic review and meta-analysis. *PloS one* 2014, *9*, e115147.

[35] Von Tungeln, L. S., Bucci, T. J., Hart, R. W., Kadlubar, F. F., Fu, P. P., Inhibitory effect of caloric restriction on tumorigenicity induced by 4-aminobiphenyl and 2-amino-1-methyl-6-phenylimidazo-[4,5-b]pyridine (PhIP) in the CD1 newborn mouse bioassay. *Cancer letters* 1996, *104*, 133-136.

[36] James, S. J., Muskhelishvili, L., Rates of apoptosis and proliferation vary with caloric intake and may influence incidence of spontaneous hepatoma in C57BL/6 x C3H F1 mice. *Cancer research* 1994, *54*, 5508-5510.

[37] van Ginhoven, T. M., van den Berg, J. W., Dik, W. A., Ijzermans, J. N., de Bruin, R. W., Preoperative dietary restriction reduces hepatic tumor load by reduced E-selectin-mediated adhesion in mice. *Journal of surgical oncology* 2010, *102*, 348-353.

[38] Houtkooper, R. H., Pirinen, E., Auwerx, J., Sirtuins as regulators of metabolism and healthspan. *Nat Rev Mol Cell Biol* 2012, *13*, 225-238.

[39] Caron, A. Z., He, X., Mottawea, W., Seifert, E. L., *et al.*, The SIRT1 deacetylase protects mice against the symptoms of metabolic syndrome. *FASEB journal : official publication of the Federation of American Societies for Experimental Biology* 2014, *28*, 1306-1316.

[40] Li, Y., Wong, K., Giles, A., Jiang, J., *et al.*, Hepatic SIRT1 attenuates hepatic steatosis and controls energy balance in mice by inducing fibroblast growth factor 21. *Gastroenterology* 2014, *146*, 539-549 e537.

[41] Purushotham, A., Schug, T. T., Xu, Q., Surapureddi, S., *et al.*, Hepatocyte-specific deletion of SIRT1 alters fatty acid metabolism and results in hepatic steatosis and inflammation. *Cell metabolism* 2009, *9*, 327-338.

[42] Rodgers, J. T., Puigserver, P., Fasting-dependent glucose and lipid metabolic response through hepatic sirtuin 1. *Proceedings of the National Academy of Sciences of the United States of America* 2007, *104*, 12861-12866.

[43] Bordone, L., Motta, M. C., Picard, F., Robinson, A., *et al.*, Sirt1 regulates insulin secretion by repressing UCP2 in pancreatic beta cells. *PLoS Biol* 2006, *4*, e31.

[44] Alcendor, R. R., Gao, S., Zhai, P., Zablocki, D., *et al.*, Sirt1 regulates aging and resistance to oxidative stress in the heart. *Circulation research* 2007, *100*, 1512-1521.

[45] Hsu, C. P., Odewale, I., Alcendor, R. R., Sadoshima, J., Sirt1 protects the heart from aging and stress. *Biol Chem* 2008, *389*, 221-231.

[46] Wang, Y. Q., Cao, Q., Wang, F., Huang, L. Y., *et al.*, SIRT1 Protects Against Oxidative Stress-Induced Endothelial Progenitor Cells Apoptosis by Inhibiting FOXO3a via FOXO3a Ubiquitination and Degradation. *J Cell Physiol* 2015, *230*, 2098-2107.

[47] Nascimento, A. F., Ip, B. C., Luvizotto, R. A., Seitz, H. K., Wang, X. D., Aggravation of nonalcoholic steatohepatitis by moderate alcohol consumption is associated with decreased SIRT1 activity in rats. *Hepatobiliary surgery and nutrition* 2013, *2*, 252-259.

[48] Rafacho, B. P., Stice, C. P., Liu, C., Greenberg, A. S., *et al.*, Inhibition of diethylnitrosamine-initiated alcohol-promoted hepatic inflammation and precancerous lesions by flavonoid luteolin is associated with increased sirtuin 1 activity in mice. *Hepatobiliary surgery and nutrition* 2015, *4*, 124-134.

[49] Schug, T. T., Xu, Q., Gao, H., Peres-da-Silva, A., *et al.*, Myeloid deletion of SIRT1 induces inflammatory signaling in response to environmental stress. *Molecular and cellular biology* 2010, *30*, 4712-4721.

[50] Canto, C., Houtkooper, R. H., Pirinen, E., Youn, D. Y., *et al.*, The NAD(+) precursor nicotinamide riboside enhances oxidative metabolism and protects against high-fat diet-induced obesity. *Cell metabolism* 2012, *15*, 838-847.

[51] Imai, S., Armstrong, C. M., Kaeberlein, M., Guarente, L., Transcriptional silencing and longevity protein Sir2 is an NAD-dependent histone deacetylase. *Nature* 2000, *403*, 795-800.

[52] Landry, J., Sutton, A., Tafrov, S. T., Heller, R. C., *et al.*, The silencing protein SIR2 and its homologs are NAD-dependent protein deacetylases. *Proceedings of the National Academy of Sciences of the United States of America* 2000, *97*, 5807-5811.

[53] Imai, S., Yoshino, J., The importance of NAMPT/NAD/SIRT1 in the systemic regulation of metabolism and ageing. *Diabetes, obesity & metabolism* 2013, *15 Suppl 3*, 26-33.

[54] Braidy, N., Guillemin, G. J., Mansour, H., Chan-Ling, T., *et al.*, Age related changes in NAD+ metabolism oxidative stress and Sirt1 activity in wistar rats. *PloS one* 2011, *6*, e19194.

[55] Revollo, J. R., Li, X., The ways and means that fine tune Sirt1 activity. *Trends in biochemical sciences* 2013, *38*, 160-167.

[56] Tao, R., Wei, D., Gao, H., Liu, Y., *et al.*, Hepatic FoxOs regulate lipid metabolism via modulation of expression of the nicotinamide phosphoribosyltransferase gene. *The Journal of biological chemistry* 2011, *286*, 14681-14690.

[57] Dahl, T. B., Haukeland, J. W., Yndestad, A., Ranheim, T., *et al.*, Intracellular nicotinamide phosphoribosyltransferase protects against hepatocyte apoptosis and is

down-regulated in nonalcoholic fatty liver disease. *The Journal of clinical endocrinology and metabolism* 2010, *95*, 3039-3047.

[58] Deng, X. Q., Chen, L. L., Li, N. X., The expression of SIRT1 in nonalcoholic fatty liver disease induced by high-fat diet in rats. *Liver international : official journal of the International Association for the Study of the Liver* 2007, *27*, 708-715.

[59] Mariani, S., Fiore, D., Basciani, S., Persichetti, A., *et al.*, Plasma levels of SIRT1 associate with non-alcoholic fatty liver disease in obese patients. *Endocrine* 2015, *49*, 711-716.

[60] Pfluger, P. T., Herranz, D., Velasco-Miguel, S., Serrano, M., Tschop, M. H., Sirt1 protects against high-fat diet-induced metabolic damage. *Proceedings of the National Academy of Sciences of the United States of America* 2008, *105*, 9793-9798.

[61] Xu, F., Gao, Z., Zhang, J., Rivera, C. A., *et al.*, Lack of SIRT1 (Mammalian Sirtuin 1) activity leads to liver steatosis in the SIRT1+/- mice: a role of lipid mobilization and inflammation. *Endocrinology* 2010, *151*, 2504-2514.

[62] Wang, R. H., Li, C., Deng, C. X., Liver steatosis and increased ChREBP expression in mice carrying a liver specific SIRT1 null mutation under a normal feeding condition. *International journal of biological sciences* 2010, *6*, 682-690.

[63] Ding, J., Li, M., Wan, X., Jin, X., *et al.*, Effect of miR-34a in regulating steatosis by targeting PPARalpha expression in nonalcoholic fatty liver disease. *Scientific reports* 2015, *5*, 13729.

[64] Hou, X., Xu, S., Maitland-Toolan, K. A., Sato, K., *et al.*, SIRT1 regulates hepatocyte lipid metabolism through activating AMP-activated protein kinase. *The Journal of biological chemistry* 2008, *283*, 20015-20026.

[65] Boily, G., Seifert, E. L., Bevilacqua, L., He, X. H., *et al.*, SirT1 regulates energy metabolism and response to caloric restriction in mice. *PloS one* 2008, *3*, e1759.

[66] Cheng, H. L., Mostoslavsky, R., Saito, S., Manis, J. P., *et al.*, Developmental defects and p53 hyperacetylation in Sir2 homolog (SIRT1)-deficient mice. *Proceedings of the National Academy of Sciences of the United States of America* 2003, *100*, 10794-10799.

[67] McBurney, M. W., Yang, X., Jardine, K., Hixon, M., *et al.*, The mammalian SIR2alpha protein has a role in embryogenesis and gametogenesis. *Molecular and cellular biology* 2003, *23*, 38-54.

[68] Zhao, G., Cui, J., Zhang, J. G., Qin, Q., *et al.*, SIRT1 RNAi knockdown induces apoptosis and senescence, inhibits invasion and enhances chemosensitivity in pancreatic cancer cells. *Gene therapy* 2011, *18*, 920-928.

[69] Jung-Hynes, B., Nihal, M., Zhong, W., Ahmad, N., Role of sirtuin histone deacetylase SIRT1 in prostate cancer. A target for prostate cancer management via its inhibition? *The Journal of biological chemistry* 2009, *284*, 3823-3832.

[70] Hu, Q., Wang, G., Peng, J., Qian, G., Jiang, W., Xie, C., Xiao, Y., Wang, X., Knockdown of *SIRT1* suppresses bladder cancer cell proliferation and migration and induces cell cycle arrest and antioxidant response through FOXO3a-mediated pathways. *BioMed Research International* 2017, *2017*.

[71] Kabra, N., Li, Z., Chen, L., Li, B., *et al.*, SirT1 is an inhibitor of proliferation and tumor formation in colon cancer. *The Journal of biological chemistry* 2009, *284*, 18210-18217.

[72] Firestein, R., Blander, G., Michan, S., Oberdoerffer, P., *et al.*, The SIRT1 deacetylase suppresses intestinal tumorigenesis and colon cancer growth. *PloS one* 2008, *3*, e2020.

[73] Qu, Y., Zhang, J., Wu, S., Li, B., *et al.*, SIRT1 promotes proliferation and inhibits apoptosis of human malignant glioma cell lines. *Neuroscience letters* 2012, *525*, 168-172.

[74] Santolla, M. F., Avino, S., Pellegrino, M., De Francesco, E. M., *et al.*, SIRT1 is involved in oncogenic signaling mediated by GPER in breast cancer. *Cell death & disease* 2015, *6*, e1834.

[75] Wang, R. H., Zheng, Y., Kim, H. S., Xu, X., *et al.*, Interplay among BRCA1, SIRT1, and Survivin during BRCA1-associated tumorigenesis. *Molecular cell* 2008, *32*, 11-20.

[76] Wang, R. H., Sengupta, K., Li, C., Kim, H. S., *et al.*, Impaired DNA damage response, genome instability, and tumorigenesis in SIRT1 mutant mice. *Cancer cell* 2008, *14*, 312-323.

[77] Chen, J., Zhang, B., Wong, N., Lo, A. W., *et al.*, Sirtuin 1 is upregulated in a subset of hepatocellular carcinomas where it is essential for telomere maintenance and tumor cell growth. *Cancer research* 2011, *71*, 4138-4149.

[78] Li, Y., Xu, S., Li, J., Zheng, L., *et al.*, SIRT1 facilitates hepatocellular carcinoma metastasis by promoting PGC-1alpha-mediated mitochondrial biogenesis. *Oncotarget* 2016, *7*, 29255-29274.

[79] Portmann, S., Fahrner, R., Lechleiter, A., Keogh, A., *et al.*, Antitumor effect of SIRT1 inhibition in human HCC tumor models in vitro and in vivo. *Molecular cancer therapeutics* 2013, *12*, 499-508.

[80] Al-Bahrani, R., Tuertcher, D., Zailaie, S., Abuetabh, Y., *et al.*, Differential SIRT1 expression in hepatocellular carcinomas and cholangiocarcinoma of the liver. *Annals of clinical and laboratory science* 2015, *45*, 3-9.

[81] Choi, H. N., Bae, J. S., Jamiyandorj, U., Noh, S. J., *et al.*, Expression and role of SIRT1 in hepatocellular carcinoma. *Oncology reports* 2011, *26*, 503-510.

[82] Hao, C., Zhu, P. X., Yang, X., Han, Z. P., *et al.*, Overexpression of SIRT1 promotes metastasis through epithelial-mesenchymal transition in hepatocellular carcinoma. *BMC cancer* 2014, *14*, 978.

[83] Wang, H., Liu, H., Chen, K., Xiao, J., *et al.*, SIRT1 promotes tumorigenesis of hepatocellular carcinoma through PI3K/PTEN/AKT signaling. *Oncology reports* 2012, *28*, 311-318.

[84] Liu, L., Liu, C., Zhang, Q., Shen, J., *et al.*, SIRT1-mediated transcriptional regulation of SOX2 is important for self-renewal of liver cancer stem cells. *Hepatology (Baltimore, Md.)* 2016, *64*, 814-827.

[85] Bae, H. J., Noh, J. H., Kim, J. K., Eun, J. W., *et al.*, MicroRNA-29c functions as a tumor suppressor by direct targeting oncogenic SIRT1 in hepatocellular carcinoma. *Oncogene* 2014, *33*, 2557-2567.

[86] Chen, H. C., Jeng, Y. M., Yuan, R. H., Hsu, H. C., Chen, Y. L., SIRT1 promotes tumorigenesis and resistance to chemotherapy in hepatocellular carcinoma and its expression predicts poor prognosis. *Annals of surgical oncology* 2012, *19*, 2011-2019.

[87] Cheng, J., Liu, C., Liu, L., Chen, X., *et al.*, MEK1 signaling promotes self-renewal and tumorigenicity of liver cancer stem cells via maintaining SIRT1 protein stabilization. *Oncotarget* 2016, *7*, 20597-20611.

[88] Gang, D., Hongwei, H., Hedai, L., Ming, Z., *et al.*, The tumor suppressor protein menin inhibits NF-kappaB-mediated transactivation through recruitment of Sirt1 in hepatocellular carcinoma. *Molecular biology reports* 2013, *40*, 2461-2466.

[89] Garcia-Rodriguez, J. L., Barbier-Torres, L., Fernandez-Alvarez, S., Gutierrez-de Juan, V., *et al.*, SIRT1 controls liver regeneration by regulating bile acid metabolism through farnesoid X receptor and mammalian target of rapamycin signaling. *Hepatology (Baltimore, Md.)* 2014, *59*, 1972-1983.

[90] Jiang, G., Wen, L., Zheng, H., Jian, Z., Deng, W., miR-204-5p targeting SIRT1 regulates hepatocellular carcinoma progression. *Cell biochemistry and function* 2016, *34*, 505-510.

[91] Mao, B., Hu, F., Cheng, J., Wang, P., *et al.*, SIRT1 regulates YAP2-mediated cell proliferation and chemoresistance in hepatocellular carcinoma. *Oncogene* 2014, *33*, 1468-1474.

[92] Song, S., Luo, M., Song, Y., Liu, T., *et al.*, Prognostic role of SIRT1 in hepatocellular carcinoma. *Journal of the College of Physicians and Surgeons--Pakistan : JCPSP* 2014, *24*, 849-854.

[93] Wang, Y., Cui, R., Zhang, X., Qiao, Y., *et al.*, SIRT1 increases YAP- and MKK3-dependent p38 phosphorylation in mouse liver and human hepatocellular carcinoma. *Oncotarget* 2016, *7*, 11284-11298.

[94] Xiong, H., Ni, Z., He, J., Jiang, S., *et al.*, LncRNA HULC triggers autophagy via stabilizing Sirt1 and attenuates the chemosensitivity of HCC cells. *Oncogene* 2017.

[95] Zhang, H., Feng, Z., Huang, R., Xia, Z., *et al.*, MicroRNA-449 suppresses proliferation of hepatoma cell lines through blockade lipid metabolic pathway related to SIRT1. *International journal of oncology* 2014, *45*, 2143-2152.

[96] Zhang, Z. Y., Hong, D., Nam, S. H., Kim, J. M., *et al.*, SIRT1 regulates oncogenesis via a mutant p53-dependent pathway in hepatocellular carcinoma. *Journal of hepatology* 2015, *62*, 121-130.

[97] Jang, K. Y., Noh, S. J., Lehwald, N., Tao, G. Z., *et al.*, SIRT1 and c-Myc promote liver tumor cell survival and predict poor survival of human hepatocellular carcinomas. *PloS one* 2012, *7*, e45119.

[98] Lou, W., Chen, Q., Ma, L., Liu, J., *et al.*, Oncolytic adenovirus co-expressing miRNA-34a and IL-24 induces superior antitumor activity in experimental tumor model. *Journal of molecular medicine (Berlin, Germany)* 2013, *91*, 715-725.

[99] Lin, Z., Fang, D., The Roles of SIRT1 in Cancer. *Genes & cancer* 2013, *4*, 97-104.

[100] Heltweg, B., Gatbonton, T., Schuler, A. D., Posakony, J., *et al.*, Antitumor activity of a small-molecule inhibitor of human silent information regulator 2 enzymes. *Cancer research* 2006, *66*, 4368-4377.

[101] Cohen, H. Y., Lavu, S., Bitterman, K. J., Hekking, B., *et al.*, Acetylation of the C terminus of Ku70 by CBP and PCAF controls Bax-mediated apoptosis. *Molecular cell* 2004, *13*, 627-638.

[102] Liu, T., Liu, P. Y., Marshall, G. M., The critical role of the class III histone deacetylase SIRT1 in cancer. *Cancer research* 2009, *69*, 1702-1705.

[103] Tian, Z., Jiang, H., Liu, Y., Huang, Y., *et al.*, MicroRNA-133b inhibits hepatocellular carcinoma cell progression by targeting Sirt1. *Experimental cell research* 2016, *343*, 135-147.

[104] Wu, Y., Meng, X., Huang, C., Li, J., Emerging role of silent information regulator 1 (SIRT1) in hepatocellular carcinoma: a potential therapeutic target. *Tumour biology : the journal of the International Society for Oncodevelopmental Biology and Medicine* 2015, *36*, 4063-4074.

[105] Yi, J., Luo, J., SIRT1 and p53, effect on cancer, senescence and beyond. *Biochimica et biophysica acta* 2010, *1804*, 1684-1689.

[106] Lee, J. T., Gu, W., SIRT1: Regulator of p53 Deacetylation. *Genes & cancer* 2013, *4*, 112-117.

[107] Wierod, L., Rosseland, C. M., Lindeman, B., Oksvold, M. P., *et al.*, Activation of the p53-p21(Cip1) pathway is required for CDK2 activation and S-phase entry in primary rat hepatocytes. *Oncogene* 2008, *27*, 2763-2771.

[108] Xu, M. Z., Yao, T. J., Lee, N. P., Ng, I. O., *et al.*, Yes-associated protein is an independent prognostic marker in hepatocellular carcinoma. *Cancer* 2009, *115*, 4576-4585.

[109] Zender, L., Spector, M. S., Xue, W., Flemming, P., *et al.*, Identification and validation of oncogenes in liver cancer using an integrative oncogenomic approach. *Cell* 2006, *125*, 1253-1267.

[110] Yagi, R., Chen, L. F., Shigesada, K., Murakami, Y., Ito, Y., A WW domain-containing yes-associated protein (YAP) is a novel transcriptional co-activator. *The EMBO journal* 1999, *18*, 2551-2562.

[111] Zhang, H., Liu, C. Y., Zha, Z. Y., Zhao, B., *et al.*, TEAD transcription factors mediate the function of TAZ in cell growth and epithelial-mesenchymal transition. *The Journal of biological chemistry* 2009, *284*, 13355-13362.

[112] Urtasun, R., Latasa, M. U., Demartis, M. I., Balzani, S., *et al.*, Connective tissue growth factor autocriny in human hepatocellular carcinoma: oncogenic role and regulation by epidermal growth factor receptor/yes-associated protein-mediated activation. *Hepatology (Baltimore, Md.)* 2011, *54*, 2149-2158.

[113] Dong, J., Feldmann, G., Huang, J., Wu, S., *et al.*, Elucidation of a universal size-control mechanism in Drosophila and mammals. *Cell* 2007, *130*, 1120-1133.

[114] D'Addario, M., Arora, P. D., McCulloch, C. A., Role of p38 in stress activation of Sp1. *Gene* 2006, *379*, 51-61.

[115] Komuro, A., Nagai, M., Navin, N. E., Sudol, M., WW domain-containing protein YAP associates with ErbB-4 and acts as a co-transcriptional activator for the carboxyl-terminal fragment of ErbB-4 that translocates to the nucleus. *The Journal of biological chemistry* 2003, *278*, 33334-33341.

[116] Whittaker, S., Marais, R., Zhu, A. X., The role of signaling pathways in the development and treatment of hepatocellular carcinoma. *Oncogene* 2010, *29*, 4989-5005.

[117] Waisberg, J., Saba, G. T., Wnt-/-beta-catenin pathway signaling in human hepatocellular carcinoma. *World journal of hepatology* 2015, *7*, 2631-2635.

[118] Wands, J. R., Kim, M., WNT/beta-catenin signaling and hepatocellular carcinoma. *Hepatology (Baltimore, Md.)* 2014, *60*, 452-454.

[119] MacDonald, B. T., Tamai, K., He, X., Wnt/beta-catenin signaling: components, mechanisms, and diseases. *Developmental cell* 2009, *17*, 9-26.

[120] Simic, P., Zainabadi, K., Bell, E., Sykes, D. B., *et al.*, SIRT1 regulates differentiation of mesenchymal stem cells by deacetylating beta-catenin. *EMBO molecular medicine* 2013, *5*, 430-440.

[121] Roberts, P. J., Der, C. J., Targeting the Raf-MEK-ERK mitogen-activated protein kinase cascade for the treatment of cancer. *Oncogene* 2007, *26*, 3291-3310.

[122] Dhillon, A. S., Hagan, S., Rath, O., Kolch, W., MAP kinase signalling pathways in cancer. *Oncogene* 2007, *26*, 3279-3290.

[123] Page, K., Li, J., Hershenson, M. B., p38 MAP kinase negatively regulates cyclin D1 expression in airway smooth muscle cells. *American journal of physiology. Lung cellular and molecular physiology* 2001, *280*, L955-964.

[124] Caunt, C. J., Sale, M. J., Smith, P. D., Cook, S. J., MEK1 and MEK2 inhibitors and cancer therapy: the long and winding road. *Nature reviews. Cancer* 2015, *15*, 577-592.

[125] Facciorusso, A., Licinio, R., Carr, B. I., Di Leo, A., Barone, M., MEK 1/2 inhibitors in the treatment of hepatocellular carcinoma. *Expert review of gastroenterology & hepatology* 2015, *9*, 993-1003.

[126] Li, L., Wang, J., Zhang, Y., Zhang, Y., *et al.*, MEK1 promotes YAP and their interaction is critical for tumorigenesis in liver cancer. *FEBS letters* 2013, *587*, 3921-3927.

[127] Koul, H. K., Pal, M., Koul, S., Role of p38 MAP Kinase Signal Transduction in Solid Tumors. *Genes & cancer* 2013, *4*, 342-359.

[128] Dziegielewska, B., Brautigan, D. L., Larner, J. M., Dziegielewski, J., T-type Ca2+ channel inhibition induces p53-dependent cell growth arrest and apoptosis through activation of p38-MAPK in colon cancer cells. *Molecular cancer research : MCR* 2014, *12*, 348-358.

[129] Deng, Q., Liao, R., Wu, B. L., Sun, P., High intensity ras signaling induces premature senescence by activating p38 pathway in primary human fibroblasts. *The Journal of biological chemistry* 2004, *279*, 1050-1059.

[130] Jian, K. L., Zhang, C., Shang, Z. C., Yang, L., Kong, L. Y., Eucalrobusone C suppresses cell proliferation and induces ROS-dependent mitochondrial apoptosis via the p38 MAPK pathway in hepatocellular carcinoma cells. *Phytomedicine : international journal of phytotherapy and phytopharmacology* 2017, *25*, 71-82.

[131] Hsieh, S. C., Huang, M. H., Cheng, C. W., Hung, J. H., *et al.*, alpha-Mangostin induces mitochondrial dependent apoptosis in human hepatoma SK-Hep-1 cells through inhibition of p38 MAPK pathway. *Apoptosis : an international journal on programmed cell death* 2013, *18*, 1548-1560.

[132] Melendez-Martinez, A. J., Nascimento, A. F., Wang, Y., Liu, C., *et al.*, Effect of tomato extract supplementation against high-fat diet-induced hepatic lesions. *Hepatobiliary surgery and nutrition* 2013, *2*, 198-208.

[133] Colditz, G. A., Branch, L. G., Lipnick, R. J., Willett, W. C., *et al.*, Increased green and yellow vegetable intake and lowered cancer deaths in an elderly population. *The American journal of clinical nutrition* 1985, *41*, 32-36.

[134] Fawzi, W., Herrera, M. G., Nestel, P., Tomato intake in relation to mortality and morbidity among Sudanese children. *The Journal of nutrition* 2000, *130*, 2537-2542.

[135] Garcia-Alonso, F. J., Jorge-Vidal, V., Ros, G., Periago, M. J., Effect of consumption of tomato juice enriched with n-3 polyunsaturated fatty acids on the lipid profile, antioxidant biomarker status, and cardiovascular disease risk in healthy women. *European journal of nutrition* 2012, *51*, 415-424.

[136] Ghavipour, M., Sotoudeh, G., Ghorbani, M., Tomato juice consumption improves blood antioxidative biomarkers in overweight and obese females. *Clin Nutr* 2014.

[137] Basu, A., Imrhan, V., Tomatoes versus lycopene in oxidative stress and carcinogenesis: conclusions from clinical trials. *European journal of clinical nutrition* 2007, *61*, 295-303.

[138] Jacob, K., Periago, M. J., Bohm, V., Berruezo, G. R., Influence of lycopene and vitamin C from tomato juice on biomarkers of oxidative stress and inflammation. *The British journal of nutrition* 2008, *99*, 137-146.

[139] Giovannucci, E., Tomatoes, tomato-based products, lycopene, and cancer: review of the epidemiologic literature. *J Natl Cancer Inst* 1999, *91*, 317-331.

[140] Wang, Y., Ausman, L. M., Greenberg, A. S., Russell, R. M., Wang, X. D., Dietary lycopene and tomato extract supplementations inhibit nonalcoholic steatohepatitis-promoted hepatocarcinogenesis in rats. *International journal of cancer* 2010, *126*, 1788-1796.

[141] Hu, K. Q., Liu, C., Ernst, H., Krinsky, N. I., *et al.*, The biochemical characterization of ferret carotene-9',10'-monooxygenase catalyzing cleavage of carotenoids in vitro and in vivo. *The Journal of biological chemistry* 2006, *281*, 19327-19338.

[142] Kiefer, C., Hessel, S., Lampert, J. M., Vogt, K., *et al.*, Identification and characterization of a mammalian enzyme catalyzing the asymmetric oxidative cleavage of provitamin A. *The Journal of biological chemistry* 2001, *276*, 14110-14116.

[143] Catalano, A., Simone, R. E., Cittadini, A., Reynaud, E., *et al.*, Comparative antioxidant effects of lycopene, apo-10'-lycopenoic acid and apo-14'-lycopenoic acid in human macrophages exposed to H2O2 and cigarette smoke extract. *Food Chem Toxicol* 2013, *51*, 71-79.

[144] Gouranton, E., Aydemir, G., Reynaud, E., Marcotorchino, J., *et al.*, Apo-10'-lycopenoic acid impacts adipose tissue biology via the retinoic acid receptors. *Biochimica et biophysica acta* 2011, *1811*, 1105-1114.

[145] Ip, B. C., Hu, K. Q., Liu, C., Smith, D. E., *et al.*, Lycopene metabolite, apo-10'-lycopenoic acid, inhibits diethylnitrosamine-initiated, high fat diet-promoted hepatic inflammation and tumorigenesis in mice. *Cancer prevention research (Philadelphia, Pa.)* 2013, *6*, 1304-1316.

[146] Chung, J., Koo, K., Lian, F., Hu, K. Q., *et al.*, Apo-10'-lycopenoic acid, a lycopene metabolite, increases sirtuin 1 mRNA and protein levels and decreases hepatic fat accumulation in ob/ob mice. *The Journal of nutrition* 2012, *142*, 405-410.

[147] Ip, B. C., Liu, C., Lichtenstein, A. H., von Lintig, J., Wang, X. D., Lycopene and apo-10'-lycopenoic acid have differential mechanisms of protection against hepatic steatosis in beta-carotene-9',10'-oxygenase knockout male mice. *The Journal of nutrition* 2015, *145*, 268-276.

[148] Lan, F., Cacicedo, J. M., Ruderman, N., Ido, Y., SIRT1 modulation of the acetylation status, cytosolic localization, and activity of LKB1. Possible role in AMP-activated protein kinase activation. *The Journal of biological chemistry* 2008, *283*, 27628-27635.

[149] Allard, J. S., Perez, E., Zou, S., de Cabo, R., Dietary activators of Sirt1. *Mol Cell Endocrinol* 2009, *299*, 58-63.

CHAPTER III

THE CAUSAL ROLE OF SIRT1 IN NON-ALCOHOLIC FATTY LIVER DISEASE

ABSTRACT

Background: The incidence of nonalcoholic fatty liver disease (NAFLD) is escalating paralleled with obesity rates in both adults and children. Mammalian sirtuin 1 (SIRT1), a highly conserved NAD^+-dependent protein deacetylase, has been identified as a metabolic regulator of lipid homeostasis and a potential target for NAFLD prevention and treatment. However, the mechanism of how SIRT1, in particularly its deacetylase activity, affects NAFLD has not been well investigated.

Method: The current investigation addressed the causal effect of systemic SIRT1 activity on NAFLD development and the potential mechanism involved in both liver and mesenteric adipose tissue. At 6 weeks of age, both SIRT1 homozygous mice carrying a point mutation (H355Y, MT, n=10) that ablates the catalytic activity and their corresponding wild type littermates (WT, n=10) were fed a high fat diet (HFD, 60% calories from fat) for 34 weeks.

Results: No changes in body weight, liver weight, and body composition (analyzed by EchoMRI-700) were observed between WT and MT mice, but MT mice showed significantly higher levels of hepatic triglyceride, and a trend toward more severe hepatic steatosis by pathological analysis. Such alteration was accompanied with higher protein levels of LXRα, SREBP-1, SCD1, involved in lipogenesis, and decreased phosphorylation of LKB1 and AMPK in the liver. In the mesenteric adipose tissue, mRNA expression of lipogenic genes (*lxrα*, *srebp-1c*, *scd1* and *fas*) increased significantly in the MT mice, as compared with those of wild-type mice. Fatty acid oxidation biomarkers (*acox1*, *acox3*, *cpt*, *ucp1*, *sirt3*) in both liver and mesenteric adipose tissue were comparable between groups. Interestingly, we observed that in MT mice, the

mRNA level of hormone sensitive lipase (*hsl*), adipose triglyceride lipase (*atgl*) and *perilipin-1*, involved in lipolysis, significantly increased in mesenteric adipose tissue (not in epididymal adipose tissue), as compared with those of WT. These changes were correlated with higher concentrations of circulating free fatty acids (FFA) and higher hepatic mRNA expression of *cd36* for FFA uptake.

Conclusion: The present study provided novel experimental evidence that under HFD-induced metabolic surplus, the lack of SIRT1 catalytic activity promoted release of FFA from mesenteric fat into systemic circulation and escalated NAFLD by interfering with lipid homeostasis in both liver and mesenteric adipose tissue.

INTRODUCTION

Obesity has become a leading epidemic concern worldwide, and the escalating incidence of nonalcoholic fatty liver disease (NAFLD) parallels the increasing obesity rates [1]. NAFLD is observed in 65%-85% of obese patients, with a higher prevalence in men compared to women [2]. NAFLD describes a range of related disorders that begin with hepatic steatosis, which can proceed to nonalcoholic steatohepatitis [3], leading to higher risk of hepatocellular carcinoma [4]. Considering the increasing prevalence of NAFLD and the devastating outcome of NAFLD progression, it is of critical importance to have a mechanistic understanding for NAFLD development in order to develop preventive and therapeutic strategies for NAFLD.

SIRT1 is an evolutionarily conserved NAD^+-dependent histone and non-histone protein deacetylase [5, 6]. As a metabolic regulator, SIRT1 has been identified to control a series of physiological activities, including reducing fatty acid synthesis [7, 8], increasing β-oxidation [9, 10], and decreasing adipocyte generation [11]. These functions of SIRT1 are exerted through coupling with NAD^+ hydrolysis, transferring the acetyl group of the substrate to cleaved NAD^+ (ADP-ribose), and generating O-acetyl-ADP-ribose [6, 12, 13]. The catalytic activity of SIRT1 is tightly regulated by the cellular NAD^+ levels [12, 14, 15] and multiple nutritional, hormonal, and environmental cues that can alter the cellular NAD^+ availability [15]. This explains the observation that SIRT1 protein level and SIRT1 activity are not always parallel [16]; therefore, it is important to determine the effect of SIRT1 activity, rather than SIRT1 protein alone.

Both animal and human studies suggest an inverse correlation between SIRT1 levels and NAFLD incidence [17, 18]. Several SIRT1 transgenic mouse models have

been established to explore the molecular mechanism of SIRT1 signaling against hepatic steatosis development [10, 19-23]. Global overexpression of SIRT1 using a knock-in Sirt1 genomic construct resulted in enhancing energy expenditure and decreasing high fat diet-induced hepatic steatosis [19]. Hepatocyte-specific deletion of SIRT1 caused hepatic steatosis [10, 22, 23], hepatic inflammation and endoplasmic reticulum stress [10]. The phenotype of heterozygous SIRT1 knockout mice presented severe hepatic steatosis on high-fat diets [8]. However, these mouse models either showed the effect of partial SIRT1 function, or focused on liver-specific SIRT1 function, owing to the fact that whole body SIRT1 gene knockout in mice would cause metabolic defect [24], developmental abnormality, and postnatal lethality [25, 26]. This produces challenges of investigating the causal effect of systemic SIRT1 activity on NALFD development. Recently, an engineered systemic SIRT1 deacetylase activity ablation mouse model achieved similar SIRT1 loss-of-function effects with SIRT1 knockout mice, but with less resultant genetic defects [27]. Using this mouse model, Caron et al. observed an increasing hepatic lipid accumulation in SIRT1 activity ablated mice [21]. This study raised an important question and also opened the door to the further investigation as to how the lack of SIRT1 activity promotes NAFLD.

As an effort along this line, in this study we used the systemic SIRT1 activity ablation (MT) and wild-type mice (WT) in the current study to investigate the underlying mechanism by which SIRT1 activity ablation exerted on high fat diet (HFD)-induced NAFLD.

MATERIALS AND METHODS

Animals and Diet

All study protocols including breeding were approved by the Institutional Animal Care and Use Committee of Tufts University. We utilized the homozygous H355Y SIRT1 mutant (MT), 129/SvJ background mouse expressing the SIRT1 protein that lacks its catalytic activity, as compared with that of a wild-type H355Y, sirt1$^{+/+}$ 129/SvJ mouse. Both MT, 129/SvJ background mice and sirt1$^{+/+}$ 129/SvJ mice exhibit hepatic steatosis similar to humans, and 129/SvJ mice are the animal model of choice in studies of high fat diet (HFD)-induced hepatic steatosis. At 4 weeks of age, SIRT1 genotypes of animals were determined by a PCR-based test performed on DNA isolated from tail-tip biopsies using the primers 5'-TGGAAGGAAAGCAATTTTGGT-3' and g'CTGAGTTACCTTAGCTTGGC-3'. Mice were fed the standard laboratory chow diet (Envigo, Huntingdon, UK) for two weeks. At 6 weeks of age, mice were fed HFD (60% calories from fat, Bioserv, Frenchland, NJ) twice a week for 34 weeks, and body weight of each mouse was recorded weekly. The macronutrient component within the diet was listed in **Appendix I**. At 38 weeks of age, EchoMRI-100 (EchoMRI, Houston, TX) was used for mice body composition measurements, as described previously [28]. Briefly, after weights were recorded for each mouse, non-anesthetized mice were placed into a cylinder and inserted into the chamber unit of the MRI machine. Total fat mass was determined and fat composition was obtained by calculating the ratio of fat mass to body weight. All mice were killed at 40 weeks of age. Serum, livers, mesenteric adipose tissue (MAT), and epididymal adipose tissue were collected. Livers were weighed, and a piece of liver tissue from left lobe of liver was fixed in 10% buffered formalin solution for

histopathological examination while the remaining liver tissues were snap frozen in liquid nitrogen and stored at -80°C for further study.

Liver Histopathology Evaluation

Five-micrometer sections of formalin-fixed and paraffin-embedded liver tissue were stained with hematoxylin and eosin (H&E) for histopathological examination. The sections were examined under light microscopy by 2 independent investigators who were blinded to the treatment groups. A ZEISS microscope with a PixeLINK USB 2.0 (PL-B623CU) digital Camera and PixeLINK µScope Microscopy Software was used for the examination. Liver steatosis was graded according to steatosis magnitude (both macro- and micro-vesicular fat accumulation) as described previously [29] (Figure 1A). Briefly, the degree of steatosis was graded based on the percentage of the liver section that was occupied by fat vacuoles at 100× magnification in 20 fields (grade 0 = <5%; grade 1 = 5–25%; grade 2 = 26–50%; grade 3 = 51–75%; grade 4 = >75%).

Liver and Plasma Triglyceride (TG) Quantification

Plasma and hepatic TG were measured using a TG colorimetric assay kit (Cayman, USA). Plasma was obtained from EDTA tubes and centrifuged at 1,000 g for 10 minutes, followed by pipetting off the top plasma layer. Liver tissue (about 40 mg) was minced and weighed, followed by homogenization in the standard diluent (0.2 ml) with an ultrasonic tissue homogenizer. The digested tissue was centrifuged for 10 minutes at 10,000 g, and the entire supernatant was transferred and diluted 1:5 with the standard diluent. The TG contents in both plasma and liver were determined based on the absorbance at 540 nm after a coupled enzymatic reaction, and was adjusted with a standard glycerol solution.

Liver Cholesterol Quantification

A commercial cholesterol kit (Cell Biolabs Inc, San Diego, CA) was utilized for total cholesterol measurement. Briefly, 50 mg liver tissue was extracted with 1000 µL mixture of chloroflorm : isopropanol : NP-40 (7:11:0.1) in a micro-homogenizer. The pellet was kept after centrifuging the mixture for 10 minutes at 15,000 rcf. Removing the trace amounts of organic solvent, dried lipids was dissolved in 200 µL Assay Diluent with sonicating and vortexing. The cholesterol concentration was calculated according to the absorption at 540 nm wavelength.

Protein Isolation and Western Blotting

Whole cell protein was extracted from frozen liver tissue as previously described [30]. For nuclear protein extraction, 50-60 mg liver protein was minced and mixed with 2ml hypertonic buffer, followed by homogenization for 30 seconds. The whole volume was then centrifuged at 5500 rpm for 5 minutes, and a second centrifugation (13000 rpm, 5 minutes) was executed after washing pellets with 1ml hypertonic buffer. Pellets were then re-suspended in 100µl high salt buffer (5M NaCl) and shake-incubated on a Vortex Genie Turbo Mixer in 4°C cold room for 10 minutes. The supernatant was transferred and centrifuged at 55000 rpm for 60 minutes using an Ultracentrifuge. The protein concentration was measured by the Comassie Plus protein quantification method (Thermo Fisher Scientific) and adjusted to 10µg/µl. For Western blotting, 5µl whole cell lysates per sample were mixed with 6 µl 2X reducing Laemmli sample buffer and boiled in 100°C water bath for 5 minutes to denature. Denatured protein was then loaded on SDS-polyacrylamide gels and resolved according to their molecular weights. For protein detection, electroblotting was executed by transferring protein onto Immobilon-P

membranes (Millipore, MA, USA), followed by non-specific blocking (5% non-fat milk) in TBST buffer and incubation with appropriate primary antibodies. The following antibodies were used for Western blotting: phosphorylated-AMPK (Thr172), phosphorylated-ACC (Ser79), phosphorylated-LKB1 (Ser428), AMPK, ACC, LKB1, SCD1 (Cell Signaling, MA, USA), LXRα (Abcam, Cambridge, UK), Ac-FoxO1, FoxO1, and SREBP-1 (Santa Cruz, TX, USA). An anti-rabbit secondary antibody (Bio-Rad, CA, USA) linked to a horseradish peroxidase reporter enzyme was applied to binding the above primary antibody, and the bands of interest were detected by a SuperSignal West Pico Chemiluminescent Substrate kit (Sigma-Aldrich) according to the manufacturer's instructions. Protein level of β-actin was used as reference for normalization. Intensities of protein bands were detected using GS-710 Calibrated Imaging Densitometer (Bio-Rad).

RNA Extraction and Quantitative Polymerase Chain Reaction (qPCR)

Total RNA was extracted from frozen liver tissue with TriPure Isolation Reagent kit (Roche, USA). Briefly, 50-100 mg frozen liver was minced, mixed with 1 ml TriPure Isolation Reagent, and centrifuged for 10 minutes at 12,000 g. Then 0.2 ml chloroform was added to each sample and the whole volume was centrifuged for 15 minutes at 12,000 g. The collected upper aqueous phase was mixed with 0.5 ml isopropanol and centrifuged for 10 minutes at 12,000 g. The RNA pellet was obtained after discarding the supernatant, washed using 75% ethanol, followed by resuspending in DEPC water and incubating for 10 minutes at 55 4°C. Complementary DNA (cDNA) was synthesized with a reverse transcription PCR kit (M-MLV, Invitrogen, CA) and the Bio-Rad PTC 200 (GMI, CA). Quantitative real-time PCR was performed using FastStart Universal SYBR

Green Master (Roche, USA). Relative gene expression was determined using the $-2^{\Delta\Delta Ct}$ method and normalized to the level of β-actin. Primer sequences are listed in **Appendix II**.

Statistical Analysis

SAS 9.3 software was utilized to perform the statistical analysis. The Mann-Whitney U test was used to compare liver steatosis score distribution. The Student *t* test was used to compare TG, FFA levels and gene and protein expressions between wild-type mice and MT mice. Logistic regression was utilized to analyze the correlation between steatosis score and hepatic TG level. Statistical significance was set as $P < 0.05$.

RESULTS

SIRT1 Mutation Increased Liver Triglyceride Level

To test whether SIRT1 deacetylase activity was reduced in our mouse model, we measured the acetylation of FoxO1, and observed significantly higher acetylated-FoxO1 to total-FoxO1 ratio in Sirt1 mutant (MT) mice, compared to wild-type (WT) mice (**Figure 1B**), indicating that the deacetylase activity of SIRT1 in MT mice was decreased. Average food consumption was similar between the two groups of mice (**Table 1**). There was no significant difference in final body weight, liver weight or liver weight/g body weight, and total fat mass between wild-type and mutant mice (**Table 1**). Hepatic cholesterol concentration was comparable between the two groups (wild-type vs. MT: 52.35 ± 5.38 vs. 53.28 ± 2.19 mg/g tissue).

To examine liver steatosis, we measured hepatic TG level using a TG quantification kit. We found that hepatic TG level was significantly higher in mutant

mice, compared to their wild-type counterparts (**Figure 1C**). The results from liver histopathological examination showed that among wild-type mice, 20% developed hepatic steatosis with a score of 1, 40% with a score of 2, and 30 with a score of 3; in contrast, all mutant mice developed hepatic steatosis with score at 2 or higher (55.6% with score 2, 44.4% with score 3; **Figure 1D**). Although overall liver steatosis was not significantly different between two groups, MT mice showed a trend toward higher liver steatosis severity as compared to wild-type mice. In addition, the hepatic TG level was significantly correlated with steatosis score ($P = 0.04$).

SIRT1 Mutation Increased Hepatic Lipid Synthesis

To address the molecular mechanism of increasing liver steatosis severity in MT mice, we quantified mRNA expressions and protein levels of the genes involved in lipogenesis and fatty acid β-oxidation. Result showed that phosphorylation of acetyl-CoA carboxylase (p-ACC), the inactive form of ACC, was significantly lower in MT mice (**Figure 2A**). This was correlated with lower phosphorylation of AMP-kinase (p-AMPK; **Figure 2B**). LKB1 phosphorylated at Ser^{428}, the upstream signaling of p-AMPK [8, 31], was also reduced in MT animals (**Figure 2C**). LXRα mRNA, but not protein level, was higher in MT mice (**Figure 2F**). The protein level of sterol regulatory element-binding protein 1 (SREBP-1) and the mRNA level of its isoform, *srebp-1c*, were found elevated in MT mice (**Figure 2D, F**). The mRNA and protein level of SCD1, one of the downstream targets of SREBP-1c [32], were promoted in MT mice (**Figure 2E, F**). Hepatic nuclear PGC1α/whole-cell PGC1α ratio and hepatic PPARα protein levels were not changed (data not shown). Other lipogenic gene mRNA (*fas*, *dgat1*, *dgat2*, *fatp2*, *pparα*) were not altered between groups (**Figure 2F**). The mRNA levels of five β-

oxidation related genes (*acox1*, *acox3*, *cpt*, *ucp1*, *ucp2*, *sirt3*) were measured in the liver, but no changes were observed between wild-type and MT mice (**Figure 2G**). These data suggest that increasing *de novo* lipogenesis, rather than decreasing β-oxidation, is a major mechanism leading to elevated liver steatosis in SIRT1 activity ablated mice.

SIRT1 Mutation Increased Lipid Synthesis in MAT

MAT can release free fatty acids (FFA) to venous drainage, which subsequently enters liver via portal vein and exposes liver to lipid accumulation [33-35]. Since the SIRT1 activity ablation in this model is systemic, we propose that lacking SIRT1 activity may affect lipid metabolism in MAT. To test this hypothesis, we examined lipogenesis and fatty acid β-oxidation related genes in MAT. We first examined the mRNA level of lipogenic genes (*scd1*, *srebp-1c*, *fas*, *dgat1*, *dgat2*, *pparγ*). Interestingly, *srebp-1c* showed a trend of increase (P = 0.07) in SIRT1 mutant mice, but its downstream targets, *scd1* and *fas* were significantly higher in MT mice (**Figure 3A**). Liver X receptor α (LXRα) is known to activate the cleavage and movement of mature SREBP-1c to the nucleus [36]. We examined *lxr-α* expression and found *lxrα* transcription significantly elevated in MT mice (**Figure 3A**). This indicates that the lack of SIRT1 activity may promote LXRα-mediated SREBP-1c maturation. We then determined the effect of SIRT1 activity ablation on fatty acid oxidation biomarkers (*acox1*, *acox3*, *cpt*, *ucp1*, *ucp2*). Results showed no difference in transcription levels of these genes between groups (**Figure 3B**). No alterations of gene expression were found in epididymal adipose tissue between two groups (data not shown). These results suggested an overall increasing lipogenesis level in MAT of MT mice. We also measured adiponectin mRNA level in both MAT and epididymal adipose tissue, as well as hepatic adiponectin receptor 1 and adiponectin

receptor 2 protein levels in WT and MT mice, but did not find significant differences between two groups (data not shown). In addition, the downstream target of adiponectin, hepatic PPARα, did not change in both mRNA levels (**Figure 2F**) and protein levels (data not shown), indicating that the difference of hepatic lipogenesis between wild-type and MT mice was not due to adiponectin activity in this mouse model.

SIRT1 Mutation Caused hepatic steatosis via MAT-liver FFA mobilization

Since hepatic steatosis could be the result of elevating fatty acid uptake by 1) up-taking triglyceride in chylomicron or VLDL remnant that derived from dietary sources, and 2) up-taking FFA released from adipose tissue, we tested the possibility that SIRT1 mutation affects liver TG uptake. We examined plasma TG level and hepatic LDL-receptor (*ldl-r*) transcription level and found no difference in these parameters between two groups (**Figure 4A**), suggesting that liver TG uptake was similar between WT and MT mice.

We then examined plasma FFA and found the level of plasma FFA was significantly higher in MT mice (**Figure 4B**), as compared with that of WT mice. Since FFA from MAT directly enters liver through the portal vein [2, 33-35], lipolysis of MAT greatly contributes to FFA transferred to liver. We further hypothesized that the increase of FFA in mutant mice was attributed to the increasing MAT lipolysis. Of four genes related to mesenteric lipolysis (*hsl*, *atgl*, *plin-1*, *plin-2*), *hsl*, *atgl* and *plin-2* significantly increased in MT mice (**Figure 4C**). CD36 is a transporter that takes up long chain fatty acids [36]. In the current study, we found that *cd36* transcription level in liver was significantly higher in MT mice (**Figure 4D**). The mRNA level of *lxrα*, as a transcription factor that up-regulates CD36 transcription, was also elevated in MT mice. To test

whether wild-type and MT mice have different hepatic TG clearance rates, we examined the mRNA of microsomal triglyceride transfer protein (*mttp*), a transporter that exports TG, but observed no difference in its expression between groups (**Figure 4D**). These data suggest that increased FFA release from MAT may enter systemic circulation, and subsequently the liver, leading to augmented liver steatosis in sirt1 mutant mice.

DISCUSSION

To our knowledge, the present study has provided the first evidence that systemic SIRT1 activity loss promoted NAFLD by targeting both liver and MAT, as well as their cross-talk. We demonstrated that the accumulating hepatic TG due to the lack of SIRT1 activity was associated with 1) increased hepatic fatty acid synthesis but unchanged β-oxidation in liver; 2) increased lipid synthesis in MAT; and 3) elevated free fatty acid transport from MAT to liver.

In the current study, the acetylated version of FoxO1 significantly increased in MT mice, supporting the observation that SIRT1 enzymatic activity in liver decreased due to a systemic SIRT1 activity ablation in this mouse model. After HFD (60% calories from fat) intervention for 34 weeks, we found that MT mice accumulated significantly higher TG level in liver. This suggests that the lack of systemic SIRT1 deacetylase activity can promote NAFLD development. Our findings were consistent with the previous studies showing that impaired SIRT1 signaling was associated with increased hepatic lipid deposition [8, 10, 19-21, 23]. It should be noted that our histopathologic analysis tended to present more severe hepatic steatosis in MT mice ($P = 0.16$). The discrepancy between our histopathologic grading and hepatic TGs was possibly due to the fact that the changes of hepatic TGs were more sensitive to detect compared to

histologic observation. Nevertheless, our steatosis grading score was significantly correlated with the hepatic TGs, which supports that systemic SIRT1 activity ablation can escalate NAFLD development. In the current study, we observed comparable hepatic total cholesterol levels, which agree with the similar mRNA expression levels of *abca1* and *cyp7a1* between WT and MT mice. ABCA1 is a key transporter that exports cholesterol from liver, and Cyp7A1 is the gene that encodes cholesterol 7α-hydroxylase, the enzyme that catalyzes the initial step in bile acid synthesis. Our data suggest that the comparable hepatic cholesterol levels in wild-type and mutant mice may be due to unchanged reverse cholesterol transport and cholesterol catabolism, or alternatively, a high fat diet-induced metabolic surplus. Taken together, we conclude that the lack of SIRT1 enzymatic activity plays a minor role on cholesterol metabolism in this model. One of the important observations in the present study was that the lack of SIRT1 deacetylase activity increased lipogenesis while maintaining fatty acid oxidation unchanged in both liver and MAT. In MT mice, increased hepatic lipogenesis was associated with reduced phosphorylations of LKB1, AMPK and ACC. LKB1 can be activated through phosphorylation at Ser^{428}, which enhances its kinase activity of phosphorylating AMPK [7, 8, 31], resulting in enhanced inhibition of ACC by phosphorylating the enzyme to the inactive form [37]. Hepatic ACC activation promotes FA synthesis and lipid accumulation [37]. Unexpectedly, we observed higher levels of LXRα mRNA in MT mice, which is not in agreement with the previous report that SIRT1 contributes to deacetylating and activating LXRα transcription *in vitro* [21]. However, these authors found that *lxrα* mRNA expression was similar in SIRT1 knock-out mice and their wild-type, suggesting that SIRT1 might regulate *lxrα* in multiple mechanistic

pathways *in vivo* [38]. One possible pathway is that SIRT1 activity ablation decreases the release of nicotinamide phosphoribosyltransferase (NAMPT), a rate limiting enzyme that catalyzes the biosynthesis of nicotinamide adenine dinucleotide (NAD) [39]. Decreased release of NAMPT from hepatocytes can attenuate the inhibition of *lxrα* transcription in MT mice [39]. It is important to note that the mRNA level of *lxrα* was also promoted in the MAT of MT mice, showing the consistence of the effect of SIRT1 activity on *lxrα* transcription in multiple tissues. To the best of our knowledge, this is the first report to reveal the effect of SIRT1 deacetylase activity on regulating *lxrα* transcription level in MAT. As one important target of LXRα, SREBP-1c plays a role as a transcription factor that regulates multiple lipogenic genes, including SCD1, FAS and ACC [32]. Compared to WT mice, the protein level of SREBP-1 in liver and the mRNA level of *srebp-1c* in both liver and MAT were significantly higher in MT mice. Data in this study showed that *scd1* mRNA consistently increased in both liver and MAT, but an elevated level of *fas* mRNA was only observed in MAT. Further study is needed to examine whether SIRT1 catalytic activity ablation affects other signaling pathways that alters FAS transcription levels specifically in MAT. It is interesting to note that the lack of SIRT1 enzymatic activity affected neither transcription of *adiponectin* in MAT nor adiponectin downstream targets in liver. Our observation that the lack of systemic SIRT1 activity did not impact adiponectin production and signaling does not agree with a previous study [40], in which adipocyte-selective SIRT1 knockout mice had reduced adiponectin production, compared to WT mice. Such a discrepancy might be due to the different effects of SIRT1 on adiponectin transcription, between SIRT1 adipocyte-specific knockout and systemic SIRT1 activity mutation.

In the present study, SIRT1 activity ablation did not affect plasma TG levels, which is consistent with previous findings that the SIRT1 protein levels were not correlated with the circulating TG levels in both human and animal studies [18, 41]. An intriguing observation in the present study is that the promoting effect of SIRT1 deacetylase activity ablation on hepatic steatosis is coupled with an increase in circulating FFA level. It has been shown that the portal vein directly connects the liver with the visceral MAT, and visceral fat content is highly correlated with the severity of hepatic steatosis in humans [42, 43]. In the present study, we found that the higher circulating FFA was associated with higher mRNA levels of *atgl*, *hsl* and *plin-2* in MT mice. ATGL is a rate-limiting lipolytic enzyme for TG hydrolysis, while HSL is the major hydrolase for diacylglyceride in the adipocytes [44, 45]. The phosphorylation of PLIN-2 is responsible for recruiting HSL to lipid droplets and meanwhile dissociates and activates ATGL. Jointly, the increased levels of *atgl*, *hsl* and *plin-2* mRNA in MT mice indicate a higher rate of lipolysis in MAT. This result is contradictory to the findings from previous studies that SIRT1 promotes lipolysis in adipocytes [44, 45]. In the study of Picard et al. [45], they reported a decreased lipolysis rate in the epididymal adipose tissue of SIRT1 heterozygous mice, which was associated with a lower level of circulating FFA. The discrepancy between that study and the current study might be due to the different adipose tissues used in the investigations. It is noted that the basal protein level of perilipins and activated HSL are different between MAT and epididymal adipose tissue, and moreover, the effect of HFD on ATGL activation is surprisingly inverse between the adipose tissue at two depots [46], leading us to hypothesize that SIRT1 differently regulates lipolysis between MAT and epididymal adipose tissue. CD36 mediates liver

FFA uptake and plays an important role in promoting steatosis [47, 48]. Interestingly, we observed an increased level of *cd36* mRNA in the liver, but not in the MAT, in MT mice, indicating that SIRT1 might regulate *cd36* transcription in a tissue-specific manner [47]. Previous studies reported that lipodystrophy occurred when fat mass was reduced and lipolysis was increased [49]. Interestingly, in the present study, we observed not only increased lipolysis, but also increased fatty acid synthesis in Sirt1 mutant animals fed high fat diet, which may lead to the dynamic homeostasis in mesenteric adipose tissue. This was supported by our body composition analyses showing that the percent fat mass and adipose tissue weight were comparable between wild-type and Sirt1 mutant mice, but significantly increased TG was found in the livers of Sirt1 mutant mice. This observation may help us to understand why some people without 'fat belly' still develop fatty liver when sirt1 activity decreases due to certain factors, such as aging, unhealthful diet, stress, or high alcohol consumption.

Taken together, the results from the current study suggest that systemic SIRT1 deacetylase activity ablation can promote hepatic steatosis by elevating lipogenesis in both liver and MAT (**Figure 5**). The lack of SIRT1 activity also promotes the release of FFA from MAT and consequent transport to liver, and increases liver FFA uptake by increasing hepatic FFA transporter (**Figure 5**). Whether SIRT1 activity is a potential molecular target for certain dietary components (e.g., tomato carotenoids) to prevent and/or mitigate development of NAFLD is currently under the investigation in this lab.

TABLE 1

Food consumption, body weights, liver weights, body fat composition of wild-type or SIRT1 ablation mice with high fat diet intervention for 34 weeks[a]

Study Group	WT	MT
Animal (n)	10	10
Food consumption (g/d)	3.2 ± 0.13	3.3 ± 0.22
Final body weight (g)	49.73 ± 1.54	46.89 ± 1.68
Liver weight (g)	1.87 ± 0.13	1.61 ± 0.11
Liver/body weight (%)	7.71 ± 0.54	9.33 ± 1.64
Fat composition (% total mass)	20.03 ± 1.03	19.93± 1.22

[a]Values are means ± SEMs (n=10) or (%). Student *t* test was used to examine the difference between WT and MT mice. Statistical significance was $P < 0.05$. WT, wild-type mice; MT, SIRT1 ablated mice.

FIGURE 1

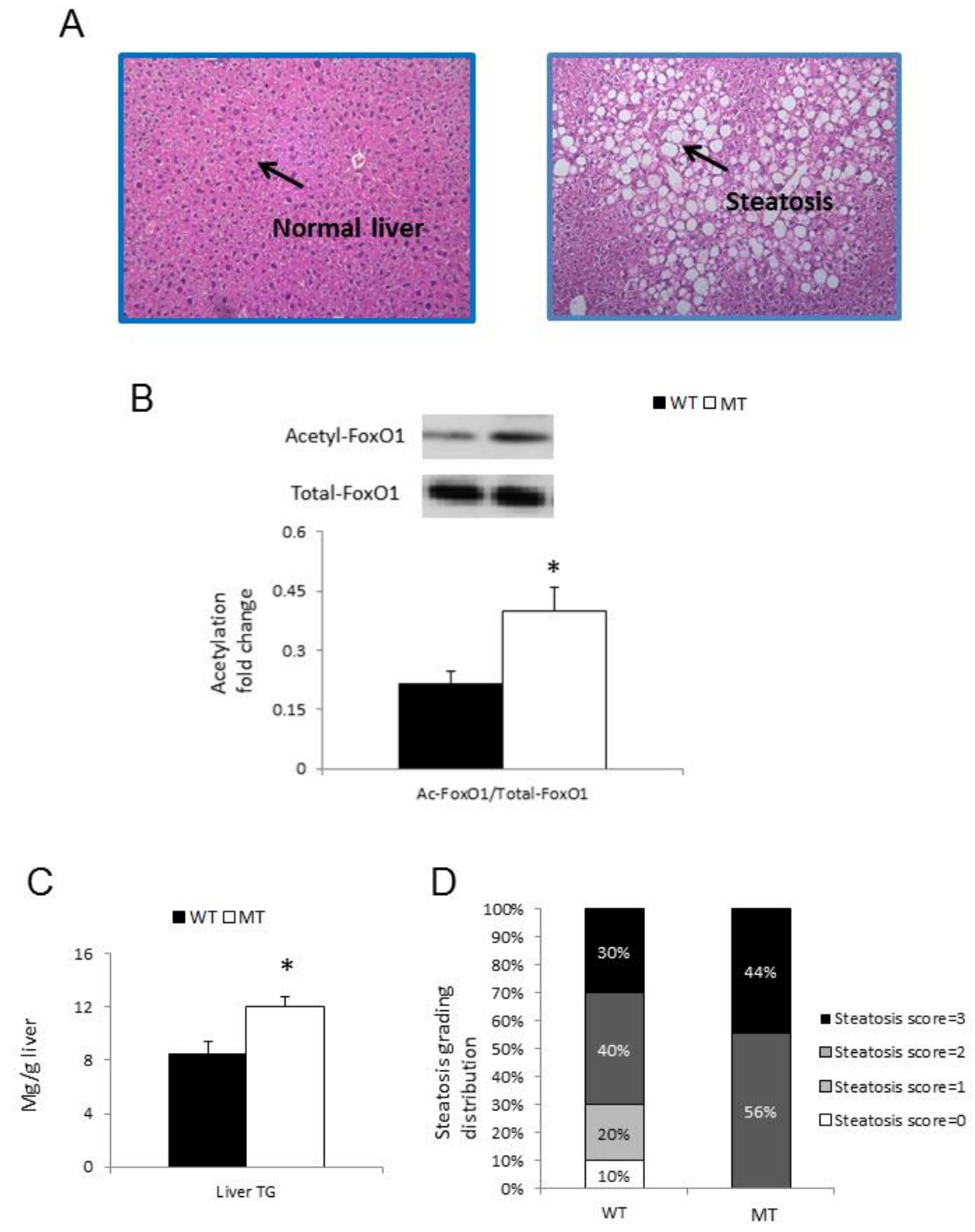
A
Normal liver
Steatosis
B
WT MT
Acetyl-FoxO1
Total-FoxO1
Acetylation fold change
0.6
0.45
0.3
0.15
0
*
Ac-FoxO1/Total-FoxO1
C
WT MT
Mg/g liver
16
12
8
4
0
*
Liver TG
D
Steatosis grading distribution
100%
90%
80%
70%
60%
50%
40%
30%
20%
10%
0%
30%
40%
20%
10%
44%
56%
WT
MT
Steatosis score=3
Steatosis score=2
Steatosis score=1
Steatosis score=0

FIGURE 2

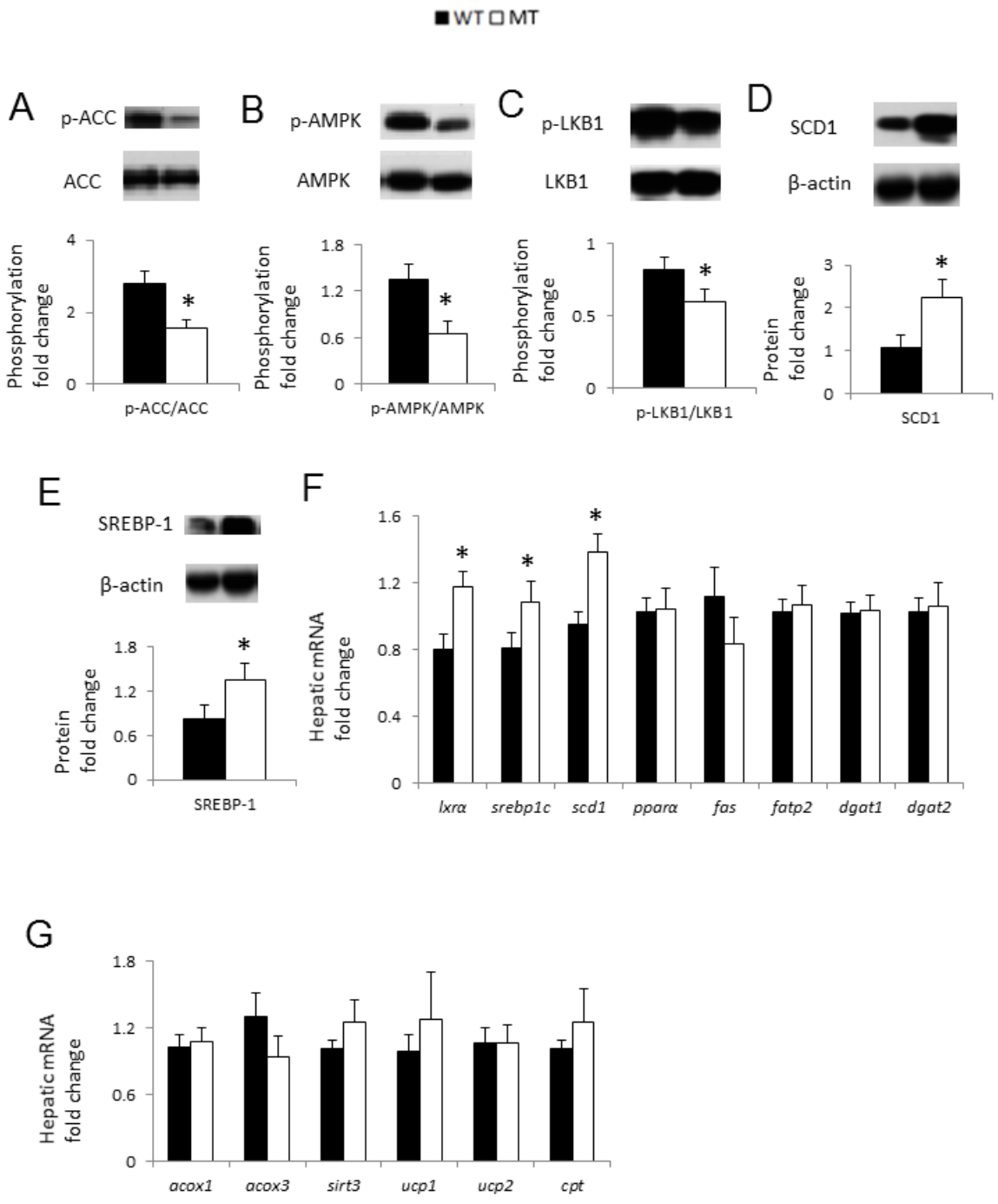
WT MT
A
p-ACC
ACC
Phosphorylation fold change
p-ACC/ACC
B
p-AMPK
AMPK
Phosphorylation fold change
p-AMPK/AMPK
C
p-LKB1
LKB1
Phosphorylation fold change
p-LKB1/LKB1
D
SCD1
β-actin
Protein fold change
SCD1
E
SREBP-1
β-actin
Protein fold change
SREBP-1
F
Hepatic mRNA fold change
lxrα
srebp1c
scd1
pparα
fas
fatp2
dgat1
dgat2
G
Hepatic mRNA fold change
acox1
acox3
sirt3
ucp1
ucp2
cpt

FIGURE 3

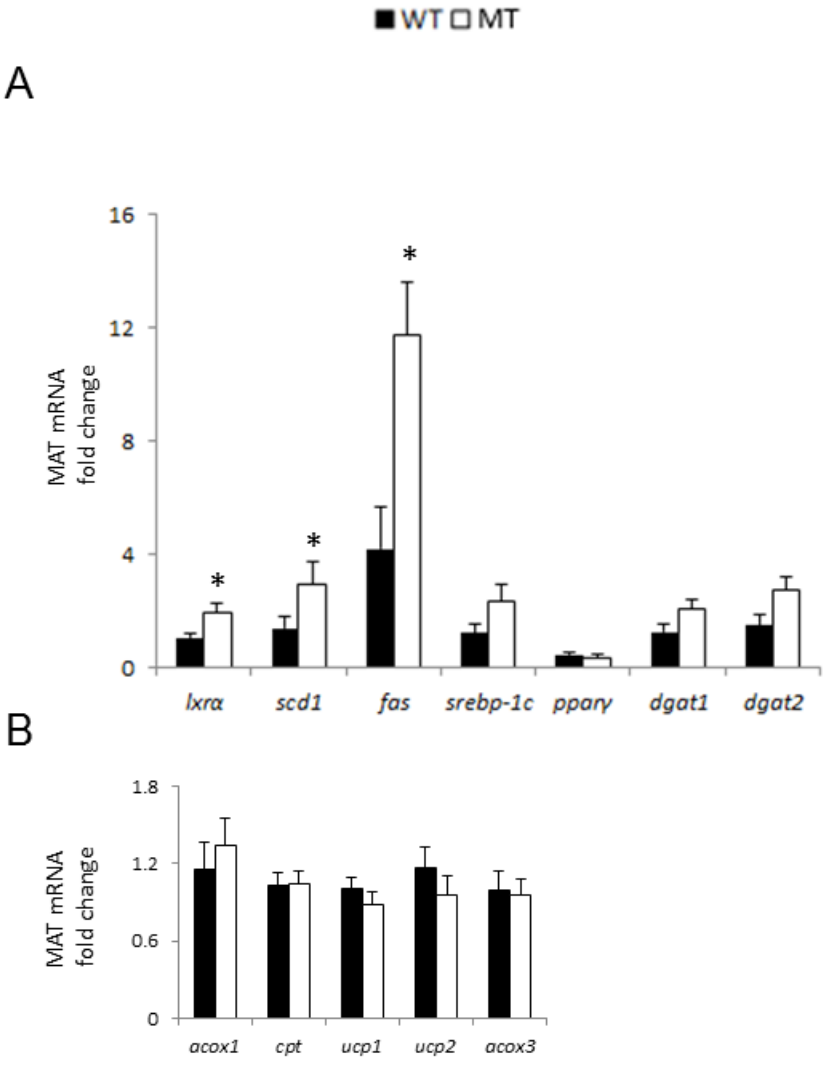
WT MT
A
MAT mRNA fold change
16
12
8
4
0
*
*
lxrα
scd1
fas
srebp-1c
pparγ
dgat1
dgat2
B
MAT mRNA fold change
1.8
1.2
0.6
0
acox1
cpt
ucp1
ucp2
acox3

FIGURE 4

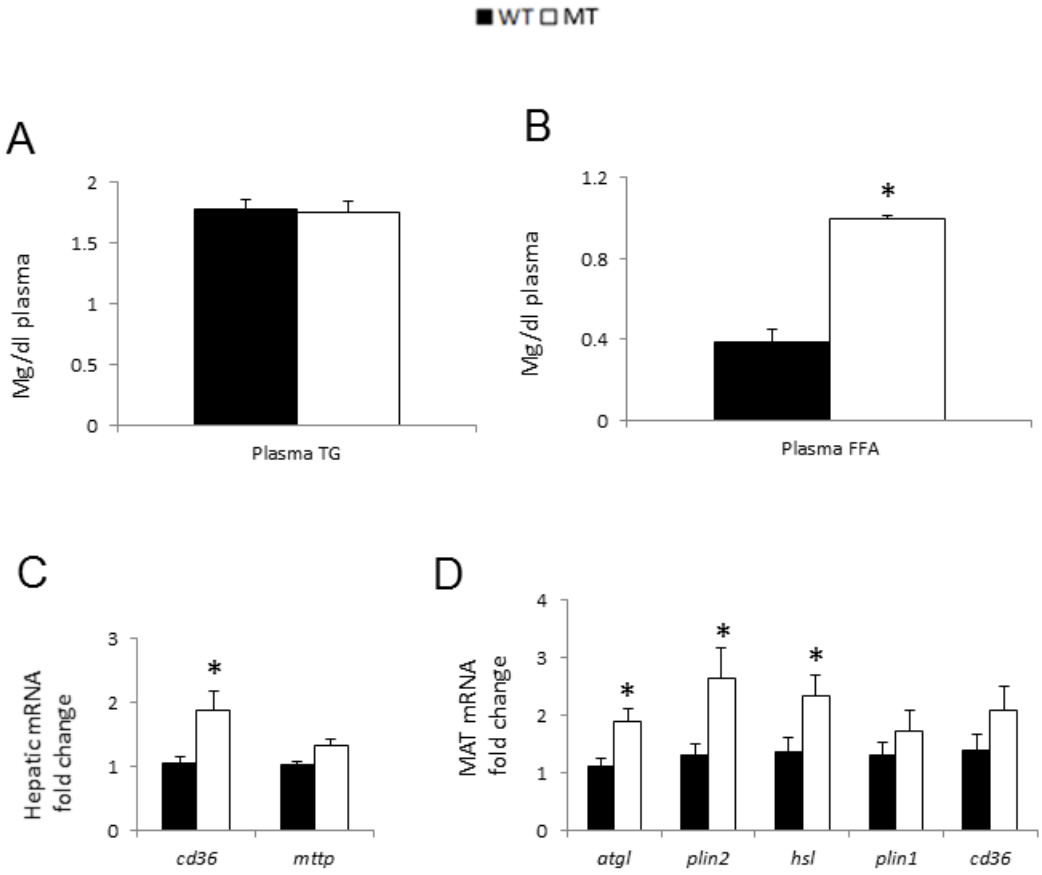
WT MT
A
Mg/dl plasma
2
1.5
1
0.5
0
Plasma TG
B
Mg/dl plasma
1.2
0.8
0.4
0
*
Plasma FFA
C
Hepatic mRNA fold change
3
2
1
0
*
cd36
mttp
D
MAT mRNA fold change
4
3
2
1
0
*
*
*
atgl
plin2
hsl
plin1
cd36

FIGURE 5

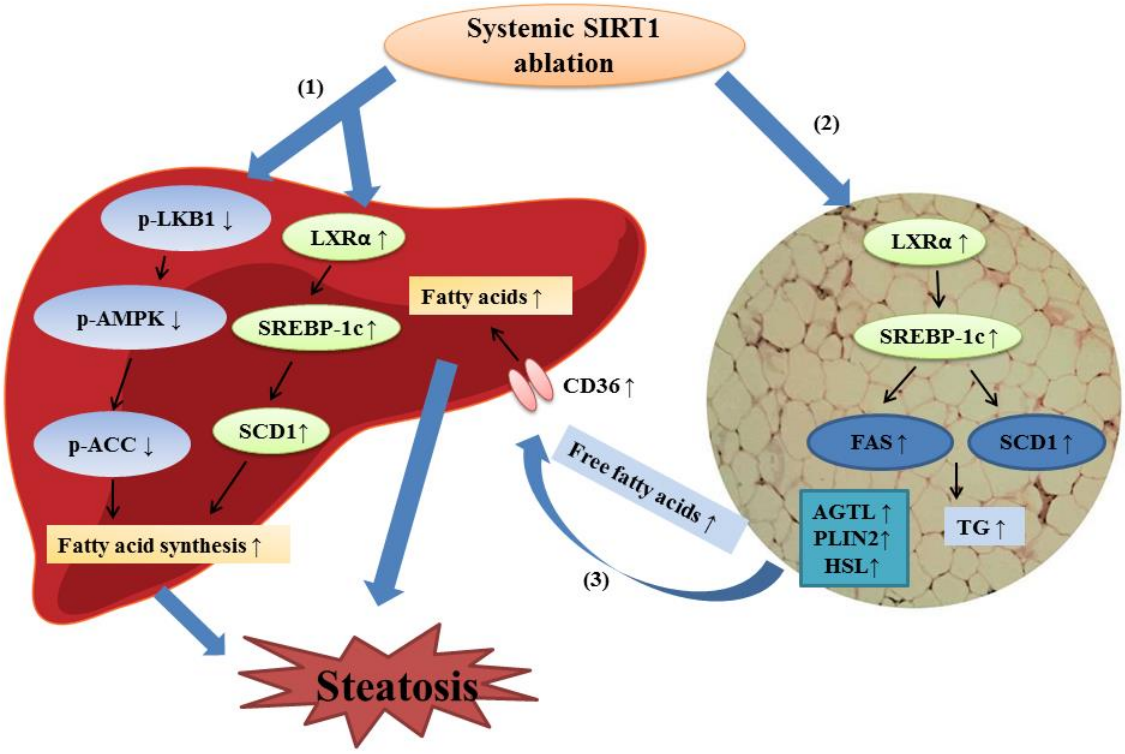
Systemic SIRT1 ablation
(1)
(2)
p-LKB1 ↓
LXRα ↑
p-AMPK ↓
SREBP-1c↑
Fatty acids ↑
CD36 ↑
p-ACC ↓
SCD1↑
Fatty acid synthesis ↑
Free fatty acids ↑
(3)
LXRα ↑
SREBP-1c↑
FAS ↑
SCD1↑
AGTL ↑
PLIN2↑
HSL↑
TG ↑
Steatosis

FIGURE LEGENDS

Figure 1. A, Graphic representation for hepatic steatosis histopathology grading. B, C, D, liver Ac-FoxO1, liver steatosis score distribution and liver TG level (WT, MT n = 10). B, graphic representation of fold changes in hepatic acetylated FoxO1, FoxO1 as loading control. C, distribution of histopathologic liver steatosis score in WT, MT. D, TG level of livers. Values are % of total mice, or means ± SMEs. Mann–Whitney U test was used to compare liver steatosis score distribution; student t test was used to compare liver Ac-FoxO1 ratio and TG level between WT and MT mice. *Different from WT, $P < 0.05$. WT, wild-type mice; MT, SIRT1 activity ablation mice.

Figure 2. Effects of SIRT1 activity ablation on lipogenesis and fatty acid oxidation biomarkers. Changes of protein or mRNA expressions in liver lysates (WT, MT n = 10) were analyzed by western-blotting or RT-PCR, and β-actin was used as loading control unless specified otherwise. Graphical representation of fold changes in: A, phosphorylated ACC (Ser79; ACC as loading control); B, phosphorylated AMPK (Thr172; AMPK as loading control); C, phosphorylated LKB1 (Ser428; LKB1 as loading control); D, SREBP-1; E, SCD1; F, mRNA of lipogenesis-associated genes: *lxrα*, *srebp1c*, *scd1*, *fas*, *pparα*, *dgat1*, *dgat2*; G, mRNA of fatty acid oxidation-associated genes: *acox1*, *acox3*, *sirt3*, *ucp1*, *ucp2*, *cpt*. Values are means ± SMEs. Student t test was used to compare liver TG level between WT and MT mice. *Different from WT, $P < 0.05$.

Figure 3. Effects of sirt1 activity ablation on lipogenesis and fatty acid oxidation biomarkers. Changes of mRNA expressions in MAT lysates (WT, MT n=7-9) were analyzed by RT-PCR, and β-actin was used as loading control unless specified otherwise.

Graphical representation of fold changes in: A, lipogenesis-associated genes: *lxrα, srebp-1c, scd1, fas, pparγ, dgat1, dgat2*; B, fatty acid oxidation-associated genes: *acox1, cpt, ucp1, ucp2, acox3*. Values are means ± SMEs. Student t test was used to compare liver TG level between WT and MT mice. *Different from WT, $P < 0.05$.

Figure 4. Effects of SIRT1 activity ablation on plasma TG, FFA concentration and FFA mobilization biomarkers in liver and MAT. Changes of mRNA expressions in liver or MAT lysates (WT, MT n=7-9) were analyzed by RT-PCR, and β-actin was used as loading control unless specified otherwise. Graphical representation of fold changes in: A, plasma TG concentration; B, FFA concentration; C, FFA uptake transporter in liver: *cd36*, TG export transporter in liver: *mttp*; D, lipolysis-associated genes: *agtl, plin-2, hsl, plin-1*, FFA uptake transporter in MAT: *cd36*. Values are means ± SMEs. Student t test was used to compare liver TG level between WT and MT mice. *Different from WT, $P < 0.05$.

Figure 5. The potential effect of systemic SIRT1 ablation on the development of nonalcoholic fatty liver disease (NAFLD) through three pathways: (1) increase TG synthesis in the liver by promoting fatty acid synthetic genes; (2) increase TG synthesis in the mesenteric adipose tissue (MAT) by promoting fatty acid synthetic genes; and (3) promote the mobilization of fatty acid from MAT to liver by increasing hepatic free fatty acid uptake.

LITERATURE CITED

[1] K. Aleksandrova, M. Stelmach-Mardas, S. Schlesinger, Obesity and Liver Cancer, Recent Results Cancer Res, 208 (2016) 177-198.

[2] E. Fabbrini, S. Sullivan, S. Klein, Obesity and nonalcoholic fatty liver disease: biochemical, metabolic, and clinical implications, Hepatology, 51 (2010) 679-689.

[3] J.C. Cohen, J.D. Horton, H.H. Hobbs, Human fatty liver disease: old questions and new insights, Science, 332 (2011) 1519-1523.

[4] G. Baffy, E.M. Brunt, S.H. Caldwell, Hepatocellular carcinoma in non-alcoholic fatty liver disease: an emerging menace, J Hepatol, 56 (2012) 1384-1391.

[5] J.S. Smith, C.B. Brachmann, I. Celic, M.A. Kenna, S. Muhammad, V.J. Starai, J.L. Avalos, J.C. Escalante-Semerena, C. Grubmeyer, C. Wolberger, J.D. Boeke, A phylogenetically conserved NAD+-dependent protein deacetylase activity in the Sir2 protein family, Proc Natl Acad Sci U S A, 97 (2000) 6658-6663.

[6] S. Imai, C.M. Armstrong, M. Kaeberlein, L. Guarente, Transcriptional silencing and longevity protein Sir2 is an NAD-dependent histone deacetylase, Nature, 403 (2000) 795-800.

[7] F. Lan, J.M. Cacicedo, N. Ruderman, Y. Ido, SIRT1 modulation of the acetylation status, cytosolic localization, and activity of LKB1. Possible role in AMP-activated protein kinase activation, J Biol Chem, 283 (2008) 27628-27635.

[8] X. Hou, S. Xu, K.A. Maitland-Toolan, K. Sato, B. Jiang, Y. Ido, F. Lan, K. Walsh, M. Wierzbicki, T.J. Verbeuren, R.A. Cohen, M. Zang, SIRT1 regulates hepatocyte lipid metabolism through activating AMP-activated protein kinase, J Biol Chem, 283 (2008) 20015-20026.

[9] Z. Gerhart-Hines, J.T. Rodgers, O. Bare, C. Lerin, S.H. Kim, R. Mostoslavsky, F.W. Alt, Z. Wu, P. Puigserver, Metabolic control of muscle mitochondrial function and fatty acid oxidation through SIRT1/PGC-1alpha, Embo j, 26 (2007) 1913-1923.

[10] A. Purushotham, T.T. Schug, Q. Xu, S. Surapureddi, X. Guo, X. Li, Hepatocyte-specific deletion of SIRT1 alters fatty acid metabolism and results in hepatic steatosis and inflammation, Cell Metab, 9 (2009) 327-338.

[11] L. Bai, W.J. Pang, Y.J. Yang, G.S. Yang, Modulation of Sirt1 by resveratrol and nicotinamide alters proliferation and differentiation of pig preadipocytes, Mol Cell Biochem, 307 (2008) 129-140.

[12] C. Canto, R.H. Houtkooper, E. Pirinen, D.Y. Youn, M.H. Oosterveer, Y. Cen, P.J. Fernandez-Marcos, H. Yamamoto, P.A. Andreux, P. Cettour-Rose, K. Gademann, C. Rinsch, K. Schoonjans, A.A. Sauve, J. Auwerx, The NAD(+) precursor nicotinamide riboside enhances oxidative metabolism and protects against high-fat diet-induced obesity, Cell Metab, 15 (2012) 838-847.

[13] J. Landry, A. Sutton, S.T. Tafrov, R.C. Heller, J. Stebbins, L. Pillus, R. Sternglanz, The silencing protein SIR2 and its homologs are NAD-dependent protein deacetylases, Proc Natl Acad Sci U S A, 97 (2000) 5807-5811.

[14] R.H. Houtkooper, C. Canto, R.J. Wanders, J. Auwerx, The secret life of NAD+: an old metabolite controlling new metabolic signaling pathways, Endocr Rev, 31 (2010) 194-223.

[15] X. Li, SIRT1 and energy metabolism, Acta Biochim Biophys Sin (Shanghai), 45 (2013) 51-60.

[16] B.J. Gurd, Y. Yoshida, J.T. McFarlan, G.P. Holloway, C.D. Moyes, G.J. Heigenhauser, L. Spriet, A. Bonen, Nuclear SIRT1 activity, but not protein content, regulates mitochondrial biogenesis in rat and human skeletal muscle, Am J Physiol Regul Integr Comp Physiol, 301 (2011) R67-75.

[17] X.Q. Deng, L.L. Chen, N.X. Li, The expression of SIRT1 in nonalcoholic fatty liver disease induced by high-fat diet in rats, Liver Int, 27 (2007) 708-715.

[18] S. Mariani, D. Fiore, S. Basciani, A. Persichetti, S. Contini, C. Lubrano, L. Salvatori, A. Lenzi, L. Gnessi, Plasma levels of SIRT1 associate with non-alcoholic fatty liver disease in obese patients, Endocrine, 49 (2015) 711-716.

[19] P.T. Pfluger, D. Herranz, S. Velasco-Miguel, M. Serrano, M.H. Tschop, Sirt1 protects against high-fat diet-induced metabolic damage, Proc Natl Acad Sci U S A, 105 (2008) 9793-9798.

[20] F. Xu, Z. Gao, J. Zhang, C.A. Rivera, J. Yin, J. Weng, J. Ye, Lack of SIRT1 (Mammalian Sirtuin 1) activity leads to liver steatosis in the SIRT1+/- mice: a role of lipid mobilization and inflammation, Endocrinology, 151 (2010) 2504-2514.

[21] A.Z. Caron, X. He, W. Mottawea, E.L. Seifert, K. Jardine, D. Dewar-Darch, G.O. Cron, M.E. Harper, A. Stintzi, M.W. McBurney, The SIRT1 deacetylase protects mice against the symptoms of metabolic syndrome, Faseb j, 28 (2014) 1306-1316.

[22] R.H. Wang, C. Li, C.X. Deng, Liver steatosis and increased ChREBP expression in mice carrying a liver specific SIRT1 null mutation under a normal feeding condition, Int J Biol Sci, 6 (2010) 682-690.

[23] J. Ding, M. Li, X. Wan, X. Jin, S. Chen, C. Yu, Y. Li, Effect of miR-34a in regulating steatosis by targeting PPARalpha expression in nonalcoholic fatty liver disease, Sci Rep, 5 (2015) 13729.

[24] G. Boily, E.L. Seifert, L. Bevilacqua, X.H. He, G. Sabourin, C. Estey, C. Moffat, S. Crawford, S. Saliba, K. Jardine, J. Xuan, M. Evans, M.E. Harper, M.W. McBurney, SirT1 regulates energy metabolism and response to caloric restriction in mice, PLoS One, 3 (2008) e1759.

[25] H.L. Cheng, R. Mostoslavsky, S. Saito, J.P. Manis, Y. Gu, P. Patel, R. Bronson, E. Appella, F.W. Alt, K.F. Chua, Developmental defects and p53 hyperacetylation in Sir2 homolog (SIRT1)-deficient mice, Proc Natl Acad Sci U S A, 100 (2003) 10794-10799.

[26] M.W. McBurney, X. Yang, K. Jardine, M. Hixon, K. Boekelheide, J.R. Webb, P.M. Lansdorp, M. Lemieux, The mammalian SIR2alpha protein has a role in embryogenesis and gametogenesis, Mol Cell Biol, 23 (2003) 38-54.

[27] E.L. Seifert, A.Z. Caron, K. Morin, J. Coulombe, X.H. He, K. Jardine, D. Dewar-Darch, K. Boekelheide, M.E. Harper, M.W. McBurney, SirT1 catalytic activity is required for male fertility and metabolic homeostasis in mice, Faseb j, 26 (2012) 555-566.

[28] J. Wang, S.M. Vanegas, X. Du, T. Noble, J.M. Zingg, M. Meydani, S.N. Meydani, D. Wu, Caloric restriction favorably impacts metabolic and immune/inflammatory profiles in obese mice but curcumin/piperine consumption adds no further benefit, Nutr Metab (Lond), 10 (2013) 29.

[29] C.P. Stice, C. Liu, K. Aizawa, A.S. Greenberg, L.M. Ausman, X.D. Wang, Dietary tomato powder inhibits alcohol-induced hepatic injury by suppressing cytochrome p450 2E1 induction in rodent models, Arch Biochem Biophys, 572 (2015) 81-88.

[30] J. Chung, K. Koo, F. Lian, K.Q. Hu, H. Ernst, X.D. Wang, Apo-10'-lycopenoic acid, a lycopene metabolite, increases sirtuin 1 mRNA and protein levels and decreases hepatic fat accumulation in ob/ob mice, J Nutr, 142 (2012) 405-410.

[31] Y. Peng, D.A. Rideout, S.S. Rakita, W.R. Gower, Jr., M. You, M.M. Murr, Does LKB1 mediate activation of hepatic AMP-protein kinase (AMPK) and sirtuin1 (SIRT1) after Roux-en-Y gastric bypass in obese rats?, J Gastrointest Surg, 14 (2010) 221-228.

[32] D. Eberle, B. Hegarty, P. Bossard, P. Ferre, F. Foufelle, SREBP transcription factors: master regulators of lipid homeostasis, Biochimie, 86 (2004) 839-848.

[33] M.U. Jakobsen, T. Berentzen, T.I. Sorensen, K. Overvad, Abdominal obesity and fatty liver, Epidemiol Rev, 29 (2007) 77-87.

[34] P. Engfeldt, P. Arner, Lipolysis in human adipocytes, effects of cell size, age and of regional differences, Horm Metab Res Suppl, 19 (1988) 26-29.

[35] P. Bjorntorp, "Portal" adipose tissue as a generator of risk factors for cardiovascular disease and diabetes, Arteriosclerosis, 10 (1990) 493-496.

[36] T. Yoshikawa, H. Shimano, M. Amemiya-Kudo, N. Yahagi, A.H. Hasty, T. Matsuzaka, H. Okazaki, Y. Tamura, Y. Iizuka, K. Ohashi, J. Osuga, K. Harada, T. Gotoda, S. Kimura, S. Ishibashi, N. Yamada, Identification of liver X receptor-retinoid X receptor as an activator of the sterol regulatory element-binding protein 1c gene promoter, Mol Cell Biol, 21 (2001) 2991-3000.

[37] M.D. Fullerton, S. Galic, K. Marcinko, S. Sikkema, T. Pulinilkunnil, Z.P. Chen, H.M. O'Neill, R.J. Ford, R. Palanivel, M. O'Brien, D.G. Hardie, S.L. Macaulay, J.D. Schertzer, J.R. Dyck, B.J. van Denderen, B.E. Kemp, G.R. Steinberg, Single phosphorylation sites in Acc1 and Acc2 regulate lipid homeostasis and the insulin-sensitizing effects of metformin, Nat Med, 19 (2013) 1649-1654.

[38] S.H. Jin, J.H. Yang, B.Y. Shin, K. Seo, S.M. Shin, I.J. Cho, S.H. Ki, Resveratrol inhibits LXRalpha-dependent hepatic lipogenesis through novel antioxidant Sestrin2 gene induction, Toxicol Appl Pharmacol, 271 (2013) 95-105.

[39] S. Schuster, M. Penke, T. Gorski, S. Petzold-Quinque, G. Damm, R. Gebhardt, W. Kiess, A. Garten, Resveratrol differentially regulates NAMPT and SIRT1 in Hepatocarcinoma cells and primary human hepatocytes, PLoS One, 9 (2014) e91045.

[40] X. Hui, M. Zhang, P. Gu, K. Li, Y. Gao, D. Wu, Y. Wang, A. Xu, Adipocyte SIRT1 controls systemic insulin sensitivity by modulating macrophages in adipose tissue, EMBO Rep, 18 (2017) 645-657.

[41] A. Purushotham, Q. Xu, X. Li, Systemic SIRT1 insufficiency results in disruption of energy homeostasis and steroid hormone metabolism upon high-fat-diet feeding, Faseb j, 26 (2012) 656-667.

[42] A. Gastaldelli, K. Cusi, M. Pettiti, J. Hardies, Y. Miyazaki, R. Berria, E. Buzzigoli, A.M. Sironi, E. Cersosimo, E. Ferrannini, R.A. Defronzo, Relationship between hepatic/visceral fat and hepatic insulin resistance in nondiabetic and type 2 diabetic subjects, Gastroenterology, 133 (2007) 496-506.

[43] A. Kotronen, H. Yki-Jarvinen, K. Sevastianova, R. Bergholm, A. Hakkarainen, K.H. Pietilainen, L. Juurinen, N. Lundbom, T.I. Sorensen, Comparison of the relative contributions of intra-abdominal and liver fat to components of the metabolic syndrome, Obesity (Silver Spring), 19 (2011) 23-28.

[44] P. Chakrabarti, T. English, S. Karki, L. Qiang, R. Tao, J. Kim, Z. Luo, S.R. Farmer, K.V. Kandror, SIRT1 controls lipolysis in adipocytes via FOXO1-mediated expression of ATGL, J Lipid Res, 52 (2011) 1693-1701.

[45] F. Picard, M. Kurtev, N. Chung, A. Topark-Ngarm, T. Senawong, R. Machado De Oliveira, M. Leid, M.W. McBurney, L. Guarente, Sirt1 promotes fat mobilization in white adipocytes by repressing PPAR-gamma, Nature, 429 (2004) 771-776.

[46] S. Wueest, F. Item, F.C. Lucchini, T.D. Challa, W. Muller, M. Bluher, D. Konrad, Mesenteric Fat Lipolysis Mediates Obesity-Associated Hepatic Steatosis and Insulin Resistance, Diabetes, 65 (2016) 140-148.

[47] J. Zhou, M. Febbraio, T. Wada, Y. Zhai, R. Kuruba, J. He, J.H. Lee, S. Khadem, S. Ren, S. Li, R.L. Silverstein, W. Xie, Hepatic fatty acid transporter Cd36 is a common target of LXR, PXR, and PPARgamma in promoting steatosis, Gastroenterology, 134 (2008) 556-567.

[48] M.W. Bradbury, Lipid metabolism and liver inflammation. I. Hepatic fatty acid uptake: possible role in steatosis, Am J Physiol Gastrointest Liver Physiol, 290 (2006) G194-198.

[49] J. Zhang, T.M. Henagan, Z. Gao, J. Ye, Inhibition of glyceroneogenesis by histone deacetylase 3 contributes to lipodystrophy in mice with adipose tissue inflammation, Endocrinology, 152 (2011) 1829-1838.

CHAPTER IV

TOMATO POWDER ATTENUATED NON-ALCOHOLIC FATTY LIVER DISEASE INDEPENDENT OF SIRT1 ACTIVITY

ABSTRACT

Background: Tomato and tomato products can induce Sirtuin 1 (SIRT1) deacetylate activity and inhibit the development of nonalcoholic fatty liver disease (NAFLD), a risk factor for hepatocellular carcinoma (HCC) development. Whether the dietary tomato feeding inhibits NAFLD and HCC dependent on SIRT1 activity remains unknown.

Methods: Mice with homozygous ablation in catalytic activity of SIRT1 (MT) and their corresponding wild type littermates (WT) were injected with diethylnitrosamine, and fed a high fat diet (HFD, 60% calories from fat) with or without tomato powder (TP, containing lycopene 100mg/kg diet) for 34 weeks.

Results: Dietary TP supplementation significantly reduced liver steatosis in both WT and MT mice through different molecular mechanisms: protective effect of TP was mediated, by increasing SIRT1 protein expression and activity, and decreasing hepatic fatty acid binding protein 1 expression and long chain fatty acid (FA) uptake in WT mice; while in MT mice, TP decreased hepatic FA synthesis through inactivating hepatic acetyl-CoA carboxylase mediated by AMPK phosphorylation, independent of SIRT1. Although we did not detect significant inflammatory responses in either WT or MT mice, TP lowered *il-6* expression in MAT and IL-6 concentration in plasma and liver, as compared with MT mice without TP; while in WT mice, dietary TP decreased caspase-1 mediated IL-1β maturation. However, neither the mutation of SIRT1 activity nor TP supplementation altered HCC incidence or severity in both WT and MT mice, which could be due to the lack of inflammation as a target of TP protection or limited efficacy in ameliorating HCC development in this mouse model.

Conclusion: Dietary TP supplementation can ameliorate HFD-induced NAFLD and inflammatory responses independent of SIRT1 activity, but not affecting carcinogen-induced HCC development.

INTRODUCTION

Nonalcoholic fatty liver disease (NAFLD) includes a wide spectrum of disease ranging from simple steatosis to nonalcoholic steatohepatitis (NASH), liver fibrosis, cirrhosis, and hepatocellular carcinoma (HCC) [1]. Obesity is a major risk factor of NAFLD [2]. In fact, an average of 76% obese patients was reported to have liver steatosis [3], and the incidence of NAFLD is still rising with paralleled to increasing obesity rates [4]. HCC accounted for 85%-90% of primary liver cancers, and is the second most common cause of cancer mortality worldwide [5-7]. According to the 18th Annual Report to the Nation on the Status of Cancer, the mortality of HCC is still increasing, despite the decline in overall cancer death rates [8, 9]. NAFLD has been observed in 30%-40% of HCC patients in the US [5]. Indeed, with the involvement of inflammatory cytokines such as IL-1β, IL-6 and TNFα, simple steatosis can further progress to NASH, or even severe fibrosis [10], which was observed in approximately 90% of HCC cases [11], highlighting the critical role of metabolism disorder on HCC development. Considering the lack of effective medical treatments for both NAFLD and HCC, preventing the incidence of NAFLD, or ameliorate NAFLD development at early stage could be an important strategy.

Tomatoes are good sources of the colorless carotenoids phytoene, phytofluene, and other micronutrients such as vitamin C, E, and flavonoids, which are all considered as anti-oxidant agents [12]. Previous studies have shown that consumption of tomato

products can inhibit systemic inflammation by reducing pro-inflammatory cytokines [13], decrease hallmarks of liver steatosis, and accelerate hepatic lipid metabolism [14]. Lycopene, a major pigment characterizing the redness of tomatoes and tomato products, is widely studied due to its biological activities [15, 16]. Accumulating evidence has shown that lycopene, and its natural cleavage product apo-10'-lycopenoic acid (ALA) [17], have protective efficacy against high fat diet (HFD)-induced liver steatosis, inflammation and cancer development [18-25], which was associated with improved hepatic Sirtuin 1 (SIRT1) expression and SIRT1 activity [18, 23, 24]. Interestingly, a marked increase of *sirt1* mRNA level was also observed in animals with lycopene-rich tomato oleoresin supplementation [26], prompting us to address the question whether the beneficial effects from natural tomato products are dependent on SIRT1 signaling.

SIRT1 is an evolutionarily conserved NAD^+-dependent deacetylase for both histone and non-histone proteins [27, 28]. By catalyzing the transfer of the acetyl-group from the substrate to cleaved nicotinamide adenine dinucleotide nicotine (NAD^+), generated from NAD+ hydrolysis, SIRT1 can regulate the expressions of multiple genes or proteins and control a series of physiological activities including energy metabolism [29-31], stress response [32, 33], and aging [34, 35]. By virtue of these functions, SIRT1 has been widely studied as a molecular target to inhibit the pathogenesis of various diseases, including HFD-induced NAFLD [30, 36, 37]. Recently, an epidemiology study reported an inverse correlation between plasma SIRT1 concentration and the severity of liver steatosis in obese patients [38], indicating an interaction between SIRT1 and liver steatosis development. It is important to note, however, people with high risk of NAFLD, such as those in aging, obesity and chronic inflammation [2, 39-41], are susceptible to

developing SIRT1 dysfunction due to depleted NAD^+ pool [42, 43], or impaired Nicotinamide phosphoribosyltransferase (NAMPT), a rate limiting enzyme in NAD^+ biosynthesis [43, 44],which highlights the importance of developing an efficient strategy to inhibit NAFLD without depending on SIRT1 activity.

Controversy regarding SIRT1 and HCC is still under debate as it could act as either a tumor suppressor or tumor promoter depending on its targets in specific signaling pathways. Dual effects of SIRT1 on cell proliferation have been documented in previous publications. It has been reported that SIRT1 can transcriptionally and post-translationally promote cell proliferation by inhibiting key cell cycle and apoptosis regulatory proteins such as p53 [45-47], BCL6 [48], Ku-70 [49] and Smad7 [50]. In contrast, SIRT1 also contains a suppressive activity in tumor cell growth by interacting and deacetylating E2F1, which indirectly decrease pRb hyper-phosphorylation and induce cyclinD/cdk4 activity [51]. Additionally, SIRT1 has been shown to directly deacetylate NF-κB, which is well-known for its anti-apoptotic function [50]. Although SIRT1 was found elevated in human HCC tissue, compared to non-HCC tissue [45, 52-56], the causality between SIRT1 and HCC remains unknown. Using transgenic mice models, two studies reported that SIRT1 was HCC promoter by increasing bile acid accumulation and impeding cell arrest at G1 [56, 57]; one study reported that SIRT1 was HCC inhibitor by decreasing expression of the ageing-associated gene p16 (Ink4a) and improving hepatic protection from both DNA damage [58]. These mouse models either showed the effect of SIRT1 overexpression, or partial SIRT1 function, given that mice with whole-body SIRT1 gene knockout developed metabolic defect [59], developmental abnormality, or postnatal lethality [60, 61]. The challenge of employing a systemic

SIRT1 knockout animal model to investigate the causal role of SIRT1 on HCC development was overcome recently by using an engineered mouse model with systemic SIRT1 deacetylase activity ablation to achieve similar SIRT1 loss-of-function effects with SIRT1 knockout mice but with less resultant genetic defects [27]. Using this mouse model, we and others observed an increasing hepatic lipid accumulation in SIRT1 activity ablated mice [21] and proposed the underlying mechanism by which systemic SIRT1ablation aggravated HFD-induced hepatic steatosis [36]. These studies raised an opportunity to the further investigation as for how the lack of SIRT1 activity affects HCC initiation and development.

To explore the causal effect of systemic SIRT1 activity on HCC development, we utilized the systemic SIRT1 activity ablated mice (MT), as compared to their wild-type (WT) counterparts, and a well-established two-hit mouse model [24, 62] in which tumor initiation by N-nitrosodiethylamine (DEN) was further promoted by HFD feeding. To examine the effect of tomato products on NAFLD, inflammation and HCC development, we fed both WT and MT mice HFD with or without tomato powder (TP), and further elucidated the underlying mechanism by which TP exhibited anti-NAFLD and HCC efficacy in both WT and MT mice.

METHODS

Animals and Diets

All study protocols were approved by the Institutional Animal Care and Use Committee of Tufts University. We utilized the 129/SvJ background, outbred CD-1 mouse strain carrying a point mutation (H355Y) expressing similar SIRT1 protein with

ablated catalytic activity, compared with their WT counterparts, as previously described [36]. At 2 weeks of age, both WT and MT mice were injected with DEN, a carcinogenic reagent mainly specific to liver, at 25 mg/kg body weight. At 4 weeks of age, genotyping was conducted by employing a PCR-based test to amplify DNA using the primers 5'-TGGAAGGAAAGCAATTTTGGT-3' and g'CTGAGTTACCTTAGCTTGGC-3'. We selected male mice for this study because the risk for males to develop liver cancer is higher than females in both humans and mice [63, 64]. At 6 weeks of age, to mimic the disorder induced by diet-induced obesity in human [65], we used mice fed high fat diet (HFD, 60% calories from fat, Bioserv, NJ) with or without TP supplementation. The macronutrient component within the HFD was listed in **Appendix I**. At 38 weeks of age, EchoMRI-100 (EchoMRI, Houston, TX) was used for mice body composition measurement, as described previously [66]. Blood and tissues were collected post-mortem.

TP Supplementation

TP was mixed in the diet to make lycopene level at 100mg/kg diet, which is equivalent to lycopene intake of 8.1 mg per day for person weighing 60-kg, as calculated in our previous study [62]. Since the average daily intake of lycopene in the United States ranges from 6.6–10.5 mg/day for men and from 5.7–10.4 mg/day for women [67], and lycopene doses used in dietary supplements are between 15-30 mg/day [62], the TP dosage used in the present study is within physiology relevance.

Tissue Processing and Liver Tumor Quantification

Livers, mesenteric adipose tissue (MAT), and epididymal adipose tissue were collected and weighed. Two investigators unaware of genotype and treatment groups

counted the number of surface liver tumors and measured the diameter of the tumors, as described [62]. A piece of liver tissue from the left lobe of liver was fixed in 10% buffered formalin solution for histopathological examination while the remaining liver tissues were snap frozen in liquid nitrogen and stored at -80°C for later analysis.

Liver Histopathology Evaluation

Paraffin-embedded liver tissues were cut into 5 μm sections and stained with hematoxylin-eosin (H&E) to evaluate histology of the tissues, as described previously [36]. The sections were examined under light microscopy by two independent investigators who were blinded to the group classification. A SEIZZ microscope with a PixeLINK USB 2.0 (PL-B623CU) digital Camera and PixeLINK μScope Microscopy Software was utilized for the histopathology examination. Hepatic steatosis was graded according to the degree of both macro- and micro-vesicular lipid accumulations, as previously described [68]. Briefly, the severity of hepatic steatosis was evaluated based on the percentage of liver section that was occupied by lipid vacuoles at 100x magnification in 20 fields according to the following criteria: grade 0 = <5%; grade 1 = 5–25%; grade 2 = 26–50%; grade 3 = 51–75%; grade 4 = >75%. The types of hepatic tumors were confirmed according to the following criteria: (i) the presence of trabecular pattern with 3+ cell-thick hepatocellular plates/cords; (ii) mitotic figure; (iii) enlarged convoluted nuclei or high nuclei/cytoplasmic ratio; (iv) the presence of tumor giant cells with compact growth pattern; and (v) the presence of endothelial cells lining of sinusoids that surround enlarged hepatocellular plates/cords, as previously described [62].

Protein Isolation and Western Blotting

Liver protein isolation was described previously [23]. For MAT protein isolation, adipose tissue was homogenized in RIPA buffer with protease (Halt) and phosphatase (PhoStop) inhibitors at 100mg tissue/100 µL buffer. We pooled 3-4 samples per group to obtain detectable signals. MAT homogenates were centrifuged at 14,500 rpm for 10 minutes at 4 °C, followed by removing the surface fat free homogenate. Repeat centrifugation and remove fat from samples. The whole volume was then centrifuged at 55,000 rpm for 1 hour using an Ultracentrifuge. Both liver and MAT protein concentrations were measured by utilizing the Comassie Plus protein quantification method (Thermo Fisher Scientific) and adjusted to 10 µg/µl. For Western blotting, 5 µl liver whole cell lysates were mixed with 5 µl Laemmli sample buffer for protein denature. Protein detection was performed by electroblotting with details published previously [36]. The following primary antibodies were used for Western blotting: p-AMPK (Thr172), p-ACC (Ser79), p-mTOR, p-MAPK (Thr202/Tyr204), p-STAT3, AMPK, ACC, SCD1, PARP, NF-κ B (Cell Signaling, MA, USA), Ac-FoxO1, FoxO1, SREBP-1, and p21 (Santa Cruz, TX, USA). The protein level of β-actin was used as internal control.

RNA Extraction and qPCR

Total RNA from either frozen liver tissue or MAT tissue was extracted using TriPure Isolation Reagent kit (Roche, USA), as the protocol indicates. Complementary DNA (cDNA) was synthesized with a reverse transcription PCR kit (M-MLV, Invitrogen, CA) and the Bio-Rad PTC 200 (GMI, CA). Quantitative real-time PCR was performed by employing the mixture of FastStart Universal SYBR Green Master (Roche, USA),

primer mix (including forward and reverse primers), PCR water and diluted cDNA. Relative gene expression was determined using the $-2^{\Delta\Delta Ct}$ method and normalized to the mRNA level of β-actin. Primer sequences are listed in **Appendix II**.

High Performance Liquid Chromatography

Quantitative analysis of LYC was performed utilizing high performance liquid chromatography (HPLC) techniques. Briefly, approximately 100 mg of liver tissue was homogenized in 3 ml of ethanol and saline (2:1 vol/vol) and extracted with 3.5 ml of hexane and ether (1:1 vol/vol). Extracts were vortexed for 1 minute followed by centrifugation at 2,000g for 10 minutes at 4°C and collection of the supernatant. Samples were extracted via this method 3 times followed by evaporation under nitrogen gas and reconstitution in 100 µl of ethanol and ether (2:1 vol/vol). 50 µl of the final extract was then injected into the HPLC system. The HPLC system consisted of a 2695 separation module and a 2998 photodiode array detector (Waters Corporate, Milford, MA). Separation was performed on a YMC C30 column (S-3 micron, 4.6 × 150 mm) (YMC, Wilmington, NC, USA) and the following gradient was used: 0 min, 90% A (methanol and 1% ammonium acetate [9:1 vol/vol]) and 10% B (methyl-ter-butyl ether); 20 min, 85% A and 15% B; 30 min, 40% A and 60% B; 40 min, 30% A and 70% B; 52 min, 90% A and 10% B. The flow was set at 1 ml/min and LYC concentrations were measured at 472 nm and quantified utilizing the area under the curve respective to an appropriate standard curve. An internal control (retinoic acid) was added to ensure efficient extraction and all procedures were performed under red light.

ELISA

The reagents for IL-1β and IL-6 ELISA were from R&D System and BD Biosciences, respectively. Cytokine concentrations in liver and plasma were quantified according to the manufacturer protocols. Briefly, the capture antibody was diluted to 4 µg/ml in Binding Solution and 100 µl of diluted antibody was added to each well. Then plates were sealed and incubated overnight at 4 °C, after which time 200 µl/well Blocking Buffer was added to block non-specific binding, and the plates were then incubated at room temperature (RT) for 1 hour. Plates were washed 3 times with PBS/Tween. After adding standards and samples, we added 100 µl diluted antibody to each well and incubated the plate for 1 hour at RT. After washing plate, we added 100 µl Av-HRP. The plate was then incubated at RT for 30 minutes. ABTS substrate solution was added to the plate for color development for1 hour at RT. OD at 405 nm was read for cytokine concentration calculation.

Analysis of Plasma Free Fatty Acids (FFA)

Plasma FFA was measure by utilizing a FFA colorimetric assay kit (Abcam, Cambridge, USA). Briefly, after adding 2 µL of acyl-coA synthetase reagent to each sample and standard well, total mixture was incubated for 30 min at 37 °C. Then 50 µL of reaction mix was added to each well and the entire plate was incubated for 30 min at 37 °C protected from light. The concentration of FFA in each well was quantified by reading the absorbance at 570 nm.

Statistical Analyses

SAS 9.3 software was employed for the statistical analysis. Differences among groups were determined by using one-way ANOVA followed by Tukey post-hoc test.

Two-way ANOVA was used to examine the effects of TP or SIRT1 mutation on continuous variables. The Mann-Whitney U test was used to compare liver steatosis score distribution among groups. The χ^2 test was used to examine the difference on liver tumor incidence. Statistical significance was set as $P < 0.05$.

RESULTS

TP Attenuated NAFLD

There was no significant difference in average food consumption, final body weight, liver weight or liver weight/body weight ratio, and total fat mass/body weight ratio among four groups (**Table 1**). Lycopene was undetectable in mice without TP supplementation. In WT+TP mice, hepatic lycopene was 7.72 ± 1.69 nmol/g liver, which was comparable with the hepatic lycopene concentration in MT+TP mice at 7.36 ± 2.02 nmol/g liver. HCC incidence, liver tumor multiplicity, and liver tumor volume were not altered by either TP supplementation, or systemic SIRT1 ablation (**Table 2**). We did not observe inflammation foci incidence in the current study. We quantified SIRT1 protein levels in four groups and found tomato powder (TP) supplementation significantly increased SIRT1 protein expression in WT mice (**Figure 1A**). To determine SIRT1 deacetylase activity, we quantified the acetylation of FoxO1, and found MT mice had significantly higher acetylated-FoxO1 to total-FoxO1 ratio, compared with WT mice (**Figure 1B**).

Using histopathology analysis, we found liver steatosis significantly decreased in animals with TP supplementation, in both WT and MT groups (**Figure 1C**), suggesting that TP can inhibit liver steatosis independent of SIRT1 deacetylase activity. We also

observed an increase of liver steatosis in MT mice, compared to WT mice, but the difference did not reach statistical significance ($P = 0.14$). Mice fed TP had substantially lower TG concentration in plasma, in both WT and MT groups. Plasma FFA concentration was comparable among four groups.

TP Decreased NAFLD in WT and MT Mice Through Different Mechanisms

To explore the underlying mechanism by which TP decreased liver steatosis, we first quantified mRNA and protein levels of genes that are involved in fatty acid synthesis and fatty acid oxidation. As a result, the phosphorylation of acetyl-CoA carboxylase (ACC), which inactivates ACC, did not change between WT and WT+TP mice, but significantly increased in MT+TP mice, compared with MT mice (**Figure 2A**). This was correlated with unchanged phosphorylation of AMP-kinase (AMPK) in WT vs. WT+TP mice, but enhanced p-AMPK in MT+TP mice, compared with MT mice (**Figure 2B**), indicating that TP inhibits ACC mediated by AMPK signaling. Other fatty acid synthetic enzymes such as stearoyl-CoA desaturase 1 (SCD1), sterol regulatory element-binding protein 1 (SREBP-1) and peroxisome proliferator-activated receptor α (PPARα) did not change among four groups (**Supplemental Figure 2A-C**). We also quantified the mRNA levels of six lipogenic genes (*acc*, *fas*, *scd1*, *srebp-1c*, *lxrα*, *pparα*), which presented comparable expressions among four groups (**Supplemental Figure 3A**). The hepatic mRNA levels of four fatty acid oxidation related genes (*acox1*, *acox3*, *cpt1*, *sirt3*) also remained unchanged among four groups (**Supplemental Figure 3B**). These data indicate that decreasing hepatic fatty acid synthesis might be a major mechanism by which TP mitigates hepatic steatosis in MT mice, but not WT mice.

It has been well-established that intrahepatic TG accumulation could be due to two mechanisms: 1) increasing *de novo* fatty acid synthesis versus fatty acid oxidation; and 2) exceeding hepatic lipid uptake compared to lipid output [70]. With the observation that in WT mice, TP inhibited hepatic steatosis development without altering hepatic lipid metabolism/catabolism, we examined the expressions of genes related to lipid transportation. Fatty acid binding protein 1 (FABP1) is mainly expressed in livers at high levels and facilitates the uptake of long chain fatty acid (LCFA) [71]. In the present study, we found that compared to WT mice, the mRNA level of *fabp1* increased in MT mice ($p = 0.087$), while *fabp1* expression was decreased in WT+TP vs. WT mice (**Figure 2C**), suggesting that the anti-NAFLD effect of TP in WT mice is associated with SIRT1-mediated decrease of LCFA uptake by the liver. Interestingly, by using two-way ANOVA analysis, we found that the mRNA of *cd36*, another fatty acid translocase that imports LCFA, significantly increased in MT mice, compared to WT mice ($p = 0.048$), while the mRNA of microsomal triglyceride transporter protein (*mttp*), a transporter that exports TG, significantly decreased in MT mice, as compared with their WT counterparts ($p = 0.016$, **Figure 2C**). Such data suggest that the lack of SIRT1 activity induces hepatic TG accumulation, possibly through increasing fatty acid uptake and inhibiting TG clearance. We also assessed the mRNA level of genes related to lipolysis in MAT (*plin-2*, *atgl*, *hsl*), which presented comparable transcription levels among the four groups (data not shown).

TP Reduced MAT Fatty Acid Synthesis

FFA released from MAT can be directly delivered to liver through portal vein [72]. We quantified the mRNA levels of eight lipogenic genes (*acc*, *fas*, *scd1*, *dgat1*,

dgat2, *lxr-α*, *srebp-1c*, *pparγ*) in MAT, and found that *acc*, *fas* mRNA levels significantly decreased with TP supplementation in both WT and MT mice. Compared to WT mice, MT mice had higher *scd1* transcription, which was decreased to normal level after TP supplementation. In WT mice, TP inhibited *dgat1* and *dgat2* mRNA, indicating decreased fatty acid synthesis (**Figure 3A**). To further investigate the underlying mechanism for the inhibited lipogenic gene expressions by TP, we determined the phosphorylation of AMPK in MAT. As a result, p-AMPK level was significantly higher in TP supplemented mice, in both WT and MT groups (**Figure 3B**). To examine the effect of TP on lipid catabolism, we measured the mRNA levels of five β-oxidation related genes (*ucp1*, *ucp2*, *cpt*, *acox1*, *acox3*), and consistent with the data in liver, these genes presented comparable mRNA expression among all four groups (data not shown).

TP Reduced Hepatic Inflammation

Cytokines and adipokines play a pivotal role in the development of NAFLD [73]. Results from ELISA showed that TP significantly lowered the concentration of hepatic IL-1β, a proinflammatory cytokine, in WT mice (**Figure 4A**). IL-1β is synthesized as a biologically inactive pro-IL-1β polypeptide and requires to be cleaved by caspase-1 to generate mature IL-1β [74]. In the present study, the mRNA level of pro-il-β was similar among groups (**Figure 4C**), but a lowered mRNA level of *caspase-1* was observed in WT+TP mice, suggesting that TP may decrease hepatic IL-1β concentration in WT mice in a post-translational manner.

In MT mice, TP supplementation significantly decreased hepatic IL-6 concentration without altering hepatic *il-6* mRNA level (**Figure 4B**). Interestingly, we found plasma IL-6 concentration significantly decreased in MT+TP mice, compared to

MT mice, indicating that reduced hepatic IL-6 in MT+ TP mice might be due to less circulating IL-6 delivered from plasma to liver (**Figure 4D**). The notion that one-third of circulating IL-6 is estimated to originate from adipose tissue [75] prompted us to examine MAT *il-6* transcription, which presented significant reduction in MT+TP mice, compared to MT mice (**Figure 4E**). Along with that, MAT *il-1β* and *mcp1* significantly increased in MT mice, compared to WT mice, and giving TP supplementation decreased both *il-1β* and *mcp1* to normal level (**Figure 4E**). These data lead us to propose that in MT mice, TP supplementation may decrease hepatic IL-6 concentration by decreasing circulating IL-6, presumably through reducing MAT *il-6* transcription.

TP Generated Limited Effects in HCC Development

Although it has been proposed that NAFLD and hepatic inflammation are major risk factors for HCC development [15, 76, 77], in the current study, TP did not affect HCC development in both WT and MT mice, despite significantly decreased hepatic steatosis and inflammation observed with TP supplementation in both WT and MT mice. Chronic MAPK activation can promote HCC development via inducing the phosphorylation on loop residues Thr202/Tyr204 by MEK1/2 [78, 79]. Unexpectedly, in the current study, we found TP supplementation increased p38 MAPK phosphorylation in both WT and MT mice (**Figure 5A**), which was associated with increasing APMK activation. Other protein/kinases related to cell proliferation or apoptosis, such as cleaved PARP, NF-κB, p-STAT3, or p-mTOR, remained unchanged among four groups (**Supplemental Figure 3A-D**). We also examined the mRNA expressions of four genes involved in regulating cell cycle (*p21*, *p27*, *p53*, *cyclin D1*), and found the mRNA and

protein levels of p21 significantly increased in MT mice, with or without TP, compared to WT mice, while other genes did not among four groups (**Figure 5B,C**).

DISCUSSION

The present study has provided first evidence that TP can inhibit carcinogen-induced, HFD-promoted liver steatosis and inflammation, independent of SIRT1 catalytic activity. In the WT mice, TP decreased NAFLD by 1) decreasing LCFA uptake in the liver; and 2) decreasing hepatic IL-1β maturation; in the MT mice, TP attenuated NAFLD development by 1) reducing *de novo* hepatic FA synthesis; and 2) reducing circulating IL-6 released from MAT, resulting in decreased hepatic IL-6 concentration.

TP increase SIRT1 protein by decreasing caspase 1 in WT. In the current study, dietary TP significantly increased hepatic SIRT1 protein level in WT+TP vs. WT mice, without interfering *sirt1* mRNA, indicating a post-transcriptional modification. This agrees with previous finding that supplementation with ALA, a lycopene metabolite, induced SIRT1 protein expression without changing *sirt1* mRNA level [24]. Chalkiadaki et al. has shown that SIRT1 can be cleaved by caspase-1, under a HFD surplus [80]. In the present study, a significant decrease of *caspase-1* mRNA was observed in mice fed with TP, suggesting that TP might be capable of inhibiting caspase-1 induction triggered by HFD and subsequently decreasing caspase-1 mediated SIRT1 cleavage. Compared to WT mice, MT mice showed substantial increase in actylated-FoxO1, indicating a significant decrease of SIRT1 deacetylase activity [36], which confirms the efficiency of SIRT1 activity ablation in our mouse model. The acetylated-FoxO1/total-FoxO1 ratio, however, was comparable between WT and WT+TP mice. This is possibly because genetic modification has greater effect on SIRT1 activity than dietary effect does.

TP decreases lipogenesis in MT mice via AMPK-ACC axis. ACC is a rate-limiting enzyme in *de novo* synthesis of fatty acids [70]. In the current study, we found p-ACC, the inactive form of ACC, was significantly lower in MT, while giving TP restored ACC phosphorylation that was impaired by SIRT1 mutation. A similar pattern was observed in AMPK phosphorylation, which was inhibited in MT mice, but restored by TP supplementation, suggesting that TP might decrease lipogenesis via AMPK-ACC axis. It should be noted that although we observed an increase of p-AMPK in WT+TP vs WT mice, the increase did not reach statistical significance, probably due to limited sample size. Controversies have been addressed recently on whether the activation of AMPK depends on SIRT1 activity [81, 82]. One previous study showed that ablating SIRT1 activity decreased liver kinase b1 (LKB1) phosphorylation at Ser^{428}, resulting in decreased AMPK phosphorylation [36]. However, in the current study, TP did not affect LKB phosphorylation (data not shown), it thus requires further investigation to determine how TP activates AMPK in the absence of SIRT1.

TP decreases hepatic steatosis in WT mice via decreasing fabp3 expression. Previous studies reported that overexpression of *fabp1* caused excessive hepatic TG accumulation [83-85], while silencing FABP1 ameliorated hepatic steatosis and inflammation in mice with NAFLD [71]. One provoking finding in our study was that compared to WT mice, MT mice had higher *fabp1* transcription, while mice in WT+TP group had lower *fabp1* mRNA level, suggesting that TP can mitigate hepatic steatosis through inhibiting FABP1-mediated LCFA uptake. Importantly, the inhibitory effect of TP on *fabp1* was blunted in MT mice, indicating that TP decreases *fabp1* transcription in a SIRT1 dependent pathway. Unexpectedly, on the contrary to decreased *fabp1*

expression, the mRNA expression of *fabp3* was significantly increased in WT+TP mice, which might be the consequence of reduced *fabp1* mRNA, given that FABP1 knock-out increased *fabp3* transcription [71]. Furthermore, since the hepatic FABP3 concentration is 200–1000 times lower than that of FABP1 [71], the impact of FABP3 on liver LCFA uptake is minimal. In the present study, we also examined the effect of SIRT1 ablation on lipid metabolism, and found that hepatic mRNA level of *cd36* significantly increased in MT mice, compared to WT mice, which was consistent with previous findings [36, 86]. Additionally, SIRT1 activity ablation caused a marked decrease of *mttp* transcription, which serves as evidence for impaired TG export in MT mice [87], ; it may help explaine increased hepatic TG concentration in MT vs. WT mice ($p = 0.04$). Dietary TP did not affect *cd36* and *mttp* transcription in both WT and MT mice.

TP imposed protective efficacy against lipogenesis in MAT. The mRNA levels of *acc* and *fas* were significantly lowered by TP supplementation and the phosphorylation of AMPK significantly increased by TP supplementation, in both WT and MT mice. Indeed, AMPK can be up-regulated by tomato products [88, 89] and contribute to down-regulating lipogenic genes, such as ACC, FAS, and SCD1 [88, 90-92]. However, mRNA expressions of these genes were not changed by inducing AMPK in the liver, indicating that TP-induced AMPK activation might regulate lipogenesis in a tissue-specific manner. Despite documented inhibitory effect of AMPK against lipolysis [90, 93], we found that plasma FFA concentration and lipolysis-related gene expressions (*plin-2*, *atgl*, *hsl*) were comparable among four groups. Genetic modification of SIRT1 did not impact lipolysis either, showing discrepancy with our previous finding that systemic ablation of SIRT1 increased MAT lipolysis, and promoted the mobilization of FFA from MAT to liver [36].

One possible explanation for the inconsistency is that in the current study, we developed HCC mouse model using injection of DEN, a widely reported carcinogen that initiates tumorigenesis by inducing Wnt/β-catenin signaling [94], which can subsequently upregulate lipolysis by activating ATGL and HSL [95], resulting in mitigated anti-lipolysis effects exerted by AMPK and SIRT1.

TP lowered il-6 expression in MAT, contributing to lowered IL-6 concentration in plasma and liver. It has been reported that lycopene-rich tomato products have anti-inflammatory functions in both animal and epidemiology studies [13, 96]. In the current study, TP decreased hepatic IL-1β concentration in WT+TP mice, compared to WT mice, whereas MT and MT+TP mice presented similar hepatic IL-1β level. The observation of unchanged hepatic mRNA expression of *il-1β* and comparable protein level of NF-κB, a well-known transcription factor for pro-inflammatory cytokines, indicates that TP reduces IL-1β via a post-translational mechanism. Accumulating evidence has shown that caspase-1 is a central regulator of HFD-induced NAFLD by proteolytically cleaving IL-1β into its active form [97, 98], while IL-1β knock-out protects mice against early stages of NAFLD by decreasing the maturation of IL-1β [98]. Caspase-1 is a downstream effector of NLRP3 (NACHT, LRR and PYD domains-containing protein-3) inflammasome [99], which can be stimulated under HFD surplus [98, 99] while attenuated by SIRT1 activation [100]. Zhou et al. reported that adenovirus-mediated SIRT1 overexpression only partially suppressed HFD-induced NLRP3 inflammasome pathway, whereas improving SIRT1 activity by replenishing NAD^+ pool completely inhibited NLRP3-mediated TNFα and IL-1β expression [101]. Therefore, SIRT1 activity, rather than its protein expression, is more important in suppressing NLRP3 pathway,

which explains why TP decreased *caspase-1* transcription only in WT mice, but not in MT mice. Compared to liver, TP had even more significant effect on inhibiting inflammatory cytokines in MAT by decreasing *il-1β, il-6* and *mcp-1* transcription, possibly due to varied lycopene, or lycopenoid distribution resultant from TP supplementation in different tissue [102]. Previous studies reported that lycopene was capable of reducing IL-6 released from adipose tissue, resulting in decreased circulating IL-6 level [25, 103]. This was concordant with our observation of decreased MAT *il-6* transcription and decreased systemic IL-6 concentration with TP supplementation, indicating that TP inhibits hepatic inflammation via MAT-liver axis. NASH is a more advanced stage of NAFLD, which can be distinguished by the presence of inflammation and hepatocyte ballooning [104]. In the present study, we did not observe the occurrence of NASH, possibly owing to the feature of 129/SvJ and CD-1 strains, as both of them exhibit less susceptibility to hepatocyte enlargement than C57BL/6 mice under the same dietary intervention [105]. Although we observed decreased IL-6 or IL-1β concentration in liver and plasma in mice fed dietary TP, it is important to note that these biomarkers represented a status of chronic inflammation possibly resultant from DEN injection, which differs from NASH that was induced metabolically [106].

No significant effects of TP or SIRT1 activity were observed in HCC development. In spite of the inhibitory effect against hepatic steatosis and inflammation, TP did not show anti-HCC benefits in our study. This might be related to the activated MAPK signaling, a paradoxical effect of enhanced p-AMPK on cell survival. Although AMPK is essential for metabolic control by inhibiting anabolic processes and stimulating catabolic pathways, it also contributes to activating p38 MAPK signaling pathway [107, 108], and

global MAPK overexpression could induce aberrant cell proliferation and survival [78, 79, 109]. Therefore, in dietary TP, the anti-HCC effect through decreasing AMPK-inhibited hepatic steatosis and inflammation might be counteracted by AMPK-induced p38 MAPK activation. It is important to note that in the current study, lack of systemic SIRT1 activity did not affect HCC development. Cyclin-dependent kinase inhibitor p21 is best known as a tumor suppressor for its activities in modulating cellular apoptosis and survival [110]. Results from our study showed that both hepatic mRNA and protein levels of p21 significantly increased by ablating SIRT1 activities, which is concordant with previous report that SIRT1 can destabilize p53, consequently inhibiting p21 [111] while inhibition of SIRT1 restored p21-dependent cell-cycle arrest [112]. Increased p21 expression possibly compromised the effects of SIRT1 ablation on inducing hepatic steatosis and inflammation, causing comparable HCC incidence between WT and MT mice. The unaltered HCC development among groups could also be due to one limitation of our study for not being able to monitor tumor growth *in vivo* at multiple time points. It has been revealed that a single injection of 20 mg/kg DEN in 129/SvJ mice resulted in 80-100% HCC after 30-55 weeks [113, 114]. Using a similar HCC mouse model, mice did not show HCC incidence at 30 week-of-age in our pilot study, which led us to extend the study period to 40 weeks for the purpose of observing tumor incidence. Indeed, we could not rule out the possibility that dietary TP affected tumorigenesis, or the transition from adenoma to carcinoma at an earlier stage. However, since TP resembles whole food, rather than pharmacologic compounds, it is within expectation that TP might be an efficient dietary strategy for preventing metabolic disorders, but not a potent treatment against HCC initiated by detrimental carcinogen exposure.

TP dose rationale. In the present study, the hepatic lycopene level (7.56 ± 1.24 nmol/g tissue) was within the range of lycopene concentration in normal human liver (0.2 - 20.7 nmol/g tissue) [115], suggesting that the TP dosage used in our study is physiologically achievable and relevant in public health. However, this concentration is lower than the hepatic lycopene concentration of 19.4 ± 4.1 nmol/g tissue in C57BL6 mice fed 100 mg lycopene/kg diet, as reported by Ip et al. [62], which is possibly due to differential absorption efficiency of lycopene in different animal strains. It is worth mentioning that lower lycopene concentrations might also contribute to limited benefits from dietary TP observed in the present study. One limitation of our study is that we did not compare the effect of TP with lycopene, since Ip et al. previously reported that lycopene exerted anti-NAFLD effects mainly by inducing PPARα and PPARγ-related genes, without affecting SIRT1 activity [25], indicating that SIRT1 was not the direct target of lycopene in impeding NAFLD development.

Taken together, we provided the first evidence that TP supplementation elicited differential mechanism of inhibitory effects against hepatic steatosis and inflammation. In WT mice, TP-mediated anti-NAFLD effects were associated with decreasing FFA uptake and inhibiting IL-1β maturation whereas in MT mice, TP ameliorated NAFLD development by decreasing hepatic lipogenesis and inhibiting the release of IL-6 from MAT to liver (**Figure 6A**). However, neither TP supplementation nor SIRT1 mutation affected HCC development. Since TP is effective irrespective of the presence or absence of SIRT1 deacetylase activity, our findings suggest that dietary TP could be an effective dietary agent for preventing NAFLD development, especially in population with impaired SIRT1 activity.

TABLE 1

Food intake, body weights, liver weights, liver/body weight, fat mass/body weight of DEN-injected, HFD-fed WT or MT mice with or without TP supplementation for 34 weeks[1].

Study group	WT (N = 18)	WT+TP (N = 16)	MT (N = 13)	MT+TP (N = 15)	Diet effect	Strain effect
Food intake, g/d	3.9 ± 0.22	3.8 ± 0.15	3.8 ± 0.34	3.7 ± 0.40	0.86	0.69
Body weights, g	44.74 ± 1.48	44.47 ± 1.43	41.50 ± 1.52	44.51 ± 1.51	0.42	0.31
Liver weights, g	1.65 ± 0.14	1.79 ± 0.27	1.64 ± 0.13	1.64 ± 0.12	0.69	0.70
Liver/body weight, %	3.58 ± 0.21	3.95 ± 0.57	4.06 ± 0.42	3.72 ± 0.29	0.91	0.75
Fat mass/body weight, %	20.05 ± 1.32	21.15 ± 1.06	19.96 ± 1.84	20.15 ± 1.75	0.57	0.63

[1]Values are means ± SEMs. One-way ANOVA followed by Tukey post-hoc test was used to compare values among four groups. Two-way ANOVA was used to examine the diet or strain effects, which are shown as *p* values. WT, wild-type; MT, mutant; TP, tomato powder.

TABLE 2

Steatosis score, HCC incidence by histopathology analysis, liver surface tumor multiplicity, tumor plasma TG concentration and plasma FFA concentration in all groups[1]

Study group	WT (N = 18)	WT+TP (N = 16)	MT (N = 13)	MT+TP (N = 15)	Diet effect	Strain effect
Steatosis score	1.72 ± 0.27	0.31 ± 0.27	2.46 ± 0.24	0.67 ± 0.21	**<0.0001**	0.14
HCC incidence, %	50[ab]	37.5[a]	64.3[b]	54.3[ab]	0.45	0.32
Tumor multiplicity, n	2.78 ± 1.04	2.06 ± 1.01	1.92 ± 0.84	1.80 ± 0.76	0.69	0.70
Tumor volume, cm^3	1.61 ± 0.82	6.71 ± 4.50	2.89 ±2.13	2.20 ± 1.34	0.48	0.64
Plasma TG, mg/dl	1.52 ± 0.27	1.26 ± 0.53	1.58 ± 0.49	1.38 ± 0.38	**0.04**	0.39
Plasma FFA, mg/dl	0.62 ± 0.28	0.73 ± 0.31	0.84 ± 0.37	0.66 ± 0.25	0.59	0.73

[1]Values are %, means ± SEMs. One-way ANOVA followed by Tukey post-hoc test was used to compare values among four groups. Two-way ANOVA was used to examine the diet or strain effects, which are shown as *p* values. Bolded font represents $p < 0.05$. WT, wild-type; MT, mutant; TP, tomato powder, TG, triglyceride; FFA, free fatty acid.

FIGURE 1

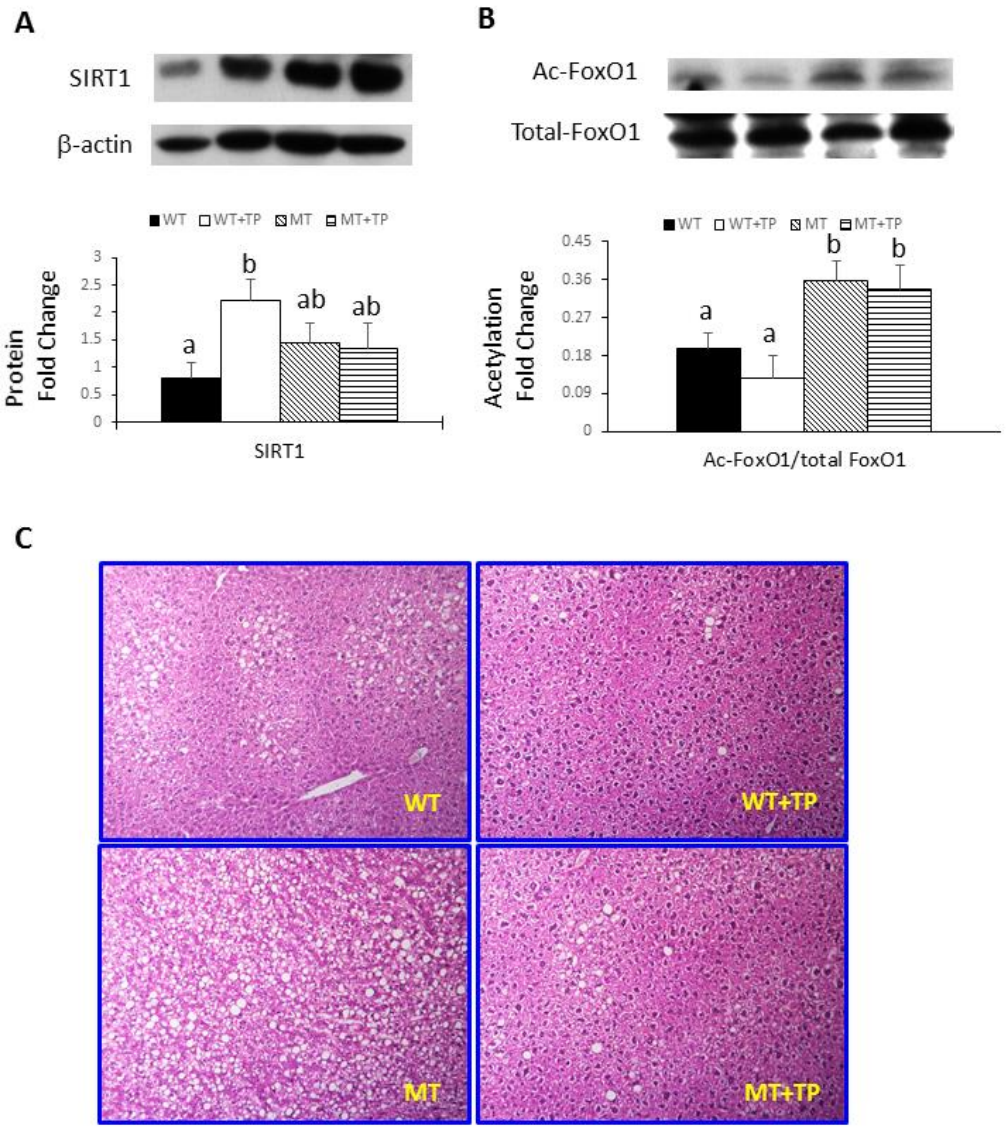
A
SIRT1
β-actin
WT WT+TP MT MT+TP
Protein Fold Change
3
2.5
2
1.5
1
0.5
0
a
b
ab
ab
SIRT1
B
Ac-FoxO1
Total-FoxO1
WT WT+TP MT MT+TP
Acetylation Fold Change
0.45
0.36
0.27
0.18
0.09
0
a
a
b
b
Ac-FoxO1/total FoxO1
C
WT
WT+TP
MT
MT+TP

FIGURE 2

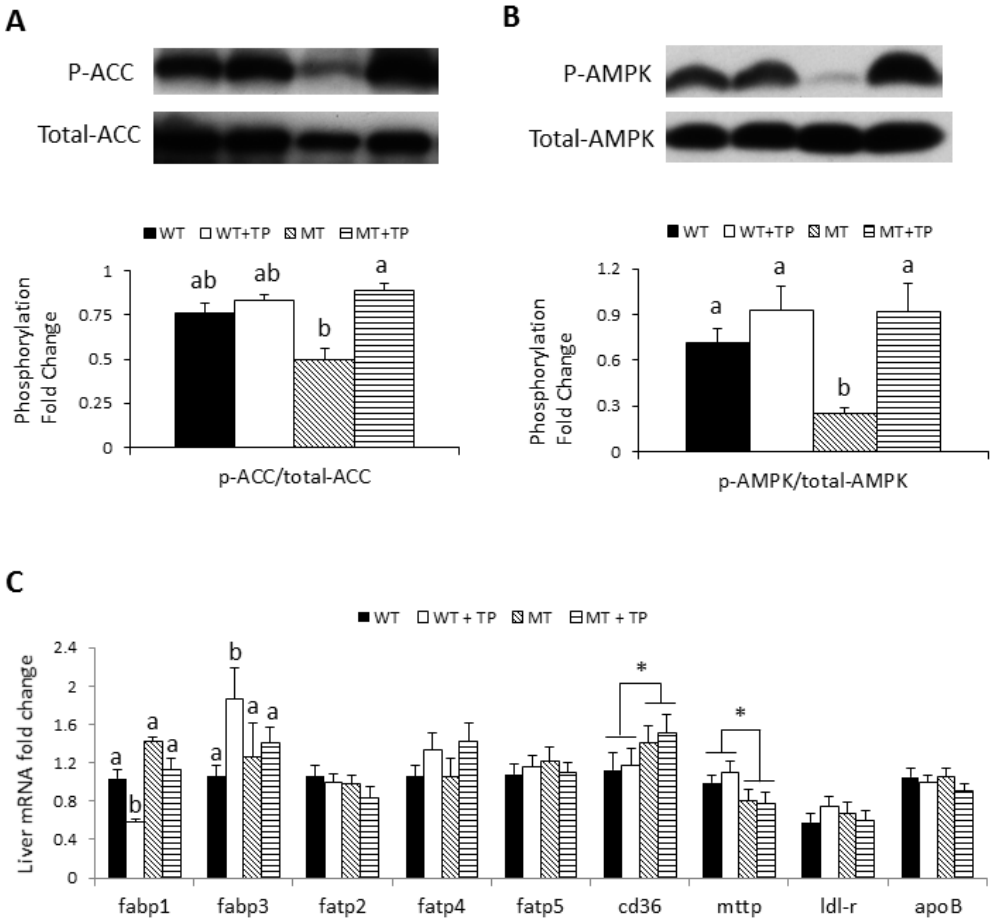
A
P-ACC
Total-ACC
WT WT+TP MT MT+TP
Phosphorylation Fold Change
p-ACC/total-ACC
B
P-AMPK
Total-AMPK
WT WT+TP MT MT+TP
Phosphorylation Fold Change
p-AMPK/total-AMPK
C
WT WT + TP MT MT + TP
Liver mRNA fold change
fabp1
fabp3
fatp2
fatp4
fatp5
cd36
mttp
ldl-r
apoB

FIGURE 3

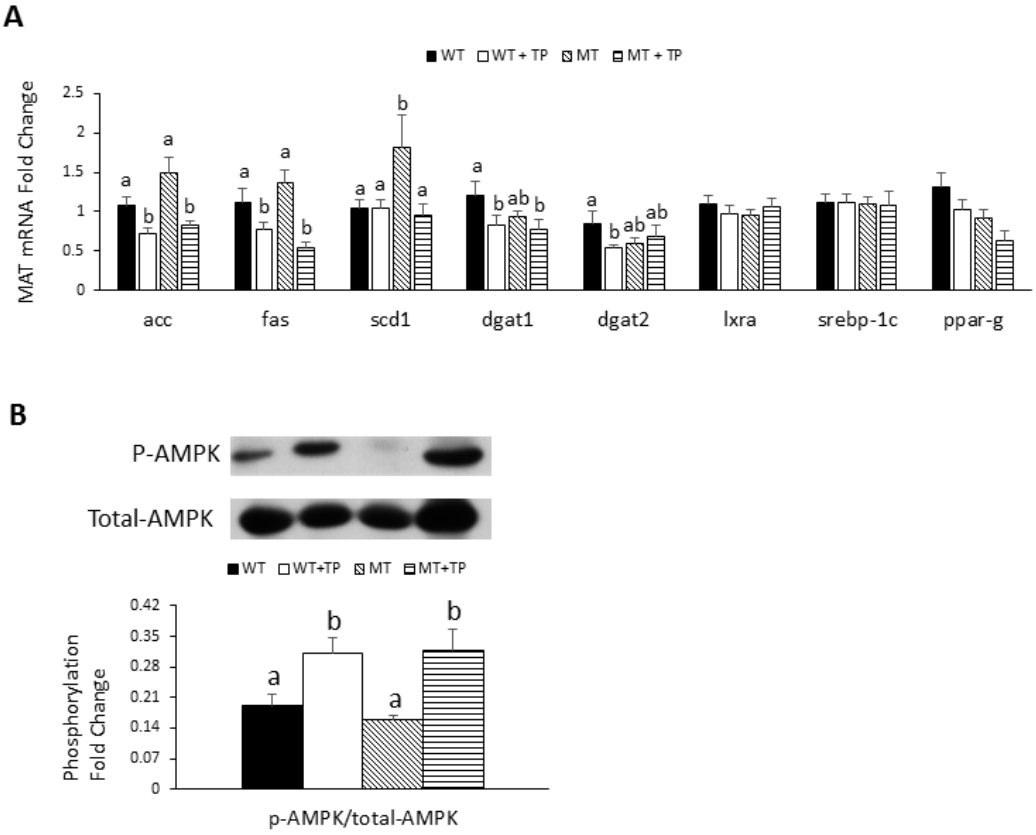
A
WT
WT + TP
MT
MT + TP
MAT mRNA Fold Change
2.5
2
1.5
1
0.5
0
a
b
a
b
a
a
a
b
a
b
a
b
a
b
b
a
b
ab
b
a
b
ab
ab
acc
fas
scd1
dgat1
dgat2
lxra
srebp-1c
ppar-g
B
P-AMPK
Total-AMPK
WT
WT+TP
MT
MT+TP
Phosphorylation Fold Change
0.42
0.35
0.28
0.21
0.14
0.07
0
a
b
a
b
p-AMPK/total-AMPK

FIGURE 4

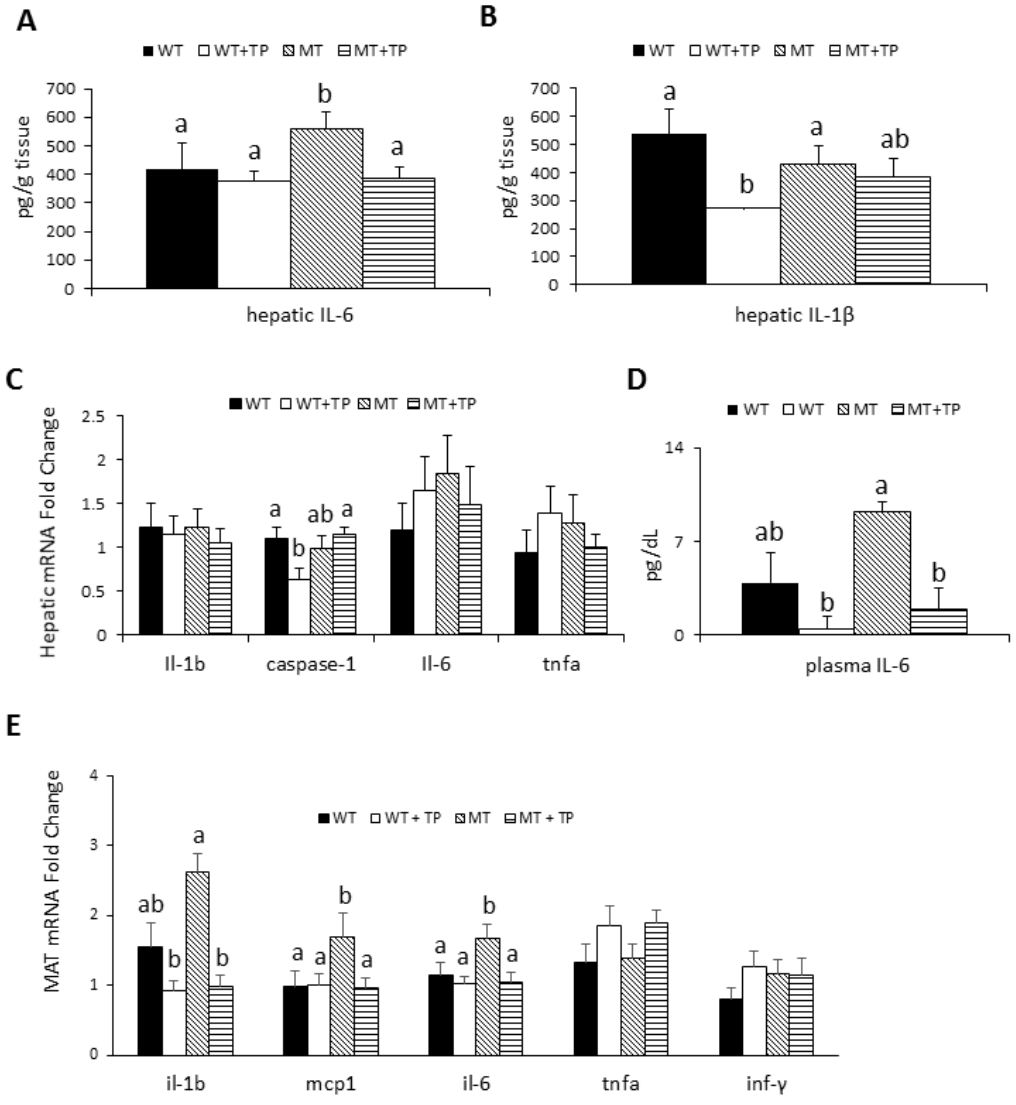
A
WT WT+TP MT MT+TP
pg/g tissue
hepatic IL-6
B
WT WT+TP MT MT+TP
pg/g tissue
hepatic IL-1β
C
WT WT+TP MT MT+TP
Hepatic mRNA Fold Change
Il-1b
caspase-1
Il-6
tnfa
D
WT WT MT MT+TP
pg/dL
plasma IL-6
E
WT WT+TP MT MT+TP
MAT mRNA Fold Change
il-1b
mcp1
il-6
tnfa
inf-γ

FIGURE 5

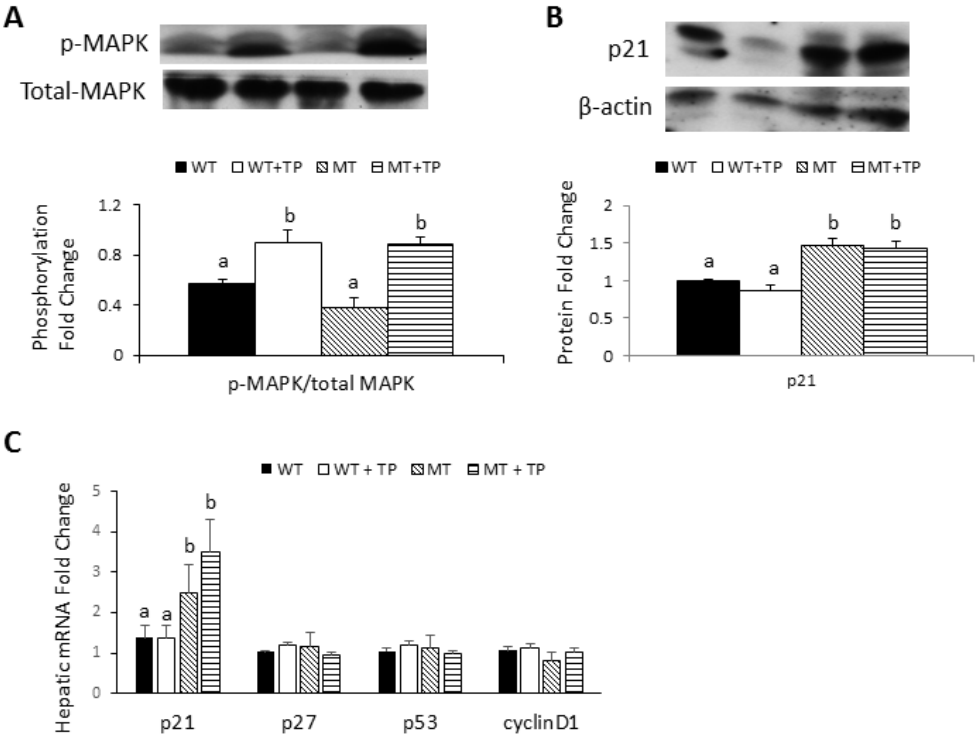
A
p-MAPK
Total-MAPK
WT WT+TP MT MT+TP
Phosphorylation Fold Change
1.2
0.8
0.4
0
a
b
a
b
p-MAPK/total MAPK
B
p21
β-actin
WT WT+TP MT MT+TP
Protein Fold Change
2
1.5
1
0.5
0
a
a
b
b
p21
C
WT WT + TP MT MT + TP
Hepatic mRNA Fold Change
5
4
3
2
1
0
a
a
b
b
p21
p27
p53
cyclinD1

FIGURE 6

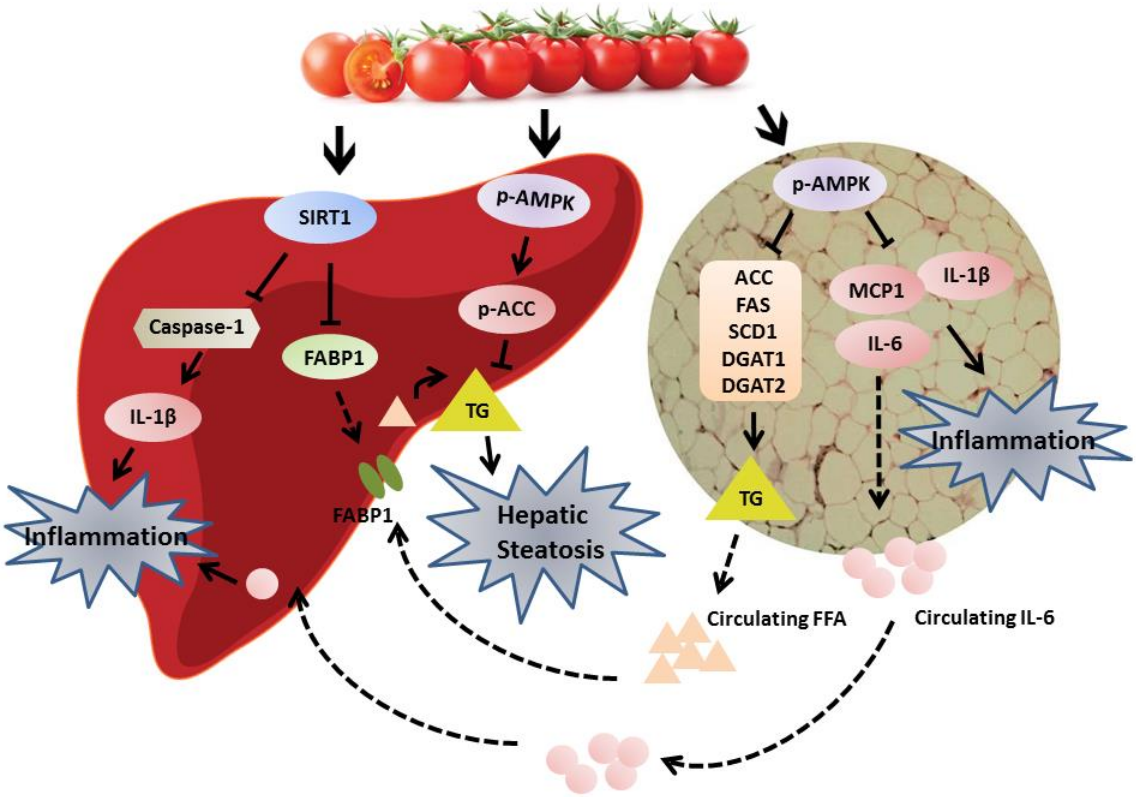
SIRT1
p-AMPK
Caspase-1
FABP1
p-ACC
IL-1β
TG
Inflammation
FABP1
Hepatic Steatosis
p-AMPK
ACC
FAS
SCD1
DGAT1
DGAT2
MCP1
IL-1β
IL-6
Inflammation
TG
Circulating FFA
Circulating IL-6

FIGURE LEGENDS

Figure 1. Hepatic SIRT1 expression and activity and histopathology of liver steatosis in WT, WT+TP, MT, or MT+TP mice. Graphic representation of protein fold changes in: **A**, SIRT1, β-actin as loading control; **B**, acetylated-FoxO1, total-FoxO1 as loading control; and **C**, representative picture of H&E stained liver at x25. Values are means ± SMEs. One-way ANOVA followed by Tukey post-hoc test was used to compare protein expressions among four groups. Different letters indicate statistical difference ($p < 0.05$). WT, wild-type; MT, mutant; TP, tomato powder.

Figure 2. Hepatic lipogenesis, lipid transportation-related gene mRNA and protein expressions in WT, WT+TP, MT, or MT+TP mice. Graphic representation of protein fold changes in: **A**, phosphorylated ACC (Ser79; ACC as loading control); **B**, phosphorylated AMPK (Thr172; AMPK as loading control); and mRNA fold changes in: **C**, lipid transportation-associated genes: *fabp1*, *fabp3*, *fatp2*, *fatp4*, *fatp5*, *cd36*, *mttp*, *ldl-r*, *apoB*. Values are means ± SMEs. One-way ANOVA followed by Tukey post-hoc test was used to compare protein or mRNA expressions among four groups. Different letters indicate statistical difference ($p < 0.05$). Two-way ANOVA was used to compared mRNA expressions between WT and MT mice. * MT different from WT, $p < 0.05$. WT, wild-type; MT, mutant; TP, tomato powder.

Figure 3. Lipogenesis and β-oxidation -related gene mRNA and protein expressions in MAT in WT, WT+TP, MT, or MT+TP mice. Graphic representation of fold changes in: **A**, mRNA of lipogenesis-associated genes: *acc*, *fas*, *scd1*, *dgat1*, *dgat2*, *lxrα*, *srebp*-1c, *pparγ*; **B**, phosphorylated AMPK (Thr172; AMPK as loading control); and **C**, mRNA of fatty acid oxidation-associated genes: *ucp1*, ucp2, *cpt1*, *acox1*, *acox3*. Values are means

± SMEs. One-way ANOVA followed by Tukey post-hoc test was used to compare protein or mRNA expressions among four groups. Different letters indicate statistical difference ($p < 0.05$). MAT, mesenteric adipose tissue; WT, wild-type; MT, mutant; TP, tomato powder.

Figure 4. Hepatic *caspase-1* mRNA expression, protein and mRNA levels of inflammatory cytokines in liver, plasma and MAT in WT, WT+TP, MT, or MT+TP mice. Graphic representation of fold changes in: **A**, hepatic IL-6 protein concentration; **B**, hepatic IL-1β protein concentration; **C**, mRNA of *caspase-1* and hepatic inflammatory cytokines: *il-1β*, *il-6*, *tnfα*; **D**, plasma IL-6 concentration; and **E**, MAT mRNA of inflammatory cytokines: *il-1β*, *mcp1*, *il-6*, *tnfα*, *inf-γ*. Values are means ± SMEs. One-way ANOVA followed by Tukey post-hoc test was used to compare protein or mRNA expressions among four groups. Different letters indicate statistical difference ($p < 0.05$). MAT, mesenteric adipose tissue; WT, wild-type; MT, mutant; TP, tomato powder.

Figure 5. Hepatic protein and mRNA expressions of cell cycle-related genes in WT, WT+TP, MT, or MT+TP mice. Graphic representation of fold changes in: **A**, phosphorylated-MPAK (Thr202/Tyr204, total-MAPK as loading control); **B**, p21 (β-actin as loading control), and **C**, hepatic mRNA of cell cycle-related genes: *p21*, *p27*, *p53*, *cyclinD1*. Values are means ± SMEs. One-way ANOVA followed by Tukey post-hoc test was used to compare protein or mRNA expressions among four groups. Different letters indicate statistical difference ($p < 0.05$). WT, wild-type; MT, mutant; TP, tomato powder.

Figure 6. TP supplementation elicited differential mechanism of inhibitory effects against hepatic steatosis and inflammation: in WT mice, TP-mediated anti-NAFLD

effects were associated with (1) increasing SIRT1 and decreasing FABP1-mediated LCFA uptake; and (2) inhibiting IL-1β maturation through suppressing caspase-1; while in MT mice, TP ameliorated NAFLD development by (1) activating AMPK signaling and decreasing *de novo* lipogenesis; and (2) inhibiting MAT IL-6 production, resulting in less liver IL-6 uptake from circulating system. WT, wild-type; MT, mutant; TP, tomato powder; NAFLD, non-alcoholic fatty liver disease; LCFA, long-chain fatty acid.

LITERATURE CITED

[1] Tiniakos DG, Vos MB, Brunt EM. Nonalcoholic fatty liver disease: pathology and pathogenesis. Annual review of pathology. 2010;5:145-71.

[2] Noureddin M, Rinella ME. Nonalcoholic Fatty liver disease, diabetes, obesity, and hepatocellular carcinoma. Clinics in liver disease. 2015;19:361-79.

[3] Lazo M, Clark JM. The epidemiology of nonalcoholic fatty liver disease: a global perspective. Seminars in liver disease. 2008;28:339-50.

[4] Aleksandrova K, Stelmach-Mardas M, Schlesinger S. Obesity and Liver Cancer. Recent results in cancer research Fortschritte der Krebsforschung Progres dans les recherches sur le cancer. 2016;208:177-98.

[5] El-Serag HB, Rudolph KL. Hepatocellular carcinoma: epidemiology and molecular carcinogenesis. Gastroenterology. 2007;132:2557-76.

[6] Ferlay J, Soerjomataram I, Dikshit R, Eser S, Mathers C, Rebelo M, et al. Cancer incidence and mortality worldwide: sources, methods and major patterns in GLOBOCAN 2012. International journal of cancer. 2015;136:E359-86.

[7] Parkin DM. Global cancer statistics in the year 2000. The Lancet Oncology. 2001;2:533-43.

[8] Ryerson AB, Eheman CR, Altekruse SF, Ward JW, Jemal A, Sherman RL, et al. Annual Report to the Nation on the Status of Cancer, 1975-2012, featuring the increasing incidence of liver cancer. Cancer. 2016;122:1312-37.

[9] Siegel RL, Miller KD, Jemal A. Cancer Statistics, 2017. CA: a cancer journal for clinicians. 2017;67:7-30.

[10] Dowman JK, Tomlinson JW, Newsome PN. Pathogenesis of non-alcoholic fatty liver disease. QJM : monthly journal of the Association of Physicians. 2010;103:71-83.

[11] De Minicis S, Marzioni M, Saccomanno S, Rychlicki C, Agostinelli L, Trozzi L, et al. Cellular and molecular mechanisms of hepatic fibrogenesis leading to liver cancer. Transl Gastrointest Cancer. 2011;1:88-94.

[12] Melendez-Martinez AJ, Nascimento AF, Wang Y, Liu C, Mao Y, Wang XD. Effect of tomato extract supplementation against high-fat diet-induced hepatic lesions. Hepatobiliary surgery and nutrition. 2013;2:198-208.

[13] Ghavipour M, Saedisomeolia A, Djalali M, Sotoudeh G, Eshraghyan MR, Moghadam AM, et al. Tomato juice consumption reduces systemic inflammation in overweight and obese females. The British journal of nutrition. 2013;109:2031-5.

[14] Martin-Pozuelo G, Navarro-Gonzalez I, Gonzalez-Barrio R, Santaella M, Garcia-Alonso J, Hidalgo N, et al. The effect of tomato juice supplementation on biomarkers and gene expression related to lipid metabolism in rats with induced hepatic steatosis. European journal of nutrition. 2015;54:933-44.

[15] Ip BC, Wang XD. Non-alcoholic steatohepatitis and hepatocellular carcinoma: implications for lycopene intervention. Nutrients. 2013;6:124-62.

[16] Wang XD. Carotenoids. In: Ross AC, Caballero B, Cousins RJ, Tucker KL, Zeigler TR, editors. Modern Nutrition in Health and Disease. Phillidelphia: Lippincott Williams & Wilkins; 2012. p. 427-39.

[17] Hu KQ, Liu C, Ernst H, Krinsky NI, Russell RM, Wang XD. The biochemical characterization of ferret carotene-9',10'-monooxygenase catalyzing cleavage of carotenoids in vitro and in vivo. The Journal of biological chemistry. 2006;281:19327-38.

[18] Wang Y, Ausman LM, Greenberg AS, Russell RM, Wang XD. Dietary lycopene and tomato extract supplementations inhibit nonalcoholic steatohepatitis-promoted hepatocarcinogenesis in rats. International journal of cancer. 2010;126:1788-96.

[19] Ahn J, Lee H, Jung CH, Ha T. Lycopene inhibits hepatic steatosis via microRNA-21-induced downregulation of fatty acid-binding protein 7 in mice fed a high-fat diet. Molecular nutrition & food research. 2012;56:1665-74.

[20] Aizawa K, Liu C, Tang S, Veeramachaneni S, Hu KQ, Smith DE, et al. Tobacco carcinogen induces both lung cancer and non-alcoholic steatohepatitis and hepatocellular carcinomas in ferrets which can be attenuated by lycopene supplementation. International journal of cancer. 2016;139:1171-81.

[21] Jiang W, Guo MH, Hai X. Hepatoprotective and antioxidant effects of lycopene on non-alcoholic fatty liver disease in rat. World journal of gastroenterology. 2016;22:10180-8.

[22] Tan HL, Moran NE, Cichon MJ, Riedl KM, Schwartz SJ, Erdman JW, Jr., et al. Beta-Carotene-9',10'-oxygenase status modulates the impact of dietary tomato and lycopene on hepatic nuclear receptor-, stress-, and metabolism-related gene expression in mice. The Journal of nutrition. 2014;144:431-9.

[23] Chung J, Koo K, Lian F, Hu KQ, Ernst H, Wang XD. Apo-10'-lycopenoic acid, a lycopene metabolite, increases sirtuin 1 mRNA and protein levels and decreases hepatic fat accumulation in ob/ob mice. The Journal of nutrition. 2012;142:405-10.

[24] Ip BC, Hu KQ, Liu C, Smith DE, Obin MS, Ausman LM, et al. Lycopene metabolite, apo-10'-lycopenoic acid, inhibits diethylnitrosamine-initiated, high fat diet-promoted hepatic inflammation and tumorigenesis in mice. Cancer prevention research (Philadelphia, Pa). 2013;6:1304-16.

[25] Ip BC, Liu C, Lichtenstein AH, von Lintig J, Wang XD. Lycopene and apo-10'-lycopenoic acid have differential mechanisms of protection against hepatic steatosis in beta-carotene-9',10'-oxygenase knockout male mice. The Journal of nutrition. 2015;145:268-76.

[26] Luvizotto RA, Nascimento AF, Miranda NC, Wang XD, Ferreira AL. Lycopene-rich tomato oleoresin modulates plasma adiponectin concentration and mRNA levels of adiponectin, SIRT1, and FoxO1 in adipose tissue of obese rats. Human & experimental toxicology. 2015;34:612-9.

[27] Imai S, Armstrong CM, Kaeberlein M, Guarente L. Transcriptional silencing and longevity protein Sir2 is an NAD-dependent histone deacetylase. Nature. 2000;403:795-800.

[28] Smith JS, Brachmann CB, Celic I, Kenna MA, Muhammad S, Starai VJ, et al. A phylogenetically conserved NAD+-dependent protein deacetylase activity in the Sir2 protein family. Proceedings of the National Academy of Sciences of the United States of America. 2000;97:6658-63.

[29] Caron AZ, He X, Mottawea W, Seifert EL, Jardine K, Dewar-Darch D, et al. The SIRT1 deacetylase protects mice against the symptoms of metabolic syndrome. FASEB journal : official publication of the Federation of American Societies for Experimental Biology. 2014;28:1306-16.

[30] Hou X, Xu S, Maitland-Toolan KA, Sato K, Jiang B, Ido Y, et al. SIRT1 regulates hepatocyte lipid metabolism through activating AMP-activated protein kinase. The Journal of biological chemistry. 2008;283:20015-26.

[31] Li X. SIRT1 and energy metabolism. Acta biochimica et biophysica Sinica. 2013;45:51-60.

[32] Brunet A, Sweeney LB, Sturgill JF, Chua KF, Greer PL, Lin Y, et al. Stress-dependent regulation of FOXO transcription factors by the SIRT1 deacetylase. Science (New York, NY). 2004;303:2011-5.

[33] Cetrullo S, D'Adamo S, Tantini B, Borzi RM, Flamigni F. mTOR, AMPK, and Sirt1: Key Players in Metabolic Stress Management. Critical reviews in eukaryotic gene expression. 2015;25:59-75.

[34] Zhou N, Lin X, Dong W, Huang W, Jiang W, Lin L, et al. SIRT1 alleviates senescence of degenerative human intervertebral disc cartilage endo-plate cells via the p53/p21 pathway. Scientific reports. 2016;6:22628.

[35] Donato AJ, Morgan RG, Walker AE, Lesniewski LA. Cellular and molecular biology of aging endothelial cells. Journal of molecular and cellular cardiology. 2015;89:122-35.

[36] Cheng J, Liu C, Hu K, Greenberg A, Wu D, Ausman LM, et al. Ablation of systemic SIRT1 activity promotes nonalcoholic fatty liver disease by affecting liver-mesenteric adipose tissue fatty acid mobilization. Biochimica et biophysica acta. 2017.

[37] Purushotham A, Xu Q, Li X. Systemic SIRT1 insufficiency results in disruption of energy homeostasis and steroid hormone metabolism upon high-fat-diet feeding. FASEB journal : official publication of the Federation of American Societies for Experimental Biology. 2012;26:656-67.

[38] Mariani S, Fiore D, Basciani S, Persichetti A, Contini S, Lubrano C, et al. Plasma levels of SIRT1 associate with non-alcoholic fatty liver disease in obese patients. Endocrine. 2015;49:711-6.

[39] Fontana L, Zhao E, Amir M, Dong H, Tanaka K, Czaja MJ. Aging promotes the development of diet-induced murine steatohepatitis but not steatosis. Hepatology (Baltimore, Md). 2013;57:995-1004.

[40] Hamaguchi M, Kojima T, Ohbora A, Takeda N, Fukui M, Kato T. Aging is a risk factor of nonalcoholic fatty liver disease in premenopausal women. World journal of gastroenterology. 2012;18:237-43.

[41] Sheedfar F, Di Biase S, Koonen D, Vinciguerra M. Liver diseases and aging: friends or foes? Aging cell. 2013;12:950-4.

[42] Braidy N, Guillemin GJ, Mansour H, Chan-Ling T, Poljak A, Grant R. Age related changes in NAD+ metabolism oxidative stress and Sirt1 activity in wistar rats. PloS one. 2011;6:e19194.

[43] Choi SE, Fu T, Seok S, Kim DH, Yu E, Lee KW, et al. Elevated microRNA-34a in obesity reduces NAD+ levels and SIRT1 activity by directly targeting NAMPT. Aging cell. 2013;12:1062-72.

[44] Garten A, Schuster S, Penke M, Gorski T, de Giorgis T, Kiess W. Physiological and pathophysiological roles of NAMPT and NAD metabolism. Nature reviews Endocrinology. 2015;11:535-46.

[45] Chen J, Zhang B, Wong N, Lo AW, To KF, Chan AW, et al. Sirtuin 1 is upregulated in a subset of hepatocellular carcinomas where it is essential for telomere maintenance and tumor cell growth. Cancer research. 2011;71:4138-49.

[46] Lin Z, Fang D. The Roles of SIRT1 in Cancer. Genes & cancer. 2013;4:97-104.

[47] Zhang ZY, Hong D, Nam SH, Kim JM, Paik YH, Joh JW, et al. SIRT1 regulates oncogenesis via a mutant p53-dependent pathway in hepatocellular carcinoma. Journal of hepatology. 2015;62:121-30.

[48] Heltweg B, Gatbonton T, Schuler AD, Posakony J, Li H, Goehle S, et al. Antitumor activity of a small-molecule inhibitor of human silent information regulator 2 enzymes. Cancer research. 2006;66:4368-77.

[49] Cohen HY, Lavu S, Bitterman KJ, Hekking B, Imahiyerobo TA, Miller C, et al. Acetylation of the C terminus of Ku70 by CBP and PCAF controls Bax-mediated apoptosis. Molecular cell. 2004;13:627-38.

[50] Liu T, Liu PY, Marshall GM. The critical role of the class III histone deacetylase SIRT1 in cancer. Cancer research. 2009;69:1702-5.

[51] Kabra N, Li Z, Chen L, Li B, Zhang X, Wang C, et al. SirT1 is an inhibitor of proliferation and tumor formation in colon cancer. The Journal of biological chemistry. 2009;284:18210-7.

[52] Al-Bahrani R, Tuertcher D, Zailaie S, Abuetabh Y, Nagamori S, Zetouni N, et al. Differential SIRT1 expression in hepatocellular carcinomas and cholangiocarcinoma of the liver. Annals of clinical and laboratory science. 2015;45:3-9.

[53] Choi HN, Bae JS, Jamiyandorj U, Noh SJ, Park HS, Jang KY, et al. Expression and role of SIRT1 in hepatocellular carcinoma. Oncology reports. 2011;26:503-10.

[54] Hao C, Zhu PX, Yang X, Han ZP, Jiang JH, Zong C, et al. Overexpression of SIRT1 promotes metastasis through epithelial-mesenchymal transition in hepatocellular carcinoma. BMC cancer. 2014;14:978.

[55] Li Y, Xu S, Li J, Zheng L, Feng M, Wang X, et al. SIRT1 facilitates hepatocellular carcinoma metastasis by promoting PGC-1alpha-mediated mitochondrial biogenesis. Oncotarget. 2016;7:29255-74.

[56] Portmann S, Fahrner R, Lechleiter A, Keogh A, Overney S, Laemmle A, et al. Antitumor effect of SIRT1 inhibition in human HCC tumor models in vitro and in vivo. Molecular cancer therapeutics. 2013;12:499-508.

[57] Garcia-Rodriguez JL, Barbier-Torres L, Fernandez-Alvarez S, Gutierrez-de Juan V, Monte MJ, Halilbasic E, et al. SIRT1 controls liver regeneration by regulating bile acid metabolism through farnesoid X receptor and mammalian target of rapamycin signaling. Hepatology (Baltimore, Md). 2014;59:1972-83.

[58] Herranz D, Munoz-Martin M, Canamero M, Mulero F, Martinez-Pastor B, Fernandez-Capetillo O, et al. Sirt1 improves healthy ageing and protects from metabolic syndrome-associated cancer. Nature communications. 2010;1:3.

[59] Boily G, Seifert EL, Bevilacqua L, He XH, Sabourin G, Estey C, et al. SirT1 regulates energy metabolism and response to caloric restriction in mice. PloS one. 2008;3:e1759.

[60] McBurney MW, Yang X, Jardine K, Hixon M, Boekelheide K, Webb JR, et al. The mammalian SIR2alpha protein has a role in embryogenesis and gametogenesis. Molecular and cellular biology. 2003;23:38-54.

[61] Seifert EL, Caron AZ, Morin K, Coulombe J, He XH, Jardine K, et al. SirT1 catalytic activity is required for male fertility and metabolic homeostasis in mice. FASEB journal : official publication of the Federation of American Societies for Experimental Biology. 2012;26:555-66.

[62] Ip BC, Liu C, Ausman LM, von Lintig J, Wang XD. Lycopene attenuated hepatic tumorigenesis via differential mechanisms depending on carotenoid cleavage enzyme in mice. Cancer prevention research (Philadelphia, Pa). 2014;7:1219-27.

[63] Hefaiedh R, Ennaifer R, Romdhane H, Ben Nejma H, Arfa N, Belhadj N, et al. Gender difference in patients with hepatocellular carcinoma. La Tunisie medicale. 2013;91:505-8.

[64] Caviglia JM, Schwabe RF. Mouse models of liver cancer. Methods in molecular biology (Clifton, NJ). 2015;1267:165-83.

[65] Buettner R, Scholmerich J, Bollheimer LC. High-fat diets: modeling the metabolic disorders of human obesity in rodents. Obesity (Silver Spring, Md). 2007;15:798-808.

[66] Wang J, Vanegas SM, Du X, Noble T, Zingg JM, Meydani M, et al. Caloric restriction favorably impacts metabolic and immune/inflammatory profiles in obese mice but curcumin/piperine consumption adds no further benefit. Nutrition & metabolism. 2013;10:29.

[67] Porrini M, Riso P. What are typical lycopene intakes? The Journal of nutrition. 2005;135:2042s-5s.

[68] Stice CP, Liu C, Aizawa K, Greenberg AS, Ausman LM, Wang XD. Dietary tomato powder inhibits alcohol-induced hepatic injury by suppressing cytochrome p450 2E1 induction in rodent models. Archives of biochemistry and biophysics. 2015;572:81-8.

[69] Liu C, Lian F, Smith DE, Russell RM, Wang XD. Lycopene supplementation inhibits lung squamous metaplasia and induces apoptosis via up-regulating insulin-like growth factor-binding protein 3 in cigarette smoke-exposed ferrets. Cancer research. 2003;63:3138-44.

[70] Nguyen P, Leray V, Diez M, Serisier S, Le Bloc'h J, Siliart B, et al. Liver lipid metabolism. Journal of animal physiology and animal nutrition. 2008;92:272-83.

[71] Mukai T, Egawa M, Takeuchi T, Yamashita H, Kusudo T. Silencing of FABP1 ameliorates hepatic steatosis, inflammation, and oxidative stress in mice with nonalcoholic fatty liver disease. FEBS open bio. 2017;7:1009-16.

[72] Ebbert JO, Jensen MD. Fat depots, free fatty acids, and dyslipidemia. Nutrients. 2013;5:498-508.

[73] Abenavoli L, Peta V. Role of adipokines and cytokines in non-alcoholic fatty liver disease. Reviews on recent clinical trials. 2014;9:134-40.

[74] Galliher-Beckley AJ, Lan LQ, Aono S, Wang L, Shi J. Caspase-1 activation and mature interleukin-1beta release are uncoupled events in monocytes. World journal of biological chemistry. 2013;4:30-4.

[75] Makki K, Froguel P, Wolowczuk I. Adipose tissue in obesity-related inflammation and insulin resistance: cells, cytokines, and chemokines. ISRN inflammation. 2013;2013:139239.

[76] Margini C, Dufour JF. The story of HCC in NAFLD: from epidemiology, across pathogenesis, to prevention and treatment. Liver international : official journal of the International Association for the Study of the Liver. 2016;36:317-24.

[77] Michelotti GA, Machado MV, Diehl AM. NAFLD, NASH and liver cancer. Nature reviews Gastroenterology & hepatology. 2013;10:656-65.

[78] Rubinfeld H, Seger R. The ERK cascade: a prototype of MAPK signaling. Molecular biotechnology. 2005;31:151-74.

[79] Murphy LO, Blenis J. MAPK signal specificity: the right place at the right time. Trends in biochemical sciences. 2006;31:268-75.

[80] Chalkiadaki A, Guarente L. High-fat diet triggers inflammation-induced cleavage of SIRT1 in adipose tissue to promote metabolic dysfunction. Cell metabolism. 2012;16:180-8.

[81] Philp A, Chen A, Lan D, Meyer GA, Murphy AN, Knapp AE, et al. Sirtuin 1 (SIRT1) deacetylase activity is not required for mitochondrial biogenesis or peroxisome proliferator-activated receptor-gamma coactivator-1alpha (PGC-1alpha) deacetylation following endurance exercise. The Journal of biological chemistry. 2011;286:30561-70.

[82] Schenk S, McCurdy CE, Philp A, Chen MZ, Holliday MJ, Bandyopadhyay GK, et al. Sirt1 enhances skeletal muscle insulin sensitivity in mice during caloric restriction. The Journal of clinical investigation. 2011;121:4281-8.

[83] Newberry EP, Xie Y, Kennedy SM, Luo J, Davidson NO. Protection against Western diet-induced obesity and hepatic steatosis in liver fatty acid-binding protein knockout mice. Hepatology (Baltimore, Md). 2006;44:1191-205.

[84] Martin GG, Atshaves BP, Huang H, McIntosh AL, Williams BJ, Pai PJ, et al. Hepatic phenotype of liver fatty acid binding protein gene-ablated mice. American journal of physiology Gastrointestinal and liver physiology. 2009;297:G1053-65.

[85] Ge Z, Zhang P, Hong T, Tang S, Meng R, Bi Y, et al. Erythropoietin alleviates hepatic insulin resistance via PPARgamma-dependent AKT activation. Scientific reports. 2015;5:17878.

[86] Falcon A, Doege H, Fluitt A, Tsang B, Watson N, Kay MA, et al. FATP2 is a hepatic fatty acid transporter and peroxisomal very long-chain acyl-CoA synthetase. American journal of physiology Endocrinology and metabolism. 2010;299:E384-93.

[87] Tietge UJ, Bakillah A, Maugeais C, Tsukamoto K, Hussain M, Rader DJ. Hepatic overexpression of microsomal triglyceride transfer protein (MTP) results in increased in vivo secretion of VLDL triglycerides and apolipoprotein B. Journal of lipid research. 1999;40:2134-9.

[88] Choi KM, Lee YS, Shin DM, Lee S, Yoo KS, Lee MK, et al. Green tomato extract attenuates high-fat-diet-induced obesity through activation of the AMPK pathway in C57BL/6 mice. The Journal of nutritional biochemistry. 2013;24:335-42.

[89] Seo KI, Lee J, Choi RY, Lee HI, Lee JH, Jeong YK, et al. Anti-obesity and anti-insulin resistance effects of tomato vinegar beverage in diet-induced obese mice. Food & function. 2014;5:1579-86.

[90] Long YC, Zierath JR. AMP-activated protein kinase signaling in metabolic regulation. The Journal of clinical investigation. 2006;116:1776-83.

[91] Motoshima H, Goldstein BJ, Igata M, Araki E. AMPK and cell proliferation--AMPK as a therapeutic target for atherosclerosis and cancer. The Journal of physiology. 2006;574:63-71.

[92] Woods A, Williams JR, Muckett PJ, Mayer FV, Liljevald M, Bohlooly YM, et al. Liver-Specific Activation of AMPK Prevents Steatosis on a High-Fructose Diet. Cell reports. 2017;18:3043-51.

[93] Kim SJ, Tang T, Abbott M, Viscarra JA, Wang Y, Sul HS. AMPK Phosphorylates Desnutrin/ATGL and Hormone-Sensitive Lipase To Regulate Lipolysis and Fatty Acid Oxidation within Adipose Tissue. Molecular and cellular biology. 2016;36:1961-76.

[94] Heindryckx F, Colle I, Van Vlierberghe H. Experimental mouse models for hepatocellular carcinoma research. International journal of experimental pathology. 2009;90:367-86.

[95] Xiao X, Li H, Yang J, Qi X, Zu X, Yang J, et al. Wnt/beta-catenin signaling pathway and lipolysis enzymes participate in methylprednisolone induced fat differential distribution between subcutaneous and visceral adipose tissue. Steroids. 2014;84:30-5.

[96] Palozza P, Parrone N, Catalano A, Simone R. Tomato lycopene and inflammatory cascade: basic interactions and clinical implications. Current medicinal chemistry. 2010;17:2547-63.

[97] Alnemri ES, Livingston DJ, Nicholson DW, Salvesen G, Thornberry NA, Wong WW, et al. Human ICE/CED-3 protease nomenclature. Cell. 1996;87:171.

[98] Dixon LJ, Flask CA, Papouchado BG, Feldstein AE, Nagy LE. Caspase-1 as a central regulator of high fat diet-induced non-alcoholic steatohepatitis. PloS one. 2013;8:e56100.

[99] Henao-Mejia J, Elinav E, Jin C, Hao L, Mehal WZ, Strowig T, et al. Inflammasome-mediated dysbiosis regulates progression of NAFLD and obesity. Nature. 2012;482:179-85.

[100] Yang SJ, Lim Y. Resveratrol ameliorates hepatic metaflammation and inhibits NLRP3 inflammasome activation. Metabolism: clinical and experimental. 2014;63:693-701.

[101] Zhou CC, Yang X, Hua X, Liu J, Fan MB, Li GQ, et al. Hepatic NAD(+) deficiency as a therapeutic target for non-alcoholic fatty liver disease in ageing. British journal of pharmacology. 2016;173:2352-68.

[102] Agarwal S, Rao AV. Tomato lycopene and its role in human health and chronic diseases. CMAJ : Canadian Medical Association journal = journal de l'Association medicale canadienne. 2000;163:739-44.

[103] Luvizotto Rde A, Nascimento AF, Imaizumi E, Pierine DT, Conde SJ, Correa CR, et al. Lycopene supplementation modulates plasma concentrations and epididymal adipose tissue mRNA of leptin, resistin and IL-6 in diet-induced obese rats. The British journal of nutrition. 2013;110:1803-9.

[104] Powell EE, Cooksley WG, Hanson R, Searle J, Halliday JW, Powell LW. The natural history of nonalcoholic steatohepatitis: a follow-up study of forty-two patients for up to 21 years. Hepatology (Baltimore, Md). 1990;11:74-80.

[105] Fengler VH, Macheiner T, Kessler SM, Czepukojc B, Gemperlein K, Muller R, et al. Susceptibility of Different Mouse Wild Type Strains to Develop Diet-Induced NAFLD/AFLD-Associated Liver Disease. PloS one. 2016;11:e0155163.

[106] Liang W, Lindeman JH, Menke AL, Koonen DP, Morrison M, Havekes LM, et al. Metabolically induced liver inflammation leads to NASH and differs from LPS- or IL-1beta-induced chronic inflammation. Laboratory investigation; a journal of technical methods and pathology. 2014;94:491-502.

[107] Li J, Miller EJ, Ninomiya-Tsuji J, Russell RR, 3rd, Young LH. AMP-activated protein kinase activates p38 mitogen-activated protein kinase by increasing recruitment of p38 MAPK to TAB1 in the ischemic heart. Circulation research. 2005;97:872-9.

[108] Ouchi N, Shibata R, Walsh K. AMP-activated protein kinase signaling stimulates VEGF expression and angiogenesis in skeletal muscle. Circulation research. 2005;96:838-46.

[109] Schultze SM, Hemmings BA, Niessen M, Tschopp O. PI3K/AKT, MAPK and AMPK signalling: protein kinases in glucose homeostasis. Expert reviews in molecular medicine. 2012;14:e1.

[110] Abbas, T., Dutta A. p21 in cancer: intricate networks and multiple activities. Nature reviews Cancer. 2009;9:400-14.

[111] Adler SR. Endocrine-Disrupting Chemicals: From Basic Research to Clinical Practice. New Jersey: Human Press; 2007.

[112] Atkins KM, Thomas LL, Barroso-Gonzalez J, Thomas L, Auclair S, Yin J, et al. The multifunctional sorting protein PACS-2 regulates SIRT1-mediated deacetylation of p53 to modulate p21-dependent cell-cycle arrest. Cell reports. 2014;8:1545-57.

[113] Park TJ, Kim JY, Oh SP, Kang SY, Kim BW, Wang HJ, et al. TIS21 negatively regulates hepatocarcinogenesis by disruption of cyclin B1-Forkhead box M1 regulation loop. Hepatology (Baltimore, Md). 2008;47:1533-43.

[114] Teoh NC, Dan YY, Swisshelm K, Lehman S, Wright JH, Haque J, et al. Defective DNA strand break repair causes chromosomal instability and accelerates liver carcinogenesis in mice. Hepatology (Baltimore, Md). 2008;47:2078-88.

[115] Schmitz HH, Poor CL, Wellman RB, Erdman JW, Jr. Concentrations of selected carotenoids and vitamin A in human liver, kidney and lung tissue. The Journal of nutrition. 1991;121:1613-21.

CHAPTER V

THE EFFICACY OF APO-10'-LYCOPENOIC ACID IS SIRT INDEPENDENT

ABSTRACT

Background: Apo-10'-lycopenoic acid (ALA) is an oxidized metabolite of apo-10'-lycopenal through lycopene cleavage by beta-carotene- 9',10'-oxygenase and also existing in tomato and tomato juice. Sirtuin 1 (SIRT1) is an NAD^+-dependent deacetylase for histone and non-histone proteins. We have previously shown that ALA supplementation can increase the expression and activity of SIRT1, and decrease the development of liver steatosis and hepatocellular carcinoma (HCC) in mice. However, whether the efficacy of ALA against NAFLD and HCC is SIRT1-dependent remains unknown.

Methods: SIRT1 homozygous mice ablated for the catalytic activity of SIRT1 (MT) and their corresponding wild type littermates (WT) were injected with diethylnitrosamine, followed by being fed a high fat diet (HFD) with ALA for 34 weeks.

Results: MT mice presented similar SIRT1 protein expression but significantly higher acetylated-FoxO1/total-FoxO1 ratio than WT mice. Dietary ALA resulted in comparable liver steatosis and HCC incidence between WT and MT mice. Unexpectedly, a trend of decreasing liver tumor multiplicity was observed in MT mice, as compared with WT mice fed the same dose of ALA ($P = 0.08$). Interestingly, the ablation of SIRT1 activity resulted in an increased hepatic retinol level, which is associated with increased vitamin A transporter *cd36* mRNA expression. The lack of SIRT1 activity was also associated with higher expressions of hepatic nuclear receptors (*rxrα*, *lxrα*, *pparγ*) and hepatic *p21*, *p27* and *p53* mRNA, but lower cyclin D1 protein levels, suggesting contribution of these nuclear receptors and retinol as well as cell cycle arrest to the reduction of hepatic tumor multiplicity.

Conclusion: ALA protects against NAFLD and HCC independent of SIRT1 activity and the lack of SIRT1 can reduce the tumor number in mice given HFD and ALA supplementation.

INTRODUCTION

Hepatocellular carcinoma (HCC) accounted for 85-90% of primary liver cancers [1, 2]. It is the fifth most common cancer among men, and the second most common cause of cancer mortality worldwide [3]. According to the 18th Annual Report to the Nation on the Status of Cancer, both the incidence and mortality of HCC are rising rapidly, despite the decline in overall cancer death rates [4, 5]. Recently, increasing evidence has linked HCC to metabolic disorders such as obesity, a major risk factor of non-alcoholic fatty liver disease (NAFLD) [6, 7]. NAFLD describes a broad spectrum of liver disease which ranges from liver steatosis to non-alcoholic steatohepatitis (NASH), and ultimately, to fibrosis and cirrhosis [1, 6, 8]. In fact, NAFLD is observed in 30%-40% HCC patients [1], and approximately 90% of HCC cases develop based on a natural history of severe fibrosis [9]. Given the poor prognosis of HCC and modifiable risk factors contributing to its cancer burden, the prevention of predisposing factors of HCC, such as obesity and NAFLD, through dietary interventions represents an important strategy to impede the progress of HCC.

Previous studies have shown that tomatoes and tomato products can impede the progression of NAFLD [10, 11], liver inflammation [12, 13] and HCC [12, 14, 15]. Lycopene, as the predominant carotenoid in tomato products, has been widely studied as an anti-carcinogenic agent due to its biological and physicochemical properties [13, 16, 17]. We have previously demonstrated that in mammalian tissues, lycopene can be preferentially cleaved by beta-carotene 9',10'-oxygenase, resulting in apo-10'-lycopenal, which can be subsequently oxidized to apo-10'-lycopenoic acid (ALA) [18]. A recent study from our lab revealed the anti-angiogenesis effect of ALA by acting as a PPARγ

antagonist (**Appendix I**). Intriguingly, recent *in vivo* studies found that ALA presented substantial anti-carcinogenesis characteristic in lung and liver through reducing cyclin D1 by promoting p21 expression [19, 20]. In the further exploration of the underlying mechanism, Ip et al. found that ALA ameliorated HCC by dose-dependently up-regulating sirtuin 1 (SIRT1) protein, which is concordant with the previous report that ALA increased SIRT1 mRNA and protein levels in genetically induced obese (ob/ob) mice [21]. However, whether this inhibitory effect of ALA on HCC is dependent on SIRT1 signaling remains to be explored.

SIRT1 is an evolutionarily conserved NAD^+-dependent deacetylase for both histone and non-histone proteins [22, 23]. It exerts catalytic function via removing the acetyl group from the lysine of the target protein, thereby regulating the expression of target genes in both transcriptional and post-translational manners [22]. Accumulating evidence from our lab and others has consistently shown that SIRT1 is involved in maintaining hepatic lipid homeostasis by modulating lipid metabolism through decreasing fatty acid synthesis [24-26], enhancing β-oxidation [27, 28], and regulating the mobilization of free fatty acids from adipose tissue to the liver [24]. In contrast, the effect of SIRT1 on HCC development is controversial due to its differential roles in specific signaling pathways. For example, SIRT1 deacetylates and inhibits p53, a key tumor inhibitor inducing apoptosis [29-31], leading to accelerated cancer cell proliferation. On the contrary, SIRT1 suppresses NF-κB [19, 32], which can induce hepatic inflammation through transactivating IL-1β. However, the causality of SIRT1 on HCC development remains unknown due to the lack of a systemic SIRT1 knock-out animal model [24]. Recently, Serfeit et al. published a novel engineered systemic SIRT1

deacetylase activity-ablated mouse model, which mimics whole-body SIRT1 knockout mice, but presents less resultant genetic defects [33]. This allows an opportunity to further study how systemic SIRT1 activity affects the inhibitory effect of ALA against NAFLD and HCC.

The present study investigated the effect of systemic SIRT1 activity ablation on carcinogen-initiated, high fat diet (HFD)-promoted HCC in mice with ALA supplementation, and elucidated the underlying mechanisms by which the lack of systemic SIRT1 activity affected HCC development in mice fed ALA.

METHODS

Animals and Diets

All animal protocols for the study were approved by the Institutional Animal Care and Use Committee at the USDA Human Nutrition Research Center on Aging (HNRCA) at Tufts University. Male 129/SvJ background mice with homozygous H355Y SIRT1 point mutation (MT) and their wild-type (WT) counterparts were utilized in the current study. At 2 weeks of age, mice were injected intraperitoneally with diethylnitrosamine (DEN, Sigma-Aldrich, MO, USA), a carcinogen well established for HCC initiation [34]. At 4 weeks of age, SIRT1 genotypes were determined by a PCR-based test performed on DNA isolated from tail-tip biopsies using the primers 5'-TGGAAGGAAAGCAATTTTGGT-3' and g'CTGAGTTACCTTAGCTTGGC-3'. All mice were housed individually and fed the standard chow diet (Envigo, Huntingdon, UK) for 2 weeks. At 6 weeks of age, mice were fed HFD (60% calories from fat, Bioserv, NJ, USA) with ALA (10 mg/kg diet) twice a week for 34 weeks. The macronutrient

component within the HFD was listed in **Appendix I**. The ALA used in this study was provided by Dr. Hansgeorg Ernst (BASF, Ludwigshafen, Germany) with 99% purity, analyzed by HPLC as previously described [19, 21]. At 40 weeks of age, livers and epidydimal adipose tissue were harvested from the animals and weighed.

ALA Dose Rationale

In the current study, ALA was provided at 10 mg/kg diet. The rationale for selecting this ALA dose was previously described [19]. Briefly, by using an established equation to calculate the dosage equivalence for human consumption [35], the ALA dosage utilized in this study is approximately equivalent to 0.36 mg ALA/day in a 60-kg adult man [19]. A/J mice fed the same ALA dose for 14 weeks accumulated circulating ALA concentration of 1.0 nmol/L [20], which is comparable to the sum of plasma apo-lycopenals (1.9 nmol/L) detected in individuals who had consumed tomato juice (with 21.8 mg lycopene/day) for 8 weeks [36].

Liver Tumor Quantification

An investigator unaware of genotype and treatment groups counted liver surface tumors and measured the diameter of the tumors, as previously described [16]. A piece of liver tissue from left lobe of liver was fixed in 10% buffered formalin solution for histopathological examination while the remaining liver tissues were snap frozen in liquid nitrogen and stored at -80°C.

Histological Examination

Tissue processing for histopathological examination was described previously [24]. Briefly, tissues from the left lobe of the liver of each mouse were processed with

fixation, dehydration, clearing, and paraffin wax infiltration and then embedded in paraffin to make tissue blocks for sectioning. Hematoxylin and eosin (H&E, Sigma Aldrich, MI, USA) was subsequently used to stain the liver tissue for histopathological analysis. A ZEISS microscope with a PixeLINK USB 2.0 (PL-B623CU) digital Camera and PixeLINK µScope Microscopy Software was used for image capture of the liver tissues.

Hepatic steatosis was graded according to the degree of both macro- and micro-vesicular lipid accumulations, as previously reported [24]. Briefly, steatosis score was assigned by evaluating the percentage of liver section that was occupied by lipid vacuoles at 100x magnification in 20 fields: grade 0 = <5%; grade 1 = 5–25%; grade 2 = 26–50%; grade 3 = 51–75%; grade 4 = >75%. The types of hepatic tumors were confirmed according to the following criteria: (i) the presence of trabecular pattern with 3+ cell-thick hepatocellular plates/cords; (ii) mitotic figure; (iii) enlarged convoluted nuclei or high nuclei/cytoplasmic ratio; (iv) the presence of tumor giant cells with compact growth pattern; and (v) the presence of endothelial cells lining of sinusoids that surround enlarged hepatocellular plates/cords, as previously described [16].

Protein Isolation and Western Blotting

Approximately 50 mg of liver tissue was extracted using whole cell lysis buffer (50 mM HEPES, 300 mM NaCl, 1.5 mM MgCl2, 1 mM EDTA, 0.5% Triton X-100, 10% Glycerol, Protease Inhibitor Cocktail (Sigma-Aldrich), Phosphatase Inhibitor Cocktail (Sigma-Aldrich), and 1 mM PMSF (phenylmethylsulfonyl fluoride)). Protein concentration was determined using standard spectrophotometer techniques using Coomassie Blue (Thermo Scientific) with bovine serum albumin (BSA, Pierce)

standards. Protein extracts were stored at -80°C until needed for analysis. Whole cell lysate protein samples from liver containing 25-100 μg protein were run in SDS-polyacrylamide gels (Protogel, National Diagnostics) with a standard protein marker for protein size determination (Bio-Rad Laboratories) followed by transfer to a methanol-activated polyvinylidene fluoride (PVDF) membrane (Immobilon-P transfer membrane PVDF). Membranes were blocked in 5% non-fat dry milk or 5% BSA in 0.1% TBS-T (25 mM Tris pH 8.0, 150 mM NaCl, 0.1% Tween-20) at room temperature for 1 hour. Blots were incubated with primary antibody at 4°C overnight. Protein concentrations of whole-tissue lysate were determined by Bradford assay (Bio-Rad, CA, USA). Primary antibodies for proliferator-activated receptor (PPAR)α were purchased from Santa Cruz (TX, USA). Primary antibodies for phosphorylated, total acetyl-CoA carboxylase (ACC) were purchased from Cell Signaling (MA, USA). Monoclonal mouse antibody against β-actin was purchased from Sigma-Aldrich (MA, USA). The secondary antibodies included horseradish anti-rabbit antibodies were purchased from Bio-Rad (CA, USA). The relative intensity of films was determined by employing GS-710 Calibrated Imaging Densitometer (Bio-Rad, CA, USA).

RNA Extraction and Real Time-PCR

Hepatic mRNA levels were determined by real-time PCR. Liver RNA was extracted using TriPure Isolation Reagent (Roche Applied Science) as per the manufacturer's instructions. RNA quality and quantity were analyzed using 1% agarose gel and spectrophotomer (Abs260) techniques, respectively. Complementary DNA (cDNA) was synthesized by reverse transcription PCR (M-MLV, Invitrogen). Real-time PCR was performed using SYBER green (Fast Start Universal SYBR Green Master,

Roche) according to the manufacturer's instructions on a 7500 Real Time PCR System (Applied Biosystems) detection system. Primer sequences used are listed in the **Appendix II**. Gene expression was determined by the $-2^{\Delta\Delta Ct}$ method relative to the control group after normalization to housekeeping gene, β-actin.

High-Performance Liquid Chromatography (HPLC) Analysis

The HPLC analysis for liver concentrations of lycopene was described in our previous publications [19-21]. Briefly, liver tissue was weighed and minced over ice, followed by adding 3 ml of saline and ethanol (1:2). Then 100 µl of retinyl acetate (RAC) was added to each tube as internal control. The mixture was homogenized. Remaining tissue on the homogenizer was washed off by 3.5 ml hexane and ether (1:1). Lycopene and retinol was extracted by vortexing the total mixture for 1 minute, followed by centrifuging for 15 minutes at 1,500 rpm at 4 °C. The upper layer of each sample was collected, and the extraction process was repeated. After all extractions, the samples were dried completely by nitrogen gas and then reconstituted with 100 µl ethanol. A 50 µl sample of final extract was injected into the HPLC system. The area under curve (AUC) was measured in each liver sample, and divided the AUC of RAC to calculate the efficiency of extraction. All procedures were conducted under red light.

Statistical Analyses

GraphPad Prism 5 was used to perform the statistical analysis. Normality and equal variance were assessed by utilizing SAS 9.3 PROC UNIVARIATE command. Mann-Whitney U test was performed to compare liver steatosis score distribution. Chi-Square test was used to compare HCC incidence. Student *t*-test was used to HPLC

results, gene and protein expressions between WT and MT groups. Statistical significance was set as $P < 0.05$.

RESULTS

SIRT1 Ablation Decreased HCC development in ALA Fed Mice

There were no significant differences in food intake, body weights, liver weights, and epididymal adipose tissue weights between the WT and MT mice fed HFD+ALA (**Table 1**). Histological assessments of liver tissue sections showed that WT and MT mice developed comparable incidence and severity of hepatic steatosis after ALA supplementation for 34 weeks. Systemic SIRT1 ablation did not alter the incidence of HCC, but showed a trend of reducing tumor multiplicity ($P = 0.08$) as compared to the WT group (**Table 2**). Consistent with histopathology results, lipid metabolism-related genes and inflammatory biomarkers were similar in the livers of WT and MT mice (data not shown).

To test mouse model, we examined hepatic SIRT1 and acetyl-FoxO1/total-FoxO1 ratio, and found acetyl-FoxO1/total-FoxO1 ratio significantly increased in MT mice, while SIRT1 protein level was not altered (**Figure 1A,B**). This indicates that SIRT1 activity is impaired in MT mice [24], but the mutation of SIRT1 activity does not affect SIRT1 protein expression.

SIRT1 Ablation Increased Hepatic Retinol Concentration In ALA Fed

By utilizing HPLC, we first examined hepatic ALA concentration. However, hepatic ALA concentration was undetectable in both WT and MT mice, similar to our previous report that hepatic ALA concentration was at picomolar levels in C57BL6 mice

[19]. Interestingly, compared to WT mice, MT mice showed significantly higher hepatic concentrations of retinol and retinyl palmitate, the esterified form of retinol (**Figure 2A, B**). The ratio of hepatic retinol over retinyl palmitate was similar between WT and MT mice (**Figure 2C**).

To further explore the underlying mechanism by which SIRT1 ablation increases hepatic retinol concentration, we examined hepatic mRNA of *cd36*, a transporter involved in cellular uptake of provitamin A carotenoids [37]. Compared to WT mice, MT mice showed significantly higher expression of hepatic cd36 mRNA, indicating that SIRT1 ablation may increase hepatic retinol concentration potentially via increasing hepatic retinol uptake.

SIRT1 Ablation Increased Hepatic Retinoid and Liver X Receptor Expressions in ALA Fed Mice

As the oxidative form of retinol, RA can increase the expression and transactivation of retinoid X receptor gene [37]. In the current study, we found that lack of SIRT1 activity increased hepatic mRNA levels of *rxrα*, *lxrα* and *pparγ* (**Figure 3A**), as well as hepatic RXRα protein expression, as compared with that of the WT mice (**Figure 3B**). However, hepatic *rarβ* expression significantly decreased in MT mice, as compared to WT mice (**Figure 3A**).

SIRT1 Ablation Induced Cell Cycle Arrest in ALA Fed Mice

Once activated, RXR can form heterodimers with other nuclear receptors such as RAR, LXR and PPARs, and consequently induce the transcription of a wide range of genes. In the current study, we found that hepatic mRNA expressions of *p27* and *p53*,

well-known tumor suppressors, significantly increased in MT mice (**Figure 4A**). Hepatic mRNA expression of p21 was also moderately elevated in MT mice, compared to WT mice ($P = 0.07$). This was correlated with increased RXRα protein expression and *lxrα* mRNA expression in MT mice, compare with the WT group. Cyclin D1 is an oncogene that upregulates G1 to S phase progression in many different cell types, and is involved in the development and progression of several cancers. In the current study, both mRNA and protein levels of hepatic cyclin D1 were significantly lower in MT mice compared to WT mice (**Figure 4B, C**). These results indicated that SIRT1 activity ablation induced cell cycle arrest by increasing tumor suppressor genes and inhibiting tumor promotor genes.

DISCUSSION

The current study provided first evidence that systemic SIRT1 ablation did not affect the efficacy of ALA on NAFLD in mice fed HFD. In addition, in mice given HFD+ALA, the lack of systemic SIRT1 activity inhibited HCC development through increasing hepatic retinol concentrations, which induced cell cycle arrest mediated by retinol and liver X receptors.

Previous studies have shown that under the surplus of HFD, mice receiving ALA supplementation developed less hepatic steatosis and HCC, which was accompanied with reduced hepatic SIRT1 protein expression and decreased SIRT1 deacetylase activity [19, 21]. In the present study, we found that the lack of systemic SIRT1 activity did not affect the efficacy of ALA on NAFLD development, indicating that ALA inhibits NAFLD independent of SIRT1 activity. An alternative mechanism by which ALA supplementation impedes NAFLD may be that ALA increases the phosphorylation of

AMPKα [19], leading to SIRT1 activation [25, 38]. The phosphorylation and expression of AMPKα, however, did not alter in the current study (data not shown), which partly explains lack of difference in NAFLD severity between WT and MT mice fed HFD+ALA.

Intriguingly, in the present study, we found that given the same HFD+ALA diet, MT mice presented significantly higher hepatic retinol and retinyl palmitate concentrations, compared to WT mice. To the best of our knowledge, this is the first study to show that SIRT1 activity affects hepatic retinol concentration and retinol storage. All-trans-retinoic acid (RA) is a natural retinol metabolite, and it presents anti-carcinogenesis benefit in various cancers such as pancreatic cancer and lung cancer in both animal studies [39, 40] and human studies [41, 42]. Lai et al. reported that higher retinol levels in the serum were significantly associated with less liver cancer in a cohort study [43], highlighting the role of retinol as a key biomarker of HCC development. One limitation of our study is that we are unable to detect hepatic RA level, since the hepatic RA concentration was too low to be detected. However, since retinol and RA levels are tightly correlated [44], we expect that hepatic RA concentration in MT mice was higher, paralleled with increasing hepatic retinol concentration, compared to that in WT mice. In the present study, the hepatic concentration of retinol was comparable to that in humans (8.7 ± 1102.2 nmol/g tissue) [45], indicating that the regulation of SIRT1 on hepatic retinol concentration is within physiological relevance.

By further exploring the underlying mechanism by which MT mice accumulated higher amount of retinol in the livers, we found that the mRNA expression of *cd36,* a transporter for lipid-soluble vitamins including retinol, substantially increased in the

livers of MT mice. This finding is consistent with the previous report that SIRT1 can decrease hepatic CD36 protein level [46]. Using the same SIRT1 ablation mouse model, we consistently observed an increasing hepatic *cd36* mRNA in mice that lack SIRT1 activity [24]. These data indicate that the lack of SIRT1 activity can increase hepatic retinol concentrations, potentially by promoting liver retinol uptake through CD36.

The transcriptional regulatory activities of RA are mediated by nuclear hormone receptors, including RARs and RXRs [47]. Binding of RA to these receptors results in recruitment of coactivator protein, which eventually promotes transcription of the downstream target gene. Additionally, RXRs can form heterodimers with other nuclear hormone receptors such as LXR and PPARs [48]. As expected, MT mice presented significantly higher RXRα mRNA and protein levels, and increased lxrα and pparγ mRNA expressions, compared to WT mice. It has been shown that the activation of PPARγ-RXRα heterodimers by their ligands, such as RA, synergistically inhibits cancer cell progression [49], mechanistically by inducing cell apoptosis via p53/p21 [50]. Concordantly, we found a higher hepatic *p53* mRNA and a trend of increasing hepatic *p21* mRNA in MT mice, which were correlated with higher RXRα protein expressed in MT mice. In the current study, MT mice showed increasing *pparγ* mRNA but similar *pparα* mRNA, compared to WT mice. The role of liver PPARα in hepatic carcinogenesis is controversial due to its paradoxical effects on cell proliferation and apoptosis [51]. On the contrary, several studies consistently report a role for PPARγ in prevention and treatment of HCC [52, 53], indicating that the activity of PPARγ might be a more potent target in impeding HCC development. In the present study, the hepatic mRNA level of *p27* significantly increased in MT mice, as compared to that in WT mice. Previous

studies have reported that p27 is not regulated by RXRα [54], but increased by the activation of LXRα [55, 56], suggesting that the increased hepatic *p27* mRNA might be resulted from activated LXRα in this study. By utilizing the same mouse model, we have consistently reported an increased *lxrα* mRNA expression after mutating SIRT1 deacetylase activity [24]. Therefore, under the surplus of HFD+ALA, whether the increase and activation of LXRα in SIRT1 MT mice are due to the ligand activity of RA, or SIRT1 genetic manipulation *per se* warrants further investigation. In the present study, we found hepatic mRNA level of *rarβ* significantly decreased in MT mice, as compared to that in WT mice. Such result is consistent with previous studies showing that promoted SIRT1 expression is associated with increased abundance of *rarβ* mRNA expression [57, 58], given that SIRT1 appears to deacetylate and coactivate RARβ [59]. Although RA acts as a ligand for RARβ activation, the decreased *rarβ* mRNA in MT mice in this study indicates that compared to retinoids, SIRT1 genetic modification might impose more potent influence on RARβ expression.

In line with the increase of hepatic mRNA expressions of *p53*, *p21* and *p27*, as critical cyclin dependent kinase inhibitors, hepatic mRNA and protein levels of cyclinD1 significantly decreased in MT mice, which partially explained the decreased tumor multiplicity in the livers of MT mice, suggesting that the lack of SIRT1 activity can inhibit HCC development by promoting cell cycle arrest via decreasing hepatic cyclinD1 level. To date, the role of SIRT1 on cancer development is still under debate. By employing the same systemic SIRT1 ablation mouse model with DEN injection and HFD intervention, the lack of SIRT1 did not alter HCC initiation or progression, despite of increased the severity of liver steatosis. However, the unaltered HCC development might

be due to the feature of 129/SvJ and CD-1 strains, which exhibit impaired immune response, compared to C57BL/6 mice [60]. During the preparation of this manuscript, we conducted a pilot study by backcrossing the outbred 129/SvJ-CD1 mice to the inbred C57BL/6 mice. We found that with DEN injection, the SIRT1 mutant mice developed less severe HCC, compared to their WT counterparts. Such data are consistent with the current study that under the setting of HFD+ALA, HCC development was ameliorated in MT mice. One major limitation of this study was that we did not have WT and MT mice fed HFD in parallel without ALA. This is because the primary objective of this study is to address whether the efficacy of ALA against NAFLD and HCC is dependent on SIRT1. Further investigation on the synergetic effects of ALA and SIRT1 ablation on HCC development with C57BL/6 background mice is currently ongoing in our laboratory.

Taken together, the present study indicates that SIRT1 is not the only target of ALA in NAFLD prevention. We also found under the surplus of ALA that lack of SIRT1 activity can inhibit the development of carcinogen-initiated, HFD-promoted HCC, potentially through increasing hepatic retinol concentration (**Figure 5**).

TABLE 1

Table 1. Food intake, body weights, liver weights, liver/body weight, epididymal fat, epididymal fat mass/body weight of DEN-injected, HFD-fed WT or MT mice with ALA supplementation for 34 weeks[1].

Study group	WT+ALA (N = 16)	MT+ALA (N = 15)	*P* Values
Food intake, g/d	3.8 ± 0.15	3.7 ± 0.40	0.86
Body weights, g	46.11 ± 1.71	47.79 ± 1.67	0.49
Liver weights, g	3.65 ± 0.33	2.80 ± 0.24	0.07
Liver/body weight, %	8.12 ± 0.93	6.15 ± 0.73	0.10
Epididymal fat, g	1.72 ± 0.15	1.86 ± 0.14	0.50
Epididymal fat mass/body weight, %	3.66 ± 0.24	3.85 ± 0.24	0.58

[1]Values are means ± SEMs. Student's *t* test was used to compare values among four groups, which are shown as *p* values. WT, wild-type; MT, mutant; ALA, apo-10'-lycopenoic acid.

TABLE 2

Table 2. Steatosis score, HCC incidence by histopathology analysis, liver surface tumor multiplicity in all groups[1]

Study group	WT+ALA (N = 16)	MT+ALA (N = 18)	Strain effect
Steatosis incidence, %	64.71	68.75	1.00
Steatosis score	0.88 ± 0.18	1.06 ± 0.22	0.30
HCC incidence, %	93.8	83.3	0.79
Tumor multiplicity > 6, %	68.8	33.3	0.08

[1]Values are %, means ± SEMs. Chi square test was used to compare steatosis score between groups. Fisher's exact test was used to compare HCC incidence and tumor multiplicity > 6 percentage within each group, which are shown as *P* values. WT, wild-type; MT, mutant; ALA, apo-10'-lycopenoic acid.

FIGURE 1

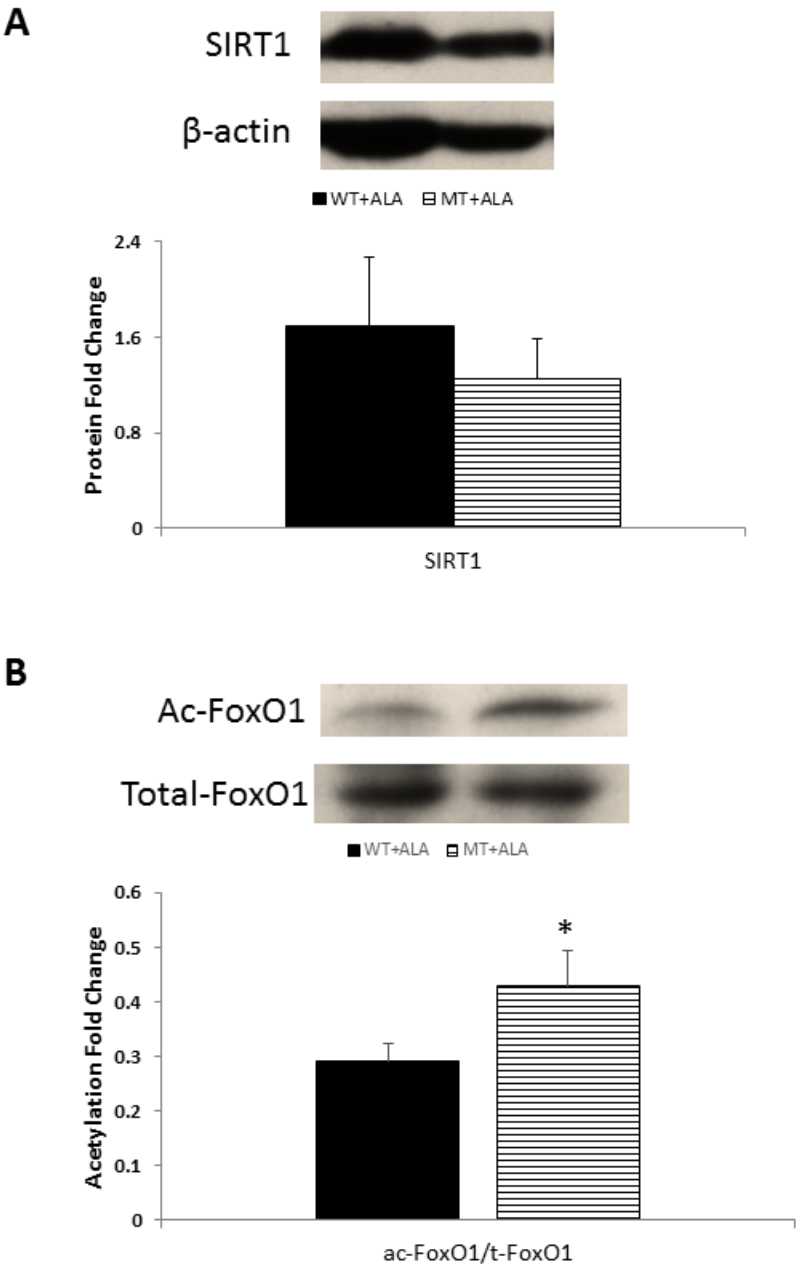
A
SIRT1
β-actin
WT+ALA
MT+ALA
Protein Fold Change
2.4
1.6
0.8
0
SIRT1
B
Ac-FoxO1
Total-FoxO1
WT+ALA
MT+ALA
Acetylation Fold Change
0.6
0.5
0.4
0.3
0.2
0.1
0
*
ac-FoxO1/t-FoxO1

FIGURE 2

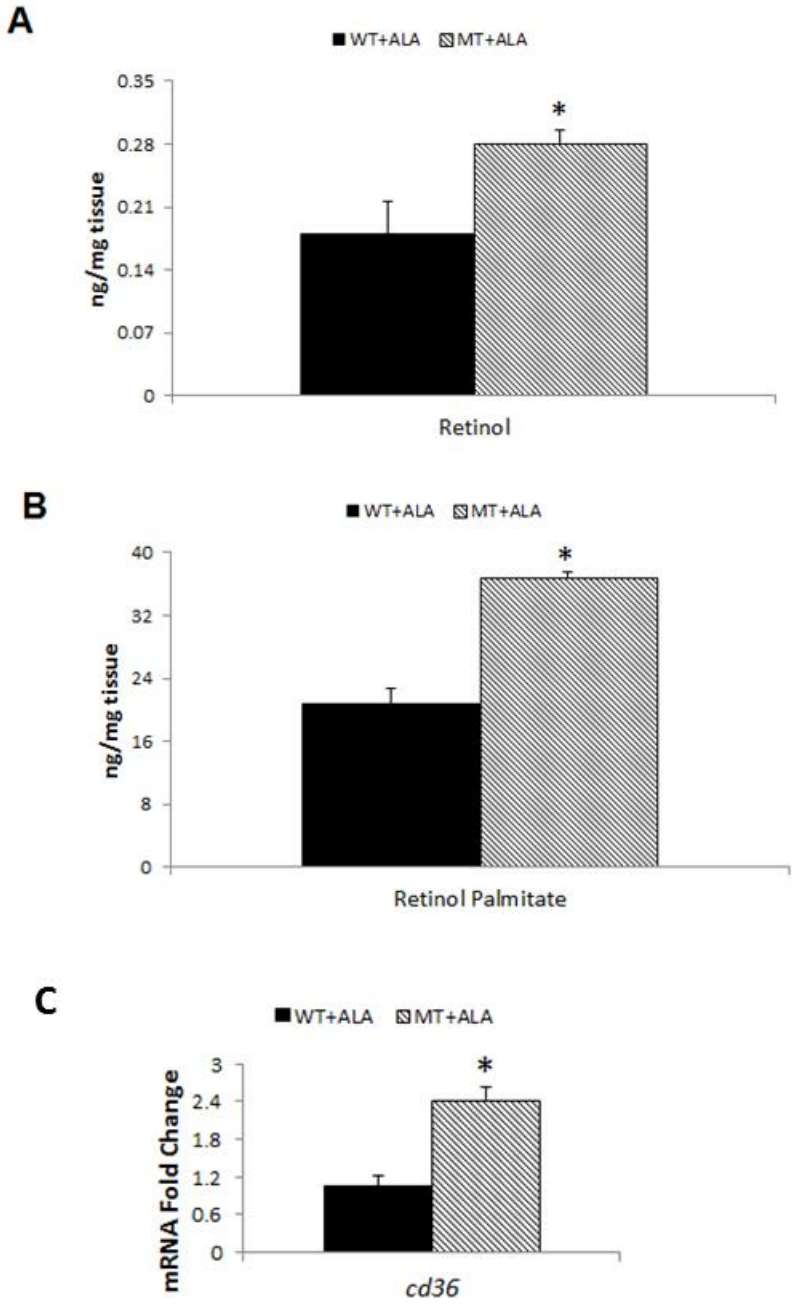
A
WT+ALA
MT+ALA
0.35
0.28
0.21
0.14
0.07
0
ng/mg tissue
*
Retinol
B
WT+ALA
MT+ALA
40
32
24
16
8
0
ng/mg tissue
*
Retinol Palmitate
C
WT+ALA
MT+ALA
3
2.4
1.8
1.2
0.6
0
mRNA Fold Change
*
cd36

FIGURE 3

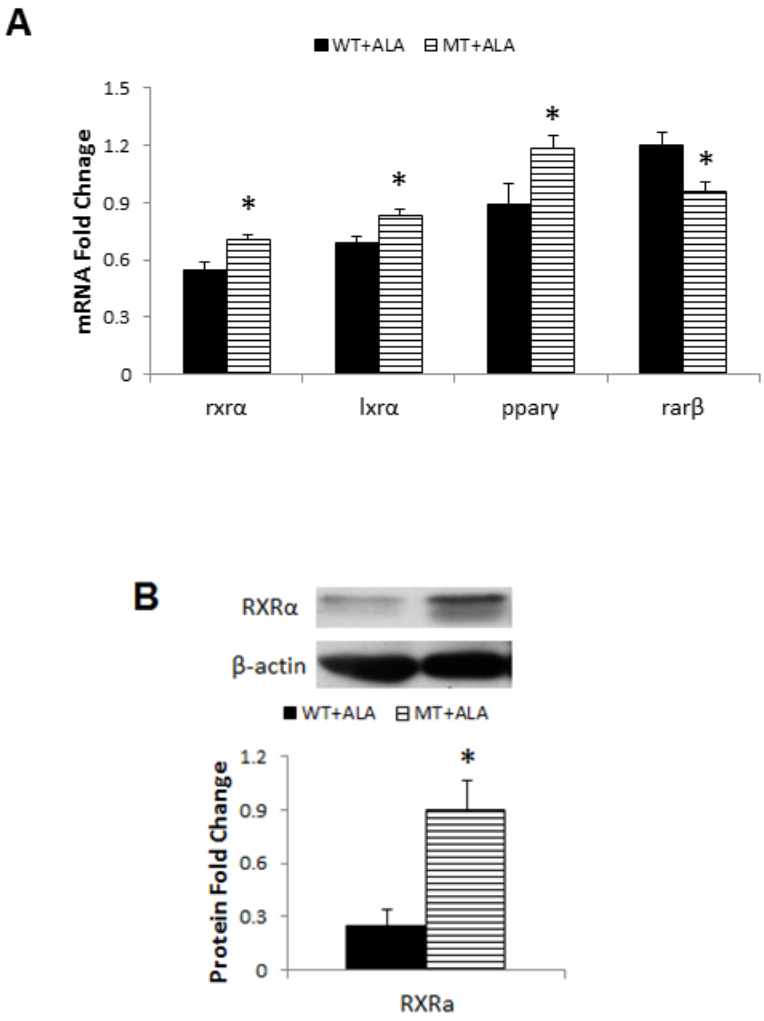
A
WT+ALA
MT+ALA
mRNA Fold Chnage
1.5
1.2
0.9
0.6
0.3
0
rxrα
lxrα
pparγ
rarβ
B
RXRα
β-actin
WT+ALA
MT+ALA
Protein Fold Change
1.2
0.9
0.6
0.3
0
RXRa

FIGURE 4

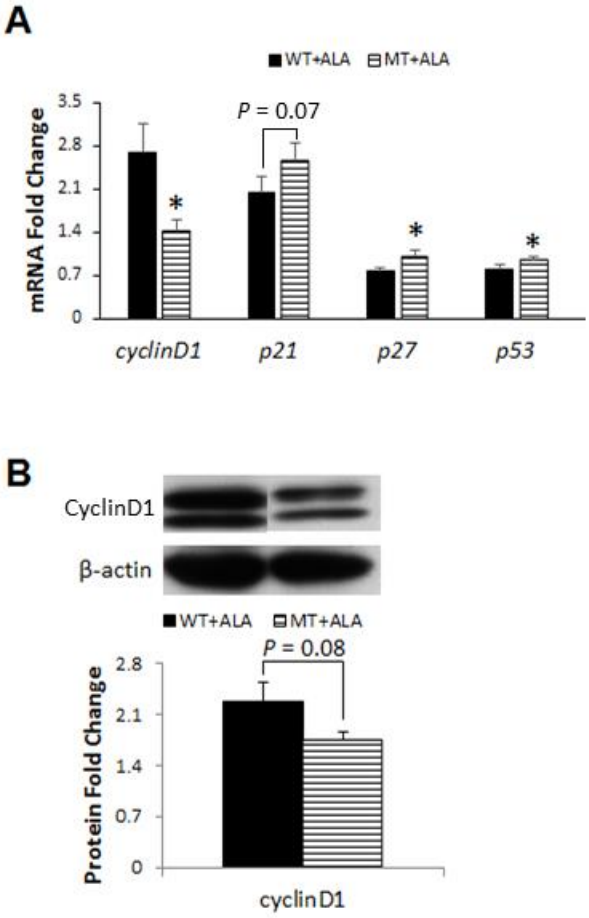
A
WT+ALA
MT+ALA
mRNA Fold Change
3.5
2.8
2.1
1.4
0.7
0
P = 0.07
*
*
*
cyclinD1
p21
p27
p53
B
CyclinD1
β-actin
WT+ALA
MT+ALA
P = 0.08
Protein Fold Change
2.8
2.1
1.4
0.7
0
cyclinD1

FIGURE 5

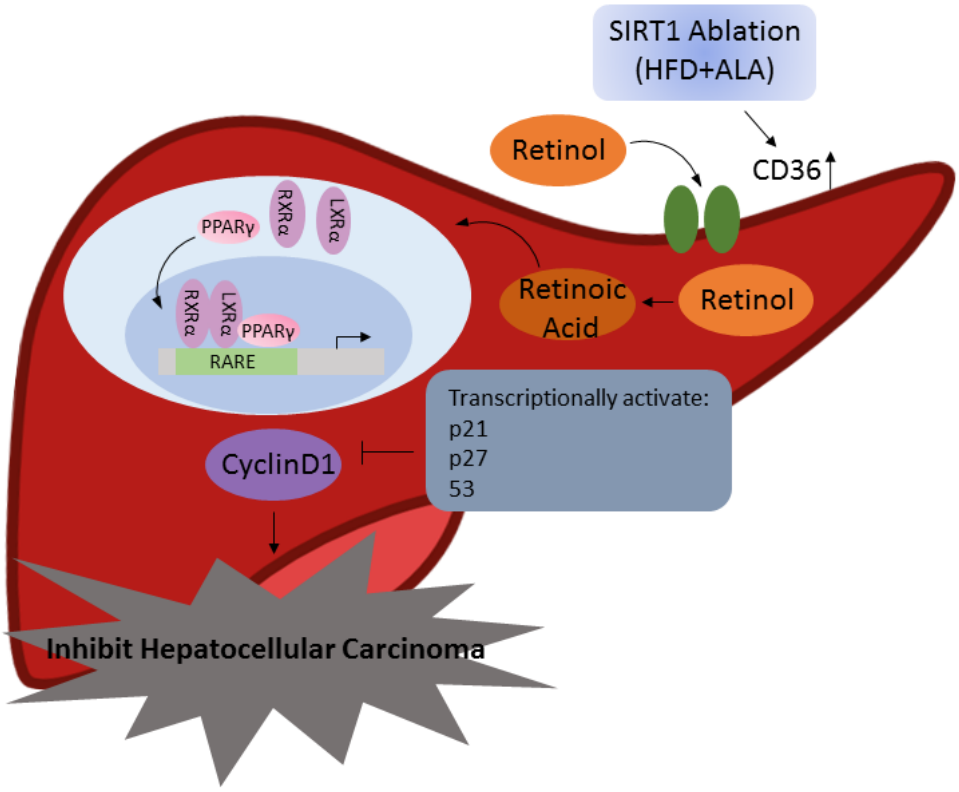
SIRT1 Ablation
(HFD+ALA)
Retinol
CD36
PPARγ
RXRα
LXRα
RXRα
LXRα
PPARγ
RARE
Retinoic
Acid
Retinol
Transcriptionally activate:
p21
p27
53
CyclinD1
Inhibit Hepatocellular Carcinoma

FIGURE LEGENDS

Figure 1. SIRT1 protein and deacetylase activity differences between WT and MT mice fed HFD+ALA. Changes of protein expression in liver lysates (WT, MT n = 10) were analyzed by Western-blotting. Graphical representation of fold changes in: A, SIRT1, β-actin used as loading control; and B, acetylated FoxO1, total-FoxO1 used as loading control. Values are means ± SEMs. Student *t* test was used to compare protein expressions between WT and MT mice. WT, wild-type mice; MT, systemic SIRT1 activity mutant mice.

Figure 2. Effects of SIRT1 activity ablation on hepatic retinol and retinyl palmitate concentration and the underlying mechanism in WT and MT mice fed HFD+ALA. Changes of hepatic retinol and retinyl palmitate levels were analyzed by HPLC (WT, MT n = 6); changes of hepatic *cd36* mRNA level was analyzed by qPCR (WT, MT n = 16). Graphic representation of fold changes in: A, hepatic retinol concentration; B, hepatic retinyl palmitate concentration; and C, hepatic *cd36* mRNA, β-actin as control. Values are means ± SEMs. Student *t* test was used to compare compound concentrations and mRNA levels between WT and MT mice. WT, wild-type mice; MT, systemic SIRT1 activity mutant mice.

Figure 3. Effects of SIRT1 activity ablation on hepatic nuclear receptor mRNA and protein expressions in WT and MT mice fed HFD+ALA. Changes of protein expression in liver lysates (WT, MT n = 10) were analyzed by Western-blotting. Changes of mRNA expression (WT, MT n = 16) were analyzed by qPCR. β-actin was used as loading control unless specified otherwise. Graphical representation of fold changes in: A, mRNA levels of: *rxrα, lxrα, pparγ*, and *rarβ*; and B, RXRα protein. Values are means ±

SEMs. Student *t* test was used to compare protein and mRNA levels between WT and MT mice. WT, wild-type mice; MT, systemic SIRT1 activity mutant mice.

Figure 4. Effects of SIRT1 activity ablation on hepatic mRNA and protein levels of cell cycle progression-related genes in WT and MT mice fed HFD+ALA. Changes of protein expression in liver lysates (WT, MT n = 10) were analyzed by Western-blotting. Changes of mRNA expression (WT, MT n = 16) were analyzed by qPCR. β-actin was used as loading control unless specified otherwise. Graphical representation of fold changes in: A, mRNA levels of: *cyclinD1*, *p21*, *p27*, *p53*; and B, cyclinD1 protein. Values are means ± SEMs. Student *t* test was used to compare protein and mRNA levels between WT and MT mice. WT, wild-type mice; MT, systemic SIRT1 activity mutant mice.

Figure 5. Graphic summary. Under the setting of HFD+ALA, SIRT1 activity ablation increased hepatic retinol uptake. This is followed by liver RXRα, LXRα and PPARγ activation, which elevates the transcription of cyclin dependent kinase inhibitors, leading to decreased cyclinD1 level, leading to impeded HCC as final event.

LITERATURE CITED

[1] El-Serag, H. B., Rudolph, K. L., Hepatocellular carcinoma: epidemiology and molecular carcinogenesis. *Gastroenterology* 2007, *132*, 2557-2576.

[2] Parkin, D. M., Global cancer statistics in the year 2000. *The Lancet. Oncology* 2001, *2*, 533-543.

[3] Ferlay, J., Soerjomataram, I., Dikshit, R., Eser, S., *et al.*, Cancer incidence and mortality worldwide: sources, methods and major patterns in GLOBOCAN 2012. *International journal of cancer* 2015, *136*, E359-386.

[4] Ryerson, A. B., Eheman, C. R., Altekruse, S. F., Ward, J. W., *et al.*, Annual Report to the Nation on the Status of Cancer, 1975-2012, featuring the increasing incidence of liver cancer. *Cancer* 2016, *122*, 1312-1337.

[5] Siegel, R. L., Miller, K. D., Jemal, A., Cancer Statistics, 2017. *CA: a cancer journal for clinicians* 2017, *67*, 7-30.

[6] Masuzaki, R., Karp, S. J., Omata, M., NAFLD as a risk factor for HCC: new rules of engagement? *Hepatology international* 2016, *10*, 533-534.

[7] Wong, C. R., Nguyen, M. H., Lim, J. K., Hepatocellular carcinoma in patients with non-alcoholic fatty liver disease. *World journal of gastroenterology* 2016, *22*, 8294-8303.

[8] Marchesini, G., Bugianesi, E., Forlani, G., Cerrelli, F., *et al.*, Nonalcoholic fatty liver, steatohepatitis, and the metabolic syndrome. *Hepatology (Baltimore, Md.)* 2003, *37*, 917-923.

[9] De Minicis, S., Marzioni, M., Saccomanno, S., Rychlicki, C., *et al.*, Cellular and molecular mechanisms of hepatic fibrogenesis leading to liver cancer. *Transl Gastrointest Cancer* 2011, *1*, 88-94.

[10] Garcia-Alonso, F. J., Gonzalez-Barrio, R., Martin-Pozuelo, G., Hidalgo, N., *et al.*, A study of the prebiotic-like effects of tomato juice consumption in rats with diet-induced non-alcoholic fatty liver disease (NAFLD). *Food & function* 2017, *8*, 3542-3552.

[11] Martin-Pozuelo, G., Navarro-Gonzalez, I., Gonzalez-Barrio, R., Santaella, M., *et al.*, The effect of tomato juice supplementation on biomarkers and gene expression related to lipid metabolism in rats with induced hepatic steatosis. *European journal of nutrition* 2015, *54*, 933-944.

[12] Wang, Y., Ausman, L. M., Greenberg, A. S., Russell, R. M., Wang, X. D., Dietary lycopene and tomato extract supplementations inhibit nonalcoholic steatohepatitis-

promoted hepatocarcinogenesis in rats. *International journal of cancer* 2010, *126*, 1788-1796.

[13] Fenni, S., Hammou, H., Astier, J., Bonnet, L., *et al.*, Lycopene and tomato powder supplementation similarly inhibit high-fat diet induced obesity, inflammatory response, and associated metabolic disorders. *Molecular nutrition & food research* 2017, *61*.

[14] Bhatia, N., Gupta, P., Singh, B., Koul, A., Lycopene Enriched Tomato Extract Inhibits Hypoxia, Angiogenesis, and Metastatic Markers in early Stage N-Nitrosodiethylamine Induced Hepatocellular Carcinoma. *Nutrition and cancer* 2015, *67*, 1268-1275.

[15] Melendez-Martinez, A. J., Nascimento, A. F., Wang, Y., Liu, C., *et al.*, Effect of tomato extract supplementation against high-fat diet-induced hepatic lesions. *Hepatobiliary surgery and nutrition* 2013, *2*, 198-208.

[16] Ip, B. C., Liu, C., Ausman, L. M., von Lintig, J., Wang, X. D., Lycopene attenuated hepatic tumorigenesis via differential mechanisms depending on carotenoid cleavage enzyme in mice. *Cancer prevention research (Philadelphia, Pa.)* 2014, *7*, 1219-1227.

[17] Ip, B. C., Liu, C., Lichtenstein, A. H., von Lintig, J., Wang, X. D., Lycopene and apo-10'-lycopenoic acid have differential mechanisms of protection against hepatic steatosis in beta-carotene-9',10'-oxygenase knockout male mice. *The Journal of nutrition* 2015, *145*, 268-276.

[18] Hu, K. Q., Liu, C., Ernst, H., Krinsky, N. I., *et al.*, The biochemical characterization of ferret carotene-9',10'-monooxygenase catalyzing cleavage of carotenoids in vitro and in vivo. *The Journal of biological chemistry* 2006, *281*, 19327-19338.

[19] Ip, B. C., Hu, K. Q., Liu, C., Smith, D. E., *et al.*, Lycopene metabolite, apo-10'-lycopenoic acid, inhibits diethylnitrosamine-initiated, high fat diet-promoted hepatic inflammation and tumorigenesis in mice. *Cancer prevention research (Philadelphia, Pa.)* 2013, *6*, 1304-1316.

[20] Lian, F., Smith, D. E., Ernst, H., Russell, R. M., Wang, X. D., Apo-10'-lycopenoic acid inhibits lung cancer cell growth in vitro, and suppresses lung tumorigenesis in the A/J mouse model in vivo. *Carcinogenesis* 2007, *28*, 1567-1574.

[21] Chung, J., Koo, K., Lian, F., Hu, K. Q., *et al.*, Apo-10'-lycopenoic acid, a lycopene metabolite, increases sirtuin 1 mRNA and protein levels and decreases hepatic fat accumulation in ob/ob mice. *The Journal of nutrition* 2012, *142*, 405-410.

[22] Smith, J. S., Brachmann, C. B., Celic, I., Kenna, M. A., *et al.*, A phylogenetically conserved NAD+-dependent protein deacetylase activity in the Sir2 protein family.

Proceedings of the National Academy of Sciences of the United States of America 2000, *97*, 6658-6663.

[23] Imai, S., Armstrong, C. M., Kaeberlein, M., Guarente, L., Transcriptional silencing and longevity protein Sir2 is an NAD-dependent histone deacetylase. *Nature* 2000, *403*, 795-800.

[24] Cheng, J., Liu, C., Hu, K., Greenberg, A., *et al.*, Ablation of systemic SIRT1 activity promotes nonalcoholic fatty liver disease by affecting liver-mesenteric adipose tissue fatty acid mobilization. *Biochimica et biophysica acta* 2017.

[25] Hou, X., Xu, S., Maitland-Toolan, K. A., Sato, K., *et al.*, SIRT1 regulates hepatocyte lipid metabolism through activating AMP-activated protein kinase. *The Journal of biological chemistry* 2008, *283*, 20015-20026.

[26] Lan, F., Cacicedo, J. M., Ruderman, N., Ido, Y., SIRT1 modulation of the acetylation status, cytosolic localization, and activity of LKB1. Possible role in AMP-activated protein kinase activation. *The Journal of biological chemistry* 2008, *283*, 27628-27635.

[27] Gerhart-Hines, Z., Rodgers, J. T., Bare, O., Lerin, C., *et al.*, Metabolic control of muscle mitochondrial function and fatty acid oxidation through SIRT1/PGC-1alpha. *The EMBO journal* 2007, *26*, 1913-1923.

[28] Purushotham, A., Schug, T. T., Xu, Q., Surapureddi, S., *et al.*, Hepatocyte-specific deletion of SIRT1 alters fatty acid metabolism and results in hepatic steatosis and inflammation. *Cell metabolism* 2009, *9*, 327-338.

[29] Chen, J., Zhang, B., Wong, N., Lo, A. W., *et al.*, Sirtuin 1 is upregulated in a subset of hepatocellular carcinomas where it is essential for telomere maintenance and tumor cell growth. *Cancer research* 2011, *71*, 4138-4149.

[30] Lin, Z., Fang, D., The Roles of SIRT1 in Cancer. *Genes & cancer* 2013, *4*, 97-104.

[31] Zhang, Z. Y., Hong, D., Nam, S. H., Kim, J. M., *et al.*, SIRT1 regulates oncogenesis via a mutant p53-dependent pathway in hepatocellular carcinoma. *Journal of hepatology* 2015, *62*, 121-130.

[32] Liu, T., Liu, P. Y., Marshall, G. M., The critical role of the class III histone deacetylase SIRT1 in cancer. *Cancer research* 2009, *69*, 1702-1705.

[33] Seifert, E. L., Caron, A. Z., Morin, K., Coulombe, J., *et al.*, SirT1 catalytic activity is required for male fertility and metabolic homeostasis in mice. *FASEB journal : official publication of the Federation of American Societies for Experimental Biology* 2012, *26*, 555-566.

[34] Tolba, R., Kraus, T., Liedtke, C., Schwarz, M., Weiskirchen, R., Diethylnitrosamine (DEN)-induced carcinogenic liver injury in mice. *Laboratory animals* 2015, *49*, 59-69.

[35] Sharma, V., McNeill, J. H., To scale or not to scale: the principles of dose extrapolation. *British journal of pharmacology* 2009, *157*, 907-921.

[36] Kopec, R. E., Riedl, K. M., Harrison, E. H., Curley, R. W., Jr., *et al.*, Identification and quantification of apo-lycopenals in fruits, vegetables, and human plasma. *Journal of agricultural and food chemistry* 2010, *58*, 3290-3296.

[37] Borel, P., Lietz, G., Goncalves, A., Szabo de Edelenyi, F., *et al.*, CD36 and SR-BI are involved in cellular uptake of provitamin A carotenoids by Caco-2 and HEK cells, and some of their genetic variants are associated with plasma concentrations of these micronutrients in humans. *The Journal of nutrition* 2013, *143*, 448-456.

[38] Fulco, M., Cen, Y., Zhao, P., Hoffman, E. P., *et al.*, Glucose restriction inhibits skeletal myoblast differentiation by activating SIRT1 through AMPK-mediated regulation of Nampt. *Developmental cell* 2008, *14*, 661-673.

[39] Shiota, G., Tsuchiya, H., Hoshikawa, Y., The liver as a target organ of retinoids. *Hepatology research : the official journal of the Japan Society of Hepatology* 2006, *36*, 248-254.

[40] Zhu, X., Wang, W., Zhang, X., Bai, J., *et al.*, All-Trans Retinoic Acid-Induced Deficiency of the Wnt/beta-Catenin Pathway Enhances Hepatic Carcinoma Stem Cell Differentiation. *PloS one* 2015, *10*, e0143255.

[41] Yu, N., Su, X., Wang, Z., Dai, B., Kang, J., Association of Dietary Vitamin A and beta-Carotene Intake with the Risk of Lung Cancer: A Meta-Analysis of 19 Publications. *Nutrients* 2015, *7*, 9309-9324.

[42] Zhang, T., Chen, H., Qin, S., Wang, M., *et al.*, The association between dietary vitamin A intake and pancreatic cancer risk: a meta-analysis of 11 studies. *Bioscience reports* 2016, *36*.

[43] Lai, G. Y., Weinstein, S. J., Albanes, D., Taylor, P. R., *et al.*, Association of serum alpha-tocopherol, beta-carotene, and retinol with liver cancer incidence and chronic liver disease mortality. *British journal of cancer* 2014, *111*, 2163-2171.

[44] Moulas, A. N., Gerogianni, I. C., Papadopoulos, D., Gourgoulianis, K. I., Serum retinoic acid, retinol and retinyl palmitate levels in patients with lung cancer. *Respirology (Carlton, Vic.)* 2006, *11*, 169-174.

[45] Schmitz, H. H., Poor, C. L., Wellman, R. B., Erdman, J. W., Jr., Concentrations of selected carotenoids and vitamin A in human liver, kidney and lung tissue. *The Journal of nutrition* 1991, *121*, 1613-1621.

[46] Falcon, A., Doege, H., Fluitt, A., Tsang, B., *et al.*, FATP2 is a hepatic fatty acid transporter and peroxisomal very long-chain acyl-CoA synthetase. *American journal of physiology. Endocrinology and metabolism* 2010, *299*, E384-393.

[47] Shirakami, Y., Sakai, H., Shimizu, M., Retinoid roles in blocking hepatocellular carcinoma. *Hepatobiliary surgery and nutrition* 2015, *4*, 222-228.

[48] de Lera, A. R., Bourguet, W., Altucci, L., Gronemeyer, H., Design of selective nuclear receptor modulators: RAR and RXR as a case study. *Nature reviews. Drug discovery* 2007, *6*, 811-820.

[49] Shimizu, M., Moriwaki, H., Synergistic Effects of PPARgamma Ligands and Retinoids in Cancer Treatment. *PPAR research* 2008, *2008*, 181047.

[50] Bonofiglio, D., Cione, E., Qi, H., Pingitore, A., *et al.*, Combined low doses of PPARgamma and RXR ligands trigger an intrinsic apoptotic pathway in human breast cancer cells. *The American journal of pathology* 2009, *175*, 1270-1280.

[51] Youssef, J., Badr, M., Peroxisome proliferator-activated receptors and cancer: challenges and opportunities. *British journal of pharmacology* 2011, *164*, 68-82.

[52] Borbath, I., Horsmans, Y., The Role of PPARgamma in Hepatocellular Carcinoma. *PPAR research* 2008, *2008*, 209520.

[53] Borbath, I., Leclercq, I., Moulin, P., Sempoux, C., Horsmans, Y., The PPARgamma agonist pioglitazone inhibits early neoplastic occurrence in the rat liver. *European journal of cancer (Oxford, England : 1990)* 2007, *43*, 1755-1763.

[54] Tanaka, T., Suh, K. S., Lo, A. M., De Luca, L. M., p21WAF1/CIP1 is a common transcriptional target of retinoid receptors: pleiotropic regulatory mechanism through retinoic acid receptor (RAR)/retinoid X receptor (RXR) heterodimer and RXR/RXR homodimer. *The Journal of biological chemistry* 2007, *282*, 29987-29997.

[55] Blaschke, F., Leppanen, O., Takata, Y., Caglayan, E., *et al.*, Liver X receptor agonists suppress vascular smooth muscle cell proliferation and inhibit neointima formation in balloon-injured rat carotid arteries. *Circulation research* 2004, *95*, e110-123.

[56] Meng, Z. X., Nie, J., Ling, J. J., Sun, J. X., *et al.*, Activation of liver X receptors inhibits pancreatic islet beta cell proliferation through cell cycle arrest. *Diabetologia* 2009, *52*, 125-135.

[57] Tang, S., Huang, G., Fan, W., Chen, Y., *et al.*, SIRT1-mediated deacetylation of CRABPII regulates cellular retinoic acid signaling and modulates embryonic stem cell differentiation. *Molecular cell* 2014, *55*, 843-855.

[58] Iskandar, A. R., Liu, C., Smith, D. E., Hu, K. Q., *et al.*, beta-cryptoxanthin restores nicotine-reduced lung SIRT1 to normal levels and inhibits nicotine-promoted lung tumorigenesis and emphysema in A/J mice. *Cancer prevention research (Philadelphia, Pa.)* 2013, *6*, 309-320.

[59] Donmez, G., Wang, D., Cohen, D. E., Guarente, L., SIRT1 suppresses beta-amyloid production by activating the alpha-secretase gene ADAM10. *Cell* 2010, *142*, 320-332.

[60] Fengler, V. H., Macheiner, T., Kessler, S. M., Czepukojc, B., *et al.*, Susceptibility of Different Mouse Wild Type Strains to Develop Diet-Induced NAFLD/AFLD-Associated Liver Disease. *PloS one* 2016, *11*, e0155163.

CHAPTER VI

DISCUSSION

SUMMARY

The primary goal of this thesis was to provide a deeper understanding of the causal role of systemic sirtuin 1 (SIRT1) activity in the development of non-alcoholic fatty liver disease (NAFLD) and hepatocellular carcinoma (HCC), and whether tomato and tomato carotenoids protect against NAFLD and HCC dependent on SIRT1 activity. First, we used a systemic deacetylase activity ablated mouse model to investigate the causal role of SIRT1 in the pathogenesis of NAFLD, which involves liver, adipose tissue, and the cross-talk between two organs. Second, we employed a hepatic carcinogen-initiated, HFD-promoted HCC model using both wild-type (WT) and systemic SIRT1 activity ablated mice (MT) to investigate the efficacy of tomato powder (TP) on the pathogenesis of NAFLD and HCC, and to explore whether TP protects against NAFLD and HCC dependent on SIRT1 activity. Finally, we fed apo-10'-lycopenoic acid (ALA) to both WT and MT mice to examine whether ALA protects against NAFLD and HCC in a SIRT1-dependent manner. The major observations from this thesis work are as follows:

1) Systemic SIRT1 activity ablation accelerated NAFLD development through three mechanisms: first, SIRT1 ablation increased hepatic triglyceride accumulation, which was accompanied with higher protein levels of LXRα, SREBP-1, and SCD1, involved in lipogenesis, and decreased phosphorylation of LKB1 and AMPK in the liver; secondly, the lack of SIRT1 activity increased lipid accumulation in MAT by increasing the mRNA expression of lipogenic genes (*lxrα, srebp-1c, scd1* and *fas*), while maintaining fatty oxidation-related biomarkers (*acox1, acox3, cpt, ucp1, sirt3*) in both liver and MAT unchanged. Finally, we observed that the mRNA level of hormone

sensitive lipase (*hsl*), adipose triglyceride lipase (*atgl*) and *perilipin-1*, involved in lipolysis, significantly increased in MAT (not in epididymal adipose tissue), as compared with those of WT. These changes were correlated with higher circulating free fatty acid (FFA) concentrations and higher hepatic mRNA expression of *cd36* for FFA uptake, indicating that systemic SIRT1 activity ablation promoted NAFLD development via increasing the mobilization of FFA from MAT to liver. This study revealed a critical role of SIRT1 in preventing NAFLD, and helped us to understand why some people without 'fat belly' still develop fatty liver when sirt1 activity decreases due to certain factors, such as aging, unhealthful diet, stress, or high alcohol consumption.

2) Supplementation with TP (equivalent to lycopene concentration at 100 mg/kg diet) significantly reduced NAFLD severity. Specifically, TP supplementation significantly reduced liver steatosis in both WT and MT mice through different molecular mechanisms: protective effect of TP was mediated by increasing SIRT1 protein expression and activity, and decreased hepatic fatty acid binding protein 1 expression and long chain fatty acid (FA) uptake in WT mice; while in MT mice, TP decreased hepatic FA synthesis through inactivating hepatic acetyl-CoA carboxylase mediated by AMPK phosphorylation, independent of SIRT1. It is important to note that, in this study, we did not detect significant inflammatory responses, exemplified by the lack of inflammatory foci, in both WT and MT mice. Regardless, we found TP lowered *il-6* expression in MAT and IL-6 concentration in plasma

and liver, as compared with MT mice without TP, while in WT mice, dietary TP decreased caspase-1 mediated IL-1β maturation. However, neither the mutation of SIRT1 activity nor TP supplementation altered HCC incidence or severity in both WT and MT mice, which could be due to the lack of inflammation as a target of TP protection or limited efficacy in ameliorating HCC development in this mouse model. This study provided the first evidence that TP, as a whole food, can inhibit NAFLD independent of SIRT1, which provided an efficient dietary strategy to inhibit the development of NAFLD, even in the population with impaired SIRT1 activity.

3) Our final study demonstrated that in mice given HFD+ALA, the lack of systemic SIRT1 activity can attenuate the development of HCC by decreasing hepatic tumor multiplicity. Interestingly, the ablation of SIRT1 activity resulted in increased expressions of hepatic nuclear receptors (*rxrα*, *lxrα*, *pparγ*) and vitamin A transporter *cd36* and hepatic retinol concentration, but decreased cyclin D1 protein levels, suggesting contribution of these nuclear receptors and retinol as well as cell cycle arrest to the reduction of hepatic tumor multiplicity. This study demonstrated that ALA protects against NAFLD and HCC independent of SIRT1 activity and the lack of SIRT1 reduced the progression of HCC in mice given HFD and ALA supplementation.

In summary, we conclude that systemic SIRT1 activity is crucial in maintaining hepatic lipid homeostasis. The lack of systemic SIRT1 activity can cause aggravated NAFLD through increasing lipogenesis in liver and MAT, as well as promoting the

mobilization of FFA from MAT to liver. As a dietary strategy in preventing NAFLD development, we recommend the consumption of tomatoes or tomato products (such as tomato juice, paste), which are whole foods that can impede the progression of fatty liver, in a SIRT1-independent manner. Although SIRT1 is involved in decreasing hepatic triglyceride accumulation, the role of SIRT1 in HCC development in still controversial. In the 2nd project, HCC incidence and severity remained comparable between WT and MT mice fed with only HFD. However, in the 3rd project, we found that in mice given HFD+ALA, SIRT1 activity mutation resulted in reduced hepatic tumor multiplicity through decreasing the expressions of vitamin A transporter *cd36* and hepatic nuclear receptors (RXRα, *lxrα*, *pparγ*), as well as hepatic retinol concentration. These studies underscore the complex regulation of SIRT1 in hepatic tumorigenesis with paradoxical functions as tumor suppressor or tumor promoter.

LIMITATIONS

This thesis work contributes a significant body of new and exciting information to the field of HFD-induced NAFLD and HCC. However, it is necessary to point out that this body of work is not without limitations. Specific limitations of this thesis work are as follows:

1) We utilized 129/SvJ background mice, which were reported to have less susceptibility to hepatocyte enlargement than C57BL/6 mice under the same dietary intervention [1]. During this thesis work, our lab also used the same systemically ablated SIRT1 mouse model to study the role of SIRT1 in lung

cancer development, and results showed that mice with 129/SvJ background developed impaired immune response to cigarette smoking, which at least partly explains why we failed to observe inflammatory foci in this thesis project. Since the development of non-alcoholic steatohepatitis (NASH) mediates the escalation of NAFLD to HCC [2], the absence of NASH might have prevented a chance for HCC development.

2) We were not able to observe HCC development by time point. It has been revealed that a single injection of 20 mg/kg DEN in 129/SvJ mice resulted in 80-100% HCC after 30-55 weeks [3, 4]. In our preliminary study, we sacrificed 3 animals in each group (WT+HFD, WT+HFD+TP, MT+HF, MT+HFD+TP) at 26 week of age and did not observe any liver surface tumors. Therefore, we extended the study duration and sacrificed animals at 40 week of age. Although there is a possibility that we could observe difference in tumor characteristic (adenoma vs. carcinoma) between wild type and SIRT1 mutant mice using histological methods, liver surface tumor incidence appeared to be similar. It is possible that liver surface tumor incidence was different between 26 week-of-age and 40 week of age, but it is logistically difficult for us to include more time points given the available number of mice and budget.
3) In the second study, we did not have lycopene-supplemented groups in comparison with TP-supplemented groups. This is due to the scope of the specific aim of this study, i.e., determining whether the efficacy of TP protecting against NAFLD is SIRT1 dependent. In the previous study by Ip et

al [5], the consumption of lycopene did not increase SIRT1 expression or activity, while ALA supplementation significantly increased SIRT1 signaling. Therefore, we did not give mice lycopene supplementation in the second study, because we have previously demonstrated that lycopene protects against NAFLD in a SIRT1-independent manner.

4) In the third study, we did not have a parallel matching group fed HFD without ALA. This is because previous study from our lab has already demonstrated that ALA supplementation can attenuate the progression of NAFLD and HCC [6, 7]. Therefore, examining the efficacy of ALA against NAFLD and HCC is beyond the scope of this study. In the third study, we aim to investigate whether the beneficial efficacy of ALA, which has been observed previously, is dependent on SIRT1 activity. Thus, two groups with WT and MT mice, both given ALA supplementation, is sufficient to test the primary hypothesis that the beneficial efficacy of ALA against NAFLD and HCC is SIRT1 dependent.
5) We need to point out that certain interpretation and mechanisms in this thesis work were based on mRNA expression only, in stead of protein levels. Therefore, further validation on protein levels are needed.
6) Finally, the results from our studies on the protective capabilities of TP supplementation on NAFLD lay an important foundation for possible future dietary intervention clinical trials. However, it should be kept in mind that these results were produced by employing animal models. While these animal models are designed to mimic human NAFLD, there is no doubt that

substantial difference exists between mice and humans. Supplementation studies can result in very different outcomes when done in different experimental models. Therefore, extrapolation of these effects in rodent models to the effect of TP supplementation in humans should be done with caution.

FUTURE DIRECTIONS

This thesis work opens up several new research directions to further the field of HFD-induced NAFLD and HCC research involving mechanistic and dietary prevention studies. Specific future directions of this thesis work are as follows:

1) In this thesis, we showed that the role of SIRT1 in HCC development is complex and controversial. However, as mentioned in the limitation section, we utilized 129/SvJ background, CD1 outbred mice, which exhibited impaired immune response and lack of inflammatory foci. The failure of developing severe hepatic inflammation might be the reason why we did not observe significant difference in HCC development between WT and MT mice, despite the observation of markedly increased hepatic steatosis in MT mice. Therefore, it would be important to backcross 129/SvJ mice to C57/BL6 mice, which is a mouse model widely used in HCC studies. In fact, during the completion of this thesis, our lab conducted a pilot study by utilizing the systemic SIRT1 ablated, C57/BL6 backcrossed mice and their WT littermates, to examine the causal role of SIRT1 in HCC development. They found that at 24 weeks of age, all mice injected carcinogen developed HCC. In addition, mice with mutated SIRT1

activity developed less tumor multiplicity than WT mice. This leads us to hypothesize that SIRT1 might be an oncogene in animals with normal immune response, which warrants further investigation.

2) As discussed in the limitation section, our study revealing the protective effects of TP against HFD-induced NAFLD and the efficacy of TP in reducing hepatic inflammatory biomarkers. However, the study is unable to demonstrate dietary TP, as whole food, has advantage for its benefit over single compounds such as lycopene, or lycopene metabolites. Therefore, an important next step for this study would be the comparison of the effects of TP, lycopene, and ALA in protecting against the progression of NAFLD or HCC.
3) A previous study in our lab has demonstrated that, compared to mice fed HFD, mice fed high refined-carbohydrates diet (HCD) developed comparable HCC, but more severe hepatic steatosis [8]. Such result is in line with emerging evidence that low-carb diet, or less refined carbohydrate diet, showed efficacy in the treatment and prevention of NAFLD [9, 10]. Therefore, a future study could utilize HCD as diet intervention to examine the role of dietary TP, or its metabolites, in HCD-induced NAFLD and HCC development.
4) This thesis work demonstrated that the lack of SIRT1activity presented causal role in exacerbating NAFLD. Interestingly, SIRT1 has been recognized as a critical regulator of circadian rhythms in multiple tissues, including liver and brain [11-13]. In the liver, SIRT1 plays its role through ensuring proper

circadian oscillation in hepatocytes due to its deacetylase activity on histone H3 at the promoter of clock-controlled genes (CCGs) [13], as well as other circadian components including BAML1 and PER2 [11, 13]. SIRT1 activity itself oscillates in a circadian manner over the day/night cycle [14, 15]. Genetic or pharmacological modulation of SIRT1 expression and SIRT1 activity could lead to altered hepatic circadian gene expression and signaling [16, 17], highlighting the importance of the SIRT1 pathway in controlling hepatic circadian rhythm. Therefore, an important next step could be the investigation of how SIRT1 prevents the development of NAFLD through its regulation of circadian rhythm. One pilot study from our lab has found that systemically ablating SIRT1 resulted in significant increase of *mTOR* mRNA expression in the brain. Since brain is the main organ controlling central circadian rhythm, it would also be important to examine brain crosstalk with liver through the modification of circadian rhythm.

5) In this thesis work, we have demonstrated that systemic SIRT1 activity ablation aggravates NAFLD by involving liver and mesenteric adipose tissue. It is important to note that the lack of systemic SIRT1 activity could also affect other tissues. Intestine plays an important role in lipid absorption, excretion and distribution. In the third study, we revealed that systemic SIRT1 activity mutation increased hepatic retinol concentration. However, the underlying mechanism remains unknown. It is possible that the deacetylase activity of SIRT1 impedes the uptake of dietary retinol by interfering with intestinal *cd36* and *sr-b1* transcription. Thus, an important further step could

be the examination of the crosstalk between intestine and liver in the development of NAFLD and HCC, and the role of SIRT1, TP or TP metabolite supplementation in the progression of NAFLD and HCC by regulating molecular signaling pathways in the intestine, as well as the cross-talk between intestine and liver.

CONCLUSION

This thesis addresses the specific molecular mechanisms by which systemic SIRT1 activity ablation aggravates NAFLD and the prevention of NAFLD and liver inflammation via the supplementation of dietary TP and lycopene metabolite, ALA. Specifically, we have demonstrated the causal role of SIRT1 in NAFLD development by increasing lipogenesis in both liver and MAT, and importantly, by promoting the mobilization of FFA from MAT to liver. In a second study, we revealed that TP supplementation is capable of preventing NAFLD including a reduction in simple hepatic steatosis and inflammatory biomarkers. This reduction occurred in both WT and mice with impaired SIRT1 activity, but interestingly, through different mechanisms: in WT mice, TP decreased hepatic steatosis by inhibiting the uptake of FFA from circulating system to the liver, and the consumption of TP decreased hepatic IL-1β concentration by promoting the cleavage and maturation of IL-1β; in MT mice, TP inhibited hepatic steatosis by decreasing hepatic lipogenesis and reduced hepatic IL-6 concentration potentially through decreasing the release of IL-6 from MAT, and decreasing circulating IL-6 from circulating system to the liver. In our last study, we demonstrated that under the surplus of HFD and ALA, systemic SIRT1 ablation resulted in attenuated HCC

progression, which was associated with increased hepatic retinol concentration and activated hepatic nuclear receptors (*rxrα*, *lxrα*, *pparγ*), as well as cycle-cycle inhibitor-mediated cell-cycle arrest. Unexpectedly, neither the mutation of SIRT1 activity nor TP supplementation altered HCC incidence or severity in both WT and MT mice, which could be due to the lack of inflammation as a target of TP protection or limited efficacy in ameliorating HCC development in this mouse model. This underscores the necessity of utilizing mice with C57/BL6 background in the future studies.

Taken together, this thesis work supports that dietary tomato powder, as a whole food approach, is an effective disease prevention strategy against NAFLD and highlights the key role of SIRT1 in preventing NAFLD progression through acting on multiple organs such as liver and MAT.

LITERATURE CITED

[1] Fengler, V. H., Macheiner, T., Kessler, S. M., Czepukojc, B., *et al.*, Susceptibility of Different Mouse Wild Type Strains to Develop Diet-Induced NAFLD/AFLD-Associated Liver Disease. *PloS one* 2016, *11*, e0155163.

[2] Tiniakos, D. G., Vos, M. B., Brunt, E. M., Nonalcoholic fatty liver disease: pathology and pathogenesis. *Annual review of pathology* 2010, *5*, 145-171.

[3] Park, T. J., Kim, J. Y., Oh, S. P., Kang, S. Y., *et al.*, TIS21 negatively regulates hepatocarcinogenesis by disruption of cyclin B1-Forkhead box M1 regulation loop. *Hepatology (Baltimore, Md.)* 2008, *47*, 1533-1543.

[4] Teoh, N. C., Dan, Y. Y., Swisshelm, K., Lehman, S., *et al.*, Defective DNA strand break repair causes chromosomal instability and accelerates liver carcinogenesis in mice. *Hepatology (Baltimore, Md.)* 2008, *47*, 2078-2088.

[5] Ip, B. C., Liu, C., Lichtenstein, A. H., von Lintig, J., Wang, X. D., Lycopene and apo-10'-lycopenoic acid have differential mechanisms of protection against hepatic steatosis in beta-carotene-9',10'-oxygenase knockout male mice. *The Journal of nutrition* 2015, *145*, 268-276.

[6] Ip, B. C., Hu, K. Q., Liu, C., Smith, D. E., *et al.*, Lycopene metabolite, apo-10'-lycopenoic acid, inhibits diethylnitrosamine-initiated, high fat diet-promoted hepatic inflammation and tumorigenesis in mice. *Cancer prevention research (Philadelphia, Pa.)* 2013, *6*, 1304-1316.

[7] Ip, B. C., Liu, C., Ausman, L. M., von Lintig, J., Wang, X. D., Lycopene attenuated hepatic tumorigenesis via differential mechanisms depending on carotenoid cleavage enzyme in mice. *Cancer prevention research (Philadelphia, Pa.)* 2014, *7*, 1219-1227.

[8] Ip, B. C., Liu, C., Smith, D. E., Ausman, L. M., Wang, X. D., High-refined-carbohydrate and high-fat diets induce comparable hepatic tumorigenesis in male mice. *The Journal of nutrition* 2014, *144*, 647-653.

[9] York, L. W., Puthalapattu, S., Wu, G. Y., Nonalcoholic fatty liver disease and low-carbohydrate diets. *Annual review of nutrition* 2009, *29*, 365-379.

[10] Eslamparast, T., Tandon, P., Raman, M., Dietary Composition Independent of Weight Loss in the Management of Non-Alcoholic Fatty Liver Disease. *Nutrients* 2017, *9*.

[11] Asher, G., Gatfield, D., Stratmann, M., Reinke, H., *et al.*, SIRT1 regulates circadian clock gene expression through PER2 deacetylation. *Cell* 2008, *134*, 317-328.

[12] Chang, H. C., Guarente, L., SIRT1 mediates central circadian control in the SCN by a mechanism that decays with aging. *Cell* 2013, *153*, 1448-1460.

[13] Nakahata, Y., Kaluzova, M., Grimaldi, B., Sahar, S., *et al.*, The NAD+-dependent deacetylase SIRT1 modulates CLOCK-mediated chromatin remodeling and circadian control. *Cell* 2008, *134*, 329-340.

[14] Nakahata, Y., Sahar, S., Astarita, G., Kaluzova, M., Sassone-Corsi, P., Circadian control of the NAD+ salvage pathway by CLOCK-SIRT1. *Science (New York, N.Y.)* 2009, *324*, 654-657.

[15] Ramsey, K. M., Yoshino, J., Brace, C. S., Abrassart, D., *et al.*, Circadian clock feedback cycle through NAMPT-mediated NAD+ biosynthesis. *Science (New York, N.Y.)* 2009, *324*, 651-654.

[16] Bellet, M. M., Nakahata, Y., Boudjelal, M., Watts, E., *et al.*, Pharmacological modulation of circadian rhythms by synthetic activators of the deacetylase SIRT1. *Proceedings of the National Academy of Sciences of the United States of America* 2013, *110*, 3333-3338.

[17] Masri, S., Rigor, P., Cervantes, M., Ceglia, N., *et al.*, Partitioning circadian transcription by SIRT6 leads to segregated control of cellular metabolism. *Cell* 2014, *158*, 659-672.

APPENDIX I

Macronutrient Component Table. Summary of macronutrient composition of diets[a]

Macronutrients	% of energy	Source
Protein	14	Casein
Carbohydrate	26	Sucrose, Maltodextrin
Fat	60	Lard

[a]Mineral mix, vitamin mix, DL-Methionine and choline chloride are added in the ingredients of diet (Bioserv, Frenchland, NJ, USA).

APPENDIX II

Primer Sequence Table. Primers sequences for RT-PCR analysis in three studies.

Genes:	Forward:	Reverse:
Acox1	TAACTTCCTCACTCGAAGCCA	AGTTCCATGACCCATCTCTGTC
Acox3	GCCTCCTTCAACTCTGGGG	TCAGTTCTTCGTAGCTTCTCTAGG
β-Actin	CTTTTCCAGCCTTCCTTCTTGG	CAGCACTGTGTTGGCATAGAGG
Atgl	ACAGTGTCCCCATTCTCAGG	CACATCTCTCGGAGGACCAT
Cd36	GCGACATGATTAATGGCACA	CCTGCAAATGTCAGAGGAAA
Cpt	GCACTGCAGCTCGCACATTACAA	CTCAGACAGTACCTCCTTCAGGAAA
Dgat1	TCCGTCCAGGGTGGTAGTG	TGAACAAAGAATCTTGCAGACGA
Dgat2	GCGCTACTTCCGAGACTACTT	GGGCCTTATGCCAGGAAACT
Fas	GCTGCGGAAACTTCAGGAAAT	AGAGACGTGTCACTCCTGGACTT
Fatp2	TCCTCCAAGATGTGCGGTACT	TAGGTGAGCGTCTCGTCTCG
Hsl	CCAGCCTGAGGGCTTACTG	CTCCATTGACTGTGACATCTCG
Mttp	CTCTTGGCAGTGCTTTTTCTCT	GAGCTTGTATAGCCCGCTCATT
Pgc1α	TATGGAGTGACATAGAGTGTGCT	CCACTTCAATCCACCCAGAAAG
Plin2	AAGAGAAGCATCGGCTACGA	GGCGATAGCCAGAGTACGTG
Pparα	GTACCACTACGGAGTTCACGCA	CATTGTGTGACATCCCGACAG
Pparγ	GGATAAAGCATCAGGCTTCCAC	AACCTGATGGCATTGTGAGACA
Scd1	CCGGAGACCCCTTAGATCGA	TAGCCTGTAAAAGATTTCTGCAAACC

Srebp1c	TAGAGCATATCCCCCAGGTG	GGTACGGGCCACAAGAAGTA
Ucp1	AGGCTTCCAGTACCATTAGGT	CTGAGTGAGGCAAAGCTGATTT
Ucp2	ATGGTTGGTTTCAAGGCCACA	CGGTATCCAGAGGGAAAGTGAT

APPENDIX III

Ablation of systemic SIRT1 activity promotes nonalcoholic fatty liver disease by affecting liver-mesenteric adipose tissue fatty acid mobilization

Junrui Cheng[1,5], Chun Liu[1], Kangquan Hu[1], Andrew Greenberg[2,5], Dayong Wu[3,5], Lynne M. Ausman[1,5], Michael W. McBurney[4] and Xiang-Dong Wang[1,5]

[1]Nutrition and Cancer Biology Lab, [2]Obesity and Metabolism Lab, [3]Nutritional Immunology Lab, JM USDA-HNRCA at Tufts University;

[4] Departments of Medicine and Biochemistry, Microbiology and Immunology Lab, University of Ottawa, Ontario, Canada; [5]Friedman School of Nutrition and Policy, Tufts University, Boston, MA, USA

Corresponding Author:

Xiang-Dong Wang, MD, PhD

Nutrition and Cancer Biology Laboratory

Jean Mayer USDA Human Nutrition Research Center on Aging at Tufts University

711 Washington Street, Room 514

Boston, MA 02111, USA

Phone: 617-556-3130

Fax: 617-556-3344

Email: xiang-dong.wang@tufts.edu

Authors' last names: Cheng, Liu, Hu, Greenberg, Wu, Ausman, McBurney, Wang

Electronic Word Count: 6,846

Total Number of Figures: 5

Total Number of Tables: 1

Online Supporting Material: 0

Running title: SIRT1 activity and liver steatosis reduction

Supported by USDA/NIFA (2015-67017) and USDA/ARS (58-1950-0014). Any opinions, findings, conclusions, and recommendations expressed in this publication are those of the authors and do not necessarily reflect the views of the sponsors.

Author disclosures: J. Cheng, C. Liu, K. Hu, A. Greenberg, D. Wu, L. Ausman, M. McBurney, and X-D. Wang, no conflicts of interest.

Abstract

Sirtuin 1 (SIRT1) has been reported to protect against nonalcoholic fatty liver disease (NAFLD) development. The mechanism of how SIRT1 deacetylase activity affects NAFLD has not been well investigated. The current investigation addressed the causal effect of systemic SIRT1 activity on NAFLD development and the underlying mechanism involved in both liver and mesenteric adipose tissue (MAT). Both SIRT1 homozygous mice ablated the catalytic activity ($sirt1^{Y/Y}$) and their corresponding wild type littermates (WT) were fed a high fat diet (HFD, 60% calories from fat) for 34 weeks. $Sirt1^{Y/Y}$ mice showed significantly higher level of hepatic triglyceride which was accompanied with higher levels of SREBP-1 and SCD1and decreased phosphorylation of LKB1 and AMPK in the liver. Compared with WT mice, mRNA expression of lipogenic genes (*lxrα*, *srebp-1c*, *scd1* and *fas*) in the MAT increased significantly in $sirt1^{Y/Y}$ mice. Fatty acid oxidation biomarkers (*acox1*, *acox3*, *cpt*, *ucp1*, *sirt3*) in both liver and MAT were comparable between groups. Interestingly, we observed that in $sirt1^{Y/Y}$ mice, the mRNA level of hormone sensitive lipase (*hsl*), adipose triglyceride lipase (*atgl*) and *perilipin-2* (*plin-2*), all involved in lipolysis, significantly increased in MAT, but not in epididymal adipose tissue. These changes positively correlated with circulating free fatty acid (FFA) concentrations and higher hepatic mRNA expression of *cd36* for FFA uptake. The present study has provided novel evidence to suggest that under HFD-induced metabolic surplus, the lack of SIRT1 catalytic activity promotes release of FFA from MAT and escalate NAFLD by interfering with lipid homeostasis in both liver and MAT.

Keywords: Non-alcoholic fatty liver disease, sirtuin 1, lipid metabolism, liver, adipose tissue

1. Introduction

Obesity has become a leading epidemic concern worldwide, and the escalating incidence of nonalcoholic fatty liver disease (NAFLD) parallels the increasing obesity rates [1]. NAFLD is observed in 65%-85% of obese patients, with a higher prevalence in men compared to women [2]. NAFLD describes a range of related disorders that begin with hepatic steatosis, which can proceed to nonalcoholic steatohepatitis [3], leading to higher risk of hepatocellular carcinoma [4]. Considering the increasing prevalence of NAFLD and the devastating outcome of NAFLD progression, it is of critical importance to have a mechanistic understanding for NAFLD development in order to develop preventive and therapeutic strategies for NAFLD.

SIRT1 is an evolutionarily conserved NAD^+-dependent histone and non-histone protein deacetylase [5, 6]. As a metabolic regulator, SIRT1 has been identified to control a series of physiological activities, including reducing fatty acid synthesis [7, 8], increasing β-oxidation [9, 10], and decreasing adipocyte generation [11]. These functions of SIRT1 are exerted through coupling with NAD^+ hydrolysis, transferring the acetyl group of the substrate to cleaved NAD^+ (ADP-ribose), and generating O-acetyl-ADP-ribose [6, 12, 13]. The catalytic activity of SIRT1 is tightly regulated by the cellular NAD^+ levels [12, 14, 15] and multiple nutritional, hormonal, and environmental cues that can alter the cellular NAD^+ availability [15]. This explains the observation that SIRT1 protein level and SIRT1 activity are not always parallel [16]; therefore, it is important to determine the effect of SIRT1 activity, rather than SIRT1 protein alone.

Both animal and human studies suggest an inverse correlation between SIRT1 levels and NAFLD incidence [17, 18]. Several SIRT1 transgenic mouse models have been established to explore the molecular mechanism of SIRT1 signaling against hepatic steatosis development [10, 19-23]. Global overexpression of SIRT1 using a knock-in Sirt1 genomic construct resulted in enhancing energy expenditure and decreasing high fat diet-induced hepatic steatosis [19]. Hepatocyte-specific deletion of SIRT1 caused hepatic steatosis [10, 22, 23], hepatic inflammation and endoplasmic reticulum stress [10]. The phenotype of heterozygous SIRT1 knockout mice presented severe hepatic steatosis on high-fat diets [8]. However, these mouse models either showed the effect of partial SIRT1 function, or focused on liver-specific SIRT1 function, owing to the fact that whole body SIRT1 gene knockout in mice would cause metabolic defect [24], developmental abnormality, and postnatal lethality [25, 26]. This produces challenges of investigating the causal effect of systemic SIRT1 activity on NALFD development. Recently, an engineered systemic SIRT1 deacetylase activity ablation mouse model achieved similar SIRT1

loss-of-function effects with SIRT1 knockout mice, but with less resultant genetic defects [27]. Using this mouse model, Caron et al. observed an increasing hepatic lipid accumulation in SIRT1 activity ablated mice [21]. This study raised an important question and also opened the door to the further investigation as for how the lack of SIRT1 activity promotes NAFLD.

As an effort along this line, in this study we used the systemic SIRT1 activity ablation ($sirt1^{Y/Y}$) and wild-type mice (WT) in the current study to investigate the underlying mechanism by which SIRT1 activity ablation exerted on high fat diet (HFD)-induced NAFLD.

2. Materials and Methods

2.1. Study design

All study protocols including breeding were approved by the Institutional Animal Care and Use Committee of Tufts University. We utilized the homozygous H355Y SIRT1 mutant ($sirt1^{Y/Y}$), 129/SvJ background mouse expressing the SIRT1 protein that lacks its catalytic activity, as compared with that of a wild-type H355Y, $sirt1^{+/+}$ 129/SvJ mouse. Both $sirt1^{Y/Y}$, 129/SvJ background mice and $sirt1^{+/+}$ 129/SvJ mice exhibit hepatic steatosis similar to humans, and 129/SvJ mice are the animal model of choice in studies of high fat diet (HFD)-induced hepatic steatosis. At 4 weeks of age, SIRT1 genotypes of animals were determined by a PCR-based test performed on DNA isolated from tail-tip biopsies using the primers 5'-TGGAAGGAAAGCAATTTTGGT-3' and g'CTGAGTTACCTTAGCTTGGC-3'. Mice were fed the standard laboratory chow diet (Envigo, Huntingdon, UK) for two weeks. At 6 weeks of age, mice were fed HFD (60% calories from fat, Bioserv, Frenchland, NJ, **Supplemental Table 1**) twice a week for 34 weeks, and body weight of each mouse was recorded weekly. At 38 weeks of age, EchoMRI-100 (EchoMRI, Houston, TX) was used for mice body composition measurement, as described previously [28]. Briefly, after weights were recorded for each mouse, non-anesthetized mice were placed into a cylinder and inserted into the chamber unit of the MRI machine. Total fat mass was determined and fat composition was obtained by calculating the ratio of fat mass to body weight. All mice were killed at 40 weeks of age. Serum, livers, mesenteric adipose tissue (MAT), and epididymal adipose tissue were collected. Livers were weighed, and a piece of liver tissue from left lobe of liver was fixed in 10% buffered formalin solution for histopathological examination while the remaining liver tissues were snap frozen in liquid nitrogen and stored at -80°C for further study.

2.2. Liver histopathology evaluation

Five-micrometer sections of formalin-fixed and paraffin-embedded liver tissue were stained with hematoxylin and eosin (H&E) for histopathological examination. The sections were examined under light microscopy by 2 independent investigators who were blinded to the treatment groups. A ZEISS microscope with a PixeLINK USB 2.0 (PL-B623CU) digital Camera and PixeLINK µScope Microscopy Software was used for the examination. Liver steatosis was graded according to steatosis magnitude (both macro- and micro-vesicular fat accumulation) as described previously [29] (**Figure 1A**). Briefly, the degree of steatosis was graded based on the percentage of the liver section that was occupied by fat vacuoles at 100× magnification in 20 fields (grade 0 = <5%; grade 1 = 5–25%; grade 2 = 26–50%; grade 3 = 51–75%; grade 4 = >75%).

2.3. Liver and plasma triglyceride (TG) quantification

Plasma and hepatic TG were measured using a TG colorimetric assay kit (Cayman, USA). Plasma was obtained in EDTA tubes and centrifuged at 1,000 g for 10 minutes, followed by pipetting off the top plasma layer. Liver tissue (about 40 mg) was minced and weighed, followed by homogenization in the standard diluent (0.2 ml) with an ultrasonic tissue homogenizer. The digested tissue was centrifuged for 10 minutes at 10,000 g, and the entire supernatant was transferred and diluted 1:5 with the standard diluent. The TG contents in both plasma and liver were determined based on the absorbance at 540 nm after a coupled enzymatic reaction, and was adjusted with a standard glycerol solution.

2.4. Liver cholesterol quantification

A commercial cholesterol kit (Cell Biolabs Inc, San Diego, CA) was utilized for total cholesterol measurement. Briefly, 50 mg liver tissue was extracted with 1000 µL mixture of chloroflorm : isopropanol : NP-40 (7:11:0.1) in a micro-homogenizer. The pellet was kept after centrifuging the mixture for 10 minutes at 15,000 rcf. Removing the trace amounts of organic solvent, dried lipids was dissolved in 200 µL Assay Diluent with sonicating and vortexing. The cholesterol concentration was calculated according to the absorption at 540 nm wavelength.

2.5. Protein isolation and Western blotting

Whole cell protein was extracted from frozen liver tissue as previously described [30]. For nuclear protein extraction, 50-60 mg liver protein was minced and mixed with 2ml hypertonic buffer, followed by homogenization for 30 seconds. The whole volume was then centrifuged at 5500 rpm for 5 minutes, and a second centrifugation (13000 rpm, 5 minutes) was executed after washing pallets with 1ml hypertonic buffer. Pellets were then re-suspended in 100µl high salt

buffer (5M NaCl) and shake-incubated a Vortex Genie Turbo Mixer in 4°C cold room for 10 minutes. The supernatant was transferred and centrifuged at 55000 rpm for 60 minutes using an Ultracentrifuge. The protein concentration was measured by the Comassie Plus protein quantification method (Thermo Fisher Scientific) and adjusted to 10μg/μl. For Western blotting, 5μl whole cell lysates per sample were mixed with 6 μl 2X reducing Laemmli sample buffer and boiled in 100°C water bath for 5 minutes to denature. Denatured protein was then loaded on SDS-polyacrylamide gels and resolved according to their molecular weights. For protein detection, electroblotting was executed by transferring protein onto Immobilon-P membranes (Millipore, MA, USA), followed by non-specific blocking (5% non-fat milk) in TBST buffer and incubation with appropriate primary antibodies. The following antibodies were used for Western blotting: phosphorylated-AMPK (Thr172), phosphorylated-ACC (Ser79), phosphorylated-LKB1 (Ser428), AMPK, ACC, LKB1, SCD1 (Cell Signaling, MA, USA), LXRα (Abcam, Cambridge, UK), Ac-FoxO1, FoxO1, and SREBP-1 (Santa Cruz, TX, USA). An anti-rabbit secondary antibody (Bio-Rad, CA, USA) linked to a horseradish peroxidase reporter enzyme was applied to binding the above primary antibody, and the bands of interest were detected by a SuperSignal West Pico Chemiluminescent Substrate kit (Sigma-Aldrich) according to the manufacturer's instructions. Protein level of β-actin was used as reference for normalization. Intensities of protein bands were detected using GS-710 Calibrated Imaging Densitometer (Bio-Rad).

2.6. RNA extraction and real-time PCR

Total RNA was extracted from frozen liver tissue with TriPure Isolation Reagent kit (Roche, USA). Briefly, 50-100 mg frozen liver was minced, mixed with 1 ml TriPure Isolation Reagent, and centrifuged for 10 minutes at 12,000 g. Then 0.2 ml chloroform was added to each sample and the whole volume was centrifuged for 15 minutes at 12,000 g. The collected upper aqueous phase was mixed with 0.5 ml isopropanol and centrifuged for 10 minutes at 12,000 g. The RNA pellet was obtained after discarding the supernatant, washed using 75% ethanol, followed by resuspending in DEPC water and incubating for 10 minutes at 55 4°C. Complementary DNA (cDNA) was synthesized with a reverse transcription PCR kit (M-MLV, Invitrogen, CA) and the Bio-Rad PTC 200 (GMI, CA). Quantitative real-time PCR was performed using FastStart Universal SYBR Green Master (Roche, USA). Relative gene expression was determined using the $-2^{\Delta\Delta Ct}$ method and normalized to the level of β-actin. Primer sequences are listed in **Supplemental Table 2**.

2.7. Statistical analysis

SAS 9.3 software was utilized to perform the statistical analysis. The Mann-Whitney U test was used to compare liver steatosis score distribution. The Student t test was used to compare TG, FFA levels and gene and protein expressions between wild-type mice and sirt1$^{Y/Y}$ mice. Logistic regression was utilized to analyze the correlation between steatosis score and hepatic TG level. Statistical significance was set as $P < 0.05$.

3. Results

3.1. SIRT1 mutation increased liver triglyceride level.

To test whether SIRT1 deacetylase activity was reduced in our mouse model, we measured the acetylation of FoxO1, and observed significantly higher acetylated-FoxO1 to total-FoxO1 ratio in Sirt1 mutant (sirt1$^{Y/Y}$) mice, compared to wild-type (WT) mice (**Figure 1B**), indicating that the deacetylase activity of SIRT1 in sirt1$^{Y/Y}$ mice was decreased. Average food consumption was similar between the two groups of mice (**Table 1**). There was no significant difference in final body weight, liver weight or liver weight/g body weight, and total fat mass between wild-type and mutant mice (**Table 1**). Hepatic cholesterol concentration was comparable between two groups (wild-type vs. sirt1$^{Y/Y}$: 52.35 ± 5.38 vs. 53.28 ± 2.19 mg/g tissue).

To examine liver steatosis, we measured hepatic TG level using a TG quantification kit. We found that hepatic TG level was significantly higher in mutant mice, compared to their wild-type counterparts (**Figure 1C**). The results from liver histopathological examination showed that among wild-type mice, 20% developed hepatic steatosis with a score of 1, 40% with a score of 2, and 30 with a score of 3; in contrast, all mutant mice developed hepatic steatosis with score at 2 or higher (55.6% with score 2, 44.4% with score 3; **Figure 1D**). Although overall liver steatosis was not significantly different between two groups, sirt1$^{Y/Y}$ mice showed a trend toward higher liver steatosis severity as compared to wild-type mice. In addition, the hepatic TG level was significantly correlated with steatosis score ($P = 0.04$).

3.2. SIRT1 mutation increased hepatic lipid synthesis.

To address the molecular mechanism of increasing liver steatosis severity in sirt1$^{Y/Y}$ mice, we quantified mRNA expressions and protein levels of the genes involved in lipogenesis and fatty acid β-oxidation. Result showed that phosphorylation of acetyl-CoA carboxylase (p-ACC), the inactive form of ACC, was significantly lower in sirt1$^{Y/Y}$ mice (**Figure 2A**). This was correlated with lower phosphorylation of AMP-kinase (p-AMPK; **Figure 2B**). LKB1 phosphorylated at Ser^{428}, the upstream signaling of p-AMPK [8, 31], was also reduced in sirt1$^{Y/Y}$ animals (**Figure**

2C). LXRα mRNA, but not protein level, was higher in sirt1$^{Y/Y}$ mice (**Figure 2F**). The protein level of sterol regulatory element-binding protein 1 (SREBP-1) and the mRNA level of its isoform, *srebp-1c*, were found elevated in sirt1$^{Y/Y}$ mice (**Figure 2D, F**). The mRNA and protein level of SCD1, one of the downstream targets of SREBP-1c [32], were promoted in sirt1$^{Y/Y}$ mice (**Figure 2E, F**). Hepatic nuclear PGC1α/whole-cell PGC1α ratio and hepatic PPARα protein levels were not changed (data not shown). Other lipogenic gene mRNA (*fas*, *dgat1*, *dgat2*, *fatp2*, *pparα*) were not altered between groups (**Figure 2F**). The mRNA levels of five β-oxidation related genes (*acox1*, *acox3*, *cpt*, *ucp1*, *ucp2*, *sirt3*) were measured in the liver, but no changes were observed between wild-type and sirt1$^{Y/Y}$ mice (**Figure 2G**). These data suggest that increasing *de novo* lipogenesis, rather than decreasing β-oxidation, is a major mechanism leading to elevated liver steatosis in SIRT1 activity ablated mice.

3.3. SIRT1 mutation increased lipid synthesis in MAT.

MAT can release free fatty acids (FFA) to venous drainage, which subsequently enters liver via portal vein and exposes liver to lipid accumulation [33-35]. Since the SIRT1 activity ablation in this model is systemic, we propose that lacking SIRT1 activity may affect lipid metabolism in MAT. To test this hypothesis, we examined lipogenesis and fatty acid β-oxidation related genes in MAT. We first examined the mRNA level of lipogenic genes (*scd1*, *srebp-1c*, *fas*, *dgat1*, *dgat2*, *pparγ*). Interestingly, *srebp-1c* showed a trend of increase (P = 0.07) in SIRT1 mutant mice, but its downstream targets, *scd1* and *fas* were significantly higher in sirt1$^{Y/Y}$ mice (**Figure 3A**). Liver X receptor α (LXRα) is known to activate the cleavage and movement of mature SREBP-1c to the nucleus [36]. We examined *lxr-α* expression and found *lxrα* transcription significantly elevated in sirt1$^{Y/Y}$ mice (**Figure 3A**). This indicates that the lack of SIRT1 activity may promote LXRα-mediated SREBP-1c maturation. We then determined the effect of SIRT1 activity ablation on fatty acid oxidation biomarkers (*acox1*, *acox3*, *cpt*, *ucp1*, *ucp2*). Results showed no difference in transcription levels of these genes between groups (**Figure 3B**). No alterations of gene expression were found in epididymal adipose tissue between two groups (data not shown). These results suggested an overall increasing lipogenesis level in MAT of sirt1$^{Y/Y}$ mice. We also measured adiponectin mRNA level in both MAT and epididymal adipose tissue, as well as hepatic adiponectin receptor 1 and adiponectin receptor 2 protein levels in WT and sirt1$^{Y/Y}$ mice, but did not find significant differences between two groups (data now shown). In addition, the downstream target of adiponectin, hepatic PPARα, did not change in both mRNA levels (**Figure 2F**) and protein levels (data not shown), indicating that the difference of hepatic

lipogenesis between wild-type and sirt1$^{Y/Y}$ mice was not due to adiponectin activity in this mouse model.

3.4. SIRT1 mutation caused hepatic steatosis via MAT-liver FFA mobilization.

Since hepatic steatosis could be the result of elevating fatty acid uptake by 1) up-taking triglyceride in chylomicron or VLDL remnant that derived from dietary sources, and 2) up-taking FFA released from adipose tissue, we tested the possibility that SIRT1 mutation affects liver TG uptake. We examined plasma TG level and hepatic LDL-receptor (*ldl-r*) transcription level and found no difference in these parameters between two groups (**Figure 4A**), suggesting that liver TG uptake was similar between WT and sirt1$^{Y/Y}$ mice.

We then examined plasma FFA and found the level of plasma FFA was significantly higher in sirt1$^{Y/Y}$ mice (**Figure 4B**), as compared with that of WT mice. Since FFA from MAT directly enters liver through the portal vein [2, 33-35], lipolysis of MAT greatly contributes to FFA transferred to liver. We further hypothesized that the increase of FFA in mutant mice was attributed to the increasing MAT lipolysis. Of four genes related to mesenteric lipolysis (*hsl*, *atgl*, *plin-1*, *plin-2*), *hsl*, *atgl* and *plin-2* significantly increased in sirt1$^{Y/Y}$ mice (**Figure 4C**). CD36 is a transporter that takes up long chain fatty acid [36]. In the current study, we found that *cd36* transcription level in liver was significantly higher in sirt1$^{Y/Y}$ mice (**Figure 4D**). The mRNA level of *lxrα*, as a transcription factor that up-regulates CD36 transcription, was also elevated in sirt1$^{Y/Y}$ mice. To test whether wild-type and sirt1$^{Y/Y}$ mice have different hepatic TG clearance rates, we examined the mRNA of microsomal triglyceride transfer protein (*mttp*), a transporter that exports TG, but observed no difference in its expression between groups (**Figure 4D**). These data suggest that increased FFA release from MAT may enter systemic circulation, and subsequently the liver, leading to augmented liver steatosis in sirt1 mutant mice.

4. Discussion

To our knowledge, the present study has provided first evidence that systemic SIRT1 activity loss promoted NAFLD by targeting both liver and MAT, as well as their cross-talk. We demonstrated that the accumulating hepatic TG due to the lack of SIRT1 activity was associated with 1) increased hepatic fatty acid synthesis but unchanged β-oxidation in liver; 2) increased lipid synthesis in MAT; and 3) elevated free fatty acid transport from MAT to liver.

In the current study, the acetylated version of FoxO1 significantly increased in sirt1$^{Y/Y}$ mice, supporting the observation that SIRT1 enzymatic activity in liver decreased due to a systemic

SIRT1 activity ablation in this mouse model. After HFD (60% calories from fat) intervention for 34 weeks, we found that sirt1$^{Y/Y}$ mice accumulated significantly higher TG level in liver. This suggests that the lack of systemic SIRT1 deacetylase activity can promote NAFLD development. Our findings were consistent with the previous studies showing that impaired SIRT1 signaling was associated with increased hepatic lipid deposition [8, 10, 19-21, 23]. It should be noted that our histopathologic analysis tended to present more severe hepatic steatosis in sirt1$^{Y/Y}$ mice (P = 0.16). The discrepancy between our histopathologic grading and hepatic TGs was possibly due to the fact that the changes of hepatic TGs were more sensitive to detect compared to histologic observation. Nevertheless, our steatosis grading score was significantly correlated with the hepatic TGs, which supports that systemic SIRT1 activity ablation can escalate NAFLD development. In the current study, we observed comparable hepatic total cholesterol levels, which agree with the similar mRNA expression levels of *abca1* and *cyp7a1* between WT and sirt1$^{Y/Y}$ mice. ABCA1 is a key transporter that exports cholesterol from liver, and Cyp7A1 is the gene that encodes cholesterol 7α-hydroxylase, the enzyme catalyzes the initial step in bile acid synthesis. Our data suggest that the comparable hepatic cholesterol levels in wild-type and mutant mice may be due to unchanged reverse cholesterol transport and cholesterol catabolism, or alternatively, a high fat diet-induced metabolic surplus. Taken together, we conclude that the lack of SIRT1 enzymatic activity plays a minor role on cholesterol metabolism in this model. One of the important observations in the present study was that the lack of SIRT1 deacetylase activity increased lipogenesis while maintaining fatty acid oxidation unchanged in both liver and MAT. In sirt1$^{Y/Y}$ mice, increased hepatic lipogenesis was associated with reduced phosphorylations of LKB1, AMPK and ACC. LKB1 can be activated through phosphorylation at Ser^{428}, which enhances its kinase activity of phosphorylating AMPK [7, 8, 31], resulting in enhanced inhibition of ACC by phosphorylating the enzyme to the inactive form [37]. Hepatic ACC activation promotes FA synthesis and lipid accumulation [37]. Unexpectedly, we observed higher levels of LXRα mRNA in sirt1$^{Y/Y}$ mice, which is not in agreement with the previous report that SIRT1 contributes to deacetylating and activating LXRα transcription *in vitro* [21]. However, these authors found that *lxrα* mRNA expression was similar in SIRT1 knock-out mice and their wild-type, suggesting that SIRT1 might regulate *lxrα* in multiple mechanistic pathways *in vivo* [38]. One possible pathway is that SIRT1 activity ablation decreases the release of Nicotinamide phosphoribosyltransferase (NAMPT), a rate limiting enzyme that catalyzes the biosynthesis of nicotinamide adenine dinucleotide (NAD) [39]. Decreased release of NAMPT from hepatocytes can attenuate the inhibition of *lxrα* transcription in sirt1$^{Y/Y}$ mice [39]. It is important to note that the mRNA level of *lxrα* was also promoted in the MAT of sirt1$^{Y/Y}$ mice, showing the consistence

of the effect of SIRT1 activity on *lxrα* transcription in multiple tissues. To our best knowledge, this is the first report to reveal the effect of SIRT1 deacetylase activity on regulating *lxrα* transcription level in MAT. As one important target of LXRα, SREBP-1c plays a role as a transcription factor that regulates multiple lipogenic genes, including SCD1, FAS and ACC [32]. Compared to WT mice, the protein level of SREBP-1 in liver and the mRNA level of *srebp-1c* in both liver and MAT were significantly higher in sirt1$^{Y/Y}$ mice. Data in this study showed that *scd1* mRNA consistently increased in both liver and MAT, but an elevated level of *fas* mRNA was only observed in MAT. Further study is needed to examine whether SIRT1 catalytic activity ablation affects other signaling pathway that alters FAS transcription level specifically in MAT. It is interesting to note that the lack of SIRT1 enzymatic activity affected neither transcription of *adiponectin* in MAT nor adiponectin downstream targets in liver. Our observation that the lack of systemic SIRT1 activity did not impact adiponectin production and signaling does not agree with a previous study [40], in which adipocyte-selective SIRT1 knockout mice had reduced adiponectin production, compared to WT mice. Such a discrepancy might be due to the different effects of SIRT1 on adiponectin transcription, between SIRT1 adipocyte-specific knockout and systemic SIRT1 activity mutation.

In the present study, SIRT1 activity ablation did not affect plasma TG levels, which is consistent with previous findings that the SIRT1 protein levels were not correlated with the circulating TG levels in both human and animal studies [18, 41]. An intriguing observation in the present study is that the promoting effect of SIRT1 deacetylase activity ablation on hepatic steatosis is coupled with an increase in circulating FFA level. It has been shown that the portal vein directly connects the liver with the visceral MAT, and visceral fat content is highly correlated with the severity of hepatic steatosis in humans [42, 43]. In the present study, we found that the higher circulating FFA was associated with higher mRNA levels of *atgl*, *hsl* and *plin-2* in sirt1$^{Y/Y}$ mice. ATGL is a rate-limiting lipolytic enzyme for TG hydrolysis, while HSL is the major hydrolase for diacylglyceride in the adipocytes [44, 45]. The phosphorylation of PLIN-2 is responsible for recruiting HSL to lipid droplets and meanwhile dissociates and activates ATGL. Jointly, the increased levels of *atgl*, *hsl* and *plin-2* mRNA in sirt1$^{Y/Y}$ mice indicate a higher rate of lipolysis in MAT. This result is contradictory to the findings from previous studies that SIRT1 promotes lipolysis in adipocytes [44, 45]. In the study of Picard et al. [45], they reported a decreased lipolysis rate in the epididymal adipose tissue of SIRT1 heterozygous mice, which was associated with a lower level of circulating FFA. The discrepancy between that study and the current study might be due to the different adipose tissues used in the investigations. It is noted that the basal

protein level of perilipins and activated HSL are different between MAT and epididymal adipose tissue, and moreover, the effect of HFD on ATGL activation is surprisingly inverse between the two adipose tissue at two depots [46], leading us to hypothesize that SIRT1 differently regulates lipolysis between MAT and epididymal adipose tissue. CD36 mediates liver FFA uptake and plays an important role in promoting steatosis [47, 48]. Interestingly, we observed an increased level of *cd36* mRNA in the liver, but not in the MAT, in sirt1$^{Y/Y}$ mice, indicating that SIRT1 might regulate *cd36* transcription in a tissue-specific manner [47]. Previous studies reported that lipodystrophy occurred when fat mass was reduced and lipolysis was increased [49]. Interestingly, in the present study, we observed not only increased lipolysis, but also increased fatty acid synthesis in Sirt1 mutant animals fed high fat diet, which may lead to the dynamic homeostasis in mesenteric adipose tissue. This was supported by our body composition analyses showing that the percent fat mass and adipose tissue weight were comparable between wild-type and Sirt1 mutant mice, but significantly increased TG was found in the livers of Sirt1 mutant mice. This observation may help us to understand why some people without 'fat belly' still develop fatty liver when sirt1 activity decreases due to certain factors, such as aging, unhealthy diet, stress, or high alcohol consumption.

Taken together, the results from the current study suggest that systemic SIRT1 deacetylase activity ablation can promote hepatic steatosis by elevating lipogenesis in both liver and MAT (**Figure 5**). The lack of SIRT1 activity also promotes the release of FFA from MAT and consequent transport to liver, and increases liver FFA uptake by increasing hepatic FFA transporter (**Figure 5**). Whether SIRT1 activity is a potential molecular target for certain dietary components (e.g., tomato carotenoids) to prevent and/or mitigate development of NAFLD is currently under the investigation in this lab.

Acknowledgement

This work was supported by USDA/NIFA (2015-67017) and USDA/ARS (58-1950-0014). Any opinions, findings, conclusions, and recommendations expressed in this publication are those of the authors and do not necessarily reflect the views of the sponsors.

Figure 1.

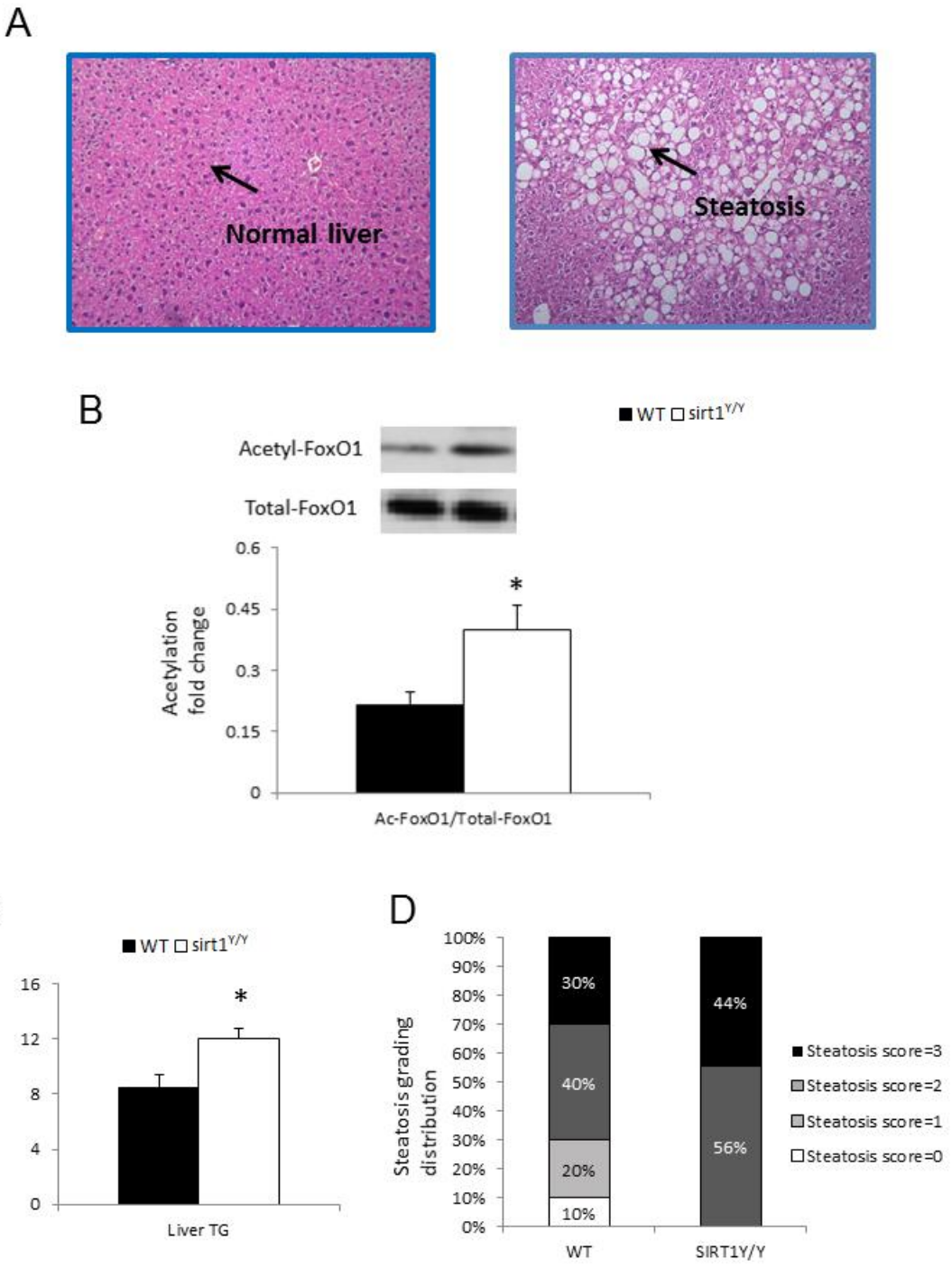
A
Normal liver
Steatosis
B
WT sirt1Y/Y
Acetyl-FoxO1
Total-FoxO1
Acetylation fold change
0.6
0.45
0.3
0.15
0
*
Ac-FoxO1/Total-FoxO1
C
WT sirt1Y/Y
Mg/g liver
16
12
8
4
0
*
Liver TG
D
Steatosis grading distribution
100%
90%
80%
70%
60%
50%
40%
30%
20%
10%
0%
30%
40%
20%
10%
44%
56%
WT
SIRT1Y/Y
Steatosis score=3
Steatosis score=2
Steatosis score=1
Steatosis score=0

Figure 2.

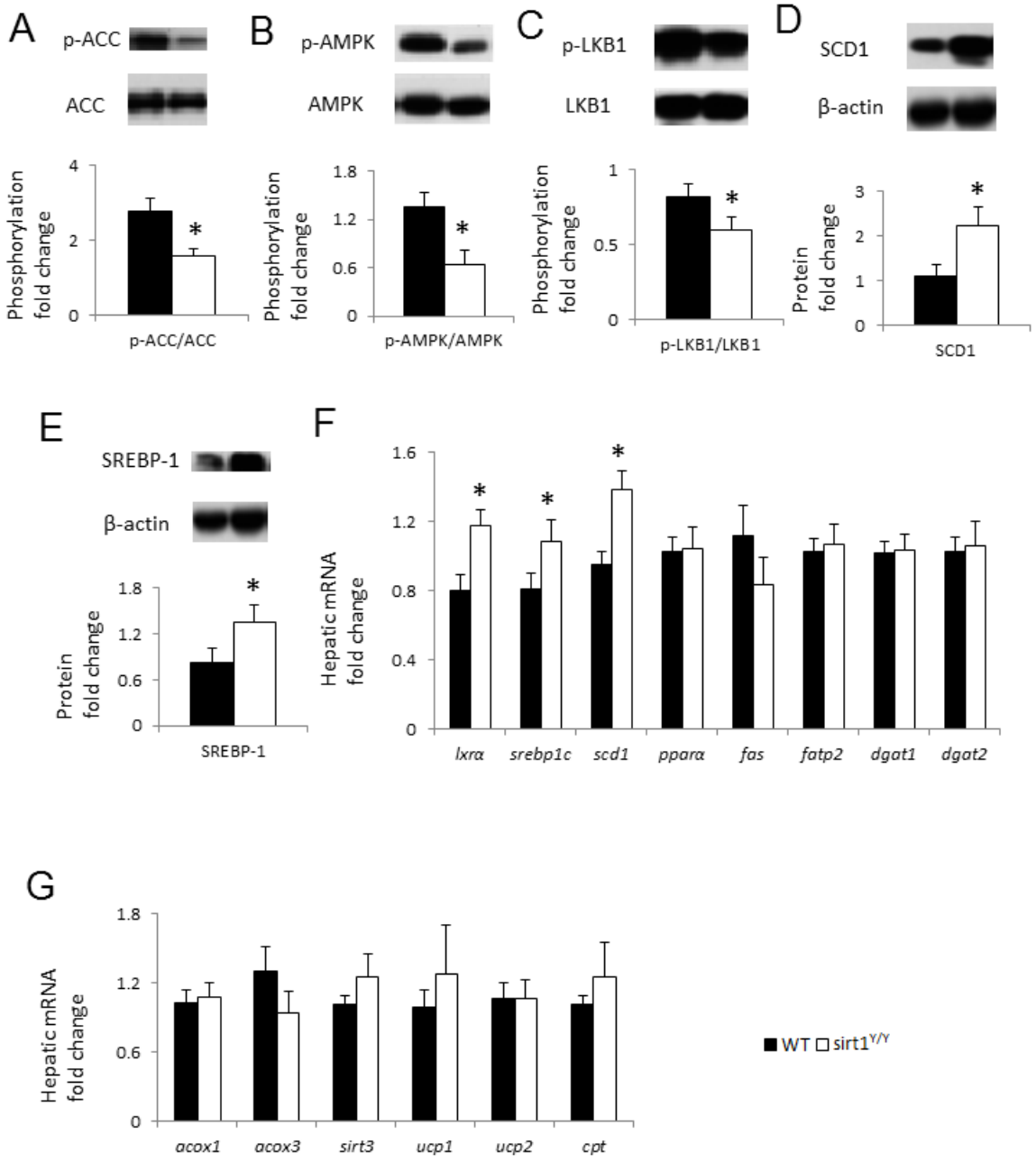
A
p-ACC
ACC
Phosphorylation fold change
p-ACC/ACC
B
p-AMPK
AMPK
Phosphorylation fold change
p-AMPK/AMPK
C
p-LKB1
LKB1
Phosphorylation fold change
p-LKB1/LKB1
D
SCD1
β-actin
Protein fold change
SCD1
E
SREBP-1
β-actin
Protein fold change
SREBP-1
F
Hepatic mRNA fold change
lxrα
srebp1c
scd1
pparα
fas
fatp2
dgat1
dgat2
G
Hepatic mRNA fold change
acox1
acox3
sirt3
ucp1
ucp2
cpt
WT
sirt1Y/Y

Figure 3.

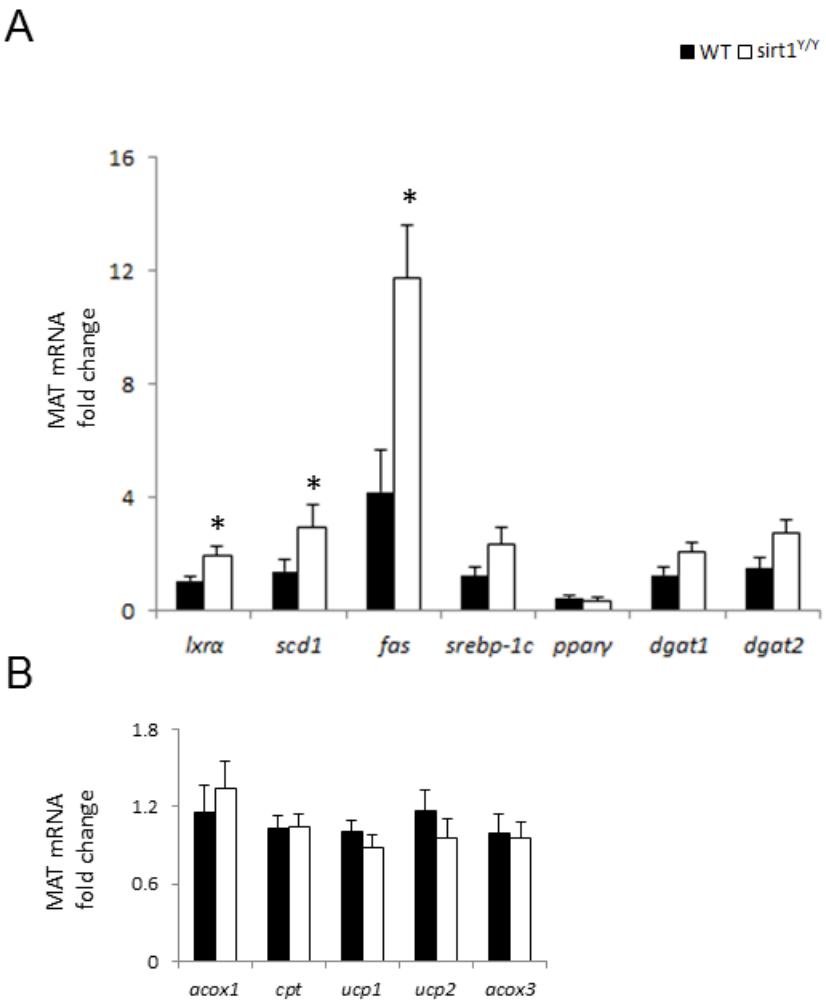
A
WT sirt1Y/Y
MAT mRNA fold change
16
12
8
4
0
*
*
*
lxrα
scd1
fas
srebp-1c
pparγ
dgat1
dgat2
B
MAT mRNA fold change
1.8
1.2
0.6
0
acox1
cpt
ucp1
ucp2
acox3

Figure 4.

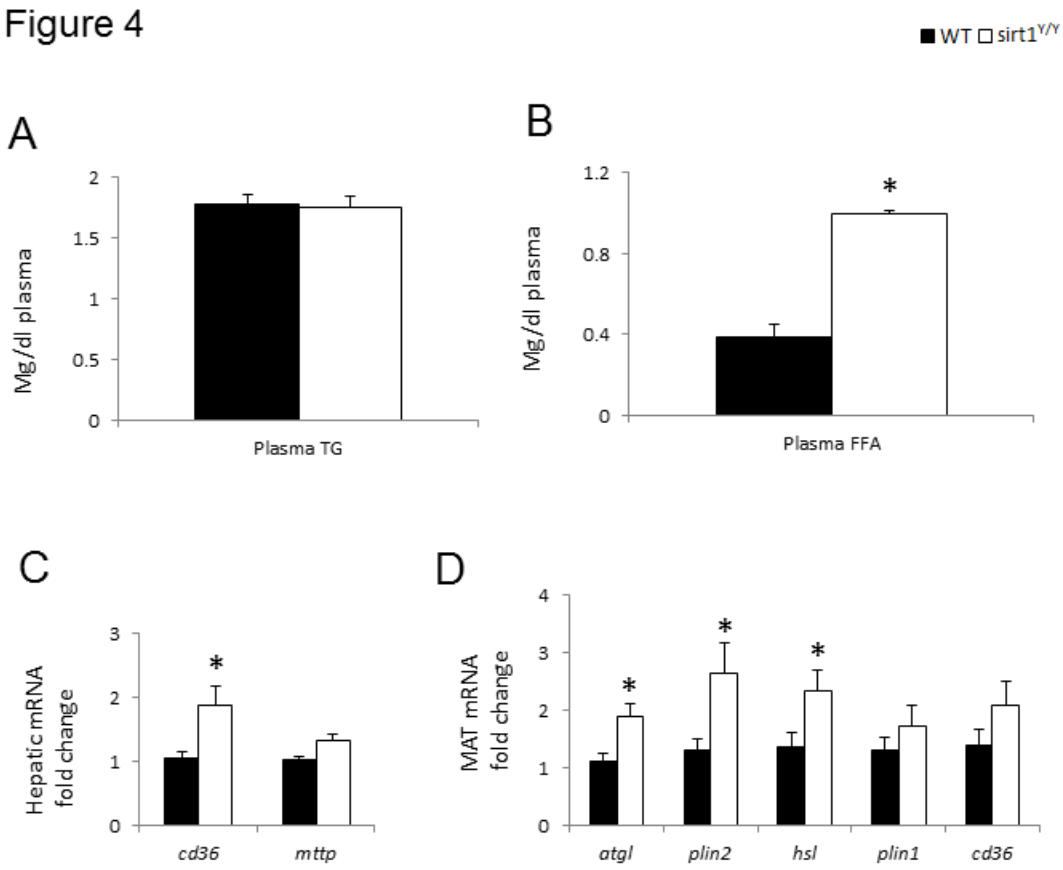
Figure 4
WT sirt1Y/Y
A
Mg/dl plasma
2
1.5
1
0.5
0
Plasma TG
B
Mg/dl plasma
1.2
0.8
0.4
0
*
Plasma FFA
C
Hepatic mRNA fold change
3
2
1
0
*
cd36
mttp
D
MAT mRNA fold change
4
3
2
1
0
*
*
*
atgl
plin2
hsl
plin1
cd36

Figure 5.

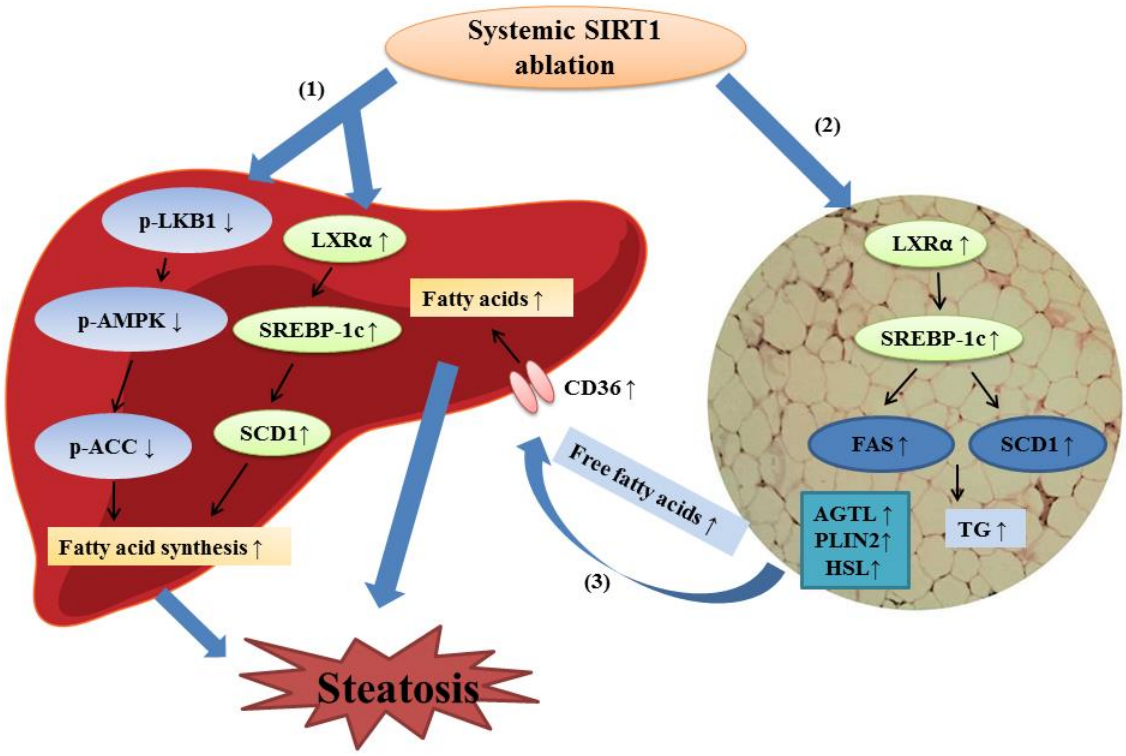
Systemic SIRT1 ablation
(1)
(2)
p-LKB1 ↓
LXRα ↑
p-AMPK ↓
SREBP-1c↑
Fatty acids ↑
CD36 ↑
p-ACC ↓
SCD1↑
Fatty acid synthesis ↑
Free fatty acids ↑
(3)
LXRα ↑
SREBP-1c↑
FAS ↑
SCD1 ↑
AGTL ↑
PLIN2↑
HSL↑
TG ↑
Steatosis

Figure Legends

Figure 1. A, Graphic representation for hepatic steatosis histopathology grading. B, C, D, liver Ac-FoxO1, liver steatosis score distribution and liver TG level (WT, sirt1$^{Y/Y}$ n = 10). B, graphic representation of fold changes in hepatic acetylated FoxO1, FoxO1 as loading control. C, distribution of histopathologic liver steatosis score in WT, sirt1$^{Y/Y}$. D, TG level of livers. Values are % of total mice, or means ± SMEs. Mann–Whitney U test was used to compare liver steatosis score distribution; student t test was used to compare liver Ac-FoxO1 ratio and TG level between WT and sirt1 $^{Y/Y}$ mice. *Different from WT, P < 0.05. WT, wild-type mice; sirt1 $^{Y/Y}$, SIRT1 activity ablation mice.

Figure 2. Effects of SIRT1 activity ablation on lipogenesis and fatty acid oxidation biomarkers. Changes of protein or mRNA expressions in liver lysates (WT, sirt$^{Y/Y}$ n = 10) were analyzed by western-blotting or RT-PCR, and β-actin was used as loading control unless specified otherwise. Graphical representation of fold changes in: A, phosphorylated ACC (Ser79; ACC as loading control); B, phosphorylated AMPK (Thr172; AMPK as loading control); C, phosphorylated LKB1 (Ser428; LKB1 as loading control); D, SREBP-1; E, SCD1; F, mRNA of lipogenesis-associated genes: *lxrα*, *srebp1c*, *scd1*, *fas*, *pparα*, *dgat1*, *dgat2*; G, mRNA of fatty acid oxidation-associated genes: *acox1*, *acox3*, *sirt3*, *ucp1*, *ucp2*, *cpt*. Values are means ± SMEs. Student t test was used to compare liver TG level between WT and sirt1 $^{Y/Y}$ mice. *Different from WT, P < 0.05.

Figure 3. Effects of sirt1 activity ablation on lipogenesis and fatty acid oxidation biomarkers. Changes of mRNA expressions in MAT lysates (WT, SIRT$^{Y/Y}$ n=7-9) were analyzed by RT-PCR, and β-actin was used as loading control unless specified otherwise. Graphical representation of fold changes in: A, lipogenesis-associated genes: *lxrα*, *srebp-1c*, *scd1*, *fas*, *pparγ*, *dgat1*, *dgat2*; B, fatty acid oxidation-associated genes: *acox1*, *cpt*, *ucp1*, *ucp2*, *acox3*. Values are means ± SMEs. Student t test was used to compare liver TG level between WT and sirt1 $^{Y/Y}$ mice. *Different from WT, P < 0.05.

Figure 4. Effects of SIRT1 activity ablation on plasma TG, FFA concentration and FFA mobilization biomarkers in liver and MAT. Changes of mRNA expressions in liver or MAT lysates (WT, sirt1$^{Y/Y}$ n=7-9) were analyzed by RT-PCR, and β-actin was used as loading control unless specified otherwise. Graphical representation of fold changes in: A, plasma TG concentration; B, FFA concentration; C, FFA uptake transporter in liver: *cd36*, TG export transporter in liver: *mttp*; D, lipolysis-associated genes: *agtl*, *plin-2*, *hsl*, *plin-1*, FFA uptake

transporter in MAT: *cd36*. Values are means ± SMEs. Student t test was used to compare liver TG level between WT and sirt1 $^{Y/Y}$ mice. *Different from WT, $P < 0.05$.

Figure 5. The potential effect of systemic SIRT1 ablation on the development of nonalcoholic fatty liver disease (NAFLD) through three pathways: (1) increase TG synthesis in the liver by promoting fatty acid synthetic genes; (2) increase TG synthesis in the mesenteric adipose tissue (MAT) by promoting fatty acid synthetic genes; and (3) promote the mobilization of fatty acid from MAT to liver by increasing hepatic free fatty acid uptake.

Reference

[1] K. Aleksandrova, M. Stelmach-Mardas, S. Schlesinger, Obesity and Liver Cancer, Recent Results Cancer Res, 208 (2016) 177-198.
[2] E. Fabbrini, S. Sullivan, S. Klein, Obesity and nonalcoholic fatty liver disease: biochemical, metabolic, and clinical implications, Hepatology, 51 (2010) 679-689.
[3] J.C. Cohen, J.D. Horton, H.H. Hobbs, Human fatty liver disease: old questions and new insights, Science, 332 (2011) 1519-1523.
[4] G. Baffy, E.M. Brunt, S.H. Caldwell, Hepatocellular carcinoma in non-alcoholic fatty liver disease: an emerging menace, J Hepatol, 56 (2012) 1384-1391.
[5] J.S. Smith, C.B. Brachmann, I. Celic, M.A. Kenna, S. Muhammad, V.J. Starai, J.L. Avalos, J.C. Escalante-Semerena, C. Grubmeyer, C. Wolberger, J.D. Boeke, A phylogenetically conserved NAD+-dependent protein deacetylase activity in the Sir2 protein family, Proc Natl Acad Sci U S A, 97 (2000) 6658-6663.
[6] S. Imai, C.M. Armstrong, M. Kaeberlein, L. Guarente, Transcriptional silencing and longevity protein Sir2 is an NAD-dependent histone deacetylase, Nature, 403 (2000) 795-800.
[7] F. Lan, J.M. Cacicedo, N. Ruderman, Y. Ido, SIRT1 modulation of the acetylation status, cytosolic localization, and activity of LKB1. Possible role in AMP-activated protein kinase activation, J Biol Chem, 283 (2008) 27628-27635.
[8] X. Hou, S. Xu, K.A. Maitland-Toolan, K. Sato, B. Jiang, Y. Ido, F. Lan, K. Walsh, M. Wierzbicki, T.J. Verbeuren, R.A. Cohen, M. Zang, SIRT1 regulates hepatocyte lipid metabolism through activating AMP-activated protein kinase, J Biol Chem, 283 (2008) 20015-20026.
[9] Z. Gerhart-Hines, J.T. Rodgers, O. Bare, C. Lerin, S.H. Kim, R. Mostoslavsky, F.W. Alt, Z. Wu, P. Puigserver, Metabolic control of muscle mitochondrial function and fatty acid oxidation through SIRT1/PGC-1alpha, Embo j, 26 (2007) 1913-1923.
[10] A. Purushotham, T.T. Schug, Q. Xu, S. Surapureddi, X. Guo, X. Li, Hepatocyte-specific deletion of SIRT1 alters fatty acid metabolism and results in hepatic steatosis and inflammation, Cell Metab, 9 (2009) 327-338.
[11] L. Bai, W.J. Pang, Y.J. Yang, G.S. Yang, Modulation of Sirt1 by resveratrol and nicotinamide alters proliferation and differentiation of pig preadipocytes, Mol Cell Biochem, 307 (2008) 129-140.
[12] C. Canto, R.H. Houtkooper, E. Pirinen, D.Y. Youn, M.H. Oosterveer, Y. Cen, P.J. Fernandez-Marcos, H. Yamamoto, P.A. Andreux, P. Cettour-Rose, K. Gademann, C. Rinsch, K. Schoonjans, A.A. Sauve, J. Auwerx, The NAD(+) precursor nicotinamide riboside enhances oxidative metabolism and protects against high-fat diet-induced obesity, Cell Metab, 15 (2012) 838-847.
[13] J. Landry, A. Sutton, S.T. Tafrov, R.C. Heller, J. Stebbins, L. Pillus, R. Sternglanz, The silencing protein SIR2 and its homologs are NAD-dependent protein deacetylases, Proc Natl Acad Sci U S A, 97 (2000) 5807-5811.
[14] R.H. Houtkooper, C. Canto, R.J. Wanders, J. Auwerx, The secret life of NAD+: an old metabolite controlling new metabolic signaling pathways, Endocr Rev, 31 (2010) 194-223.
[15] X. Li, SIRT1 and energy metabolism, Acta Biochim Biophys Sin (Shanghai), 45 (2013) 51-60.
[16] B.J. Gurd, Y. Yoshida, J.T. McFarlan, G.P. Holloway, C.D. Moyes, G.J. Heigenhauser, L. Spriet, A. Bonen, Nuclear SIRT1 activity, but not protein content, regulates mitochondrial biogenesis in rat and human skeletal muscle, Am J Physiol Regul Integr Comp Physiol, 301 (2011) R67-75.
[17] X.Q. Deng, L.L. Chen, N.X. Li, The expression of SIRT1 in nonalcoholic fatty liver disease induced by high-fat diet in rats, Liver Int, 27 (2007) 708-715.

[18] S. Mariani, D. Fiore, S. Basciani, A. Persichetti, S. Contini, C. Lubrano, L. Salvatori, A. Lenzi, L. Gnessi, Plasma levels of SIRT1 associate with non-alcoholic fatty liver disease in obese patients, Endocrine, 49 (2015) 711-716.
[19] P.T. Pfluger, D. Herranz, S. Velasco-Miguel, M. Serrano, M.H. Tschop, Sirt1 protects against high-fat diet-induced metabolic damage, Proc Natl Acad Sci U S A, 105 (2008) 9793-9798.
[20] F. Xu, Z. Gao, J. Zhang, C.A. Rivera, J. Yin, J. Weng, J. Ye, Lack of SIRT1 (Mammalian Sirtuin 1) activity leads to liver steatosis in the SIRT1+/- mice: a role of lipid mobilization and inflammation, Endocrinology, 151 (2010) 2504-2514.
[21] A.Z. Caron, X. He, W. Mottawea, E.L. Seifert, K. Jardine, D. Dewar-Darch, G.O. Cron, M.E. Harper, A. Stintzi, M.W. McBurney, The SIRT1 deacetylase protects mice against the symptoms of metabolic syndrome, Faseb j, 28 (2014) 1306-1316.
[22] R.H. Wang, C. Li, C.X. Deng, Liver steatosis and increased ChREBP expression in mice carrying a liver specific SIRT1 null mutation under a normal feeding condition, Int J Biol Sci, 6 (2010) 682-690.
[23] J. Ding, M. Li, X. Wan, X. Jin, S. Chen, C. Yu, Y. Li, Effect of miR-34a in regulating steatosis by targeting PPARalpha expression in nonalcoholic fatty liver disease, Sci Rep, 5 (2015) 13729.
[24] G. Boily, E.L. Seifert, L. Bevilacqua, X.H. He, G. Sabourin, C. Estey, C. Moffat, S. Crawford, S. Saliba, K. Jardine, J. Xuan, M. Evans, M.E. Harper, M.W. McBurney, SirT1 regulates energy metabolism and response to caloric restriction in mice, PLoS One, 3 (2008) e1759.
[25] H.L. Cheng, R. Mostoslavsky, S. Saito, J.P. Manis, Y. Gu, P. Patel, R. Bronson, E. Appella, F.W. Alt, K.F. Chua, Developmental defects and p53 hyperacetylation in Sir2 homolog (SIRT1)-deficient mice, Proc Natl Acad Sci U S A, 100 (2003) 10794-10799.
[26] M.W. McBurney, X. Yang, K. Jardine, M. Hixon, K. Boekelheide, J.R. Webb, P.M. Lansdorp, M. Lemieux, The mammalian SIR2alpha protein has a role in embryogenesis and gametogenesis, Mol Cell Biol, 23 (2003) 38-54.
[27] E.L. Seifert, A.Z. Caron, K. Morin, J. Coulombe, X.H. He, K. Jardine, D. Dewar-Darch, K. Boekelheide, M.E. Harper, M.W. McBurney, SirT1 catalytic activity is required for male fertility and metabolic homeostasis in mice, Faseb j, 26 (2012) 555-566.
[28] J. Wang, S.M. Vanegas, X. Du, T. Noble, J.M. Zingg, M. Meydani, S.N. Meydani, D. Wu, Caloric restriction favorably impacts metabolic and immune/inflammatory profiles in obese mice but curcumin/piperine consumption adds no further benefit, Nutr Metab (Lond), 10 (2013) 29.
[29] C.P. Stice, C. Liu, K. Aizawa, A.S. Greenberg, L.M. Ausman, X.D. Wang, Dietary tomato powder inhibits alcohol-induced hepatic injury by suppressing cytochrome p450 2E1 induction in rodent models, Arch Biochem Biophys, 572 (2015) 81-88.
[30] J. Chung, K. Koo, F. Lian, K.Q. Hu, H. Ernst, X.D. Wang, Apo-10'-lycopenoic acid, a lycopene metabolite, increases sirtuin 1 mRNA and protein levels and decreases hepatic fat accumulation in ob/ob mice, J Nutr, 142 (2012) 405-410.
[31] Y. Peng, D.A. Rideout, S.S. Rakita, W.R. Gower, Jr., M. You, M.M. Murr, Does LKB1 mediate activation of hepatic AMP-protein kinase (AMPK) and sirtuin1 (SIRT1) after Roux-en-Y gastric bypass in obese rats?, J Gastrointest Surg, 14 (2010) 221-228.
[32] D. Eberle, B. Hegarty, P. Bossard, P. Ferre, F. Foufelle, SREBP transcription factors: master regulators of lipid homeostasis, Biochimie, 86 (2004) 839-848.
[33] M.U. Jakobsen, T. Berentzen, T.I. Sorensen, K. Overvad, Abdominal obesity and fatty liver, Epidemiol Rev, 29 (2007) 77-87.
[34] P. Engfeldt, P. Arner, Lipolysis in human adipocytes, effects of cell size, age and of regional differences, Horm Metab Res Suppl, 19 (1988) 26-29.
[35] P. Bjorntorp, "Portal" adipose tissue as a generator of risk factors for cardiovascular disease and diabetes, Arteriosclerosis, 10 (1990) 493-496.

[36] T. Yoshikawa, H. Shimano, M. Amemiya-Kudo, N. Yahagi, A.H. Hasty, T. Matsuzaka, H. Okazaki, Y. Tamura, Y. Iizuka, K. Ohashi, J. Osuga, K. Harada, T. Gotoda, S. Kimura, S. Ishibashi, N. Yamada, Identification of liver X receptor-retinoid X receptor as an activator of the sterol regulatory element-binding protein 1c gene promoter, Mol Cell Biol, 21 (2001) 2991-3000.
[37] M.D. Fullerton, S. Galic, K. Marcinko, S. Sikkema, T. Pulinilkunnil, Z.P. Chen, H.M. O'Neill, R.J. Ford, R. Palanivel, M. O'Brien, D.G. Hardie, S.L. Macaulay, J.D. Schertzer, J.R. Dyck, B.J. van Denderen, B.E. Kemp, G.R. Steinberg, Single phosphorylation sites in Acc1 and Acc2 regulate lipid homeostasis and the insulin-sensitizing effects of metformin, Nat Med, 19 (2013) 1649-1654.
[38] S.H. Jin, J.H. Yang, B.Y. Shin, K. Seo, S.M. Shin, I.J. Cho, S.H. Ki, Resveratrol inhibits LXRalpha-dependent hepatic lipogenesis through novel antioxidant Sestrin2 gene induction, Toxicol Appl Pharmacol, 271 (2013) 95-105.
[39] S. Schuster, M. Penke, T. Gorski, S. Petzold-Quinque, G. Damm, R. Gebhardt, W. Kiess, A. Garten, Resveratrol differentially regulates NAMPT and SIRT1 in Hepatocarcinoma cells and primary human hepatocytes, PLoS One, 9 (2014) e91045.
[40] X. Hui, M. Zhang, P. Gu, K. Li, Y. Gao, D. Wu, Y. Wang, A. Xu, Adipocyte SIRT1 controls systemic insulin sensitivity by modulating macrophages in adipose tissue, EMBO Rep, 18 (2017) 645-657.
[41] A. Purushotham, Q. Xu, X. Li, Systemic SIRT1 insufficiency results in disruption of energy homeostasis and steroid hormone metabolism upon high-fat-diet feeding, Faseb j, 26 (2012) 656-667.
[42] A. Gastaldelli, K. Cusi, M. Pettiti, J. Hardies, Y. Miyazaki, R. Berria, E. Buzzigoli, A.M. Sironi, E. Cersosimo, E. Ferrannini, R.A. Defronzo, Relationship between hepatic/visceral fat and hepatic insulin resistance in nondiabetic and type 2 diabetic subjects, Gastroenterology, 133 (2007) 496-506.
[43] A. Kotronen, H. Yki-Jarvinen, K. Sevastianova, R. Bergholm, A. Hakkarainen, K.H. Pietilainen, L. Juurinen, N. Lundbom, T.I. Sorensen, Comparison of the relative contributions of intra-abdominal and liver fat to components of the metabolic syndrome, Obesity (Silver Spring), 19 (2011) 23-28.
[44] P. Chakrabarti, T. English, S. Karki, L. Qiang, R. Tao, J. Kim, Z. Luo, S.R. Farmer, K.V. Kandror, SIRT1 controls lipolysis in adipocytes via FOXO1-mediated expression of ATGL, J Lipid Res, 52 (2011) 1693-1701.
[45] F. Picard, M. Kurtev, N. Chung, A. Topark-Ngarm, T. Senawong, R. Machado De Oliveira, M. Leid, M.W. McBurney, L. Guarente, Sirt1 promotes fat mobilization in white adipocytes by repressing PPAR-gamma, Nature, 429 (2004) 771-776.
[46] S. Wueest, F. Item, F.C. Lucchini, T.D. Challa, W. Muller, M. Bluher, D. Konrad, Mesenteric Fat Lipolysis Mediates Obesity-Associated Hepatic Steatosis and Insulin Resistance, Diabetes, 65 (2016) 140-148.
[47] J. Zhou, M. Febbraio, T. Wada, Y. Zhai, R. Kuruba, J. He, J.H. Lee, S. Khadem, S. Ren, S. Li, R.L. Silverstein, W. Xie, Hepatic fatty acid transporter Cd36 is a common target of LXR, PXR, and PPARgamma in promoting steatosis, Gastroenterology, 134 (2008) 556-567.
[48] M.W. Bradbury, Lipid metabolism and liver inflammation. I. Hepatic fatty acid uptake: possible role in steatosis, Am J Physiol Gastrointest Liver Physiol, 290 (2006) G194-198.
[49] J. Zhang, T.M. Henagan, Z. Gao, J. Ye, Inhibition of glyceroneogenesis by histone deacetylase 3 contributes to lipodystrophy in mice with adipose tissue inflammation, Endocrinology, 152 (2011) 1829-1838.

APPENDIX IV

Tomato powder inhibits hepatic steatosis and inflammation potentially through restoring SIRT1 activity and adiponectin function independent of carotenoid cleavage enzymes in mice

Cheng-Chung Li1, Chun Liu1, Maobin Fu2, Kang-Quan Hu1, Koichi Aizawa1.2, Shingo Takahashi2, Suganuma Hiroyuki2, Junrui Cheng1, Johannes von Lintig3 and Xiang-Dong Wang1

1Nutrition and Cancer Biology Laboratory, Jean Mayer USDA-Human Nutrition Research Center on Aging at Tufts University, Boston, MA 02111, USA;
2Nature & Wellness Research Department, Research & Development Division, Kagome Co., Ltd., Tochigi, Japan; and
3Department of Pharmacology, School of Medicine, Case Western Reserve University, Cleveland, Ohio, USA

Running title: Dietary tomato prevents fatty liver and inflammation

Corresponding Author:
Xiang-Dong Wang, MD, PhD
Nutrition and Cancer Biology Laboratory
Jean Mayer USDA Human Nutrition Research Center on Aging at Tufts University
711 Washington Street, Room 514
Boston, MA 02111, USA
Phone: 617-556-3130
Fax: 617-556-3344
Email: xiang-dong.wang@tufts.edu

Abbreviations: TP, Tomato powder; HFD, high fat diet; NAFLD, nonalcoholic fatty liver disease; BCO1, beta-carotene-15, 15'-oxygenase; BCO2, beta-carotene-9', 10'-oxygenase; NASH, nonalcoholic steatohepatitis; NAD, Nicotinamide adenine dinucleotide; NAMPT, nicotinamide phosphoribosyltransferase; ACC, acetyl-CoA carboxylase; KO, knock-out; HPLC, High-performance liquid chromatography; ELISA, enzyme-linked immunosorbent assay; FoxO1, fork head box protein O1; adipoR2, adiponectin receptor2; PPARα , peroxisome proliferator-activated receptor α; AMPK, AMP-activated protein kinase; OUT, operational taxonomic unit; DCA, deoxycholic acid.

Key words: Tomato, non-alcoholic fatty liver disease, adiponectin, sirtuin 1, microbiome
Authors' last names: Li, Liu, Fu, Hu, Aizawa, Takahashi, Hiroyuki, Cheng, von Lintig, Wang

Author disclosures: Li, Liu, Fu, Hu, Aizawa, Takahashi, Hiroyuki, Cheng, von Lintig, and Wang, no conflicts of interest.

Electronic Word Count: 9330
Total Number of Figures: 6
Total Number of Tables: 1
Online Supporting Material: total 3: 1 Tables; 2 Figures

Abstract

Scope: Beta-carotene-15,15'-oxygenase (BCO1) and beta-carotene-9',10'-oxygenase (BCO2) metabolize lycopene to biologically active metabolites, which can ameliorate nonalcoholic fatty liver disease (NAFLD). We investigated the effects of tomato powder (TP containing substantial lycopene (2.3 mg/g)) on NAFLD development and gut microbiome in the absence of both BCO1 and BCO2 in mice.

Method and Results: BCO1-/-/BCO2-/- double knockout mice were fed a high fat diet (HFD) alone (n=9) or with TP feeding (n=9) for 24 weeks. TP feeding significantly reduced pathological severity of steatosis and hepatic triglyceride levels in BCO1-/-/BCO2-/- mice ($P<0.04$ vs. HFD alone). This was associated with increased SIRT1 activity, nicotinamide phosphoribosyltransferase expression and AMPK phosphorylation, and subsequently decreased lipogenesis, hepatic fatty acid uptake, and increasing fatty acid β-oxidation ($P<0.05$). TP feeding significantly decreased mRNA expression of pro-inflammatory genes (tnf-α, il-1β and il-6) in both liver and mesenteric adipose tissue, which were associated with increased plasma adiponectin and hepatic adiponectin receptor-2. Multiplexed 16S rRNA gene sequencing was performed using DNA extracted from cecum fecal samples. TP feeding increased microbial richness and decreased relative abundance of the genus Clostridium.

Conclusion: Dietary TP can inhibit NAFLD independent of carotenoid cleavage enzymes, potentially through increasing SIRT1 activity and adiponectin production and decreasing Clostridium abundance.

1. Introduction

One of the consequences of the current obesity epidemic is an increased prevalence of nonalcoholic fatty liver disease (NAFLD), a major form of chronic liver disease in adults and children [1-3]. Nonalcoholic fatty liver (or steatosis) can progress to nonalcoholic steatohepatitis, which is closely associated with insulin resistance, oxidative stress and inflammatory responses [4]. This ultimately leads to cirrhosis and end-stage liver disease, such as liver cancer. The increasing incidence of liver cancer in the United States has paralleled the epidemic of obesity [5, 6].

There is substantial evidence that high fat diet (HFD)-induced obesity is associated with chronic low-grade systemic inflammation [7, 8], which is believed to contribute to metabolic disorders, and the progression of NAFLD [2, 9]. Emerging literature also implicates that HFD consumption can result in alterations in gut microbiota [10-12], subsequently followed by increasing intestinal permeability [13, 14], bacteria translocation, and the production of lipopolysaccharide and metabolic endotoxemia [15-17]. This cascade ultimately leads to the development of a low-grade inflammatory state in the host, typically in liver and adipose tissue [7, 8, 12, 14, 16, 18]. Under metabolic surplus in obese individuals, adipose tissue expansion signals immune cells to infiltrate the adipose tissue and secrete TNFα and IL-6 [19] [20]. These pro-inflammatory cytokines from adipose tissue can be released into systemic circulation along with free fatty acids from adipose tissue [21 , 22-25], perturbing the function of other tissues including the liver [22, 26, 27].

Furthermore adiponectin, an adipokine secreted by adipocytes, can be down-regulated in obesity and plays an important role in maintaining energy homeostasis, and anti-diabetic and anti-inflammatory functions [28] [29]. Several studies have indicated that the cross-talk between the liver and adipose tissue may be implicated in the progression of NAFLD [30]. Release of various cytokines and adipokines is involved in the network of communication between adipose tissue, and the liver, and some are associated with NAFLD progression [31]. As such, increasing levels of adiponectin by dietary agents may play a protective role against obesity-related complications [32].

Currently there is not an effective medical treatment for NAFLD. The prevention of NAFLD through dietary interventions could be an important and feasible strategy. Epidemiological studies indicate that high intake of lycopene-rich tomatoes and related products are associated with a decreased risk of various chronic diseases [33]. Lycopene, the pigment principally responsible for the characteristic deep-red color of ripe tomatoes and tomato products, has attracted attention due

to its biological activities [20, 34]. Compared to a healthy population, patients with NAFLD were shown to have significantly lower circulating lycopene concentrations, suggesting a potential association between NAFLD development and lycopene status [35], although the cause and consequence in such observational studies remains unclear. Indeed, our studies found that both tomato extract, lycopene, and lycopene metabolites exhibit biological activities against metabolic disorders and NAFLD [36]. We and others have shown that lycopene can be preferentially catalyzed by beta-carotene-9, 10'-oxygenase (BCO2) to generate apolycopenoids [37]. Furthermore apo-10'-lycopenoic acid, a lycopene metabolite formed by BCO2 cleavage, attenuated hepatic steatosis in obese (ob/ob) mice [38] and was effective in alleviating HFD-induced steatosis and hepatic inflammation in the absence of BCO2 [39]. Additionally, apo-10'-lycopenoic acid treatment induces sirturin 1 (SIRT1) activity, a Nicotinamide adenine dinucleotide (NAD+)-dependent protein deacetylase, which can modulate energy homeostasis, lipid metabolism, and inflammatory responses through deacetylation of its downstream transcriptional factors [40, 41], and decreases severity of NAFLD [39, 42, 43]. We have recently reported that the lack of SIRT1 activity interferes with lipid metabolism and increases fatty acid uptake in the liver, which was associated with free fatty acid mobilization of mesenteric adipose tissue (MAT) [44]. These studies suggest that SIRT1 activity might act as a potential molecular target for tomato lycopene, abundant in tomatoes, to slowing the progression NAFLD. However, more supporting evidence is needed for this notion.

In addition to BCO2, a central cleavage product apo-15'-lycopenal was detected in vitro when lycopene was incubated with human recombinant beta-carotene-15, 15'-oxygenase (BCO1) [45]. The existence of genetic variation of BCO1 and BCO2 caused by single nucleotide polymorphisms, and their subsequent impact on carotenoids' metabolism in humans has been previously described [46, 47]. However, the effects of tomato, a whole food containing substantial lycopene, on NAFLD development in the absence of both BCO1 and BCO2 are unknown. A recent study showed that both tomato powder (TP) and lycopene similarly inhibit HFD-induced obesity, the inflammatory response, and associated metabolic disorders [48]. Therefore, the role of BCO1 and BCO2 on the biological activities of whole tomato against NAFLD development warrants further investigation.

In the present study, we investigated the effects of whole tomato (tomato powder, TP) on HFD-induced hepatic steatosis and inflammatory responses in the absence of both BCO1 and BCO2 in mice. We also explored the possibility that TP supplementation is capable of altering the gut microbiome.

2. Materials and methods

2.1 Animals, diets, and experimental design

All animal protocols for the study were approved by the Institutional Animal Care and Use Committee at the USDA Human Nutrition Research Center on Aging (HNRCA) at Tufts University. Male BCO1-/-BCO2-/- double knock-out (KO) mice were previously established by appropriate crossings [49]. Mice were bred in an Association for Assessment and Accreditation of Laboratory Animal Care (AAALAC)-accredited animal facility at the HNRCA at Tufts University. All of mice were housed individually, in a controlled temperature and humidity room with 12-hour light/dark cycle and fed with standard chow diet (Harlan Laboratories, IN, USA). At 6 weeks of age, mice were divided by weight-matching into 2 groups (n = 9 in each group) and fed a powdered HFD (F3282, 60% calories from fat; BioServ, NJ, USA; diet information cited in Ip et al. [9]) alone (HFD group), or with tomato powder (TP, 41.9 g/kg diet, Kagome, Inc, Japan) supplementation (HFD+TP group) for 24 weeks. TP, contains all nutrients found in a whole tomato including 238.8 mg of lycopene, 10.9 mg of β-carotene, and a trace amount of phytoene per 100 grams. We adjusted TP supplementation for lycopene (100 mg/kg in diet) as described in our previous study, in which this dosage of dietary lycopene inhibited HFD-induced fatty liver disease [9, 39]. Briefly, an established equation was used to calculate the dosage equivalence for human consumption [50, 51], which indicated that the lycopene supplemented dose of 100 mg/kg diet is equivalent to approximately 8.1 mg lycopene/day in a 60 kg adult man. The average human dietary lycopene is approximately 8 mg/day [34]. This dosage is less than that used in lycopene dietary supplements and in clinical trials for lycopene treatment in patients with prostate cancer (range from 30 mg to 120 mg/day). At 30 weeks of age, all mice were anesthetized with isoflurane and sacrificed. Blood samples were collected by cardiac puncture in tubes containing EDTA-Na2. The liver and MAT were rapidly harvested and stored at −80°C for further analysis. Cecum samples were collected from all mice at the end of the study.

2.2 Histopathological examination

Tissues from the left lobe of the liver of each mouse were fixed in a 10% buffered formalin phosphate for 5 days. After fixation, liver tissues were washed by running water to remove any formalin followed by phosphate buffered saline. After final washing with 70% ethanol, liver tissues were placed in a tissue processor for histological tissue processing (dehydration, clearing, and paraffin wax infiltration) and then embedded in paraffin to make tissue blocks for sectioning. Five-micrometer sections of formalin-fixed and paraffin-embedded liver tissue were stained with hematoxylin and eosin (H&E, Sigma Aldrich, MI, USA) for histopathological analysis. The sections were examined under light microscopy by two independent investigators who were blinded to the treatment groups. A ZEISS microscope with a PixeLINK USB 2.0 (PL-B623CU) digital Camera and PixeLINK μScope Microscopy Software was used for quantification and image capture for all histopathological analyses.

Hepatic steatosis was graded according to steatosis magnitude (both macro- and micro-vesicular fat accumulation). Briefly, the degree of steatosis was graded based on the percentage of the liver section that was occupied by fat vacuoles at 100 × magnification in 20 fields (grade 0 = < 5% [normal liver]; grade 1 = 5–25%; grade 2 = 26–50%; grade 3 = 51–75%; grade 4 = > 75%).

2.3 High-performance liquid chromatography (HPLC) analysis

Hepatic lycopene concentration was analyzed using HPLC techniques as previously described [52]. Lycopene concentrations were measured at 472 nm and quantified utilizing the area under the curve respective to an appropriate standard curve. An internal control (echinenone) was added to ensure efficiency of extraction and all procedures were carried out under red light.

2.4 Triglyceride (TG) and adiponectin measurement

Weighed liver samples (50 mg) were used to analyze TG content. TG content was determined using a Triglyceride Colorimetric Assay Kit (Cayman Chemical, MI, USA) according to the manufacture's protocol. Plasma adiponectin concentration was measured using enzyme-linked immunosorbent assay (ELISA) kits (R&D Systems, MN, USA). The surfaces of the microplates were coated with an adiponectin mouse monoclonal antibody. Procedures were conducted by following the manufacturer's instructions. The adiponectin ELISA had an intraplate coefficient of variation (CV) range of 5.8–6.7%, with the mean minimum assay detection limit of 0.003 ng/mL.

2.5 RNA extraction and real-time polymerase chain reaction (PCR) analysis

Total RNA extraction was conducted using Trizol reagent (Roche Applied Science, IN, USA). RNA was reverse transcribed using a complementary DNA synthesis kit (Invitrogen, CA, USA). Real-time PCR analysis was performed using the ABI 7500 Real-Time PCR System (Applied Biosystems, Foster City, CA, USA) with a SYBR Green qPCR Mix (Roche Applied Science, Penzberg, Germany). Primers for determination of mRNA expression of genes are listed in Supplemental Table 1. The mRNA levels were calculated by the equation 2-ΔΔCT and presented as the fold change in gene expression normalized to the internal control, β-actin.

2.6 Protein extraction and western blotting

Protein extraction from frozen liver tissues and Western blotting were performed as described previously [42]. Protein concentrations of whole-tissue lysate were determined by Bradford assay (Bio-Rad, CA, USA). Primary antibodies for SIRT1, for both acetylated -fork head box protein O1 (FoxO1), and total-FoxO1, adiponectin receptor2 (adipoR2), and peroxisome proliferator-activated receptor (PPAR)α were purchased from Santa Cruz (TX, USA). The antibodies against phosphorylated, total-AMP-activated protein kinase (AMPK), and phosphorylated, total-acetyl-CoA carboxylase (ACC) were purchased from Cell Signaling (MA, USA). The antibody against nicotinamide phosphoribosyltransferase (NAMPT) was purchased from Abcam (MA, USA). Monoclonal mouse antibody against β-actin was purchased from Sigma-Aldrich (MA, USA). The secondary antibodies included horseradish peroxidase-conjugated anti-rabbit, anti-mouse antibodies (Bio-Rad, CA, USA). The relative intensity was measured to quantify protein levels using GS-710 Calibrated Imaging Densitometer (Bio-Rad, CA, USA). All blots were quantified and normalized against β-actin to adjust for the amount of proteins loaded.

2.7 DNA extraction and 16s rRNA gene sequencing

DNA was directly extracted from cecal samples using the QIAamp fast DNA Stool Mini Kit (Qiagen, Hilden, Germany) according to the manufacturer's instructions and stored at -80°C until further analysis. For each sample, the V1-V2 region of 16S rDNA was amplified using 27Fmod (5'-agrgtttgatymtggctcag-3') and 338R (5'-tgctgcctcccgtaggagt-3') described by Kim et al. [53]. Subsequent amplification step was performed to add Illumina sequencing adapters and multiplexing indices using the Nextera XT Index Kit. Library quantification, normalization and pooling were conducted according to the manufacturer's instructions. Pooled libraries were denatured using fresh NaOH and mixed with Illumina-generated PhiX control libraries before sequencing. Sequencing was carried out using a paired-end, 2 × 300-bp cycle run on an Illumina MiSeq sequencing system (Illumina, San Diego, CA) and MiSeq v3 reagent kits (600 Cycles, 15

Gb output). FastQ files were generated at the end of each run for quality control. The quality of the run was internally checked using PhiX Control and then each pair-end sequence was assigned to its sample according to multiplexing indexes.

2.8 Data processing and microbial community analysis

Pair end reads were joined by command fastq-join contained in package ea-utils [54] and then processed using a pipeline constructed by Kim et al [53]. First, reads lacking both forward and reverse primers were removed based on BLAST search. Second, denoising was conducted by removing reads with average quality scores below 25. After primer sequences were trimmed, 5,000 high-quality reads per sample were selected for the operational taxonomic unit (OTU) and UniFrac distance analysis. All reads were assigned a unique name labeled by sample ID and then merged into a single file. OTUs were generated using a 97% pairwise-identity cutoff with the UCLUST program3 [55]. Two databases, described by Kim et al. [53], were used for determining specific taxa of 16S OTUs. Alpha-diversity indices (ACE, Chao1, Shannon's index and Simpson's index) were calculated using vegan (R package, v2.2-1). Weighted and unweighted UniFrac analyses were used to measure beta-diversity between microbial communities, and results were plotted using principal coordinate analysis. Clustering analysis was conducted based on genus-level classification data using hclust (method: ward.D2) [56] implemented in stats (R package, v3.3.1), and dendrogram was generated using R (v3.3.1).

2.9 Statistical analysis

GraphPad Prism 5 was used to perform the statistical analyses. Normality and equal variance were assessed by using SAS 9.3 PROC UNIVARIATE command. Student t-test and Mann-Whitney test were used to examine the differences between HFD and HFD+TP groups. Data are expressed as means and SEM or medians. A P value < 0.05 was considered significant. Comparisons of diversity indices and phylogenetic taxa among different groups were performed using Student's t-test and Tukey's HSD test (R packages, v3.3.1). Differences were considered significant when P value < 0.05.

3. Results

3.1 Dietary TP alleviated HFD-induced hepatic steatosis and TG accumulation in BCO1-/-BCO2-/- double KO mice

There were no differences in initial body weights, MAT weights, or liver weights between the HFD and HFD+TP groups (Table 1). Compared to an undetectable amount of lycopene in the livers of

mice fed only HFD, the lycopene concentration in the livers of HFD+TP fed mice was 14.0 ± 2.3 nmol/g (Table 1). We only detected a trace amount of both β-carotene and phytoene in the livers of BCO1-/-BCO2-/- double KO mice. This could be due to the fact that the concentrations of β-carotene and phytoene were much lower than that of lycopene in TP. Histological assessments of liver tissue sections showed that all HFD-fed mice developed hepatic steatosis by the age of 30 weeks, similar to our previous study utilizing BCO2 KO mice [57]. TP supplementation for 24 weeks did not alter the incidence of hepatic steatosis, but significantly decreased severity of hepatic steatosis (hepatic steatosis scores ranged from grade 1 to 3 with the median value of 2, $P = 0.048$) as compared to the HFD group (hepatic steatosis scores ranged from grade 2 to 4 with the median value of 3) (Figure 1A, B). Consistently, total hepatic TG concentration was significantly reduced with TP supplementation in the HFD fed group ($P = 0.045$), as compared with that of the HFD fed alone (Figure 1C).

3.2 Amelioration of HFD-induced hepatic steatosis by TP was associated with increased SIRT1 activity in BCO1-/-BCO2-/- double KO mice

We examined both mRNA and protein levels of SIRT1 and did not find any differences between the two groups (Figure 2A, B). However, we found that acetylation of FoxO1 was significantly decreased in mice fed TP ($P = 0.03$), suggesting an increased SIRT1 deacetylase activity with TP supplementation (Figure 2C). Since SIRT1 deacetylates target proteins accompanied with the hydrolysis of NAD+, we also examined the expression of NAMPT, which is the rate-limiting enzyme for NAD+ biosynthesis. We found that both hepatic mRNA and protein expression of NAMPT was significantly increased in the HFD+TP group ($P = 0.038$), as compared with that of the HFD alone group (Figure 2D, E).

3.3 TP supplementation decreased liver lipid synthesis and uptake, and enhanced fatty acid oxidation in BCO1-/-BCO2-/- double KO mice

AMPK is a phylogenetically conserved serine/threonine protein kinase. The phosphorylation and activation of AMPK has been reported to stimulate energy-consuming biosynthetic pathways, such as fatty acid and sterol synthesis [58]. Acetyl-CoA carboxylase (ACC) and Stearoyl-CoA desaturase-1 (SCD1) play important roles in catalyzing fatty acid synthesis. The activity of ACC is switched off by phosphorylation [59]. In the current study, the mRNA expressions of acc and scd1 were comparable between HFD and HFD+TP groups (data not shown). However, we found that TP supplementation significantly increased both phosphorylated-AMPK ($P = 0.03$, Figure 3A) and phosphorylated-ACC ($P = 0.04$, Figure 3B), and decreased the mRNA level of dgat1 ($P = 0.04$,

Figure 3D), indicating that TP decreased de novo lipogenesis in HFD+TP mice, compared to mice with HFD alone. In addition, as compared to the HFD alone group, TP feeding significantly 1) increased both mRNA and protein levels of PPARα (P = 0.05, Figure 3C); 2) up-regulated the mRNA expression of genes related to fatty acid oxidation (cpt1, acox1); and 3) decreased liver fatty acid transporter cd36 transcription (P = 0.03, Figure 3D).

3.4 TP upregulated adiponectin production and decreased mRNA of pro-inflammatory cytokines in MAT of BCO1-/-BCO2-/- double KO mice

Leptin and resistin mRNA expression in MAT did not differ between the HFD group and the HFD+TP group; however, TP supplementation significantly increased mRNA expression of Pparγ and Adiponectin in MAT (P = 0.05, Figure 4A). Consistent with increased adiponectin expression in MAT, significantly higher concentrations of plasma adiponectin were observed in the HFD+TP group, compared to the HFD group (34%, P = 0.0001) (Figure 4B). It is important to note that plasma adiponectin concentrations were inversely correlated with hepatic steatosis score (R2 = 0.62, P = 0.02) and that TP feeding significantly decreased the mRNA expressions of three pro-inflammatory biomarkers (tnf-α, il-1β, and il-6) in MAT (P = 0.03, Figure 4C).

3.5 TP supplementation significantly up-regulated adipoR2 expression and decreased mRNA expression of pro-inflammatory biomarkers in the liver

To further explore the cross-talk between adipose tissue and the liver, we assessed adipoR2 which is the major receptor in the liver for adiponectin uptake. Results showed that TP supplementation significantly up-regulated the mRNA and protein expressions of adipoR2, P = 0.03, (Figure 5A, B). Consistent with our findings in MAT, TP supplementation decreased the mRNA of three pro-inflammatory biomarkers (tnf-α, il-1β, and il-6, P = 0.03), and increased the mRNA expression of anti-inflammatory IL-10 (P = 0.001), in the livers of mice compared to that of mice without TP supplementation (Figure 5C). The hepatic mRNA level of Mcp-1 remained unchanged between the HFD group and the HFD+TP group (Figure 5C).

3.6 Dietary TP feeding resulted in relative higher microbiota diversity in HFD-fed BCO1-/-BCO2-/- KO mice

Using pyrosequencing data obtained from the cecum samples, we explored to what extent intestinal microbiota responded to TP supplementation on the overall cecum microbiota community composition under the same HFD surplus. Alpha-diversity indices including OTU richness, Chao 1, ACE and Shannon diversity index was estimated for gut microbial community differences

between HFD alone and HPD with TP feeding (Figure 6). As compared to mice on HFD alone (Figure 6A), the observed OTUs (P = 0.04), and ACE (P = 0.04) of the gut microbiota in the HFD+TP group were significantly higher. This indicates that dietary TP supplementation increased microbiota richness in HFD-fed mice. Another microbial richness index, Chao 1, showed a relative increase in the HFD+TP group, but this finding was not significant (P = 0.06). There was no significant difference in microbial evenness measured by Shannon's index (Figure 6A, B).

In addition, we examined the intestinal microbiota response in mice fed semi-purified powder HFD and HFD+TP diets (Supplemental Figure 1). The distribution of beta-diversity measures (patterns of separation) was compared between HFD with or without TP feeding using standard chow diet fed mice as a relative control group. We carried out a UniFrac analysis, a measure of community dissimilarity based on microbial abundance and evolutionary relatedness, which showed that samples clustered primarily by HFD-feeding. Meanwhile a clear patterns of separation by TP feeding was observed between HFD and HFD+TP groups in PCoA plot of unweighted UniFrac distances (Supplemental Figure 1). A clustering dendrogram was also constructed using ward.D2 method implemented in stats (R package, v3.3.1) based on genus-level classification data to improve visualization of the relationships among different groups (Supplemental Figure 1). The separation between samples of the HFD and HFD+TP groups indicated that TP supplementation accounted for differences of microbial community between the two groups. As compared with the standard chow diet group (as a relative control), our results suggested that microbiota richness decreased in the HFD group, but was partially recovered in HFD+TP group.

3.7 Dietary TP feeding resulted in a relative lower abundance of Clostridium in HFD-fed BCO1-/- BCO2-/- KO mice

To explore the possibility that TP is capable of altering the microbial profile and bacteria composition, we examined the relative abundance of both gram-positive (mainly Firmicutes) and gram-negative (mainly Bacteroidetes) bacteria. We did not find any difference between HFD group and HFD+TP group (data not shown). However, we found that the relative abundance of Clostridium was significant lower in the HFD+TP group, compared with HFD alone (P = 0.05, Figure 6C). At the species level of Clostridium, dietary TP supplementation did not affect the most abundant species of Clostridium, Clostridium sp. Culture-57 (data not shown). However, TP feeding decreased the relative abundance of Clostridium sp. ID4 (P = 0.04, Figure 6D) and Clostridium disporicum (P = 0.07, Figure 6E), which were the second and third most abundant species of Clostridium, respectively, in this study. We also found that the relative abundance of

Clostridium, in particular Clostridium sp. ID4, was significantly higher in the HFD group but remained the same in the HFD+TP group, as compared with chow diet fed mice (Supplemental Figure 2).

4. Discussion

Consumption of tomato and tomato products is inversely associated with the incidence of a number of chronic diseases and ameliorates risk factors of metabolic diseases [33]. Recently, both BCO1 and BCO2 enzymes have been reported to play critical roles in the metabolism of lycopene, one of the most abundant carotenoids in tomatoes. Genetic variation of BCO1 and BCO2 can affect the metabolism of a variety of carotenoids, including lycopene, and this has been shown in humans [47]. One recent study reported that apolycopenoids, implicated in protecting against NAFLD [20, 42], could be detected in human plasma after consuming tomato juice for 8 weeks [60]. These apolycopenoids in plasma could derive directly from foods, or from postprandial metabolic processing by human enzymes. In this present study, we showed that dietary TP supplementation alleviated severity of hepatic steatosis and modulated inflammatory responses in MAT and liver induced by the HFD in BCO1-/-BCO2-/- double KO mice. The present study provides evidence that TP (whole food) consumption can prevent NAFLD independent of BCO1 and BCO2 enzyme activities.

SIRT1, a NAD+-dependent protein deacetylase, is a key regulator of hepatic lipid metabolism. The protective effects of SIRT1 against hepatic steatosis induced by HFD have previously been demonstrated in a moderate overexpression of SIRT1 mouse model [61]. In the present study, TP supplementation significantly reduced FoxO1 acetylation without changing total FoxO1 expression in liver, indicating an increased deacetylase activity of SIRT1. It has been reported that NAMPT is a rate-limiting enzyme of NAD+ biosynthesis, which generates nicotinamide mononucleotide from nicotinamide in a salvage pathway and directly regulates SIRT1 activity [62, 63]. In the present study, we found an increased NAMPT level in the HFD+TP group, which may account for the increased SIRT1 deacetylase activity after TP supplementation. It has been shown that NAD+ precursor nicotinamide riboside feeding increased NAD+ levels in liver which enhanced oxidation metabolism and protected against HFD-induced metabolic dysfunction via activated SIRT1 [64, 65]. Intriguingly, nicotinamide riboside feeding ameliorated the steatosis that normally accompanies liver regeneration, but the overexpressing NAMPT in mice was similar to that of mice treated with nicotinamide riboside, and exhibited enhanced liver regeneration and reduced steatosis following partial hepatectomy [66]. Therefore, our observation that dietary TP feeding inhibits

hepatic steatosis and inflammation through up-regulating SIRT1 activity and NAMPT expression could be a potential molecular mechanism for TP protection.

AMPK has long been recognized as a central regulator of mammalian metabolic function [67]. In the liver, SIRT1 is required for AMPK activation [68], and the activation of SIRT1-AMPK axis has been identified as a strategy for the treatment of hepatic steatosis in NAFLD [69]. Our study revealed that in parallel with increasing SIRT1 activity in HFD+TP fed mice, TP supplementation significantly enhanced the phosphorylation of AMPK, which negatively regulated dgat1 transcription [70], and inactivated ACC, a rate-limiting enzyme for de novo fatty acid synthesis [67, 71, 72]. In addition, we observed that TP increased both mRNA and protein expressions of PPARα, which is a pivotal transcription factor that regulates a variety of genes related to energy homeostasis [73]. This potentially explained the elevated transcription level of PPARα-target genes, fatty acid transporter cd36 and β-oxidation related genes, cpt1 and acox1, in the livers of TP-fed mice. These data suggested that in liver, TP supplementation ameliorated NAFLD via three mechanisms: 1) decreasing de novo fatty acid synthesis; 2) increasing fatty acid oxidation; and 3) reducing liver fatty acid uptake.

Adiponectin is one of the most abundant adipokines secreted by adipocytes. Accumulating evidence shows that adipokine secretion is involved in the cross-talk between adipose tissue and liver in protecting against the pathogenesis of NAFLD by modulating lipid metabolism and inflammatory responses [74-76]. Decreased adiponectin transcription in adipose tissue and reduced adiponectin concentration in plasma have been reported in patients with obesity and NAFLD [77, 78]. Our present findings showed that TP supplementation caused a significant increase in adiponectin mRNA expression in MAT, and circulating adiponectin concentration in HFD-fed BCO1-/-BCO2-/- double KO mice, which was in agreement with our previous report that lycopene-rich tomato oleoresin modulates plasma adiponectin concentration and mRNA levels of adiponectin in adipose tissue of obese rats [79], indicating the induction of adiponectin by TP per se and independent of carotenoid cleavage enzymes.

Considering that adiponectin transcription in adipose tissue can be upregulated in response to PPARγ activation [80, 81], we examined pparγ in MAT and found that TP supplementation increased pparγ mRNA expression, which might be the potential mechanism by which TP enhanced adiponectin production. Furthermore, we observed a significantly inverse correlation between adiponectin circulating level and hepatic steatosis grade. This is consistent with a study performed by Bajaj, et al, who found that lower adiponectin plasma levels were inversely correlated with

hepatic fat contents [82], and further supported by our observation that HFD+TP fed mice had significantly higher hepatic adipoR2 protein than HFD mice. This might be due to the effect of TP on increasing SIRT1 activity, as SIRT1-FoxO1 signaling contributed to increased adipoR2 expression through upregulated binding of FoxO1 to adipoR2 promoter sites [83, 84]. It should be noted that in liver, adiponectin can activate PPARα transcription [85], which is in concordance with our finding that TP supplementation increased hepatic PPARα mRNA. Since impaired adiponectin secretion and decreased adipoR2 have both been documented in NAFLD patients [77, 78, 86], it is possible that TP can be used as a preventive measure against NAFLD development by targeting both liver and MAT.

Metabolic inflammation induced by HFD is frequently observed in adipose tissue and liver [30, 87], and both tissue can secrete pro-inflammatory cytokines [88]. In this study, our data showed that HFD+TP fed mice had significantly lower mRNA expression of pro-inflammatory biomarkers (tnf-α, il-1β, and il-6) in MAT and liver, and increased hepatic expression of IL-10, which is an anti-inflammatory cytokine. Similar anti-inflammatory efficacy of tomato products was observed in a clinical trial, showing that overweight/obese subjects who consumed 330 ml/d tomato juice for 20 days had significantly lower circulating IL-6 and TNF-α, compared to those only consumed water [89]. It is possible that decreased mRNA expression of hepatic pro-inflammatory biomarkers by TP supplementation was due to reduction of resident macrophage (Kupffer cell) activation. This hypothesis is supported by the results from De Stefano et al., who showed that lycopene treatment inhibited the activation of macrophage [90]. In addition, we previously observed that both lycopene and apolycopenoids supplementation inhibited the protein level of NF-κB p65 [9, 42], a key transcription factor for the activation of IL-6 [91], IL-1β [92] and inducing TNFα signaling [92]. Therefore, decreasing NF-κB p65 could represent one of the potential mechanisms by which TP inhibited pro-inflammatory cytokines in both liver and MAT.

Gut microbiota appears to contribute to the adverse consequences of HFD on the metabolic phenotype, aggravating the associated low-grade inflammation [12]. Recently, it has been shown that HFD feeding rather than obesity drives taxonomical and functional changes in the gut microbiota in mice [93]. In the present study, we evaluated bacterial community dynamics that were potentially affected by TP feeding. As compared to mice on HFD diet alone, we observed that dietary TP supplementation increased microbial richness under HFD perturbations. Since a decrease in gut microbial diversity was observed in NAFLD patients compared to healthy control, a lowered microbiota diversity might contribute to increased risk of NAFLD progression [94-97].

Our results suggest that TP feeding may improve the lowered microbial diversity caused by HFD, which may be associated with the amelioration of TP against HFD-induced NAFLD.

Interestingly, we found that dietary TP feeding resulted in a relative lower abundance of Clostridium in HFD-fed mice, as compared with that of HFD alone. Clostridium has been reported to contribute to developing diseases like fatty liver [98, 99], obesity [100], and inflammatory bowel diseases [101]. In addition, Clostridium spp carries 7α/β-dehydroxylation to the primary bile acids [102], resulting in deoxycholic acid (DCA), a secondary bile acid that may impose strong antimicrobial activity (e.g. damage of the bacterial cell membrane by interaction with phospholipids) due to their amphipathic properties. It has been reported that DCA has 10 times the bactericidal activity of cholic acid [103], therefore an increase in the proportion of DCA following HFD feeding might be the potential mechanism of altered microbiota composition in our study. A limitation of our study was that we did not measure both primary and secondary bile acids in feces due to the exploratory nature of the study and limited amount of fecal sample. In addition, although Clostidium spp. ID4 is more abundant in the HFD group, which may link this strain with NAFLD progression, the biological properties and species of Clostidium spp. ID4 has not yet been characterized. Whether decreasing Clostidium spp. ID4 is a potential mechanism of TP ameliorating HFD-induced NAFLD needs further investigation. Lastly diet modification, notably using dietary fibers, is a way to restore a high richness in the gut microbiota. Although our present study provides new evidence on the role of TP feeding on gut microbial richness, it is not clear whether TP restores high fat diet-reduced gut microbiota richness due to its fiber or carotenoid components, which is currently under the investigation in our laboratory.

One of the important observations in the present study was that hepatic lycopene concentration (14.0 ± 2.3 nmol/g tissue) was within the range of lycopene concentrations in normal human liver (0.2 - 20.7 nmol/g tissue) [104], which indicates that the TP-supplemented dosage is achievable at a physiologically relevant condition in human. In addition, hepatic lycopene concentration in BCO1-/-/BCO2-/- double KO mice fed with TP (equal to 100 mg lycopene/kg diet) was comparable to the BCO2-/- KO mice supplemented with 100 mg lycopene/kg diet in our previous study [39], suggesting that BCO2 is a major cleavage enzyme for lycopene. A limitation of this study was that we could not determine whether the potential beneficial effects of TP resulted from individual or synergistic contributions of nutrient components contained in TP products, such as lycopene, □-carotene, phytoene, phytofluene, vitamin E, vitamin C or polyphenols etc. [89], as all have protective efficacy against lipid dysregulation and inflammation [9, 39, 42, 105-107]. It is likely that these nutrients contribute individually to protecting against NALFD, however, it is worth highlighting that, independent of carotenoid cleavage enzymes BCO1 and BCO2, TP

supplementation can produce synergistic effects of individual nutrients and maximize the beneficial effects of dietary intervention [89, 108, 109].

Taken together, the present study demonstrated that dietary TP can inhibit NAFLD independent of carotenoid cleavage enzymes, potentially through suppressing inflammatory responses and increasing SIRT1 activity and adiponectin production in adipose tissue. Additionally, dietary TP can increase gut microbial richness and decrease the abundance of Clostridium, which may be associated with lower incidence of HFD-induced NAFLD.

Author contribution:

X-D Wang, J.V.L., K. A. conceived and designed the experiment. C-C L., C.L., M.F., K.H., K.A., S.T., S.H., J.C., performed the experiment. C-C Li., C.L., M.F., analyzed the data. C-C Li., M.F., J.C., J.V.L., X-D. W. wrote the manuscript. All authors reviewed and approved the manuscript.

Acknowledgement:

This work was supported by USDA/NIFA (AFRI 2015-67017- 23141) and USDA/ARS (58-1950-51000-074S). The authors thank Ms. Meghan Faherty for her assistance to the manuscript editing. Any opinions, findings, conclusions, and recommendations expressed in this publication are those of the authors and do not necessarily reflect the views of the sponsors.

Figure 1.

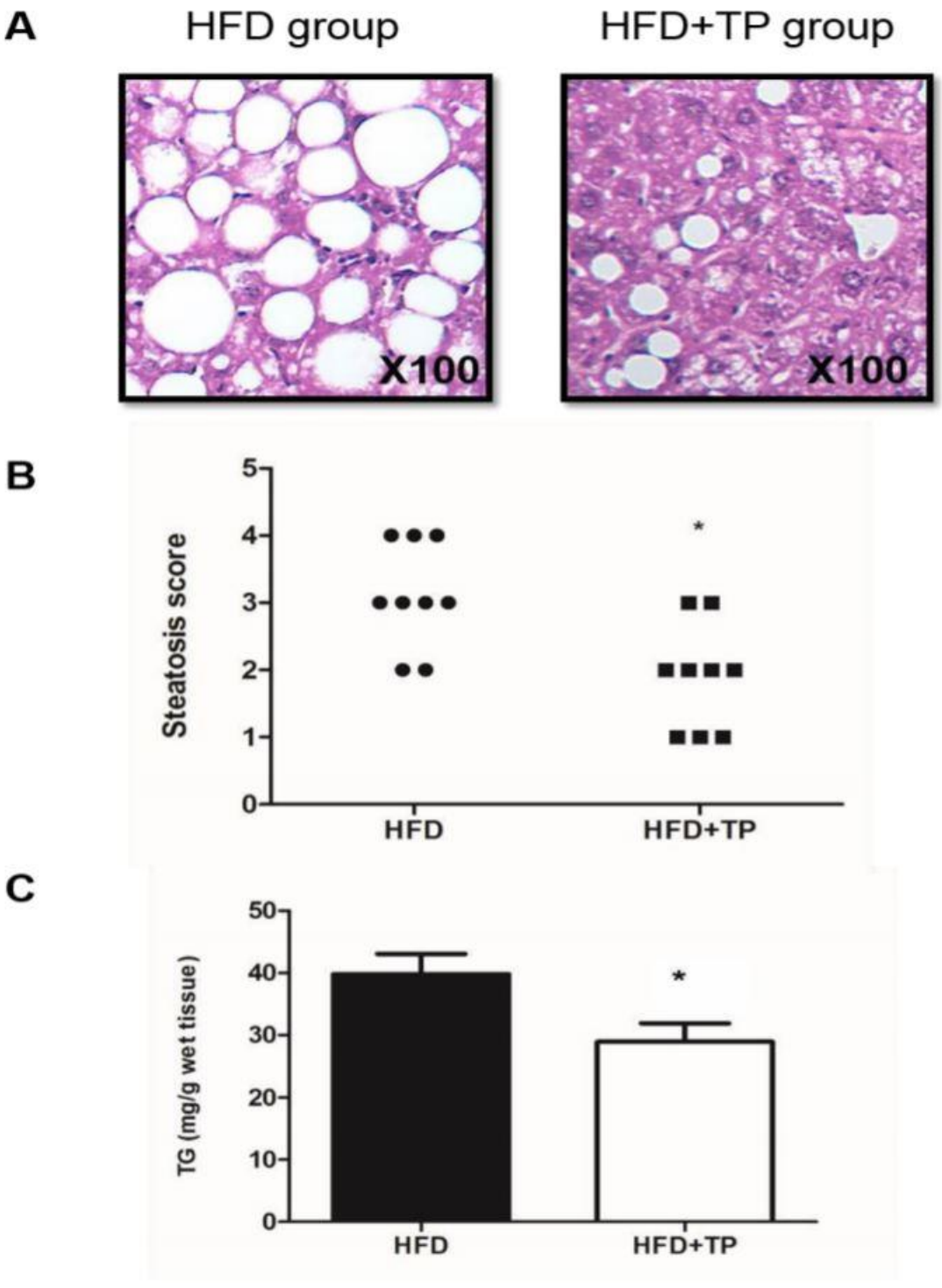
A
HFD group
HFD+TP group
X100
X100
B
Steatosis score
5
4
3
2
1
0
*
HFD
HFD+TP
C
TG (mg/g wet tissue)
50
40
30
20
10
0
*
HFD
HFD+TP

Figure 2.

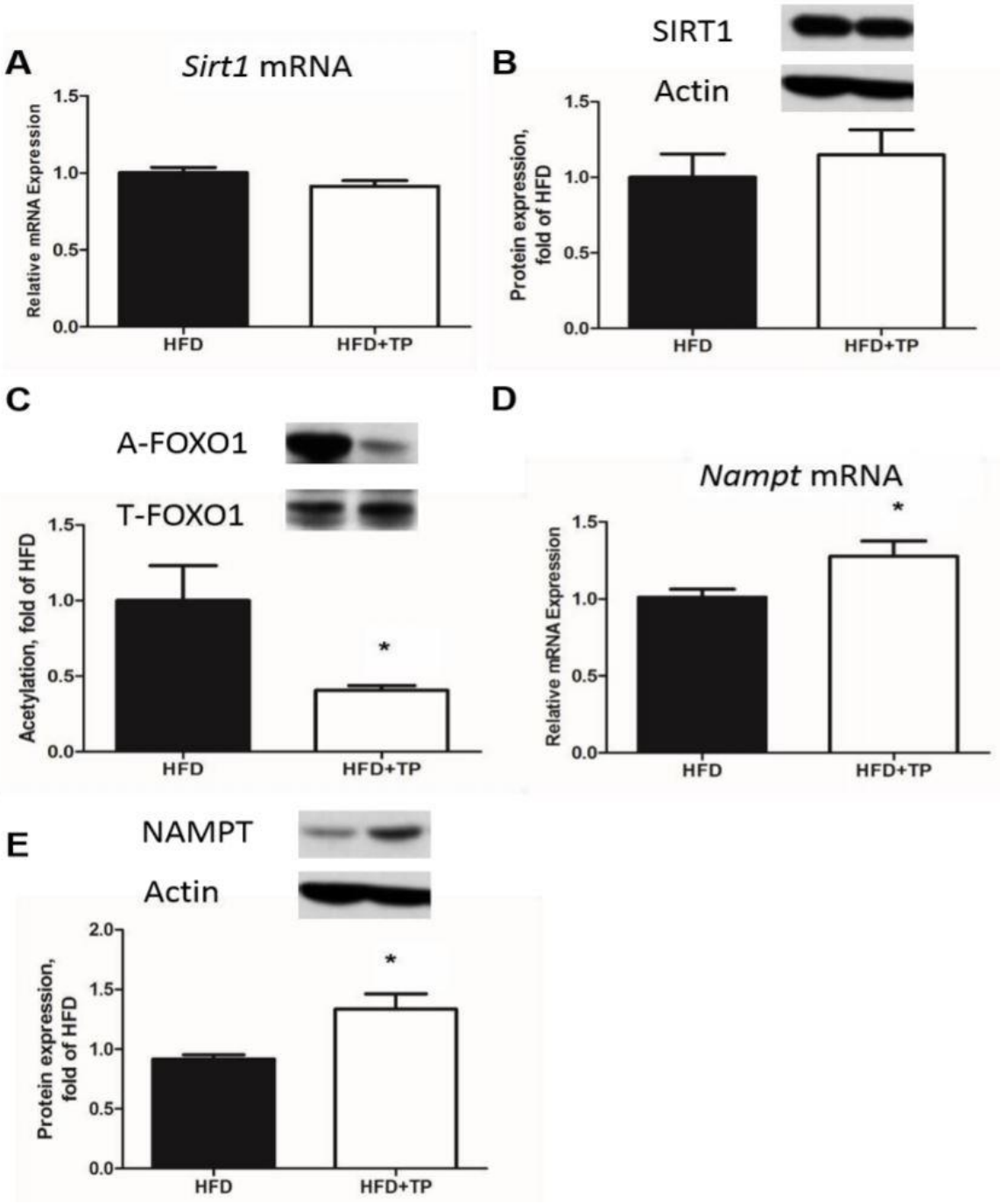
A
Sirt1 mRNA
Relative mRNA Expression
1.5
1.0
0.5
0.0
HFD
HFD+TP
B
SIRT1
Actin
Protein expression, fold of HFD
1.5
1.0
0.5
0.0
HFD
HFD+TP
C
A-FOXO1
T-FOXO1
Acetylation, fold of HFD
1.5
1.0
0.5
0.0
*
HFD
HFD+TP
D
Nampt mRNA
Relative mRNA Expression
1.5
1.0
0.5
0.0
*
HFD
HFD+TP
E
NAMPT
Actin
Protein expression, fold of HFD
2.0
1.5
1.0
0.5
0.0
*
HFD
HFD+TP

Figure 3.

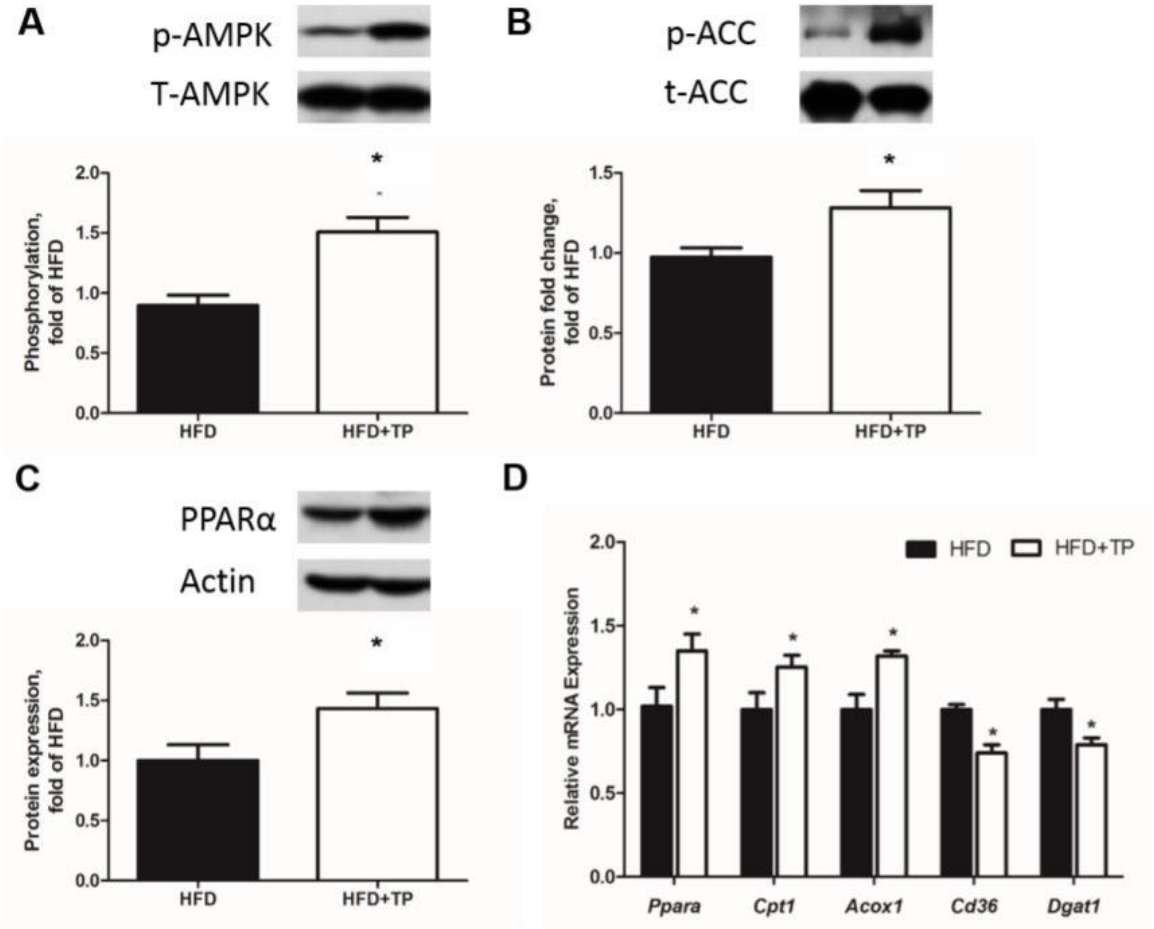
A
p-AMPK
T-AMPK
Phosphorylation, fold of HFD
HFD
HFD+TP
B
p-ACC
t-ACC
Protein fold change, fold of HFD
HFD
HFD+TP
C
PPARα
Actin
Protein expression, fold of HFD
HFD
HFD+TP
D
HFD
HFD+TP
Relative mRNA Expression
Ppara
Cpt1
Acox1
Cd36
Dgat1

Figure 4.

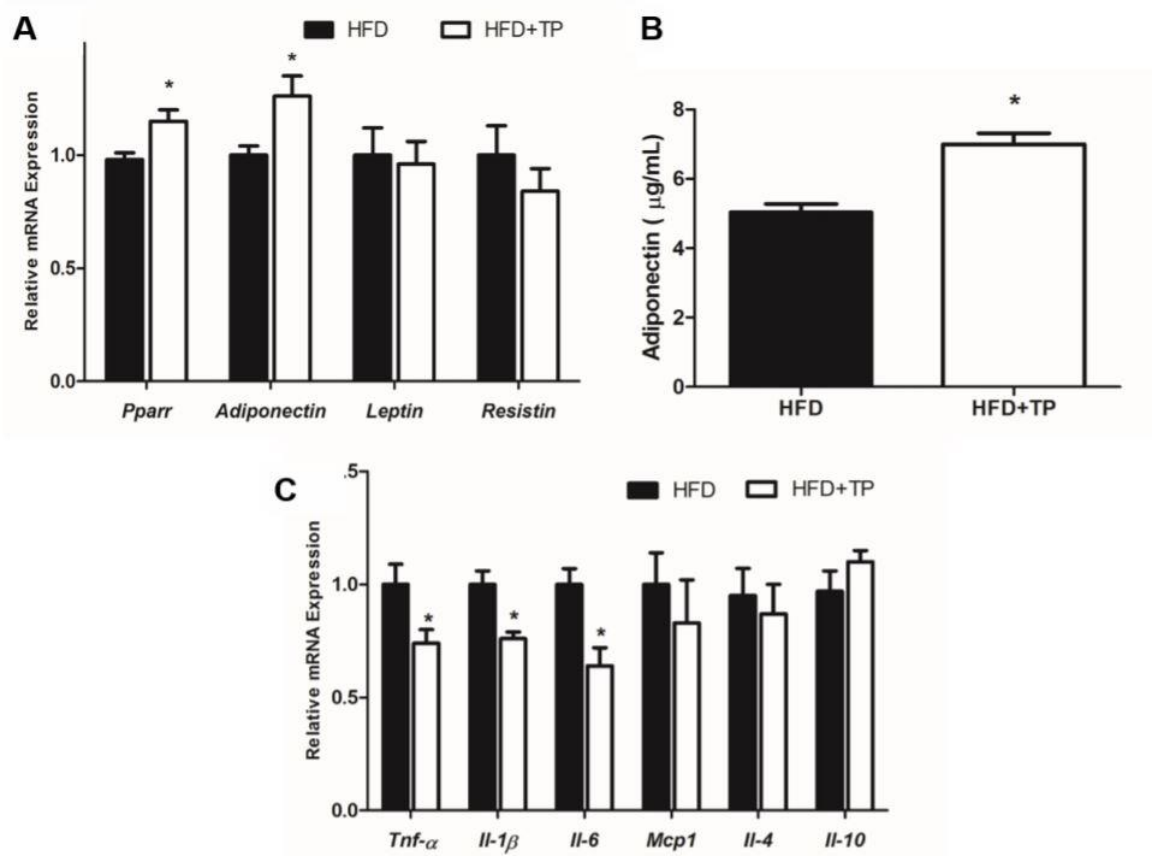
A
HFD
HFD+TP
Relative mRNA Expression
1.0
0.5
0.0
*
*
Pparr
Adiponectin
Leptin
Resistin
B
Adiponectin (μg/mL)
8
6
4
2
0
*
HFD
HFD+TP
C
HFD
HFD+TP
Relative mRNA Expression
1.0
0.5
0.0
*
*
*
Tnf-α
Il-1β
Il-6
Mcp1
Il-4
Il-10

Figure 5.

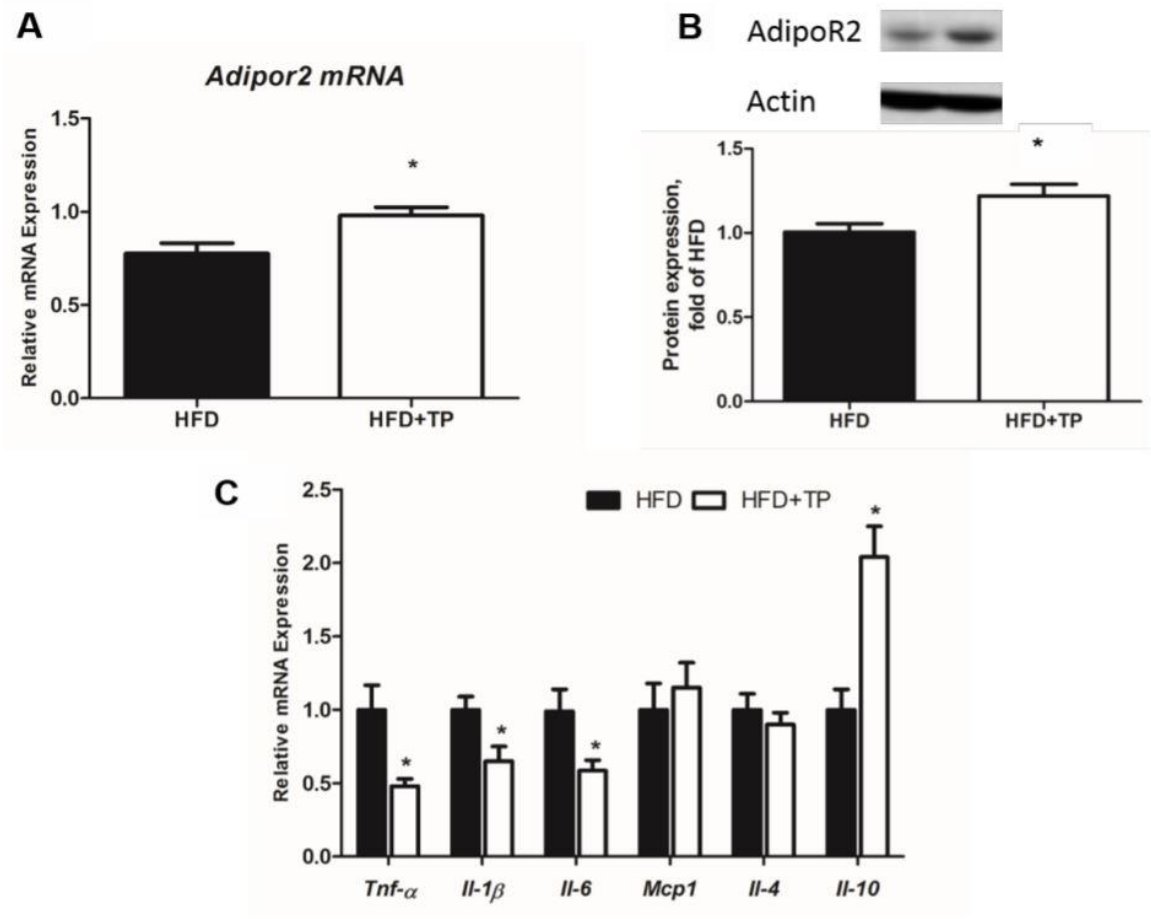
A
Adipor2 mRNA
Relative mRNA Expression
1.5
1.0
0.5
0.0
*
HFD
HFD+TP
B
AdipoR2
Actin
Protein expression, fold of HFD
1.5
1.0
0.5
0.0
*
HFD
HFD+TP
C
HFD
HFD+TP
Relative mRNA Expression
2.5
2.0
1.5
1.0
0.5
0.0
*
Tnf-α
Il-1β
Il-6
Mcp1
Il-4
Il-10

Figure 6.

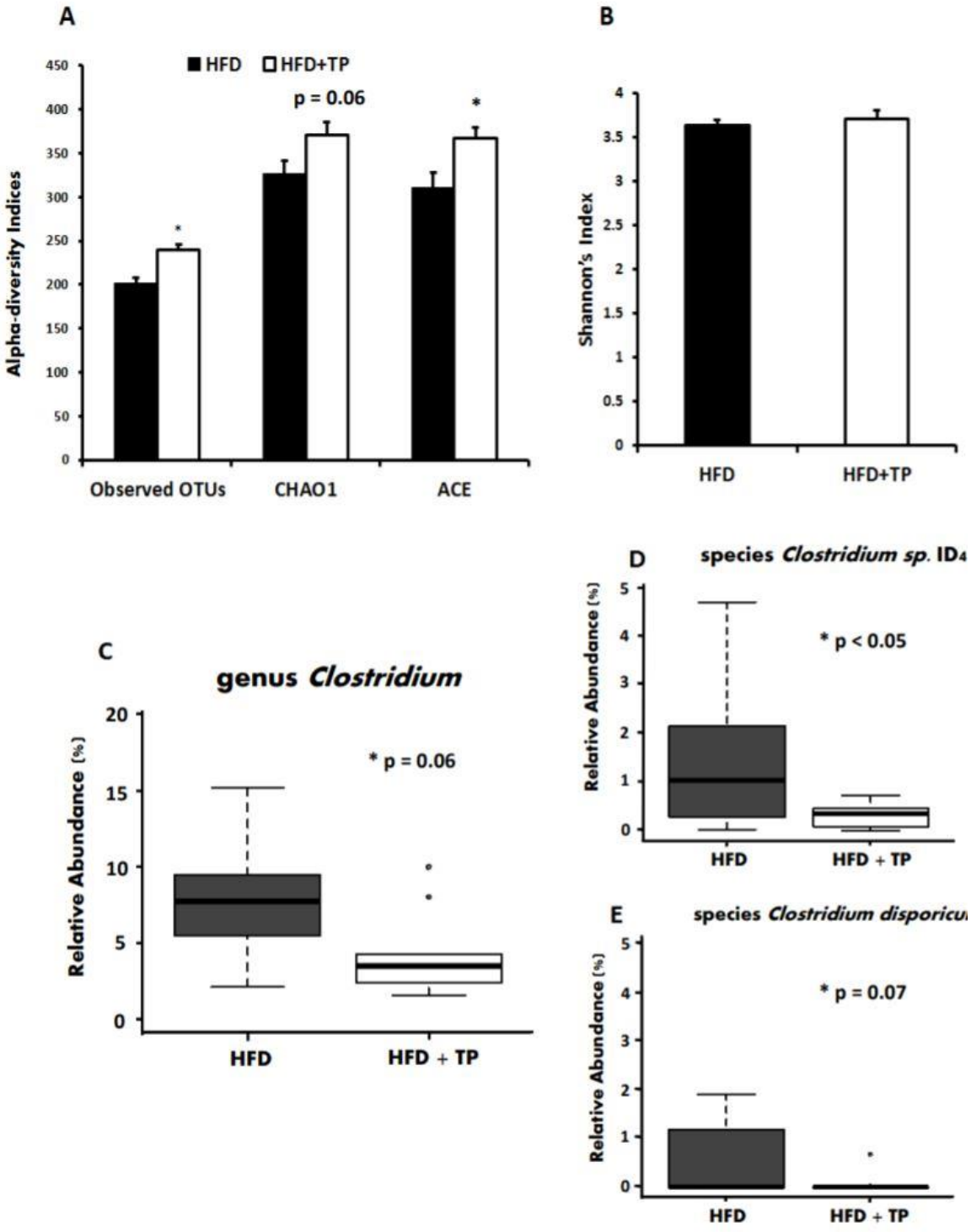
A
HFD
HFD+TP
p = 0.06
*
*
Alpha-diversity Indices
450
400
350
300
250
200
150
100
50
0
Observed OTUs
CHAO1
ACE
B
Shannon's Index
4
3.5
3
2.5
2
1.5
1
0.5
0
HFD
HFD+TP
C
genus Clostridium
* p = 0.06
Relative Abundance (%)
20
15
10
5
0
HFD
HFD + TP
D
species Clostridium sp. ID4
* p < 0.05
Relative Abundance (%)
5
4
3
2
1
0
HFD
HFD + TP
E
species Clostridium disporicu
* p = 0.07
Relative Abundance (%)
5
4
3
2
1
0
HFD
HFD + TP

Figure legends

Figure 1. Histopathological examination of steatosis in BCO1-/-BCO2-/- double KO mice fed with a HFD alone or HFD supplemented with TP. (A) The representative images of livers with H&E staining were presented from HFD and HFD+TP fed mice. (B) Distribution of steatosis score. Non-parametric test was conducted to compare the difference of the two groups. *Significantly different from the HFD, P = 0.048 (C) Hepatic TG concentration. Differences between groups were analyzed by Student's t-test. *Significantly different from the HFD, P = 0.045. BCO1, beta-carotene-15, 15'-oxygenas; BCO2, beta-carotene-9', 10'-oxygenase; KO, knockout; HFD, high fat diet; TP, tomato powder; TG, triglyceride.

Figure 2. Effects of TP on hepatic mRNA and protein expressions associated with SIRT1 and SIRT1 activity in HFD-fed BCO1-/-BCO2-/- double KO mice. Beta-actin was used as control unless specified otherwise. Graphical representation of fold changes in (A) sirt1 mRNA; (B) SIRT1 protein, (C) Acetylated-FoxO1, total-FoxO1 as loading control; (D) nampt mRNA; and (E) NAMPT protein. Values are expressed as mean ± SEM, n = 9. Differences between groups were analyzed by Student's t-test. *Significantly different from the HFD, P < 0.05. BCO1, beta-carotene-15, 15'-oxygenas; BCO2, beta-carotene-9', 10'-oxygenase; KO, knockout; HFD, high fat diet; TP, tomato powder; SIRT1, sirtuin1; NAMPT, nicotinamide phosphoribosyltransferase; FOXO, foxhead box protein O.

Figure 3. Effects of TP on hepatic protein and mRNA expressions of genes related to lipid metabolism in HFD-fed BCO1-/-BCO2-/- double KO mice. Beta-actin was used as control unless specified otherwise. Graphical representation of fold changes in (A) phosphorylated-AMPK, total-AMPK as loading control; (B) phosphorylated-ACC, total-ACC as loading control; and (C) PPARα; and (D) pparα, cpt1, acox1, dgat1, and cd36 mRNA. Values are expressed as mean ± SEM and n = 9. Differences between groups were analyzed by Student's t-test. *Significantly different from the HFD, P < 0.05. BCO1, beta-carotene-15, 15'-oxygenas; BCO2, beta-carotene-9', 10'-oxygenase; KO, knockout; HFD, high fat diet; TP, tomato powder; AMPK, AMP-activated protein kinase; ACC, acetyl-CoA carboxylase; PPAR, peroxisome proliferator-activated receptor, CPT1, carnitine palmitoyltransferase ACOX1, acyl-CoA oxidase 1; DGAT, diglyceride acyltransferase.

Figure 4. Effects of TP on hepatic mRNA expressions of adipokines and cytokines in MAT and plasma adiponectin levels in HFD-fed BCO1-/-BCO2-/- double KO mice. Beta-actin was used as control unless specified otherwise. Graphical representation of fold changes in (A) pparα,

adiponectin, leptin, and resistin mRNA; (B) plasma adiponectin concentration; and (C) tnf-α, il-1β, il-6, mcp1, il-4, and il-10 mRNA. Values are expressed as mean ± SEM and n = 9. Differences between groups were analyzed by Student's t-test. *Significantly different from the HFD, $P < 0.05$. BCO1, beta-carotene-15, 15'-oxygenas; BCO2, beta-carotene-9', 10'-oxygenase; KO, knockout; HFD, high fat diet; TP, tomato powder; TNF, tumor necrosis factor; IL, interleukin.

Figure 5. Effects of TP on hepatic mRNA and protein levels of adipoR2 and mRNA expressions of cytokines in HFD-fed BCO1-/-BCO2-/- double KO mice. Beta actin was used as control unless specified otherwise. Graphical representation of fold changes in (A) adipor2 mRNA; (B) adipoR2 protein; and (C) tnf-α, il-1β, il-6, mcp1, il-4, and il-10 mRNA. Values are expressed as mean ± SEM and n = 9. Differences between groups were analyzed by Student's t-test. *Significantly different from the HFD, $P < 0.05$. BCO1, beta-carotene-15, 15'-oxygenas; BCO2, beta-carotene-9', 10'-oxygenase; KO, knockout; HFD, high fat diet; TP, tomato powder; adipoR, adiponectin receptor.

Figure 6. Effects of TP on microbiota richness and Clostridium abundance in HFD-fed BCO1-/-BCO2-/- double KO mice. (A) Observed OTUs, Chao1 and ACE, representing community richness; (B) Shannon's Index, representing community evenness, (C) relative abundance of Clostridium; (D) relative abundance of Clostridium spp. ID4; and (E) relative abundance of Clostridium disporicum. Values are expressed as mean ± SEM and n = 9. Differences between groups were analyzed by Student's t-test. *Significantly different from the HFD, $P < 0.05$. BCO1, beta-carotene-15, 15'-oxygenas; BCO2, beta-carotene-9', 10'-oxygenase; KO, knockout; HFD, high fat diet; TP, tomato powder.

References

[1] Roberts, D. L., Dive, C., Renehan, A. G., Biological mechanisms linking obesity and cancer risk: new perspectives. Annual review of medicine 2010, 61, 301-316.

[2] Sun, B., Karin, M., Obesity, inflammation, and liver cancer. Journal of hepatology 2012, 56, 704-713.

[3] Sun, B., Karin, M., NF-kappaB signaling, liver disease and hepatoprotective agents. Oncogene 2008, 27, 6228-6244.

[4] Khandekar, M. J., Cohen, P., Spiegelman, B. M., Molecular mechanisms of cancer development in obesity. Nature reviews. Cancer 2011, 11, 886-895.

[5] Page, J. M., Harrison, S. A., NASH and HCC. Clinics in liver disease 2009, 13, 631-647.

[6] Baffy, G., Brunt, E. M., Caldwell, S. H., Hepatocellular carcinoma in non-alcoholic fatty liver disease: an emerging menace. Journal of hepatology 2012, 56, 1384-1391.

[7] Lakhan, S. E., Kirchgessner, A., Gut microbiota and sirtuins in obesity-related inflammation and bowel dysfunction. Journal of translational medicine 2011, 9, 202.

[8] Miele, L., Valenza, V., La Torre, G., Montalto, M., Cammarota, G., Ricci, R., Masciana, R., Forgione, A., Gabrieli, M. L., Perotti, G., Vecchio, F. M., Rapaccini, G., Gasbarrini, G., Day, C. P., Grieco, A., Increased intestinal permeability and tight junction alterations in nonalcoholic fatty liver disease. Hepatology (Baltimore, Md.) 2009, 49, 1877-1887.

[9] Ip, B. C., Liu, C., Ausman, L. M., von Lintig, J., Wang, X. D., Lycopene attenuated hepatic tumorigenesis via differential mechanisms depending on carotenoid cleavage enzyme in mice. Cancer prevention research (Philadelphia, Pa.) 2014, 7, 1219-1227.

[10] Murphy, E. A., Velazquez, K. T., Herbert, K. M., Influence of high-fat diet on gut microbiota: a driving force for chronic disease risk. Current opinion in clinical nutrition and metabolic care 2015, 18, 515-520.

[11] Moreira, A. P., Texeira, T. F., Ferreira, A. B., Peluzio Mdo, C., Alfenas Rde, C., Influence of a high-fat diet on gut microbiota, intestinal permeability and metabolic endotoxaemia. The British journal of nutrition 2012, 108, 801-809.

[12] Tilg, H., Kaser, A., Gut microbiome, obesity, and metabolic dysfunction. The Journal of clinical investigation 2011, 121, 2126-2132.

[13] Shen, W., Wolf, P. G., Carbonero, F., Zhong, W., Reid, T., Gaskins, H. R., McIntosh, M. K., Intestinal and systemic inflammatory responses are positively associated with sulfidogenic bacteria abundance in high-fat-fed male C57BL/6J mice. The Journal of nutrition 2014, 144, 1181-1187.

[14] Brun, P., Castagliuolo, I., Di Leo, V., Buda, A., Pinzani, M., Palu, G., Martines, D., Increased intestinal permeability in obese mice: new evidence in the pathogenesis of

nonalcoholic steatohepatitis. American journal of physiology. Gastrointestinal and liver physiology 2007, 292, G518-525.

[15] Cani, P. D., Bibiloni, R., Knauf, C., Waget, A., Neyrinck, A. M., Delzenne, N. M., Burcelin, R., Changes in gut microbiota control metabolic endotoxemia-induced inflammation in high-fat diet-induced obesity and diabetes in mice. Diabetes 2008, 57, 1470-1481.

[16] Farhadi, A., Gundlapalli, S., Shaikh, M., Frantzides, C., Harrell, L., Kwasny, M. M., Keshavarzian, A., Susceptibility to gut leakiness: a possible mechanism for endotoxaemia in non-alcoholic steatohepatitis. Liver international: official journal of the International Association for the Study of the Liver 2008, 28, 1026-1033.

[17] Kim, K. A., Gu, W., Lee, I. A., Joh, E. H., Kim, D. H., High fat diet-induced gut microbiota exacerbates inflammation and obesity in mice via the TLR4 signaling pathway. PloS one 2012, 7, e47713.

[18] Cani, P. D., Neyrinck, A. M., Fava, F., Knauf, C., Burcelin, R. G., Tuohy, K. M., Gibson, G. R., Delzenne, N. M., Selective increases of bifidobacteria in gut microflora improve high-fat-diet-induced diabetes in mice through a mechanism associated with endotoxaemia. Diabetologia 2007, 50, 2374-2383.

[19] Hotamisligil, G. S., Inflammation and metabolic disorders. Nature 2006, 444, 860-867.

[20] Ip, B. C., Wang, X. D., Non-alcoholic steatohepatitis and hepatocellular carcinoma: implications for lycopene intervention. Nutrients 2013, 6, 124-162.

[21] Park, E. J., Lee, J. H., Yu, G. Y., He, G., Ali, S. R., Holzer, R. G., Osterreicher, C. H., Takahashi, H., Karin, M., Dietary and genetic obesity promote liver inflammation and tumorigenesis by enhancing IL-6 and TNF expression. Cell 2010, 140, 197-208.

[22] Solinas, G., Karin, M., JNK1 and IKKbeta: molecular links between obesity and metabolic dysfunction. FASEB journal: official publication of the Federation of American Societies for Experimental Biology 2010, 24, 2596-2611.

[23] Nov, O., Kohl, A., Lewis, E. C., Bashan, N., Dvir, I., Ben-Shlomo, S., Fishman, S., Wueest, S., Konrad, D., Rudich, A., Interleukin-1beta may mediate insulin resistance in liver-derived cells in response to adipocyte inflammation. Endocrinology 2010, 151, 4247-4256.

[24] Rajala, M. W., Obici, S., Scherer, P. E., Rossetti, L., Adipose-derived resistin and gut-derived resistin-like molecule-beta selectively impair insulin action on glucose production. The Journal of clinical investigation 2003, 111, 225-230.

[25] Patton, J. S., Shepard, H. M., Wilking, H., Lewis, G., Aggarwal, B. B., Eessalu, T. E., Gavin, L. A., Grunfeld, C., Interferons and tumor necrosis factors have similar catabolic effects on 3T3 L1 cells. Proceedings of the National Academy of Sciences of the United States of America 1986, 83, 8313-8317.

[26] Wanless, I. R., Lentz, J. S., Fatty liver hepatitis (steatohepatitis) and obesity: an autopsy study with analysis of risk factors. Hepatology (Baltimore, Md.) 1990, 12, 1106-1110.

[27] Wree, A., Kahraman, A., Gerken, G., Canbay, A., Obesity affects the liver - the link between adipocytes and hepatocytes. Digestion 2011, 83, 124-133.

[28] Huang, H., Park, P. H., McMullen, M. R., Nagy, L. E., Mechanisms for the anti-inflammatory effects of adiponectin in macrophages. Journal of gastroenterology and hepatology 2008, 23 Suppl 1, S50-53.

[29] Torres-Leal, F. L., Fonseca-Alaniz, M. H., Rogero, M. M., Tirapegui, J., The role of inflamed adipose tissue in the insulin resistance. Cell biochemistry and function 2010, 28, 623-631.

[30] Duval, C., Thissen, U., Keshtkar, S., Accart, B., Stienstra, R., Boekschoten, M. V., Roskams, T., Kersten, S., Muller, M., Adipose tissue dysfunction signals progression of hepatic steatosis towards nonalcoholic steatohepatitis in C57BL/6 mice. Diabetes 2010, 59, 3181-3191.

[31] Braunersreuther, V., Viviani, G. L., Mach, F., Montecucco, F., Role of cytokines and chemokines in non-alcoholic fatty liver disease. World journal of gastroenterology 2012, 18, 727-735.

[32] Shehzad, A., Iqbal, W., Shehzad, O., Lee, Y. S., Adiponectin: regulation of its production and its role in human diseases. Hormones (Athens, Greece) 2012, 11, 8-20.

[33] Story, E. N., Kopec, R. E., Schwartz, S. J., Harris, G. K., An update on the health effects of tomato lycopene. Annual review of food science and technology 2010, 1, 189-210.

[34] Wang, X. D., Carotenoids. In: Ross, A. C., Caballero, B., Cousins, R. J., Tucker, K. L., Zeigler, T. R. (Eds.), Modern Nutrition in Health and Disease, Lippincott Williams & Wilkins, Phillidelphia 2012, pp. 427-439.

[35] Erhardt, A., Stahl, W., Sies, H., Lirussi, F., Donner, A., Haussinger, D., Plasma levels of vitamin E and carotenoids are decreased in patients with Nonalcoholic Steatohepatitis (NASH). European journal of medical research 2011, 16, 76-78.

[36] Wang, Y., Ausman, L. M., Greenberg, A. S., Russell, R. M., Wang, X. D., Dietary lycopene and tomato extract supplementations inhibit nonalcoholic steatohepatitis-promoted hepatocarcinogenesis in rats. International journal of cancer 2010, 126, 1788-1796.

[37] Wang, X. D., Lycopene metabolism and its biological significance. The American journal of clinical nutrition 2012, 96, 1214s-1222s.

[38] Chung, J., Koo, K., Lian, F., Hu, K. Q., Ernst, H., Wang, X. D., Apo-10'-lycopenoic acid, a lycopene metabolite, increases sirtuin 1 mRNA and protein levels and decreases hepatic fat accumulation in ob/ob mice. The Journal of nutrition 2012, 142, 405-410.

[39] Ip, B. C., Liu, C., Lichtenstein, A. H., von Lintig, J., Wang, X. D., Lycopene and apo-10'-lycopenoic acid have differential mechanisms of protection against hepatic steatosis in beta-carotene-9',10'-oxygenase knockout male mice. The Journal of nutrition 2015, 145, 268-276.

[40] Purushotham, A., Schug, T. T., Xu, Q., Surapureddi, S., Guo, X., Li, X., Hepatocyte-specific deletion of SIRT1 alters fatty acid metabolism and results in hepatic steatosis and inflammation. Cell metabolism 2009, 9, 327-338.

[41] Herranz, D., Munoz-Martin, M., Canamero, M., Mulero, F., Martinez-Pastor, B., Fernandez-Capetillo, O., Serrano, M., Sirt1 improves healthy ageing and protects from metabolic syndrome-associated cancer. Nature communications 2010, 1, 3.

[42] Ip, B. C., Hu, K. Q., Liu, C., Smith, D. E., Obin, M. S., Ausman, L. M., Wang, X. D., Lycopene metabolite, apo-10'-lycopenoic acid, inhibits diethylnitrosamine-initiated, high fat diet-promoted hepatic inflammation and tumorigenesis in mice. Cancer prevention research (Philadelphia, Pa.) 2013, 6, 1304-1316.

[43] Xu, F., Gao, Z., Zhang, J., Rivera, C. A., Yin, J., Weng, J., Ye, J., Lack of SIRT1 (Mammalian Sirtuin 1) activity leads to liver steatosis in the SIRT1+/- mice: a role of lipid mobilization and inflammation. Endocrinology 2010, 151, 2504-2514.

[44] Cheng, J., Liu, C., Hu, K., Greenberg, A., Wu, D., Ausman, L. M., McBurney, M. W., Wang, X. D., Ablation of systemic SIRT1 activity promotes nonalcoholic fatty liver disease by affecting liver-mesenteric adipose tissue fatty acid mobilization. Biochimica et biophysica acta 2017.

[45] dela Sena, C., Narayanasamy, S., Riedl, K. M., Curley, R. W., Jr., Schwartz, S. J., Harrison, E. H., Substrate specificity of purified recombinant human beta-carotene 15,15'-oxygenase (BCO1). The Journal of biological chemistry 2013, 288, 37094-37103.

[46] Ferrucci, L., Perry, J. R., Matteini, A., Perola, M., Tanaka, T., Silander, K., Rice, N., Melzer, D., Murray, A., Cluett, C., Fried, L. P., Albanes, D., Corsi, A. M., Cherubini, A., Guralnik, J., Bandinelli, S., Singleton, A., Virtamo, J., Walston, J., Semba, R. D., Frayling, T. M., Common variation in the beta-carotene 15,15'-monooxygenase 1 gene affects circulating levels of carotenoids: a genome-wide association study. American journal of human genetics 2009, 84, 123-133.

[47] Lietz, G., Oxley, A., Leung, W., Hesketh, J., Single nucleotide polymorphisms upstream from the beta-carotene 15,15'-monoxygenase gene influence provitamin A conversion efficiency in female volunteers. The Journal of nutrition 2012, 142, 161s-165s.

[48] Fenni, S., Hammou, H., Astier, J., Bonnet, L., Karkeni, E., Couturier, C., Tourniaire, F., Landrier, J. F., Lycopene and tomato powder supplementation similarly inhibit high-fat diet induced obesity, inflammatory response, and associated metabolic disorders. Molecular nutrition & food research 2017.

[49] Palczewski, G., Widjaja-Adhi, M. A., Amengual, J., Golczak, M., von Lintig, J., Genetic dissection in a mouse model reveals interactions between carotenoids and lipid metabolism. Journal of lipid research 2016, 57, 1684-1695.

[50] Sharma, V., McNeill, J. H., To scale or not to scale: the principles of dose extrapolation. British journal of pharmacology 2009, 157, 907-921.

[51] Reagan-Shaw, S., Nihal, M., Ahmad, N., Dose translation from animal to human studies revisited. FASEB journal: official publication of the Federation of American Societies for Experimental Biology 2008, 22, 659-661.

[52] Melendez-Martinez, A. J., Nascimento, A. F., Wang, Y., Liu, C., Mao, Y., Wang, X. D., Effect of tomato extract supplementation against high-fat diet-induced hepatic lesions. Hepatobiliary surgery and nutrition 2013, 2, 198-208.

[53] Kim, S. W., Suda, W., Kim, S., Oshima, K., Fukuda, S., Ohno, H., Morita, H., Hattori, M., Robustness of gut microbiota of healthy adults in response to probiotic intervention revealed by high-throughput pyrosequencing. DNA research: an international journal for rapid publication of reports on genes and genomes 2013, 20, 241-253.

[54] Aronesty, E., ea-utils: "Command-line tools for processing biological sequencing data". DOI: https://expressionanalysis.github.io/ea-utils/, 2011.

[55] Edgar, R. C., Search and clustering orders of magnitude faster than BLAST. Bioinformatics (Oxford, England) 2010, 26, 2460-2461.

[56] Murtagh, F., Legendre, P., Ward ’s Hierarchical Agglomerative Clustering Method: Which Algorithms Implement Ward ’s Criterion? Journal of Classification 2014, 31, 274-295.

[57] Ip, B. C., Liu, C., Smith, D. E., Ausman, L. M., Wang, X. D., High-refined-carbohydrate and high-fat diets induce comparable hepatic tumorigenesis in male mice. The Journal of nutrition 2014, 144, 647-653.

[58] Viollet, B., Foretz, M., Guigas, B., Horman, S., Dentin, R., Bertrand, L., Hue, L., Andreelli, F., Activation of AMP-activated protein kinase in the liver: a new strategy for the management of metabolic hepatic disorders. The Journal of physiology 2006, 574, 41-53.

[59] Ha, J., Daniel, S., Broyles, S. S., Kim, K. H., Critical phosphorylation sites for acetyl-CoA carboxylase activity. The Journal of biological chemistry 1994, 269, 22162-22168.

[60] Kopec, R. E., Riedl, K. M., Harrison, E. H., Curley, R. W., Jr., Hruszkewycz, D. P., Clinton, S. K., Schwartz, S. J., Identification and quantification of apo-lycopenals in fruits, vegetables, and human plasma. Journal of agricultural and food chemistry 2010, 58, 3290-3296.

[61] Pfluger, P. T., Herranz, D., Velasco-Miguel, S., Serrano, M., Tschop, M. H., Sirt1 protects against high-fat diet-induced metabolic damage. Proceedings of the National Academy of Sciences of the United States of America 2008, 105, 9793-9798.

[62] Revollo, J. R., Grimm, A. A., Imai, S., The NAD biosynthesis pathway mediated by nicotinamide phosphoribosyltransferase regulates Sir2 activity in mammalian cells. The Journal of biological chemistry 2004, 279, 50754-50763.

[63] Imai, S., Yoshino, J., The importance of NAMPT/NAD/SIRT1 in the systemic regulation of metabolism and ageing. Diabetes, obesity & metabolism 2013, 15 Suppl 3, 26-33.

[64] Sultani, G., Samsudeen, A. F., Osborne, B., Turner, N., NAD+: a key metabolic regulator with great therapeutic potential. Journal of neuroendocrinology 2017.

[65] Canto, C., Menzies, K. J., Auwerx, J., NAD(+) Metabolism and the Control of Energy Homeostasis: A Balancing Act between Mitochondria and the Nucleus. Cell metabolism 2015, 22, 31-53.

[66] Mukherjee, S., Chellappa, K., Moffitt, A., Ndungu, J., Dellinger, R. W., Davis, J. G., Agarwal, B., Baur, J. A., Nicotinamide adenine dinucleotide biosynthesis promotes liver regeneration. Hepatology (Baltimore, Md.) 2017, 65, 616-630.

[67] Kahn, B. B., Alquier, T., Carling, D., Hardie, D. G., AMP-activated protein kinase: ancient energy gauge provides clues to modern understanding of metabolism. Cell metabolism 2005, 1, 15-25.

[68] Price, N. L., Gomes, A. P., Ling, A. J., Duarte, F. V., Martin-Montalvo, A., North, B. J., Agarwal, B., Ye, L., Ramadori, G., Teodoro, J. S., Hubbard, B. P., Varela, A. T., Davis, J. G., Varamini, B., Hafner, A., Moaddel, R., Rolo, A. P., Coppari, R., Palmeira, C. M., de Cabo, R., Baur, J. A., Sinclair, D. A., SIRT1 is required for AMPK activation and the beneficial effects of resveratrol on mitochondrial function. Cell metabolism 2012, 15, 675-690.

[69] Tian, Y., Ma, J., Wang, W., Zhang, L., Xu, J., Wang, K., Li, D., Resveratrol supplement inhibited the NF-kappaB inflammation pathway through activating AMPKalpha-SIRT1 pathway in mice with fatty liver. Molecular and cellular biochemistry 2016, 422, 75-84.

[70] Wu, C., Guo, Y., Su, Y., Zhang, X., Luan, H., Zhang, X., Zhu, H., He, H., Wang, X., Sun, G., Sun, X., Guo, P., Zhu, P., Cordycepin activates AMP-activated protein kinase (AMPK) via interaction with the gamma1 subunit. Journal of cellular and molecular medicine 2014, 18, 293-304.

[71] Hardie, D. G., AMPK: a key regulator of energy balance in the single cell and the whole organism. International journal of obesity (2005) 2008, 32 Suppl 4, S7-12.

[72] Fullerton, M. D., Galic, S., Marcinko, K., Sikkema, S., Pulinilkunnil, T., Chen, Z. P., O'Neill, H. M., Ford, R. J., Palanivel, R., O'Brien, M., Hardie, D. G., Macaulay, S. L., Schertzer, J. D., Dyck, J. R., van Denderen, B. J., Kemp, B. E., Steinberg, G. R., Single phosphorylation sites in Acc1 and Acc2 regulate lipid homeostasis and the insulin-sensitizing effects of metformin. Nature medicine 2013, 19, 1649-1654.

[73] Contreras, A. V., Torres, N., Tovar, A. R., PPAR-alpha as a key nutritional and environmental sensor for metabolic adaptation. Advances in nutrition (Bethesda, Md.) 2013, 4, 439-452.

[74] Polyzos, S. A., Kountouras, J., Zavos, C., Tsiaousi, E., The role of adiponectin in the pathogenesis and treatment of non-alcoholic fatty liver disease. Diabetes, obesity & metabolism 2010, 12, 365-383.

[75] Zou, C. C., Liang, L., Hong, F., Fu, J. F., Zhao, Z. Y., Serum adiponectin, resistin levels and non-alcoholic fatty liver disease in obese children. Endocrine journal 2005, 52, 519-524.

[76] Finelli, C., Tarantino, G., What is the role of adiponectin in obesity related non-alcoholic fatty liver disease? World journal of gastroenterology 2013, 19, 802-812.

[77] Kern, P. A., Di Gregorio, G. B., Lu, T., Rassouli, N., Ranganathan, G., Adiponectin expression from human adipose tissue: relation to obesity, insulin resistance, and tumor necrosis factor-alpha expression. Diabetes 2003, 52, 1779-1785.

[78] Pagano, C., Soardo, G., Esposito, W., Fallo, F., Basan, L., Donnini, D., Federspil, G., Sechi, L. A., Vettor, R., Plasma adiponectin is decreased in nonalcoholic fatty liver disease. European journal of endocrinology 2005, 152, 113-118.

[79] Luvizotto, R. A., Nascimento, A. F., Miranda, N. C., Wang, X. D., Ferreira, A. L., Lycopene-rich tomato oleoresin modulates plasma adiponectin concentration and mRNA levels of adiponectin, SIRT1, and FoxO1 in adipose tissue of obese rats. Human & experimental toxicology 2015, 34, 612-619.

[80] Maeda, N., Takahashi, M., Funahashi, T., Kihara, S., Nishizawa, H., Kishida, K., Nagaretani, H., Matsuda, M., Komuro, R., Ouchi, N., Kuriyama, H., Hotta, K., Nakamura, T., Shimomura, I., Matsuzawa, Y., PPARgamma ligands increase expression and plasma concentrations of adiponectin, an adipose-derived protein. Diabetes 2001, 50, 2094-2099.

[81] Bouskila, M., Pajvani, U. B., Scherer, P. E., Adiponectin: a relevant player in PPARgamma-agonist-mediated improvements in hepatic insulin sensitivity? International journal of obesity (2005) 2005, 29 Suppl 1, S17-23.

[82] Bajaj, M., Suraamornkul, S., Piper, P., Hardies, L. J., Glass, L., Cersosimo, E., Pratipanawatr, T., Miyazaki, Y., DeFronzo, R. A., Decreased plasma adiponectin concentrations are closely related to hepatic fat content and hepatic insulin resistance in pioglitazone-treated type 2 diabetic patients. The Journal of clinical endocrinology and metabolism 2004, 89, 200-206.

[83] Liang, X., Hu, M., Rogers, C. Q., Shen, Z., You, M., Role of SIRT1-FoxO1 signaling in dietary saturated fat-dependent upregulation of liver adiponectin receptor 2 in ethanol-administered mice. Antioxidants & redox signaling 2011, 15, 425-435.

[84] Feige, J. N., Lagouge, M., Canto, C., Strehle, A., Houten, S. M., Milne, J. C., Lambert, P. D., Mataki, C., Elliott, P. J., Auwerx, J., Specific SIRT1 activation mimics low energy levels

and protects against diet-induced metabolic disorders by enhancing fat oxidation. Cell metabolism 2008, 8, 347-358.

[85] Larter, C. Z., Farrell, G. C., Insulin resistance, adiponectin, cytokines in NASH: Which is the best target to treat? Journal of hepatology 2006, 44, 253-261.

[86] Kaser, S., Moschen, A., Cayon, A., Kaser, A., Crespo, J., Pons-Romero, F., Ebenbichler, C. F., Patsch, J. R., Tilg, H., Adiponectin and its receptors in non-alcoholic steatohepatitis. Gut 2005, 54, 117-121.

[87] Gerner, R. R., Wieser, V., Moschen, A. R., Tilg, H., Metabolic inflammation: role of cytokines in the crosstalk between adipose tissue and liver. Canadian journal of physiology and pharmacology 2013, 91, 867-872.

[88] Stojsavljevic, S., Gomercic Palcic, M., Virovic Jukic, L., Smircic Duvnjak, L., Duvnjak, M., Adipokines and proinflammatory cytokines, the key mediators in the pathogenesis of nonalcoholic fatty liver disease. World journal of gastroenterology 2014, 20, 18070-18091.

[89] Ghavipour, M., Saedisomeolia, A., Djalali, M., Sotoudeh, G., Eshraghyan, M. R., Moghadam, A. M., Wood, L. G., Tomato juice consumption reduces systemic inflammation in overweight and obese females. The British journal of nutrition 2013, 109, 2031-2035.

[90] De Stefano, D., Maiuri, M. C., Simeon, V., Grassia, G., Soscia, A., Cinelli, M. P., Carnuccio, R., Lycopene, quercetin and tyrosol prevent macrophage activation induced by gliadin and IFN-gamma. European journal of pharmacology 2007, 566, 192-199.

[91] Libermann, T. A., Baltimore, D., Activation of interleukin-6 gene expression through the NF-kappa B transcription factor. Molecular and cellular biology 1990, 10, 2327-2334.

[92] Cogswell, J. P., Godlevski, M. M., Wisely, G. B., Clay, W. C., Leesnitzer, L. M., Ways, J. P., Gray, J. G., NF-kappa B regulates IL-1 beta transcription through a consensus NF-kappa B binding site and a nonconsensus CRE-like site. Journal of immunology (Baltimore, Md. : 1950) 1994, 153, 712-723.

[93] Xiao, L., Sonne, S. B., Feng, Q., Chen, N., Xia, Z., Li, X., Fang, Z., Zhang, D., Fjaere, E., Midtbo, L. K., Derrien, M., Hugenholtz, F., Tang, L., Li, J., Zhang, J., Liu, C., Hao, Q., Vogel, U. B., Mortensen, A., Kleerebezem, M., Licht, T. R., Yang, H., Wang, J., Li, Y., Arumugam, M., Wang, J., Madsen, L., Kristiansen, K., High-fat feeding rather than obesity drives taxonomical and functional changes in the gut microbiota in mice. Microbiome 2017, 5, 43.

[94] Zhang, C., Zhang, M., Pang, X., Zhao, Y., Wang, L., Zhao, L., Structural resilience of the gut microbiota in adult mice under high-fat dietary perturbations. The ISME journal 2012, 6, 1848-1857.

[95] Parks, B. W., Nam, E., Org, E., Kostem, E., Norheim, F., Hui, S. T., Pan, C., Civelek, M., Rau, C. D., Bennett, B. J., Mehrabian, M., Ursell, L. K., He, A., Castellani, L. W., Zinker, B., Kirby, M., Drake, T. A., Drevon, C. A., Knight, R., Gargalovic, P., Kirchgessner, T.,

Eskin, E., Lusis, A. J., Genetic control of obesity and gut microbiota composition in response to high-fat, high-sucrose diet in mice. Cell metabolism 2013, 17, 141-152.

[96] Lecomte, V., Kaakoush, N. O., Maloney, C. A., Raipuria, M., Huinao, K. D., Mitchell, H. M., Morris, M. J., Changes in gut microbiota in rats fed a high fat diet correlate with obesity-associated metabolic parameters. PloS one 2015, 10, e0126931.

[97] Ling, Z., Li, Z., Liu, X., Cheng, Y., Luo, Y., Tong, X., Yuan, L., Wang, Y., Sun, J., Li, L., Xiang, C., Altered fecal microbiota composition associated with food allergy in infants. Applied and environmental microbiology 2014, 80, 2546-2554.

[98] Jiang, W., Wu, N., Wang, X., Chi, Y., Zhang, Y., Qiu, X., Hu, Y., Li, J., Liu, Y., Dysbiosis gut microbiota associated with inflammation and impaired mucosal immune function in intestine of humans with non-alcoholic fatty liver disease. Scientific reports 2015, 5, 8096.

[99] Qin, N., Yang, F., Li, A., Prifti, E., Chen, Y., Shao, L., Guo, J., Le Chatelier, E., Yao, J., Wu, L., Zhou, J., Ni, S., Liu, L., Pons, N., Batto, J. M., Kennedy, S. P., Leonard, P., Yuan, C., Ding, W., Chen, Y., Hu, X., Zheng, B., Qian, G., Xu, W., Ehrlich, S. D., Zheng, S., Li, L., Alterations of the human gut microbiome in liver cirrhosis. Nature 2014, 513, 59-64.

[100] Yoshimoto, S., Loo, T. M., Atarashi, K., Kanda, H., Sato, S., Oyadomari, S., Iwakura, Y., Oshima, K., Morita, H., Hattori, M., Honda, K., Ishikawa, Y., Hara, E., Ohtani, N., Obesity-induced gut microbial metabolite promotes liver cancer through senescence secretome. Nature 2013, 499, 97-101.

[101] Monaghan, T. M., Cockayne, A., Mahida, Y. R., Pathogenesis of Clostridium difficile Infection and Its Potential Role in Inflammatory Bowel Disease. Inflammatory bowel diseases 2015, 21, 1957-1966.

[102] Degirolamo, C., Rainaldi, S., Bovenga, F., Murzilli, S., Moschetta, A., Microbiota modification with probiotics induces hepatic bile acid synthesis via downregulation of the Fxr-Fgf15 axis in mice. Cell reports 2014, 7, 12-18.

[103] Islam, K. B., Fukiya, S., Hagio, M., Fujii, N., Ishizuka, S., Ooka, T., Ogura, Y., Hayashi, T., Yokota, A., Bile acid is a host factor that regulates the composition of the cecal microbiota in rats. Gastroenterology 2011, 141, 1773-1781.

[104] Schmitz, H. H., Poor, C. L., Wellman, R. B., Erdman, J. W., Jr., Concentrations of selected carotenoids and vitamin A in human liver, kidney and lung tissue. The Journal of nutrition 1991, 121, 1613-1621.

[105] Bai, S. K., Lee, S. J., Na, H. J., Ha, K. S., Han, J. A., Lee, H., Kwon, Y. G., Chung, C. K., Kim, Y. M., beta-Carotene inhibits inflammatory gene expression in lipopolysaccharide-stimulated macrophages by suppressing redox-based NF-kappaB activation. Experimental & molecular medicine 2005, 37, 323-334.

[106] Wei, J., Lei, G. H., Fu, L., Zeng, C., Yang, T., Peng, S. F., Association between Dietary Vitamin C Intake and Non-Alcoholic Fatty Liver Disease: A Cross-Sectional Study among Middle-Aged and Older Adults. PloS one 2016, 11, e0147985.

[107] Cindrova-Davies, T., Spasic-Boskovic, O., Jauniaux, E., Charnock-Jones, D. S., Burton, G. J., Nuclear factor-kappa B, p38, and stress-activated protein kinase mitogen-activated protein kinase signaling pathways regulate proinflammatory cytokines and apoptosis in human placental explants in response to oxidative stress: effects of antioxidant vitamins. The American journal of pathology 2007, 170, 1511-1520.

[108] Basu, A., Imrhan, V., Tomatoes versus lycopene in oxidative stress and carcinogenesis: conclusions from clinical trials. European journal of clinical nutrition 2007, 61, 295-303.

[109] Shi, J., Kakuda, Y., Yeung, D., Antioxidative properties of lycopene and other carotenoids from tomatoes: synergistic effects. BioFactors (Oxford, England) 2004, 21, 203-210.

APPENDIX V

Apo-10'-lycopenoic acid inhibits cancer cell migration and angiogenesis and induces peroxisome proliferator-activated receptor γ

Junrui Cheng, Benchun Miao, Kang-Quan Hu, Xueyan Fu, and Xiang-Dong Wang*

Nutrition and Cancer Biology Laboratory, Jean Mayer United States Department of Agriculture Human Nutrition Research Center on Aging at Tufts University, Boston MA 02111 USA

*To whom correspondence should be addressed. Tel: +1 617 5563130; Fax: +1 617 5563344; Email: xiang-dong.wang@tufts.edu

Key words: lycopene metabolites, PPARγ, angiogenesis, cell migration, metastasis

Abbreviations: ALA, apo-10'-lycopenoic acid; **PPARγ**, peroxisome proliferator-activated receptor; **HCC**, hepatocellular carcinoma; **MMP-2**, matrix metalloproteinase-2; **VEGF**, vascular endothelial growth factor; **EGF**, Epidermal growth factor; **bFGF**, basic fibroblast growth factor; **PDGF**, platelet-derived growth factor; **PPRE**, PPAR response element.

Abstract

Scope

We have previously shown that apo-10'-lycopenoic acid (ALA), a derivative of lycopene through cleavage by carotene- 9',10'-oxygenase, inhibits tumor progression and metastasis in both liver and lung cancer animal models. The underlying mechanism remains unknown. We hypothesized that ALA inhibits cancer cell motility and angiogenesis by upregulating peroxisome proliferator-activated receptor γ (PPARγ) which is involved in controlling angiogenesis, tumor progression and metastasis.

Methods and Results

ALA treatment, in dose-dependent manner, was effective at inhibiting migration and invasion of liver and lung cancer cells (HuH7 and A549) in both transwell and wound healing models, as well as suppressing actin remodeling and ruffling/lamellipodia formation in HuH7 and immortalized lung BEAS-2B cells. ALA treatment resulted in suppression of angiogenesis in both tube formation and aortic ring assays and inhibition of matrix metalloproteinase-2 expression and activation in both HuH7 and A549 cells. Additionally, ALA dose-dependently increased the mRNA expression and protein levels of PPARγ in human THLE-2 liver cells. Furthermore, ALA produced concentration-dependent increases in transcription activity of the PPRE but this effect was less effective as compared with rosiglitazone.

Conclusion

ALA inhibits cancer cell motility and angiogenesis and induces PPARγ expression, which could be one of the potential mechanisms for ALA protecting against tumor progression.

1. Introduction

Dietary intervention is one of the main strategies for preventing cancer development and increasing cancer survival rates. Lycopene, the pigment principally responsible for the characteristic deep-red color of ripe tomato and tomato products, is the most predominant carotenoid in human plasma. Lycopene has attracted attention due to its biological and physicochemical properties, especially related to its effects as a natural antioxidant, anti-inflammatory and anti-carcinogenic agent against certain types of cancers, including those of the liver [1] and lung [2]. Two epidemiology studies revealed inverse association between plasma lycopene levels and early liver cancer stage [3] and lung cancer risk [4]. Concordantly, animal studies reported inhibitory effects of lycopene against cancer development in liver [5, 6], lung [7] and colon [8, 9], with strong evidence implicating lycopene as an anti-inflammatory or anti-carcinogenic agent.

Lycopene is an open chain hydrocarbon containing 11 conjugated and 2 non-conjugated double bonds arranged in a linear array. It is susceptible to oxidative cleavage and isomerization from trans- to cis-forms with the potential formation of putative bioactive metabolites [10]. Numerous oxidative metabolites of lycopene have been identified in both in vitro and in vivo systems, raising the possibility that the chemopreventive effect of lycopene could be, at least in part, due to its metabolites [11]. Indeed, apolycopenoids exist in tomatoes and tomato products and a series of apolycopenoids including apo-10'-lycopenal have been identified in human plasmas of individuals who consumed tomato juice [12]. We have previously demonstrated that in mammalian tissues, lycopene can be cleaved by carotene 9',10'-oxygenase at 9',10'-double bond, producing apo-10'-lycopenal that can be oxidized into apo-10'-lycopenoic acid (ALA, Figure 1A) [13]. Recently, we have found that animals with ALA supplementation had comparable tumor incidence, as compared with non-ALA treated group, but ALA significantly decreased tumor multiplicity in both hepatocellular carcinoma (HCC) and lung cancer models [5, 14]. Additionally, ALA supplementation decreased lung tumor incidence in diethylnitrosamine-initiated, high fat diet-promoted HCC model, suggesting a role of ALA on mitigating tumor progression or metastasis, rather than preventing the initiation of primary tumor [5]. Interestingly, ALA is

structurally similar to acyclic retinoic acid, a chemical that has been reported to inhibit the recurrence of HCC in a clinical trial [15]. However, the underlying mechanism of how ALA inhibits tumor growth and metastasis has not been investigated.

Angiogenesis plays an important role in the growth and spread of tumor cells by providing oxygen and nutrients [16, 17]; it is also an essential component of the metastatic pathway [18]. Multiple studies have shown that lycopene and its oxidative metabolite, such as apo-8'-lycopenal, inhibits angiogenesis by decreasing vascular endothelial growth factor (VEGF), matrix metalloproteinase (MMP)-2, MMP-9 and inhibiting the adhesion, invasion and migration of tumor cells [19-24]. Whether lycopene enzymatic metabolite, ALA, possesses anti-angiogenic efficacy remains unknown.

The nuclear transcription factor peroxisome proliferator-activated receptor γ (PPARγ) is involved in controlling cell growth, inflammatory responses and tumorigenesis [25, 26]. Inhibiting angiogenesis is one of the major mechanisms by which PPARγ arrests tumor cell progression and metastasis [27-30]. The activation of PPARγ was found to inhibit epithelial cell proliferation and migration via inhibiting VEGF, VEGF receptors, MMPs and phosphorylated Akt [31-35]. PPARγ agonists such as rosiglitazone, troglitazone and pioglitazone have been widely studied as anti-inflammation and anti-cancer agents [36-38]. Unfortunately, these agonists were withdrawn from the market after reports of severe adverse effects (such as liver dysfunction, heart failure and water retention) appeared in clinical trials [39]. Previous studies have demonstrated that several lycopene metabolites modulate the activity of various transcription systems, including ligand-activated nuclear receptors, such as the retinoic acid receptor and retinoid X receptor, which could be potential mechanisms for lycopene metabolites in the prevention of cancer and other chronic diseases [41, 42]. We have shown that ALA transactivated the promoter of the RARβ gene and induced the expression of this receptor [14]. However, ALA may affect multiple transcriptional pathways and, specifically, whether ALA inhibits cancer cell motility and angiogenesis by inducing PPARγ remains enigmatic. PPARγ can form heterodimer with RXR, subsequently binding to PPAR response element (PPRE) and regulate target genes [43].

In the current study, we examined whether ALA inhibits cell migration, invasion and angiogenesis and induces PPARγ expression in cells

2. Method

2.1 Materials

The ALA used in this study was provided by Dr. Hansgeorg Ernst (BASF, Ludwigshafen, Germany) with 99% purity, analyzed by HPLC as previously described [5, 44]. The rabbit anti-matrix metalloproteinase-2 (MMP-2) and PPARγ antibody were purchased from Santa Cruz Biotechnology. The secondary HRP-conjugated antibodies were purchased from Cell Signaling Technology. Epidermal growth factor (EGF) and basic fibroblast growth factor (bFGF) were purchased from Becton-Dickinson. Platelet-derived growth factor (PDGF), hydrocortisone, tetramethyl rhodamine isothiocyanate (TRITC)-labeled phalloidin and all other reagents and chemicals were purchased from Sigma. PPRE-x3-TK-LUC reporter vector that contains three copies of a consensus PPRE upstream of the thymidine kinase promoter-luciferase fusion gene was purchased from Addgene (Cambridge, MA USA).

2.2 Cells and cell culture

Human cancer cell lines (A549, BEAS-2B, HuH7) and THLE-2 human liver cell lines were purchased from the American Type Culture Collection. Human micro-vascular endothelial cell line (HMEC-1) was provided from the Centre for Disease Control and Prevention (Atlanta, Georgia). A549 and HuH7 cells were cultured in DMEM medium with 10% fetal bovine serum (FBS), and BEAS-2B cells were cultured in RPMI1640 medium with 10% FBS. HMEC-1 cells were cultured in MCDB 131 medium supplemented with 10% FBS, 10 ng/ml EGF and 1 μg/ml hydrocortisone. THLE-2 cells were cultured in 10% fetal bovine serum BEGM supplemented with Bullet kit CC3170 (Lonza Walkersville, MD), 5ng/ml EGF and 70ng/ml phosphoethanolamine. All media were supplemented with 100 units/ml penicillin, 100 μg/ml streptomycin, and 2 mM glutamine. All cells were cultured in a humidified atmosphere of 95% air and 5% CO_2 at 37 °C.

2.3 Cell viability assay

Cells were seeded into opaque-walled 96-well plates at the density of $5-10\times10^3$ cells per well in 100 μl of the according media. ALA was added at a series of concentrations and incubated for different time. A luminescence-based commercial kit (CellTiter-Glo, Promega, Madison, WI) was used. Each well was added with 30 μl of the cell lysis (or ATP disodium salt as standard), mixed for 10 min at room temperature, and the luminescence was measured by utilizing a Wallac Victor 3 plate reader (Perkin-Elmer, Wellesley, MA) and calculated according to an ATP standard curve.

2.4 Fluorescent immunocytochemistry

Cells were seeded on sterilized glass coverslips, followed by with or without ALA treatment at doses ranging from 2.5-40 μM. Cells were incubated in a 5% CO_2 incubator until they were 50-70% confluent. The cells were then fixed with 4% polyformaldehyde for 30 min, permeabilized with 0.1% Triton X-100 for 20 min, and incubated with 200 ng/ml TRITC-labeled phalloidin for 30 minutes. All images were obtained by employing Zeiss Axiovert 200 fluorescent microscope.

2.5 Cell migration assays

2.5.1 Transwell model

Migration of cells was analyzed by utilizing 24-transwell Boyden chamber (Costar, Bedford, MA) with a 8.0 μm pore polycarbonate membrane (10-μm thickness and 6.5-μm diameter), as described [45]. Briefly, cells were placed in serum-free media and seeded in the upper compartment of each well (5×10^4 cells/well) with or without ALA at different concentrations (2.5-40 μM). Subsequently, add 600 μl of serum-free media supplemented with fibronectin into the bottom of the lower chamber. Following an incubation period of 12 hours at 37°C, the cells were fixed with 70% ethanol and stained with 0.1% crystal violet. After removing the non-migrated cells on the upper surface of the filter, the migrated cells on the lower side were photographed using a microscope in five random fields. Then cells were lysed with 10% acetic acid, and colorimetric determination was made at 595 nm using Wallac Victor 3 plate reader.

2.5.2 Wound healing model

Cells were seeded into fibronectin-coated 96-well plates (2×10^4 cells/well) for 100% confluence in 24 hours as described [45]. A 200 μl pipette tip was used to press firmly against the plate to obtain a "wound". The media and cell debris were aspirated, and replaced by fresh serum-free media with or without ALA treatment at different doses (2.5-40 μM). After incubation at 37°C for 12 hours, the snapshot pictures of cells were photographed using a microscope in five random fields. The distance of wounded cell monolayers in images was measured and the inhibition rates of migration were calculated by comparing wound closure overtime.

2.5.3 Cell invasion assay

Cell invasion assay was performed using 24-transwell Boyden as described in Transwell model. The upper chamber was pre-coated with 1 mg/ml of Matrigel (BD Biosciences) with four-hour incubation at 37°C to form a basement membrane. The assays were performed and the results were analyzed as described above in Transwell model.

2.5.4 Tube formation assay

The tube formation assay was performed in 96-well plates. Wells were pre-coated with 70 μl of the Matrigel basement membrane matrix (BD Biosciences) per well for 4 hours at 37°C. HMEC-1 cells were suspended in serum-free MCDB 131 medium and plated on Matrigel at a density of 2×10^4 cells per well. ALA was added at indicated concentrations (2.5-40 μM). After an eight-hour incubation at 37°C, phase-contrast images of the endothelial tubes were obtained using Nikon TE2000 microscope, and the tube formation was assessed by counting the number of closed tubes in five random fields from each well.

2.5.5 Aortic ring assay

The aortas were isolated from 6-week old Sprague-Dawley rats and immediately transferred to a culture dish with serum-free medium. The fibroadipose tissue around the aortas was carefully removed and the aortas were cut into 1-mm long aortic ring

fragments. After three consecutive washes in serum-free medium, the aortic rings were embedded into 70 μl Matrigel in 96-well plate and fed with 100 μl of serum-free M199 medium with or without ALA at different concentrations (2.5-40 μM). The medium was replaced every 24-hour. Phase-contrast images were obtained on day 6, and the numbers of microvessel outgrowths per ring were counted.

2.6 Real-time PCR

Total RNA was isolated from the liver by TriPure Isolation Reagent (Roche Diagnostics, Indianapolis, IN) as the protocol indicates. Then cDNA was prepared from the RNA samples using M-MLV reverse transcriptase (Invitrogen, Carlsbad, CA) and an automated thermal cycler (MJ Research PTC-200, Bio-Rad Laboratories, Hercules, CA). The detection of mRNA level in each well was carried out using 20 μl reaction mixture containing 10 μl 2X SYBR Green Supermix, 2 μl of 10 μM primer mix (including forward and reverse primers), 3 μl PCR water and 5 μl cDNA diluted in Rnase-free water. Cycling conditions were 50 °C for 2 minutes and 95 °C for 10 minutes; followed by 40 cycles at 95 °C for 15 seconds and 600 °C for 1 minute. Primers were designed using the Primer Express version 2.0 software (Applied Biosystems, Foster City, CA). Quantification of gene expression was normalized to the levels of GAPDH and then calculated by reference to the average values for the control group using the comparative Ct method. For each sample and each gene, PCR reactions were carried out in duplicate and repeated twice.

2.7 Western blotting

Samples separated by SDS-PAGE were transferred to nitrocellulose membranes. After being blocked in 5% non-fat milk at room temperature for 1 hour, the membranes were rinsed and incubated at 4°C overnight with primary antibodies (1:1000). A horseradish peroxidase-conjugated secondary antibody (Bio-Rad) was used to detect protein concentration. The blots were then developed using the ECL Western blotting system (Amersham, Piscataway, NJ) and analyzed by computerized densitometry (Bio-Rad GS-710, Bio-Rad Laboratories, Hercules, CA). Beta-actin antibody was used as internal control for equal loading of proteins.

2.8 Luciferase reporter assay

To test for transcriptional activity of ALA, Cos7 cells ($4x10^4$ cells/well) in a 6-well plate were transiently transfected with 1.5 μg peroxisome proliferator response element (PPRE)-x3-TK-LUC reporter and 50 ng pRL-TK Renilla luciferase vector using Fugene 6 transfection reagent (Roche Applied Science) as indicated by the manufacturers. After transfection for 24 hours, cells were trypsinized, re-plated by 1:12 in 24-well plate and incubated for 24 hours. Afterwards, cells were treated with ALA for overnight. The luciferase activities were measured with the Dual-Luciferase Reporter System by a Lumi-Scint luminometer (BioScan, Inc., DC). Rosiglitazone, a PPARγ agonist was used as positive control. Luciferase activities were normalized against Renilla activities to adjust for transfection efficiency.

2.9 Statistics

Student's t test and analysis of variance (ANOVA) were performed using SAS 9.3. $P<0.05$ was considered significant. The data shown are representatives of at least three independent experiments with similar results, and the data points represent the mean of at least triplicate measurements with error bars corresponding to standard deviation.

3. Results

3.1 ALA inhibits cell migration and invasion

To analyze the anti-migration activity of ALA, we first examined the effect of ALA (Fig. 1) on migration of cancer and endothelial cells. As shown in Fig. 1B,D, ALA at different concentrations (2.5-40 μM) substantially inhibited migration of liver cancer cell HuH7, lung cancer cell A549, as well as lung immortalized BEAS-2B cell in a concentration-dependent manner in Transwell assay. Similar inhibition of ALA on cell migration was also observed in a wound healing assay (Fig. 1C,E). In addition, ALA significantly inhibited migration of endothelial cell HMEC-1 concentration-dependently in both Transwell and wound healing assay, suggesting its possible effect on angiogenesis (Fig. 2A-C).

We next investigated the effect of ALA on invasion of cancer and endothelial cells. As shown in Fig. 3A,B, ALA, at different concentrations (2.5-40 μM), efficiently suppressed invasion of A549, BEAS-2B and HMEC-1 cells through Matrigel dose-dependently in a Transwell invasion assay. Importantly, ALA had no significant cytotoxic effects on both cancer and endothelial cells in parallel experiments at the same concentrations used in migration and invasion experiments ($P>0.05$) (Fig. 1F, Fig. 2D), suggesting that the inhibitory effect of ALA on cell migration and invasion is not a consequence of cellular toxicity.

3.2 ALA inhibits angiogenesis

Endothelial cell migration plays a central role in the process of forming vessel loops from solid sprouts during angiogenesis [46]. Considering the efficient inhibition of endothelial cell migration by ALA, we examined the ability of ALA to attenuate angiogenesis in vitro using endothelial tube formation and aortic ring assays. As shown in Fig. 4A,B, treatment with ALA resulted in efficient inhibition of tube formation in a concentration-dependent manner (2.5-40 μM). Microvessel growth from rat aorta sections is a joint phenomenon combining both endothelial cell migration and tube formation, and thus provides a close mimic of in vivo angiogenesis [47]. Consistent with tube formation results, ALA treatment remarkably suppressed microvessel outgrowth in aortic ring sprouting experiment (Fig. 4C,D). These data suggest that ALA is capable of blocking angiogenesis through attenuation of endothelial cell motility.

3.3 ALA inhibits ruffling/lamellipodia formation

Cell motility is driven by actin rearrangement and lamellipodia formation at the leading edge of cells [48]. The reduction of cell migration, invasion and angiogenesis caused by ALA led us to examine whether ALA can influence actin reorganization and reduce ruffling/lamellipodia formation. As shown in Fig. 5A,B, pre-treatment with ALA efficiently inhibited PDGF/bFGF-stimulated actin remodeling and ruffles/lamellipodia formation in HuH7, BEAS-2B and HMEC-1 cells. This effect provides underlying mechanical explanation for the inhibition of cell migration and angiogenesis by ALA.

3.4 ALA inhibits MMP-2 levels and induces PPARγ expression

MMP-2 is a representative member of matrix metalloproteinase family proteins, which play crucial roles in cell invasion by degrading basement membranes [49-52]. Therefore, we next quantified the expression and activation of MMP-2. As a result, ALA (2.5-40 μM) reduced both pro- and activated MMP-2 levels in a dose-dependent manner (Fig. 6A), indicating that ALA could suppress activated MMP-2 by decreasing the protein expression of pro-MMP-2.

It has been shown that the activation of PPARγ by its ligands is involved in inhibiting angiogenesis and carcinogenesis in a variety of cancer cells [3, 27, 53]. To investigate whether the anti-angiogenic effects of ALA is due to inducing PPARγ, we firstly examined both mRNA and protein expression of PPARγ in THLE cells after ALA treatment at different doses (5-20 μM). There is a substantial increase of both PPARγ mRNA (Fig. 6B) and protein levels of PPARγ (Fig. 6C) in the cells treated with ALA for 48 hours.

PPRE is a sequence identified on a number of genes in their promoters that bound to PPARs for inducting transcription activity [54]. To further examine whether ALA can transactivate PPRE, we transfected Cos7 cells with a luciferase reporter that contained a potent PPRE. After treating cells with ALA at different concentrations (5, 15 and 20 μM) for 24 hours, luciferase activities increased with ALA in a dose-response manner (Fig. 6D). However, as compared to the positive control by rosiglitazone, a well-known PPARγ agonist [55, 56], the magnitude of the increase of transactivation activity of ALA at 20 microM concentration was less than that induced by rosiglitazone at 2 microM (Fig. 6D).

4. Discussion

In the present study, we present evidence that ALA is effective at inhibiting migration and invasion of human cancer cells and endothelial cells by suppressing ruffling/lamellipodia formation. Specifically, we found that the migration and invasion activities in two cancer cell lines (A549, a human adenocarcinoma cells and HuH7, a well-differentiated hepatocyte-derived carcinoma cells) substantially decreased with ALA treatment, indicating that anti-migration and anti-invasion effect are intrinsic

properties of ALA. This provided an underlying mechanism explaining the anti-tumorigenesis and metastatic effect of ALA treatment observed in our previous *in vivo* study [5, 14].

We further demonstrated that ALA treatment inhibited angiogenesis, which is a rate-limiting step in tumor growth and progression [31]. It is well-known that the induction of a tumor vasculature, or 'angiogenic switch', is required to allow tumor progression, invasion, and metastasis [16, 17]. By conducting tube formation assay and aorta ring assay, we observed that in both studies, ALA treatment decreased vessel formation in a dose-response manner, consistently demonstrating that ALA contains anti-angiogenic effects. Further investigation showed that ALA treatment blocked lamellipodia formation, a process occurs before angiogenic sprouts [57], providing underlying mechanism of how ALA inhibits angiogenesis. We previously reported that the ALA treatment inhibited hepatic inflammatory foci and IL-6 expression and tumor multiplicity in both liver and lungs, which was associated with the reduction of NF-κB protein expression [5]. Since NF-κB plays an important role in lamellipodia formation [58], the effect of ALA blocking lamellipodia formation could be due to its inhibitory function of NF-κB, thereby mitigating tumor progression or metastasis.

Matrix metalloproteinases have been implicated in increased metastatic potential of tumors, majorly via interactions with extracellular matrix and angiogenesis [59]. MMP-2 is one of the most investigated metalloproteinases for angiogenesis [49-52]. In our study, MMP-2 substantially decreased in ALA-treated cells, indicating that decreasing MMP-2 contributes to the anti-angiogenic effect of ALA. Similar MMP-2 inhibitive effect has been reported in *in vitro* studies using lycopene or apo-8'-lycopenal treatments [20, 23]. Interestingly, accumulating evidence revealed that PPARγ activation can inhibit MMP-2 [29, 60, 61], raising the possibility that the MMP-2 inhibitory effect of ALA might be related to PPARγ activation. Indeed, in present study, ALA treatment increased both transcription and protein levels of PPARγ. It has been shown that some well-known PPARγ ligands, such as rosiglitazone and troglitazone, can inhibit tumor metastasis majorly by blocking angiogenesis but exhibit serious side effects [39]. In our study, ALA treatment increased both PPARγ protein concentration without any

cytotoxicity in cell viability assay. This finding indicated that the anti-migration and anti-invasion effects of ALA could be associated with PPARγ function.

In the current study, the effective concentrations of ALA to inhibition of migration and invasion of human cancer cells and induction of PPARγ were ranged between 2.5 to 40 μmol/L, which are similar to the concentrations of well-known PPARγ agonists, such as rosiglitazone, used in previous cell culture studies [55, 56]. However, we should point out that the magnitude of the increase of transactivation activity of ALA, even at much higher concentrations, was less than that induced by rosiglitazone. These data suggest that the PPRE transactivation activity of ALA could be due to its induction of PPARγ, not as a direct agonist of PPARγ, as rosiglitazone. Additionally, the ALA concentrations we used in the present study are much higher than the reported plasma concentrations of lycopene and apolycopenals in humans who consumed tomato products and tomato juice [12, 62]. One of potential explanations was due to the low uptake of fat-soluble carotenoids in cells, or further cellular metabolism of carotenoids, as we reported previously that the intracellular concentration of carotenoids were much lower than their concentrations in cell culture medium [14, 45]. This was also supported with our *in vivo* studies that ALA supplementation in genetically-induced obese mice and in high fat diet promoted, metabolic syndrome-associated HCC mouse model has restored the reduction of expression and activity of Sirtuin 1, a class III deacetylase, and inhibited hepatic steatosis [44, 63] and HCC [5], but ALA concentration in tissue was in picomolar range [5]. Therefore, we believe that the ALA dosage used in our study is physiologically relevant to the biological effects of lycopene metabolites.

In summary, the present study indicates that ALA can inhibit cancer cell motility and angiogenesis and upregulate PPARγ , which could be one of the potential mechanisms by which ALA protects against cancer metastasis. This study has a potential implication that ALA could be used as an adjunctive agent for the therapeutic treatment that may improve survival of cancer patients.

Author contributions:

JC and BM made equal contribution as first author.

JC, BM, KH and XF conducted experimental studies.

JC, BM, and XDW wrote the manuscript.

XDW supervised the study.

The work was supported by US Department of Agriculture/NIFA (AFRI 2015-67017-23141) and US Department of Agriculture/ARS (1950-51000-074S). Any opinions, findings, conclusion, or recommendations expressed in this publication are those of the author(s) and do not necessarily reflect the views of the U.S. Department of Agriculture.

Author Disclosures: All of the authors have no conflicts of interest.

Figure 1.

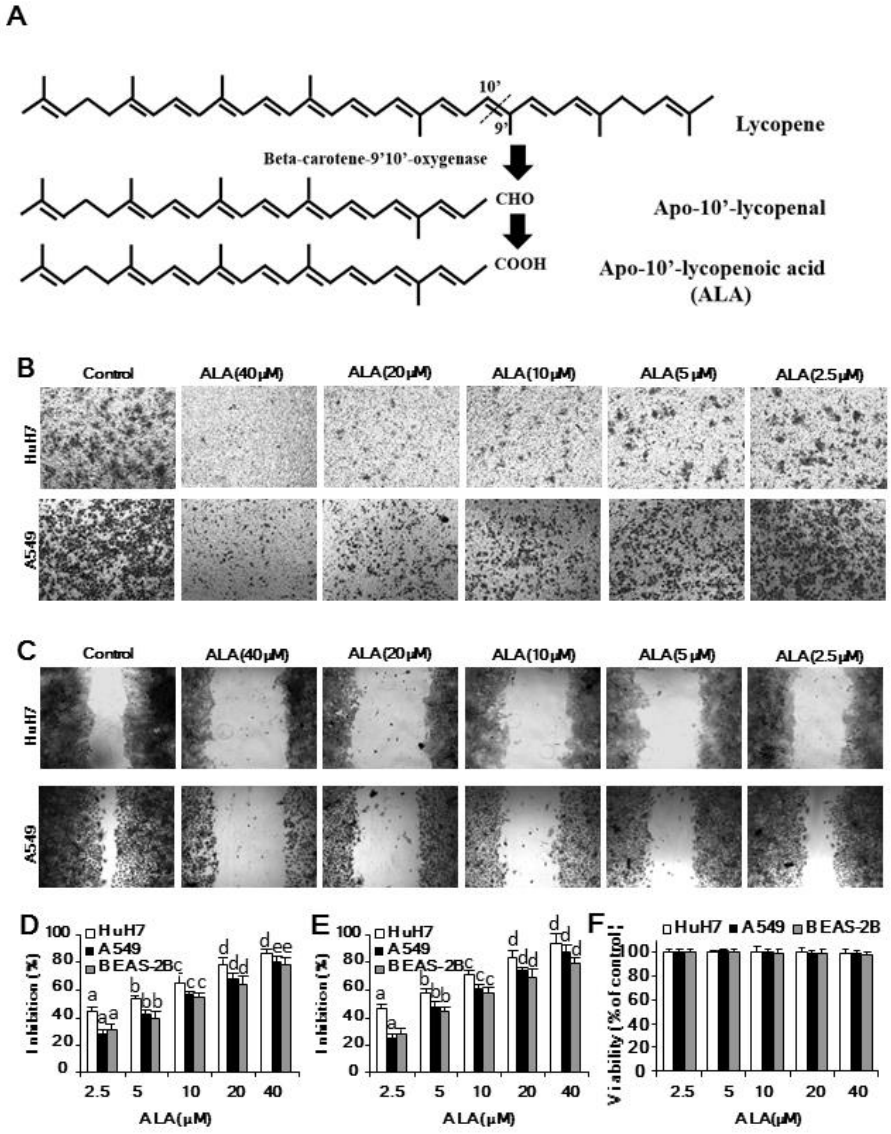
A
10'
9'
Lycopene
Beta-carotene-9'10'-oxygenase
CHO
Apo-10'-lycopenal
COOH
Apo-10'-lycopenoic acid
(ALA)
B
Control
ALA(40μM)
ALA(20μM)
ALA(10μM)
ALA(5μM)
ALA(2.5μM)
HuH7
A549
C
Control
ALA(40μM)
ALA(20μM)
ALA(10μM)
ALA(5μM)
ALA(2.5μM)
HuH7
A549
D
HuH7
A549
BEAS-2B
Inhibition (%)
ALA(μM)
E
HuH7
A549
BEAS-2B
Inhibition (%)
ALA(μM)
F
HuH7
A549
BEAS-2B
Viability (% of control)
ALA(μM)

Figure 2.

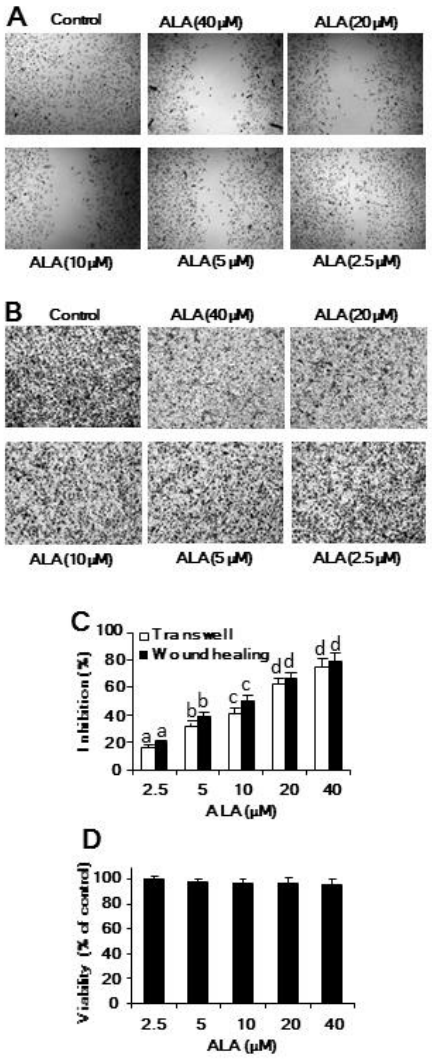
A
Control
ALA(40μM)
ALA(20μM)
ALA(10μM)
ALA(5μM)
ALA(2.5μM)
B
Control
ALA(40μM)
ALA(20μM)
ALA(10μM)
ALA(5μM)
ALA(2.5μM)
C
Transwell
Wound healing
Inhibition (%)
100
80
60
40
20
0
a a
b b
c c
d d
d d
2.5
5
10
20
40
ALA (μM)
D
Viability (% of control)
100
80
60
40
20
0
2.5
5
10
20
40
ALA (μM)

Figure 3.

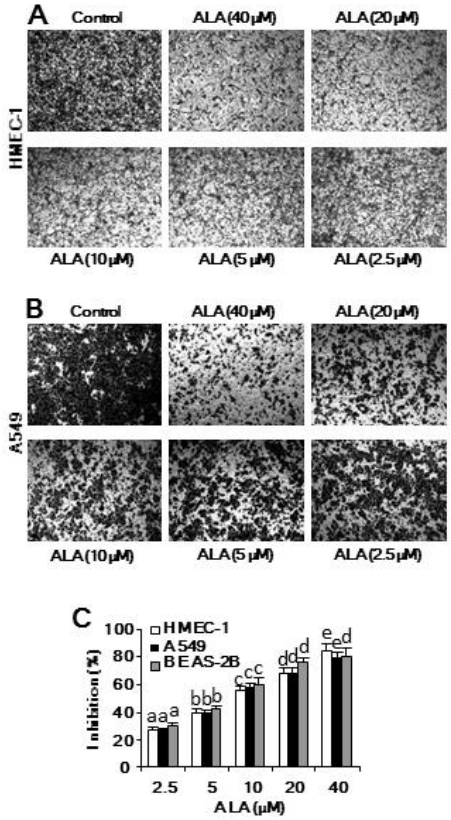
A
Control
ALA(40μM)
ALA(20μM)
HMEC-1
ALA(10μM)
ALA(5μM)
ALA(2.5μM)
B
Control
ALA(40μM)
ALA(20μM)
A549
ALA(10μM)
ALA(5μM)
ALA(2.5μM)
C
HMEC-1
A549
BEAS-2B
Inhibition (%)
100
80
60
40
20
0
2.5
5
10
20
40
ALA (μM)

Figure 4.

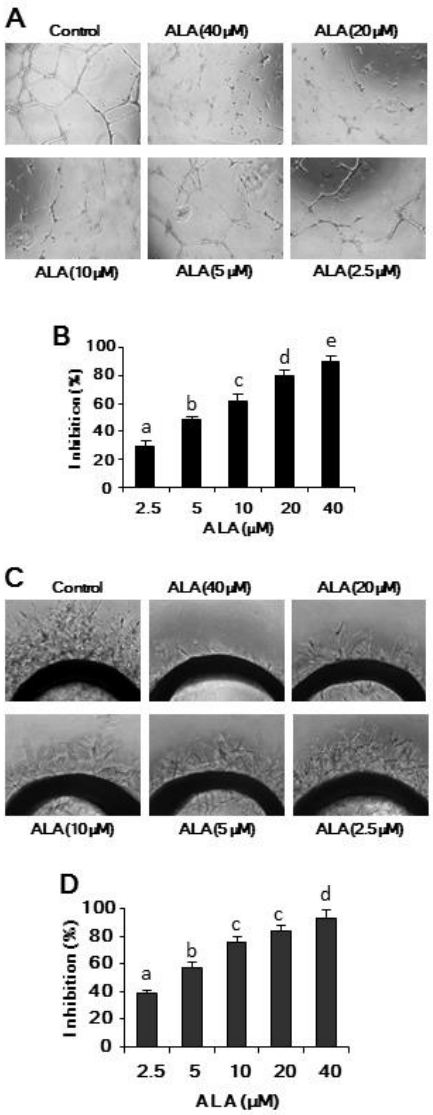
A
Control
ALA(40μM)
ALA(20μM)
ALA(10μM)
ALA(5μM)
ALA(2.5μM)
B
Inhibition (%)
100
80
60
40
20
0
a
b
c
d
e
2.5
5
10
20
40
ALA (μM)
C
Control
ALA(40μM)
ALA(20μM)
ALA(10μM)
ALA(5μM)
ALA(2.5μM)
D
Inhibition (%)
100
80
60
40
20
0
a
b
c
c
d
2.5
5
10
20
40
ALA (μM)

Figure 5.

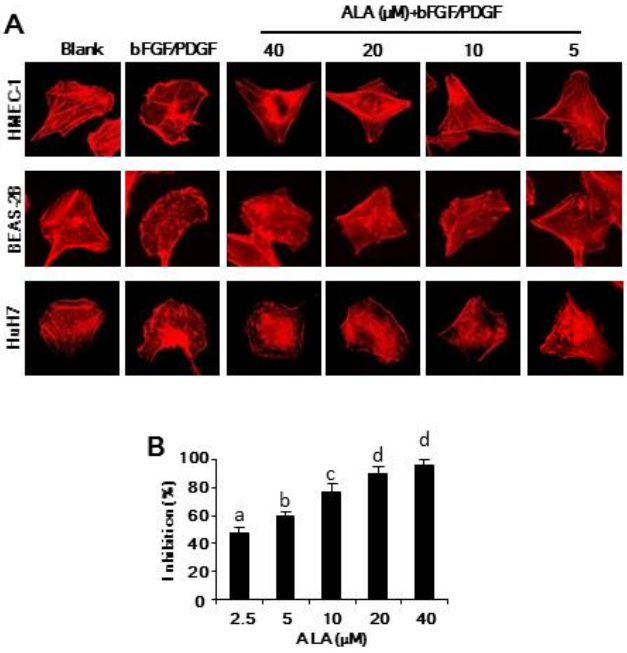
A
ALA (μM)+bFGF/PDGF
Blank
bFGF/PDGF
40
20
10
5
HMEC-1
BEAS-2B
Hul7
B
Inhibition (%)
100
80
60
40
20
0
a
b
c
d
d
2.5
5
10
20
40
ALA (μM)

Figure 6.

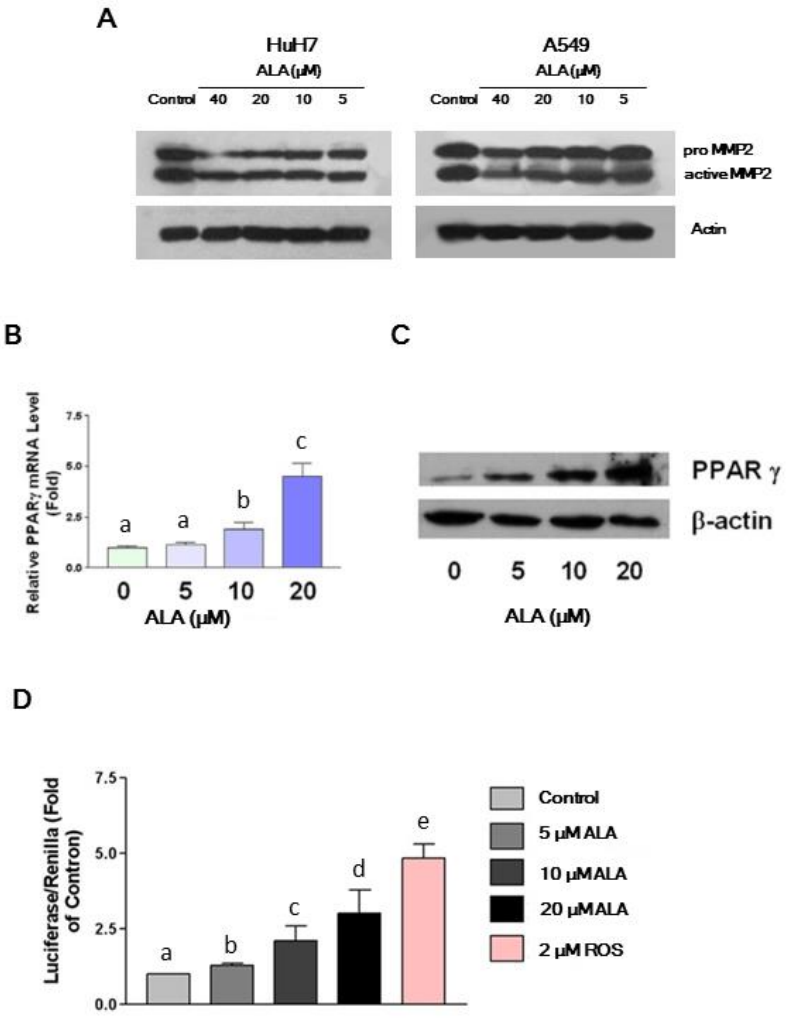
A
HuH7
ALA(μM)
Control 40 20 10 5
A549
ALA(μM)
Control 40 20 10 5
pro MMP2
active MMP2
Actin
B
Relative PPARγ mRNA Level (Fold)
7.5
5.0
2.5
0.0
a a b c
0 5 10 20
ALA (μM)
C
PPAR γ
β-actin
0 5 10 20
ALA (μM)
D
Luciferase/Renilla (Fold of Contron)
7.5
5.0
2.5
0.0
a b c d e
Control
5 μM ALA
10 μM ALA
20 μM ALA
2 μM ROS

Figure legends

Figure 1. ALA inhibits migration of cancer cells

(A) Metabolic pathway of lycopene to ALA.

(B) ALA inhibits migration of lung cells in a Transwell assay. A549 and HuH7 cells were treated with ALA (2.5-40 μM) for 12 hours. The non-migrated cells on the upper surface of the filter were removed, and the migrated cells on the lower side were stained and photographed, and the representative images are shown, then cells were lysed and colorimetric determination was made at 595 nm.

(C) ALA inhibits migration of lung cells in a wound healing assay. A scratch was introduced into a monolayer of A549 and HuH7 cells, followed by treatment with ALA (2.5-40 μM) for 12 hours. The width of wounded cell monolayer was measured in five random fields, and representative images are shown (the original wound edges are labeled with white lines).

(D) Quantitation of the inhibition from Transwell assay using A549, HuH7 and BEAS-2B cells.

(E) Quantitation of the inhibition from wound healing assay in using A549, HuH7 and BEAS-2B cells.

(F) ALA inhibits lung cell migration at non-cytotoxic concentrations. A549, HuH7 and BEAS-2B cells were treated with ALA (2.5-40 μM) for 12 hours, and cell viability was evaluated using ATP assay.

Different alphabets indicate statistically significant ($P < 0.05$).

Figure 2. ALA inhibits migration of endothelial cells

(A) ALA inhibits migration of endothelial cells in a Transwell assay. HMEC-1 cells were treated with ALA (2.5-40 μM) for 12 hours. The non-migrated cells on the upper surface of the filter were removed, and the migrated cells on the lower side were stained and photographed, and the representative images are shown, then cells were lysed and colorimetric determination was made at 595 nm.

(B) ALA inhibits migration of endothelial cells in a wound healing assay. A scratch was introduced into a monolayer of HMEC-1 cells, followed by treatment with ALA (2.5-40 μM) for 12 hours. The width of wounded cell monolayer was measured in five random fields, and representative images are shown (the original wound edges are labeled with white lines).

(C) Quantitation of the inhibition from Transwell and wound healing assays in (A,B).

(D) ALA inhibits endothelial cell migration at non-cytotoxic concentrations. HMEC-1 cells were treated with ALA (2.5-40 μM) for 12 hours, and cell viability was evaluated using ATP assay.

Different alphabets indicate statistically significant ($P < 0.05$).

Figure 3. ALA inhibits cell invasion

(A, B) ALA inhibits invasion of cancer and endothelial cells. HMEC-1 (A) and A549 (B) cells were treated with ALA (2.5-40 μM) for 12 hours. The non-invasion cells on the upper surface of the filter were removed, and the invasion cells on the lower side were stained and photographed, and the representative images are shown, then cells were lysed and colorimetric determination was made at 595 nm.

(C) Quantitation of the inhibition from Transwell invasion assay utilizing HMEC-1, A549 and BEAS-2B cells (A,B).

Different alphabets indicate statistically significant ($P < 0.05$).

Figure 4. ALA inhibits angiogenesis

(A) ALA inhibits tube formation of endothelial cells. HMEC-1 cells were seeded on matrigel and treated with ALA for 12 hours. The representative images are shown. The tube formation was assessed by counting the number of closed tubes in five random fields from each well and the inhibition was calculated.

(B) Quantitation of the effects of ALA on endothelial cell tube formation from (A).

(C) ALA suppresses microvessel outgrowth in the aortic ring sprouting experiment. The rat aortic rings were embedded in matrigel and treated with ALA for 6 days, followed by counting the number of microvessel outgrowths under a microscope. The representative images are shown and the inhibition was calculated.

(D) Quantitation of the effects of ALA on microvessel outgrowth from (C).

Different alphabets indicate statistically significant ($P < 0.05$).

Figure 5. ALA inhibits lamellipodia formation

HuH7, BEAS-2B and HMEC-1 cells were serum starved and treated with ALA (2.5-40 μM) for 12 hours, followed by PDGF (100 ng/ml, for cancer cells) or bFGF (10 ng/ml, for HMEC-1 cells) stimulation for 30 min. Then cells were stained with TRITC-labeled phalloidin and analyzed using fluorescent microscopy. The representative fluorescent images are shown (A, the lamellipodia are indicated by arrowheads). The number of cells

with significant lamellipodia was counted randomly in five fields and the inhibition was calculated (B).

Different alphabets indicate statistically significant ($P < 0.05$).

Figure 6. ALA suppresses MMP2 and induces PPARγ

HuH7 and A549 cells were treated with ALA (0.5-40 μM) for 24 hours. The protein levels of pro- and active MMP-2 were measured using western blotting and β-actin as loading control (A). THLE2 were treated with ALA (5-20 μM) for 48 hours. PPARγ mRNA expression was analyzed by RT-PCR (B). PPARγ protein levels were measured using western blotting (C). Beta-actin was used as loading control in RT-PCR and western blotting. Cos7 cells were transfected with PPRE-x3-TK-LUC reporter and pRL-TK Renilla luciferase vector. The cells were treated with ALA at different concentrations (5 and 20 μM) and rosiglitazone (2 μM) for 24 hours and luciferase fold change representing the effect of ALA on PPRE-transactivation activity (D).

Different alphabets indicate statistically significant ($P < 0.05$).

5. Reference

[1] Ip, B. C., Wang, X. D., Non-alcoholic steatohepatitis and hepatocellular carcinoma: implications for lycopene intervention. *Nutrients* 2013, *6*, 124-162.
[2] Palozza, P., Simone, R. E., Catalano, A., Mele, M. C., Tomato lycopene and lung cancer prevention: from experimental to human studies. *Cancers* 2011, *3*, 2333-2357.
[3] Kataria, Y., Deaton, R. J., Enk, E., Jin, M., *et al.*, Retinoid and carotenoid status in serum and liver among patients at high-risk for liver cancer. *BMC gastroenterology* 2016, *16*, 30.
[4] Holick, C. N., Michaud, D. S., Stolzenberg-Solomon, R., Mayne, S. T., *et al.*, Dietary carotenoids, serum beta-carotene, and retinol and risk of lung cancer in the alpha-tocopherol, beta-carotene cohort study. *American journal of epidemiology* 2002, *156*, 536-547.
[5] Ip, B. C., Hu, K. Q., Liu, C., Smith, D. E., *et al.*, Lycopene metabolite, apo-10'-lycopenoic acid, inhibits diethylnitrosamine-initiated, high fat diet-promoted hepatic inflammation and tumorigenesis in mice. *Cancer prevention research (Philadelphia, Pa.)* 2013, *6*, 1304-1316.
[6] Wang, Y., Ausman, L. M., Greenberg, A. S., Russell, R. M., Wang, X. D., Dietary lycopene and tomato extract supplementations inhibit nonalcoholic steatohepatitis-promoted hepatocarcinogenesis in rats. *International journal of cancer* 2010, *126*, 1788-1796.
[7] Liu, C., Lian, F., Smith, D. E., Russell, R. M., Wang, X. D., Lycopene supplementation inhibits lung squamous metaplasia and induces apoptosis via up-regulating insulin-like growth factor-binding protein 3 in cigarette smoke-exposed ferrets. *Cancer research* 2003, *63*, 3138-3144.
[8] Tang, F. Y., Pai, M. H., Wang, X. D., Consumption of lycopene inhibits the growth and progression of colon cancer in a mouse xenograft model. *Journal of agricultural and food chemistry* 2011, *59*, 9011-9021.
[9] Tang, F. Y., Pai, M. H., Kuo, Y. H., Wang, X. D., Concomitant consumption of lycopene and fish oil inhibits tumor growth and progression in a mouse xenograft model of colon cancer. *Molecular nutrition & food research* 2012, *56*, 1520-1531.
[10] Wang, X. D., in: Krinsky, N., Mayne, S., Sies, H. (Eds.), *Carotenoid oxidative/degradative products and their biological activities. In: Carotenoids in Health and Disease*, Marcel Dekker, New York 2004, pp. 313-335.
[11] Wang, X. D., Lycopene metabolism and its biological significance. *The American journal of clinical nutrition* 2012, *96*, 1214s-1222s.
[12] Kopec, R. E., Riedl, K. M., Harrison, E. H., Curley, R. W., Jr., *et al.*, Identification and quantification of apo-lycopenals in fruits, vegetables, and human plasma. *Journal of agricultural and food chemistry* 2010, *58*, 3290-3296.
[13] Hu, K. Q., Liu, C., Ernst, H., Krinsky, N. I., *et al.*, The biochemical characterization of ferret carotene-9',10'-monooxygenase catalyzing cleavage of carotenoids in vitro and in vivo. *The Journal of biological chemistry* 2006, *281*, 19327-19338.
[14] Lian, F., Smith, D. E., Ernst, H., Russell, R. M., Wang, X. D., Apo-10'-lycopenoic acid inhibits lung cancer cell growth in vitro, and suppresses lung tumorigenesis in the A/J mouse model in vivo. *Carcinogenesis* 2007, *28*, 1567-1574.
[15] Muto, Y., Moriwaki, H., Ninomiya, M., Adachi, S., *et al.*, Prevention of second primary tumors by an acyclic retinoid, polyprenoic acid, in patients with hepatocellular carcinoma. Hepatoma Prevention Study Group. *The New England journal of medicine* 1996, *334*, 1561-1567.
[16] Bergers, G., Benjamin, L. E., Tumorigenesis and the angiogenic switch. *Nature reviews. Cancer* 2003, *3*, 401-410.
[17] Eichmann, A., Bouvrée, K., Pardanaud, L., in: D. Marmé, Fusenig, N. (Eds.), *Tumor Angiogenesis: Basic Mechanisms and Cancer Therapy*, Springer Science & Business Media, New York 2007, pp. 31-45.
[18] Takeda, A., Stoeltzing, O., Ahmad, S. A., Reinmuth, N., *et al.*, Role of angiogenesis in the development and growth of liver metastasis. *Annals of surgical oncology* 2002, *9*, 610-616.

[19] Bhatia, N., Gupta, P., Singh, B., Koul, A., Lycopene Enriched Tomato Extract Inhibits Hypoxia, Angiogenesis, and Metastatic Markers in early Stage N-Nitrosodiethylamine Induced Hepatocellular Carcinoma. *Nutrition and cancer* 2015, *67*, 1268-1275.
[20] Chen, M. L., Lin, Y. H., Yang, C. M., Hu, M. L., Lycopene inhibits angiogenesis both in vitro and in vivo by inhibiting MMP-2/uPA system through VEGFR2-mediated PI3K-Akt and ERK/p38 signaling pathways. *Molecular nutrition & food research* 2012, *56*, 889-899.
[21] Elgass, S., Cooper, A., Chopra, M., Lycopene inhibits angiogenesis in human umbilical vein endothelial cells and rat aortic rings. *The British journal of nutrition* 2012, *108*, 431-439.
[22] Hwang, E. S., Lee, H. J., Inhibitory effects of lycopene on the adhesion, invasion, and migration of SK-Hep1 human hepatoma cells. *Experimental biology and medicine (Maywood, N.J.)* 2006, *231*, 322-327.
[23] Yang, C. M., Hu, T. Y., Hu, M. L., Antimetastatic effects and mechanisms of apo-8'-lycopenal, an enzymatic metabolite of lycopene, against human hepatocarcinoma SK-Hep-1 cells. *Nutrition and cancer* 2012, *64*, 274-285.
[24] Yang, C. M., Huang, S. M., Liu, C. L., Hu, M. L., Apo-8'-lycopenal induces expression of HO-1 and NQO-1 via the ERK/p38-Nrf2-ARE pathway in human HepG2 cells. *Journal of agricultural and food chemistry* 2012, *60*, 1576-1585.
[25] Yu, J., Shen, B., Chu, E. S., Teoh, N., *et al.*, Inhibitory role of peroxisome proliferator-activated receptor gamma in hepatocarcinogenesis in mice and in vitro. *Hepatology (Baltimore, Md.)* 2010, *51*, 2008-2019.
[26] Sharma, C., Pradeep, A., Pestell, R. G., Rana, B., Peroxisome proliferator-activated receptor gamma activation modulates cyclin D1 transcription via beta-catenin-independent and cAMP-response element-binding protein-dependent pathways in mouse hepatocytes. *The Journal of biological chemistry* 2004, *279*, 16927-16938.
[27] Kotlinowski, J., Jozkowicz, A., PPAR Gamma and Angiogenesis: Endothelial Cells Perspective. *Journal of diabetes research* 2016, *2016*, 8492353.
[28] Chuang, C. H., Yeh, C. L., Yeh, S. L., Lin, E. S., *et al.*, Quercetin metabolites inhibit MMP-2 expression in A549 lung cancer cells by PPAR-gamma associated mechanisms. *The Journal of nutritional biochemistry* 2016, *33*, 45-53.
[29] Li, Y., Zhang, D. W., Lin, D. Q., Cao, L. Q., Peroxisome proliferator-activated receptor-gamma inhibits pancreatic cancer cell invasion and metastasis via regulating MMP-2 expression through PTEN. *Molecular medicine reports* 2015, *12*, 6255-6260.
[30] Yoshizumi, T., Ohta, T., Ninomiya, I., Terada, I., *et al.*, Thiazolidinedione, a peroxisome proliferator-activated receptor-gamma ligand, inhibits growth and metastasis of HT-29 human colon cancer cells through differentiation-promoting effects. *International journal of oncology* 2004, *25*, 631-639.
[31] Keshamouni, V. G., Arenberg, D. A., Reddy, R. C., Newstead, M. J., *et al.*, PPAR-gamma activation inhibits angiogenesis by blocking ELR+CXC chemokine production in non-small cell lung cancer. *Neoplasia (New York, N.Y.)* 2005, *7*, 294-301.
[32] Biscetti, F., Gaetani, E., Flex, A., Aprahamian, T., *et al.*, Selective activation of peroxisome proliferator-activated receptor (PPAR)alpha and PPAR gamma induces neoangiogenesis through a vascular endothelial growth factor-dependent mechanism. *Diabetes* 2008, *57*, 1394-1404.
[33] Funovics, P., Brostjan, C., Nigisch, A., Fila, A., *et al.*, Effects of 15d-PGJ(2) on VEGF-induced angiogenic activities and expression of VEGF receptors in endothelial cells. *Prostaglandins & other lipid mediators* 2006, *79*, 230-244.
[34] Goetze, S., Eilers, F., Bungenstock, A., Kintscher, U., *et al.*, PPAR activators inhibit endothelial cell migration by targeting Akt. *Biochemical and biophysical research communications* 2002, *293*, 1431-1437.
[35] Kim, K. Y., Ahn, J. H., Cheon, H. G., Anti-angiogenic action of PPARgamma ligand in human umbilical vein endothelial cells is mediated by PTEN upregulation and VEGFR-2 downregulation. *Molecular and cellular biochemistry* 2011, *358*, 375-385.

[36] Tachibana, K., Yamasaki, D., Ishimoto, K., Doi, T., The Role of PPARs in Cancer. *PPAR research* 2008, *2008*, 102737.
[37] Borbath, I., Horsmans, Y., The Role of PPARgamma in Hepatocellular Carcinoma. *PPAR research* 2008, *2008*, 209520.
[38] Reddy, A. T., Lakshmi, S. P., Reddy, R. C., PPARgamma as a Novel Therapeutic Target in Lung Cancer. *PPAR research* 2016, *2016*, 8972570.
[39] Nesto, R. W., Bell, D., Bonow, R. O., Fonseca, V., *et al.*, Thiazolidinedione use, fluid retention, and congestive heart failure: a consensus statement from the American Heart Association and American Diabetes Association. October 7, 2003. *Circulation* 2003, *108*, 2941-2948.
[40] Justus, C. R., Leffler, N., Ruiz-Echevarria, M., Yang, L. V., In vitro cell migration and invasion assays. *Journal of visualized experiments : JoVE* 2014.
[41] Aydemir, G., Kasiri, Y., Birta, E., Beke, G., *et al.*, Lycopene-derived bioactive retinoic acid receptors/retinoid-X receptors-activating metabolites may be relevant for lycopene's anti-cancer potential. *Molecular nutrition & food research* 2013, *57*, 739-747.
[42] Sharoni, Y., Linnewiel-Hermoni, K., Khanin, M., Salman, H., *et al.*, Carotenoids and apocarotenoids in cellular signaling related to cancer: a review. *Molecular nutrition & food research* 2012, *56*, 259-269.
[43] Shimizu, M., Moriwaki, H., Synergistic Effects of PPARgamma Ligands and Retinoids in Cancer Treatment. *PPAR research* 2008, *2008*, 181047.
[44] Chung, J., Koo, K., Lian, F., Hu, K. Q., *et al.*, Apo-10'-lycopenoic acid, a lycopene metabolite, increases sirtuin 1 mRNA and protein levels and decreases hepatic fat accumulation in ob/ob mice. *The Journal of nutrition* 2012, *142*, 405-410.
[45] Iskandar, A. R., Miao, B., Li, X., Hu, K. Q., *et al.*, Beta-Cryptoxanthin Reduced Lung Tumor Multiplicity and Inhibited Lung Cancer Cell Motility by Downregulating Nicotinic Acetylcholine Receptor alpha7 Signaling. *Cancer prevention research (Philadelphia, Pa.)* 2016, *9*, 875-886.
[46] Gerhardt, H., VEGF and endothelial guidance in angiogenic sprouting. *Organogenesis* 2008, *4*, 241-246.
[47] Miao, B., Skidan, I., Yang, J., You, Z., *et al.*, Inhibition of cell migration by PITENINs: the role of ARF6. *Oncogene* 2012, *31*, 4317-4332.
[48] Mogilner, A., Oster, G., Cell motility driven by actin polymerization. *Biophysical journal* 1996, *71*, 3030-3045.
[49] Ali-Labib, R., Louka, M. L., Galal, I. H., Tarek, M., Evaluation of matrix metalloproteinase-2 in lung cancer. *Proteomics. Clinical applications* 2014, *8*, 251-257.
[50] Basset, P., Okada, A., Chenard, M. P., Kannan, R., *et al.*, Matrix metalloproteinases as stromal effectors of human carcinoma progression: therapeutic implications. *Matrix biology : journal of the International Society for Matrix Biology* 1997, *15*, 535-541.
[51] Giannelli, G., Bergamini, C., Marinosci, F., Fransvea, E., *et al.*, Clinical role of MMP-2/TIMP-2 imbalance in hepatocellular carcinoma. *International journal of cancer* 2002, *97*, 425-431.
[52] Zhang, Q., Chen, X., Zhou, J., Zhang, L., *et al.*, CD147, MMP-2, MMP-9 and MVD-CD34 are significant predictors of recurrence after liver transplantation in hepatocellular carcinoma patients. *Cancer biology & therapy* 2006, *5*, 808-814.
[53] Cao, L. Q., Shao, Z. L., Liang, H. H., Zhang, D. W., *et al.*, Activation of peroxisome proliferator-activated receptor-gamma (PPARgamma) inhibits hepatoma cell growth via downregulation of SEPT2 expression. *Cancer letters* 2015, *359*, 127-135.
[54] Tugwood, J. D., Issemann, I., Anderson, R. G., Bundell, K. R., *et al.*, The mouse peroxisome proliferator activated receptor recognizes a response element in the 5' flanking sequence of the rat acyl CoA oxidase gene. *The EMBO journal* 1992, *11*, 433-439.

[55] Quintanilla, R. A., Jin, Y. N., Fuenzalida, K., Bronfman, M., Johnson, G. V., Rosiglitazone treatment prevents mitochondrial dysfunction in mutant huntingtin-expressing cells: possible role of peroxisome proliferator-activated receptor-gamma (PPARgamma) in the pathogenesis of Huntington disease. *The Journal of biological chemistry* 2008, *283*, 25628-25637.
[56] Sozio, M. S., Lu, C., Zeng, Y., Liangpunsakul, S., Crabb, D. W., Activated AMPK inhibits PPAR-{alpha} and PPAR-{gamma} transcriptional activity in hepatoma cells. *American journal of physiology. Gastrointestinal and liver physiology* 2011, *301*, G739-747.
[57] Yang, H., Fang, L., Zhan, R., Hegarty, J. M., *et al.*, Polo-like kinase 2 regulates angiogenic sprouting and blood vessel development. *Developmental biology* 2015, *404*, 49-60.
[58] Guo, A. K., Hou, Y. Y., Hirata, H., Yamauchi, S., *et al.*, Loss of p53 enhances NF-kappaB-dependent lamellipodia formation. *Journal of cellular physiology* 2014, *229*, 696-704.
[59] Rojiani, M. V., Alidina, J., Esposito, N., Rojiani, A. M., Expression of MMP-2 correlates with increased angiogenesis in CNS metastasis of lung carcinoma. *International journal of clinical and experimental pathology* 2010, *3*, 775-781.
[60] Chen, R., Xue, J., Xie, M., Osthole regulates TGF-beta1 and MMP-2/9 expressions via activation of PPARalpha/gamma in cultured mouse cardiac fibroblasts stimulated with angiotensin II. *Journal of pharmacy & pharmaceutical sciences : a publication of the Canadian Society for Pharmaceutical Sciences, Societe canadienne des sciences pharmaceutiques* 2013, *16*, 732-741.
[61] Yiqin, Y., Meilin, X., Jie, X., Keping, Z., Aspirin inhibits MMP-2 and MMP-9 expression and activity through PPARalpha/gamma and TIMP-1-mediated mechanisms in cultured mouse celiac macrophages. *Inflammation* 2009, *32*, 233-241.
[62] Reynaud, E., Aydemir, G., Ruhl, R., Dangles, O., Caris-Veyrat, C., Organic synthesis of new putative lycopene metabolites and preliminary investigation of their cell-signaling effects. *Journal of agricultural and food chemistry* 2011, *59*, 1457-1463.
[63] Ip, B. C., Liu, C., Lichtenstein, A. H., von Lintig, J., Wang, X. D., Lycopene and apo-10'-lycopenoic acid have differential mechanisms of protection against hepatic steatosis in beta-carotene-9',10'-oxygenase knockout male mice. *The Journal of nutrition* 2015, *145*, 268-276.